Facing the resurgence of rotavirus:

Development of novel antiviral agents

Sunrui Chen

陈荪睿 著

Cover design: Qun Pan and the author of this thesis.
Layout design: The author of this thesis.

Printed by:

ISBN:

Facing the resurgence of rotavirus: Development of novel antiviral agents

Het gevecht tegen de wederopstanding van het rotavirus: ontwikkeling van nieuwe middelen

Thesis

to obtain the degree of Doctor from the
Erasmus University Rotterdam
by command of the
rector magnificus

Prof. dr. R.C.M.E. Engels

and in accordance with the decision of the Doctorate Board

The public defense shall be held on

Tuesday 15th December 2020 at 11：30

by

Sunrui Chen

born in Wuhan, Hubei Province, China

Erasmus University Rotterdam

Doctoral Committee:

Promoter:

Prof. dr. M.P. Peppelenbosch

Inner Committee:

Prof. dr. C.C. Baan

Prof. dr. L.J.W. van der Laan

Prof. dr. J.C.H. Hardwick

Copromoter:

Dr. Q. Pan

CONTENTS

Summary and Discussion

Dutch Summary

Acknowledgements

Publications

PhD Portfolio

Curriculum Vitae

Chapter 1

General Introduction and Outline of

This Thesis

GENERAL INTRODUCTION

Pathogenesis and virology of rotavirus

In this thesis I shall focus on rotavirus. Rotavirus is a member of the so-called *Reoviridae* family and was discovered as a novel pathogen by Dr. Ruth Bishop together with colleagues at the Royal Children's Hospital (RCH) in 1973[1]. The name rotavirus was first coined one year later by Thomas Henry Flewett and in 1978 rotavirus was officially defined[2]. Since, it has become clear that it constitutes a major health concern.

Indeed data from 2015 show that diarrheal disease is the fourth leading cause of death among children under 5 years old, responsible for almost 500 000 deaths in that year [3]. As one of the leading causal factors for pediatric diarrhea globally, it is estimated that rotavirus infection develops in 25% of cases in moderate-to-severe illnesses [4] and associates with approximately 125,000-200,000 deaths each year[3, 5], contributing to 30% of all death due to diarrhea for the first two years after birth [6].

Though among young children, diarrhea-associated mortality number has decreased since 1990 by approximately 65% [7], due to limited resources and poor hygiene practices, situations are still unsatisfactory in many developing countries and especially India, Nigeria, Pakistan, and the Democratic Republic of the Congo need to be named in this respect as they together account for half of the global mortally due to pediatric diarrhea [8].

Although primarily a health concern in infants, it is important to realize that rotavirus infection is not restricted by age. Especially orthotopic organ transplantation patients are effected, the average incidence of rotavirus infection is 3.03% among them, with intestinal transplant recipients, liver transplant recipients and hematopoietic stem cell transplant patients being under the highest risk for suffering from rotavirus infection-caused chronic diarrhea [9]. Improved treatment options are called for.

Rational novel avenues for the treatment of rotavirus may be designed following an understanding of rotavirus biology. Rotavirus is a non-enveloped virus which has a double-stranded RNA genome containing 11 segments and is surrounded by multilayered icosahedral protein capsid. Its genome encodes 12 proteins including 6 viral proteins and 6 non-structural

proteins (10). VP1, VP2 and VP3 proteins make up the rotavirus core particle. VP1 protein is the RNA-dependent RNA polymerase (RdRP) of rotavirus catalyzing viral RNA synthesis (11). VP2 protein consists of 120 molecules and VP3 is a guanylyl transferase (12, 13). There is also a VP4 protein, with a length of 775 or 776 amino acids and this constitutes an 84 KDa spike protein, part of the outer capsid. VP4 needs to be cleaved into VP5* and VP8* before the virus is infectious. This process will activate the virus, and it helps the virus to penetrate the target cell's interior (14). VP6 forms the bulk of the capsid. It is highly antigenic and constitutes the intermediate shell of the virions (15). VP7 forms as trimers the icosahedral lattice of the rotavirus outer capsid, in addition it also plays an important role in the virus' uncoating process once it enters host cells (16). Although there is a lot of information on the biology of the virus, this has still to be translated into improved therapeutic strategies.

Vaccination and treatment against rotavirus infection

Up to 2019, there were four rotavirus vaccines that had been prequalified by the WHO for global use: Rotarix (GlaxoSmithKline Biologicals SA, Rixensart, Belgium; prequalified in 2009), RotaTeq (Merck & Co., Inc. , West point, PA, USA; prequalified in 2008), Rotavac (Bharat Biotech, Hyderabad, India; prequalified in 2018), and ROTASIIL (Serum Institute of India PVT. LTD., Pune, India; prequalified in 2018) (17). Among these vaccines, Rotarix and RotaTeq were used in 97 countries in the end of 2018, while Rotavac and ROTASIIL were only used in India and the Palestine district. Besides these vaccines, which are used on international scale, two additional rotavirus vaccines have come available for nationwide-restricted use only: Rotavin-M1 (Center of Research and Production of Vaccines and Biologicals, Hanoi, Vietnam) is available in Vietnam only and the Lanzhou Lamb Rotavirus (LLR) vaccine (Lanzhou Institute of Biological Products Co., Ltd., Lanzhou, China), which now serves the private market in China (17). More widespread use of the latter two vaccines is hampered by the unique immunological profiles elicited, In past decade, rotavirus vaccines have made a remarkable impact on the global burden of disease (18). Nevertheless, initial optimism has recently subsided.

Though rotavirus vaccination programs have generated a huge breakthrough in preventing young children to contract rotavirus-related diarrhea, for patients who have already been infected by rotavirus, vaccination is not effective and specific medical treatment

counteracting ongoing rotavirus-mediated disease is still lacking. Indeed, even in developed countries, treatment is largely confined to supportive care and mainly involves rehydration and maintenance of fluid and electrolyte balance (19, 20). Even for many developing countries, the lack of coverage of rotavirus vaccination precludes efficient protection of the population at large. In addition, in severe cases, which include immunocompromised patients subject to rotavirus infection, virus-specific treatment is needed. Therefore, further steps should be taken to reduce the burden of mortality and morbidity and especially more research on the development of novel antiviral therapies is required and might even be considered urgent (21). Furthermore, as rotavirus is especially a scourge for resource-limited regions, cost efficacy should also be taken into account. An obvious solution is to investigate the potential for effective treatment based on the existing approved reagents, especially broad-spectrum antiviral agents come to mind in this respect.

Viral-host interaction

Evolutionary pressure and especially the need for efficient production of novel viral particles as well as the fight with the cell-autonomous innate immune system has shaped viral biology. Many viral mRNAs have acquired a variety of sophisticated strategies to compete with cellular mRNAs that are already present in the cytoplasm. This allows the selective translation of viral mRNAs, since they circumvent the need to possess the required components to initiate the translation of mRNA (22, 23). In this the eukaryotic translation initiation factor 4F (eIF4F) is important to consider. eIF4F is a protein complex containing three constituent proteins: a eukaryotic translation initiation factor 4A (eIF4A), a eukaryotic translation initiation factor 4E (eIF4E), and a eukaryotic translation initiation factor 4G (eIF4G)(24). This complex plays a pivotal role in cap-dependent mRNA protein translation initiated by recruiting mRNA to a ribosome (25). Moreover, it is essential in the regulation of interferon (INF) signaling(26), which closely relates to anti-viral immunity.

Innate immune responses are at the front line of this battle, playing a critical role against rotavirus infection and the critical role of INF signaling in this fight is well-established (27). Cytokine production, a broad term that includes the production of IFNs , are induced following the recognition of rotavirus viral proteins and/or RNA by the infected host cell (28). IFNs constitute a group of related humoral factors that exert potent antiviral activities and are

further subclassified into three groups: type I INFs (IFN-α, IFN-β, IFN-δ and others), type II INFs (IFN-γ) and type III INFs (IFN-λ1, IFN-λ2 and IFN-λ3)(29, 30). They bind to distinct cognate but evolutionary related receptors and all signal through the Janus kinase signal transducer and activator of transcription (JAK-STAT) pathway (30, 31). Following engagement of IFNs with their receptors, STAT1 and STAT2 are activated through phosphorylation and subsequently form complexes of STAT proteins that will translocate to the nucleus and bind to IFN regulatory factor 9 (IRF9) to form the IFN-stimulated gene factor 3 complex (ISGF3). ISGF3 induces transcription of numerous IFN-stimulated genes (ISGs) which cooperatively exert antiviral effect against various kinds of viruses (32). Moreover, recognition of rotavirus and IFN induction are indispensable to promote the development of adaptive B-cell mediated immune response and thus links innate immunity to adaptive immunity (33). The resulting evolutionary pressure on rotavirus has fostered the pathogen in developing its own strategies to evade such host immune responses. For instance, rotavirus can inhibit the production of IFNs in infected cells by blocking the activation of STAT1 and STAT2 proteins (34). Although many details are still unclear, one of the viral nonstructural proteins, NSP1, was reported to mediate this inhibition of IFN signaling in rotavirus infected primary mouse cells (35). Further understanding of the interaction of rotavirus with the host innate immune machinery may well be essential for developing novel rational avenues for managing rotavirus-provoked disease.

Nucleotide biosynthesis and viral infection

Cellular nucleotides, which are classified as either purines or pyrimidines, are the building blocks of RNA and DNA. Cellular demand for nucleotides is met either through the activity of the *de novo* synthesis pathway or through the salvage pathway (36) and also viruses require these pathways to obtain the nucleotides essential for their replication. Therefore, host enzymes or other molecules involved in nucleoside biosynthesis pathways represent potential targets for antiviral strategies.

Pyrimidine biosynthesis is a relatively linear sequential process in which the enzyme dihydroorotate dehydrogenase (DHODH) represents the fourth and, importantly, rate-limiting step. The enzyme is located in the inner membrane of mitochondria where it catalyzes the conversion of dihydroorotate to orotate (37). The thus produced orotate is then a substrate

for uridine monophosphate (UMP) synthase and the UMP resulting from the reaction serves as an essential precursor for synthesis of all other pyrimidine nucleotides. Several studies have reported that the inhibition of DHODH enzyme suppresses a range of different viruses' replication (6, 38-40). Apparently viral replication is more dependent on pyrimidine biosynthesis relative to host demands for these nucleotides.

Gemcitabine is a cytidine analogue, it has been reported to inhibit pyrimidine biosynthesis resulting in depletion of nucleotide pool (43) and might thus be useful for combating viral replication. By inference from the dependency of viral replication on pyrimidine biosynthesis, also purine biosynthesis might be target for anti-viral therapy. A common strategy for interfering with purine biosynthesis is the use of poorly-metabolizable analogues of intermediate products its biosynthetic pathway. 6-thioguanine (6-TG), a thio analogue of the naturally occurring purine base guanine, has been used clinically since 1950s (41). Metabolized 6-TG can bind to Rac1 to form a 6-TGNP•Rac1 complex that inhibits the activation of Rac1, an important regulator of cell physiology (42). The usefulness for interfering with nucleotide biosynthesis for combating rotavirus infection, however, remains largely obscure at best, prompting studies in this respect.

Organoid models for studying rotavirus infection

Lack of insight into the biology of rotavirus was also due to the absence of appropriate cellular model systems that truly recapitulated the infection process *in vivo*. An exciting development in this respect is advent of organoid technology. In 2009, the group of Prof. dr. Hans Clevers from Hubrecht institute (Utrecht, Netherlands) established primary intestinal organoids from intestinal stem cells (ISCs) (44). Subsequently the same research team generated liver organoids as well. Organoid technology is largely possible through exploiting the properties of the Lgr5-positive (Lgr5$^+$) stem cells (45, 46). Compared to conventional 2D cultured immortalized cell lines, organoids model systems are superior in various respects: 1. 2D cultured immortalized cells are cancer cells, which by definition involves genetic alterations and thus never truly mimic the situation in healthy cells *in vivo*; although there are certainly differences between organoids and real body structures, at least the genetic dimension is absent in organoid models. 2. As organoids have the capacity to form different types of stem cell-derived progeny they allow study of the interactions between these different cell types,

at least more so as compared to conventional model systems. 3. Organoids are 3D structures, hence studying spatial effects is greatly facilitated compared to 2D cultures. 4. Establishing immortalized cell lines is cumbersome and does not really allow personalized medicine. Indeed, much of the knowledge on intestinal cell biology generated in the last century depended on the use of a handful of cell lines. Organoids models perform much better in this respect and might allow precision medicine, also potentially with respect to rotavirus-mediated disease. Overall, for rotavirus research the organoid model appears highly promising and I decided in the course of this thesis research to grab the momentum and opportunity involved.

Biliary atresia and rotavirus infection

Effective research into rotavirus-mediated disease requires full understanding of the entire spectrum of clinical manifestations associated with rotavirus infection. In this case biliary atresia (BA) has been overlooked. BA is a neonatal disease of the liver and bile duct and is characterized by a progressive fibro-inflammatory obliteration of both the intrahepatic and extrahepatic bile duct. If untreated, patients have a high risk for developing chronic cholestasis and biliary cirrhosis. Also, in infants BA is one of the leading causes of end-stage liver disease requiring liver transplantation (47, 48). The pathogenesis of BA remains unknown, however the evidence points to multiple pathogenic mechanisms being involved in the development of BA, including gene mutation (49), exposure to environmental toxins (50), dysregulation of the immune system, and most importantly, viral factors (51-56).

Various lines of evidence led me to speculate that rotavirus is one of the viral factors causing biliary atresia. In rodents experimental rotavirus infection provokes aspects of neonate biliary atresia. Remarkable findings in respect are that both blood-borne viral antigens (antigenemia) and infectious virus (viremia) have been detected in this mouse model while other data indicates as well that rotavirus infection is not limited to the intestinal mucosa but may escape into the circulation, thus potentially reaching bile duct structures (57-61). If rotavirus indeed causes biliary atresia in children, this will constitute an important extra-intestinal clinical manifestation of rotavirus-mediated pathology and would have important consequences with respect to our thinking on how rotavirus infection should be managed and prevented.

Aim of this thesis

Following the introduction of rotavirus vaccines on a global scale the burden provoked by this virus to mankind has been decreasing. Nevertheless, especially in developing countries, the rotavirus-associated misery is still depressingly common, in particular with respect to infants. In addition, persistent rotavirus infection commonly occurs in immunocompromised patients, irrespective whether this concerns pediatric or adult patients and whether they hail from developing or developed countries. Finally, the full amount of clinical manifestations caused by rotavirus infections may be underestimated, for instance rotavirus may be one of the causative agents of biliary atresia in neonates. Overall, there is clear need for obtaining better insight into the role of rotavirus in pathophysiology and to define novel ways of dealing with rotavirus-induced disease, especially for patients in which disease has already manifested itself and thus vaccination is no longer an option. Excitingly, the advent of the 3D organoid model also opens new possibilities to perform research into rotavirus, previously impossible. In conjunction, I considered the case for investigating rotavirus biology imperative.

Outline of this thesis

Although it is well-recognized that rotavirus infection causes thousands of deaths among children under 5 years old, the full spectrum of rotavirus-mediated disease may still be underestimated. There is substantial evidence indicating the possible involvement of rotavirus in BA development, at least in a subset of patients, but *in lieu* of concrete proof this issue remains largely ignored both by medical professionals as well as by policy decision makers. Therefore, **in Chapter 2**, exploiting the novel possibilities offered by the recently developed organoid technology, I investigated the role of rotavirus in BA development and I demonstrated that human biliary organoids are susceptible to rotavirus infection, and this leads to active virus-host interactions and causes severe cytopathogenesis. Furthermore, I demonstrated that antiviral drugs and neutralizing antibodies can counteract the infection and BA-like morphological changes, suggesting their potential for mitigating BA in patients.

Thus, encouraged to further identify novel avenues for treating rotavirus infection, I investigated the viral mRNA translation process. **In Chapter 3**, I investigated the function of eukaryotic translation initiation factor 4F (eIF4F) complex in rotavirus replication. I dissect the effects of loss-of-function of the three components of eIF4F, including eIF4A, eIF4E and eIF4G, and establish the resulting consequences on the levels of rotavirus genomic RNA and viral

protein VP4. Consistent with the observations made, I observe that knockdown of the negative regulator of eIF4F and programmed cell death protein 4 (PDCD4) inhibits the expression of viral mRNA and the VP4 protein. More importantly, I established that eIF4F complex can regulate the IFN signaling pathway in the context of rotavirus infection. **In Chapter 4** I further extend these observations. Host immune responses determine the outcome of viral infections, and IFNs are produced as the first and the main anti-viral cytokines to combat the virus infection. In this chapter I show that rotavirus predominantly induces type III IFNs (IFN-λ1), and to a lesser degree type I IFNs (IFN-α and IFN-β) in human intestinal cells on the RNA level. However, I was not able to detect IFN protein and thus this interferon response is not sufficient to effectively inhibit rotavirus replication. In contrast, however, I establish a significant role of constitutive IFN signaling for limiting rotavirus replication, as for instance evident from experiments involving the silencing of STAT1, STAT2 and IRF9 genes. In addition, exogenous IFN treatment impaired rotavirus replication irrespective of IFN type used. Again making this observation was also facilitated by the use of organoid technology. IFNs significantly upregulated a panel of well-known anti-viral ISGs and inhibition of the JAK-STAT cascade abrogated ISG induction and the anti-rotavirus effects of IFNs. Thus overall, I was able to substantially advance our understanding of the interaction between rotavirus infection and intestinal epithelial innate immunity.

Viral replication heavily relies on the host to supply nucleosides. So, limiting nucleoside availability might inhibit rotavirus replication. I**n Chapter 5**, I demonstrate that two specific DHODH enzyme inhibitors, brequinar (BQR) and leflunomide (LFM) robustly inhibit rotavirus replication in the conventional human intestinal Caco2 cell line model as well as in human primary intestinal organoids. These antiviral effects are evident both when using the laboratory strain SA11 as well as when using the rotavirus strain 2011K which was isolated from clinical sample in my host institution. Mechanistic studies indicated that BQR and LFM exerted their anti-rotavirus effect through targeting DHODH and by depleting the pyrimidine nucleotide pool. Therefore, targeting pyrimidine biosynthesis represents a potential approach for developing antiviral strategies against rotavirus. **In Chapter 6**, I aimed at testing on the other side of the nucleoside coin, *in casu* purine biosynthesis, by testing another immunosuppressive drug 6-TG, a purine biosynthesis inhibitor. I observed, however, that 6-TG although significantly inhibits rotavirus replication, gene knockdown or knockout of Rac1,

an alternative cellular target of 6-TG, also significantly inhibited rotavirus replication, indicating a previously not-suspected accessory role for Rac1 in rotavirus infection. I further demonstrated that 6-Thioguanine (6-TG) can effectively inhibit the active form of Rac1 (GTP-Rac1) and essentially mediates the anti-rotavirus effect of 6-TG. Consistently, ectopic over-expression of GTP-Rac1 facilitates but an inactive Rac1 (N17) or a specific Rac1 inhibitor (NSC23766) inhibits rotavirus replication. In conclusion, I identified 6-TG as an effective inhibitor of rotavirus replication but that unexpectedly acts through inhibition of Rac1 activation. **In Chapter 7**, I screened a library of safe-in-man broad-spectrum antivirals and identified gemcitabine, a widely used anticancer drug, as a potent inhibitor of rotavirus infection. I confirmed this effect in 2D cell cultures and 3D cultured human intestinal organoids with both laboratory-adapted rotavirus strains and five clinical isolates. Supplementation of UTP or uridine largely abolished the anti-rotavirus activity of gemcitabine, suggesting its function through inhibition of pyrimidine biosynthesis pathway.

Overall, I feel I have been able to significantly advance our understanding of rotavirus disease and it potential management and I hope these studies will allow better treatment of disease.

References

1. Bishop RJJog, hepatology. 2009. Discovery of rotavirus: Implications for child health. 24:S81-S85.
2. Flewett T, Bryden A, Davies H, Woode G, Bridger J, Derrick JJTL. 1974. Relation between viruses from acute gastroenteritis of children and newborn calves. 304:61-63.
3. Troeger C, Forouzanfar M, Rao PC, Khalil I, Brown A, Reiner Jr RC, Fullman N, Thompson RL, Abajobir A, Ahmed MJTLID. 2017. Estimates of global, regional, and national morbidity, mortality, and aetiologies of diarrhoeal diseases: a systematic analysis for the Global Burden of Disease Study 2015. 17:909-948.
4. Kotloff KL, Nataro JP, Blackwelder WC, Nasrin D, Farag TH, Panchalingam S, Wu Y, Sow SO, Sur D, Breiman RFJTL. 2013. Burden and aetiology of diarrhoeal disease in infants and young children in developing countries (the Global Enteric Multicenter Study, GEMS): a prospective, case-control study. 382:209-222.
5. Troeger C, Khalil IA, Rao PC, Cao S, Blacker BF, Ahmed T, Armah G, Bines JE, Brewer TG, Colombara DVJJp. 2018. Rotavirus vaccination and the global burden of rotavirus diarrhea among children younger than 5 years. 172:958-965.
6. Wang Y, Wang W, Xu L, Zhou X, Shokrollahi E, Felczak K, Van Der Laan LJ, Pankiewicz KW, Sprengers D, Raat NJJAa, chemotherapy. 2016. Cross talk between nucleotide synthesis pathways with cellular immunity in constraining hepatitis E virus replication. 60:2834-2848.
7. Wang H, Naghavi M, Allen C, Barber RM, Bhutta ZA, Carter A, Casey DC, Charlson FJ, Chen AZ, Coates MMJTl. 2016. Global, regional, and national life expectancy, all-cause mortality, and cause-specific mortality for 249 causes of death, 1980–2015: a systematic analysis for the Global Burden of Disease Study 2015. 388:1459-1544.
8. Tate JE, Burton AH, Boschi-Pinto C, Parashar UJCID. 2016. World Health Organization Coordinated Global Rotavirus Surveillance Network. Global, regional, and national estimates of rotavirus mortality in children< 5 years of age, 2000–2013. 62:S96-S105.
9. Yin Y, Metselaar HJ, Sprengers D, Peppelenbosch MP, Pan QJAJoT. 2015. Rotavirus in organ transplantation: drug‐virus‐host interactions. 15:585-593.
10. Estes MK, Cohen JJM, Reviews MB. 1989. Rotavirus gene structure and function. 53:410-449.
11. Lu X, McDonald SM, Tortorici MA, Tao YJ, Vasquez-Del Carpio R, Nibert ML, Patton JT, Harrison SCJS. 2008. Mechanism for coordinated RNA packaging and genome replication by rotavirus polymerase VP1. 16:1678-1688.
12. Zeng CQ-Y, Labbé M, Cohen J, Prasad BV, Chen D, Ramig RF, Estes MKJV. 1994. Characterization of rotavirus VP2 particles. 201:55-65.
13. Vásquez M, Sandino AM, Pizarro JM, Fernández J, Valenzuela S, Spencer EJJogv. 1993. Function of rotavirus VP3 polypeptide in viral morphogenesis. 74:937-941.
14. Ludert JE, Krishnaney AA, Burns JW, Vo PT, Greenberg HBJJogv. 1996. Cleavage of rotavirus VP4 in vivo. 77:391-395.
15. Beards G, Campbell A, Cottrell N, Peiris J, Rees N, Sanders R, Shirley J, Wood H, Flewett TJJocm. 1984. Enzyme-linked immunosorbent assays based on polyclonal and monoclonal antibodies for rotavirus detection. 19:248-254.
16. Dormitzer PR, Greenberg HB, Harrison SCJV. 2000. Purified recombinant rotavirus VP7 forms soluble, calcium-dependent trimers. 277:420-428.
17. Burke RM, Tate JE, Kirkwood CD, Steele AD, Parashar UDJCoiid. 2019. Current and new rotavirus vaccines. 32:435.
18. Burnett E, Parashar UD, Tate JEJTJoID. 2020. Global impact of rotavirus vaccination on diarrhea hospitalizations and deaths among children< 5 years old: 2006–2019.
19. Yin Y, Bijvelds M, Dang W, Xu L, van der Eijk AA, Knipping K, Tuysuz N, Dekkers JF, Wang Y, de Jonge JJAr. 2015. Modeling rotavirus infection and antiviral therapy using primary intestinal organoids. 123:120-131.

20. Rossignol J-F, Abu-Zekry M, Hussein A, Santoro MGJTL. 2006. Effect of nitazoxanide for treatment of severe rotavirus diarrhoea: randomised double-blind placebo-controlled trial. 368:124-129.

21. Chen S, Ding S, Yin Y, Xu L, Li P, Peppelenbosch MP, Pan Q, Wang WJAr. 2019. Suppression of pyrimidine biosynthesis by targeting DHODH enzyme robustly inhibits rotavirus replication. 167:35-44.

22. Chaudhry Y, Nayak A, Bordeleau M-E, Tanaka J, Pelletier J, Belsham GJ, Roberts LO, Goodfellow IGJJoBC. 2006. Caliciviruses differ in their functional requirements for eIF4F components. 281:25315-25325.

23. Burgui I, Yánguez E, Sonenberg N, Nieto AJJov. 2007. Influenza virus mRNA translation revisited: is the eIF4E cap-binding factor required for viral mRNA translation? 81:12427-12438.

24. Montero H, García-Román R, Mora SIJV. 2015. eIF4E as a control target for viruses. 7:739-750.

25. Gingras A-C, Raught B, Sonenberg NJArob. 1999. eIF4 initiation factors: effectors of mRNA recruitment to ribosomes and regulators of translation. 68:913-963.

26. Colina R, Costa-Mattioli M, Dowling RJ, Jaramillo M, Tai L-H, Breitbach CJ, Martineau Y, Larsson O, Rong L, Svitkin YVJN. 2008. Translational control of the innate immune response through IRF-7. 452:323-328.

27. Holloway G, Coulson BSJJoGV. 2013. Innate cellular responses to rotavirus infection. 94:1151-1160.

28. Deal EM, Jaimes MC, Crawford SE, Estes MK, Greenberg HBJPP. 2010. Rotavirus structural proteins and dsRNA are required for the human primary plasmacytoid dendritic cell IFNα response. 6:e1000931.

29. Randall RE, Goodbourn SJJogv. 2008. Interferons and viruses: an interplay between induction, signalling, antiviral responses and virus countermeasures. 89:1-47.

30. Donnelly RP, Kotenko SVJJoI, Research C. 2010. Interferon-lambda: a new addition to an old family. 30:555-564.

31. Platanias LCJNRI. 2005. Mechanisms of type-I-and type-II-interferon-mediated signalling. 5:375-386.

32. Schneider WM, Chevillotte MD, Rice CMJAroi. 2014. Interferon-stimulated genes: a complex web of host defenses. 32:513-545.

33. Deal EM, Lahl K, Narváez CF, Butcher EC, Greenberg HBJTJoci. 2013. Plasmacytoid dendritic cells promote rotavirus-induced human and murine B cell responses. 123:2464-2474.

34. Arnold MM, Sen A, Greenberg HB, Patton JTJPP. 2013. The battle between rotavirus and its host for control of the interferon signaling pathway. 9:e1003064.

35. Feng N, Sen A, Nguyen H, Vo P, Hoshino Y, Deal E, Greenberg HJJov. 2009. Variation in antagonism of the interferon response to rotavirus NSP1 results in differential infectivity in mouse embryonic fibroblasts. 83:6987-6994.

36. Evans DR, Guy HIJJoBC. 2004. Mammalian pyrimidine biosynthesis: fresh insights into an ancient pathway. 279:33035-33038.

37. Munier-Lehmann Hln, Vidalain P-O, Tangy Fdr, Janin YLJJomc. 2013. On dihydroorotate dehydrogenases and their inhibitors and uses. 56:3148-3167.

38. Hoffmann H-H, Kunz A, Simon VA, Palese P, Shaw MLJPotNAoS. 2011. Broad-spectrum antiviral that interferes with de novo pyrimidine biosynthesis. 108:5777-5782.

39. Luthra P, Naidoo J, Pietzsch CA, De S, Khadka S, Anantpadma M, Williams CG, Edwards MR, Davey RA, Bukreyev AJAr. 2018. Inhibiting pyrimidine biosynthesis impairs Ebola virus replication through depletion of nucleoside pools and activation of innate immune responses. 158:288-302.

40. Tan YH, Driscoll JS, Mui SM. 2005. Dihydroorotate dehydrogenase inhibitors for the treatment of viral-mediated diseases. Google Patents.

41. Munshi PN, Lubin M, Bertino JRJTo. 2014. 6-thioguanine: a drug with unrealized potential for cancer therapy. 19:760.

42. Shin J-Y, Wey M, Umutesi HG, Sun X, Simecka J, Heo JJJoBC. 2016. Thiopurine prodrugs mediate immunosuppressive effects by interfering with Rac1 protein function. 291:13699-13714.

43. Lee K, Kim D-E, Jang K-S, Kim S-J, Cho S, Kim CJO. 2017. Gemcitabine, a broad-spectrum antiviral drug, suppresses enterovirus infections through innate immunity induced by the inhibition of pyrimidine biosynthesis and nucleotide depletion. 8:115315.

44. Sato T, Vries RG, Snippert HJ, Van De Wetering M, Barker N, Stange DE, Van Es JH, Abo A, Kujala P, Peters PJJN. 2009. Single Lgr5 stem cells build crypt-villus structures in vitro without a mesenchymal niche. 459:262-265.

45. Huch M, Gehart H, Van Boxtel R, Hamer K, Blokzijl F, Verstegen MM, Ellis E, Van Wenum M, Fuchs SA, de Ligt JJC. 2015. Long-term culture of genome-stable bipotent stem cells from adult human liver. 160:299-312.

46. Huch M, Dorrell C, Boj SF, Van Es JH, Li VS, Van De Wetering M, Sato T, Hamer K, Sasaki N, Finegold MJJN. 2013. In vitro expansion of single Lgr5+ liver stem cells induced by Wnt-driven regeneration. 494:247-250.

47. Balistreri WF, Grand R, Hoofnagle JH, Suchy FJ, Ryckman FC, Perlmutter DH, Sokol RJJH. 1996. Biliary atresia: current concepts and research directions. Summary of a symposium. 23:1682-1692.

48. Hartley JL, Davenport M, Kelly DAJTL. 2009. Biliary atresia. 374:1704-1713.

49. Cheng G, Tang CS-M, Wong EH-M, Cheng WW-C, So M-T, Miao X, Zhang R, Cui L, Liu X, Ngan ES-WJJoh. 2013. Common genetic variants regulating ADD3 gene expression alter biliary atresia risk. 59:1285-1291.

50. Walesky C, Goessling WJH. 2016. Nature and nurture: Environmental toxins and biliary atresia. 64:717-719.

51. Mahjoub F, Shahsiah R, Ardalan FA, Iravanloo G, Sani MN, Zarei A, Monajemzadeh M, Farahmand F, Mamishi SJDp. 2008. Detection of Epstein Barr Virus by Chromogenic In Situ Hybridization in cases of extra-hepatic biliary atresia. 3:1-4.

52. Riepenhoff-Talty M, Gouvea V, Evans M, Svensson L, Hoffenberg E, Sokol R, Uhnoo I, Greenberg S, Schäkel K, Zhaori GJJoID. 1996. Detection of group C rotavirus in infants with extrahepatic biliary atresia. 174:8-15.

53. Morecki R, Glaser JH, Cho S, Balistreri WF, Horwitz MSJNEJoM. 1982. Biliary atresia and reovirus type 3 infection. 307:481-484.

54. Fischler B, Ehrnst A, Forsgren M, Örvell C, Nemeth AJJopg, nutrition. 1998. The viral association of neonatal cholestasis in Sweden: a possible link between cytomegalovirus infection and extrahepatic biliary atresia. 27:57-64.

55. Fischler B, Woxenius S, Nemeth A, Papadogiannakis NJJops. 2005. Immunoglobulin deposits in liver tissue from infants with biliary atresia and the correlation to cytomegalovirus infection. 40:541-546.

56. Greenberg HB, Estes MKJG. 2009. Rotaviruses: from pathogenesis to vaccination. 136:1939-1951.

57. Blutt SE, Kirkwood CD, Parreño V, Warfield KL, Ciarlet M, Estes MK, Bok K, Bishop RF, Conner MEJTl. 2003. Rotavirus antigenaemia and viraemia: a common event? 362:1445-1449.

58. Blutt SE, Conner MEJCoig. 2007. Rotavirus: to the gut and beyond! 23:39-43.

59. Blutt SE, Matson DO, Crawford SE, Staat MA, Azimi P, Bennett BL, Piedra PA, Conner MEJPM. 2007. Rotavirus antigenemia in children is associated with viremia. 4:e121.

60. Patel M, Rench MA, Boom JA, Tate JE, Sahni LC, Hull JA, Gentsch JR, Parashar UD, Baker CJJTPidj. 2010. Detection of rotavirus antigenemia in routinely obtained serum specimens to augment surveillance and vaccine effectiveness evaluations. 29:836-839.

61. Ramani S, Paul A, Saravanabavan A, Menon VK, Arumugam R, Sowmyanarayanan TV, Samuel P, Gagandeep KJCid. 2010. Rotavirus antigenemia in Indian children with rotavirus gastroenteritis and asymptomatic infections. 51:1284-1289.

Chapter 2

Rotavirus infection and cytopathogenesis in human biliary organoids potentially recapitulate biliary atresia development

Sunrui Chen, Pengfei Li, Yining Wang, Yuebang Yin, Petra E. de Ruiter, Monique M. A. Verstegen, Maikel P. Peppelenbosch, Luc J. W. van der Laan, Qiuwei Pan

Abstract

Biliary atresia (BA) is a neonatal liver disease characterized by progressive fibro-inflammatory obliteration of both intrahepatic and extrahepatic bile duct. The etiologies of BA remain largely unknown, but rotavirus infection has been implicated at least for a subset of patients and this causal relation has been well-demonstrated in mouse models. In this study, we aim to further consolidate this evidence in human biliary organoids. We obtained seven batches of human biliary organoids cultured from fetal liver, adult liver and bile duct tissues. We found that these organoids are highly susceptible and support the full life cycle of rotavirus infection in 3D culture. The robust infection triggers active virus-host interactions, including interferon-based host defense mechanisms and injury response. We have observed direct cytopathogenesis in organoids upon rotavirus infection, which may partially recapitulate the development of BA. Importantly, we have demonstrated the efficacy of mycophenolic acid and interferon-alpha but not ribavirin in inhibiting rotavirus in biliary organoids. Furthermore, a neutralizing antibody targeting rotavirus VP7 protein effectively inhibits the infection in organoids. Thus, we have substantiated the causal evidence of rotavirus inducing BA in humans and provided potential strategies to combat the disease.

Importance

There are substantial evidence indicating the possible involvement of rotavirus in biliary atresia (BA) development at least in a subset of patients, but concrete proof remains lacking. In mouse model, it has been well-demonstrated that rotavirus can infect the biliary epithelium to cause biliary inflammation and obstruction, representing the pathogenesis of BA in humans. By using the recently developed organoids technology, we now have demonstrated that human biliary organoids are susceptible to rotavirus infection, and this provokes active virus-host interactions and causes severe cytopathogenesis. Thus, our model recapitulates some essential aspects of BA development. Furthermore, we have demonstrated that antiviral drugs and neutralizing antibodies are capable of counteracting the infection and BA-like morphological changes, suggesting their potential for mitigating BA in patients.

Keywords

Biliary atresia, Rotavirus infection, Human organoids

Observation

Biliary atresia (BA) is characterized by progressive fibro-inflammatory obliteration of the bile ducts, resulting in chronic cholestasis and biliary cirrhosis. It is one of the leading causes for liver transplantation in infants (1, 2). Exposure to rotavirus in mice has demonstrated the infection in biliary epithelium, resulting in BA-like biliary inflammation and obstruction (3). Nevertheless, whether rotavirus is a causal agent for BA in patients remains controversial, also because of a paucity of preclinical models. Organoid technology provides an excellent way forward here. These 3D cultured organoids are superior in recapitulating the architecture, composition, diversity, organization and functionality of cell types of the tissue/organ of origin. Human organoids have been increasingly explored to advance the research in disease modeling (4, 5). Although it is feasible to culture hepatocyte-like organoids from liver tissue, it remains technically challenging with stringent requirement of experimental protocols (6). In contrast, organoids resembling cholangiocyte-phenotype are relatively easy to be cultured from the hepatic and extrahepatic bile duct compartments (7-9). In this study, we explored the feasibility of employing human biliary organoids cultured from fetal liver, adult liver and bile duct for recapitulating BA development.

The canonical compartment for rotavirus infection is the small intestinal enterocyte. We have previously shown that human intestinal organoids (HIOs) sustain rotavirus infection (4) and we now again confirmed these results (see Fig. S1A-C in the supplemental material). BA is a disorder that typically first manifests itself during mid-gestation and murine experimentation has demonstrated rotavirus-induced BA development. Hence, we first tested if biliary fetal liver organoids (FLOs) support rotavirus infection. Inoculation of FLOs with rotavirus resulted in an increase of cellular viral RNA by a factor of 10^3-10^5 at 24 hours and 10^4-10^6 fold at 48 hours post-inoculation (Fig. 1A) with a concomitant increase in levels of rotavirus VP4 protein (Fig. 1B). Thus the human fetal biliary epithelium is highly permissive for rotavirus infection, comparable to the level in intestinal epithelium (Fig. S1A). In apparent agreement, supernatant harvested from infected FLOs effectively infected and replicated in Caco2 intestinal epithelial model as shown by qRT-PCR quantification of viral RNA (Fig 1C). Next, we performed TCID$_{50}$ assay to compare the level of infectious viral particles between the baseline

of inoculation and five batches of organoids at 48 hours post-inoculation. We harvested rotavirus from the organoids through repeated freezing and thawing and demonstrated 10^2-10^3 times increase of infectious virus titers (Fig. 1D). This was further confirmed by cytopathic effects in Caco2 cells at 48 hours post-inoculation with rotavirus harvested from these five batches of organoids and the control (see Fig. S2 in the supplemental material). Collectively, these results convincingly showed effective replication and production of infectious viral particles by infected fetal biliary organoids. Similar results were obtained in biliary organoids derived from adult human liver and bile duct (Fig. 1A-C). Thus, the human biliary epithelium is highly susceptible to rotavirus infection and supports its full life cycle.

To better understand the consequences of rotavirus infection in biliary epithelium, we performed a genome-wide transcriptomic analysis of FLOs upon infection. Volcano plots of the results showed significant down-regulation of 103 and up-regulation of 512 genes in response to rotavirus, compared to uninfected organoids (Fig. 1E). Most of the highly up-regulated genes, including IFIT2, IFITM3, OASL, DDX58, MX2, IFI35, HERC5 and BST2, are interferon-stimulated genes (ISGs). Other genes, such as CXCL11 and NLRC5 are related to inflammatory response. Gene ontology (GO) enrichment analysis of these differentially expressed genes confirmed the essential involvement of "immune system process" (Fig. 1F). Interestingly, "response to stress", "cell death" and "extracellular space" were also identified as the top regulated processes, with obvious relations to the development and pathogenesis of BA (Fig. 1E).
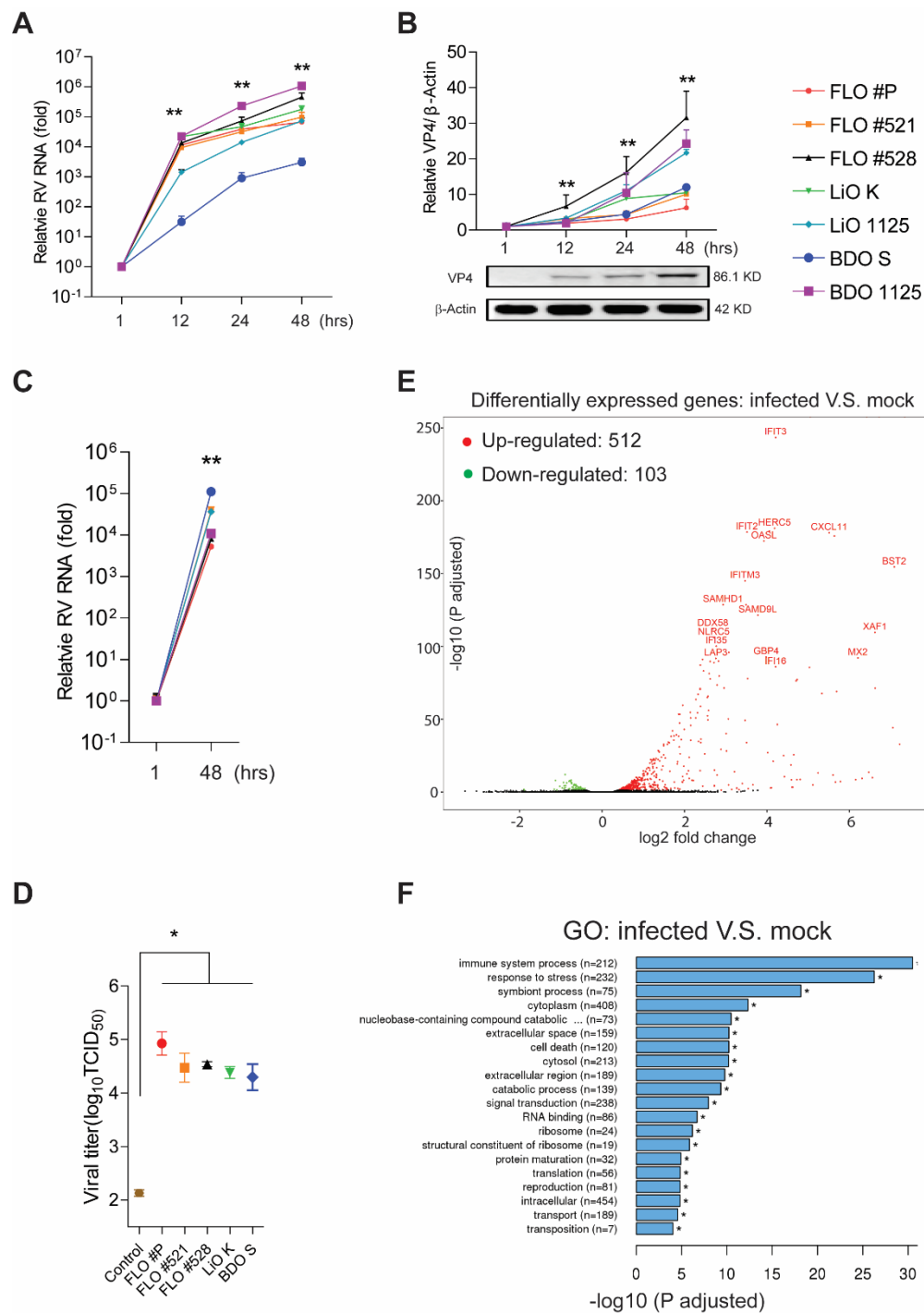
Figure 1. Characterizing rotavirus infection in human biliary organoids. (A) The dynamics of cellular viral RNA levels upon inoculation of SA11 rotavirus at different time points of post-inoculation. The level at post-inoculation 1 hour (hr) was set as 1. Three batches of human fetal liver organoids (FLOs), two adult liver (LiOs) and two bile duct organoids (BDOs) were tested. (B) Expression of rotavirus VP4 protein in the organoids determined by Western blotting. (C) Inoculation of human intestinal Caco2 cell line with supernatant from rotavirus infected organoids for 48 hrs. Relative cellular viral RNA levels were quantified. (D) TCID$_{50}$ of five batches of rotavirus infected organoids at 48 hrs post-inoculation compared with the basal level at incubation. Organoids after inoculation were thoroughly washed to remove free viruses and

subjected to repeated freezing and thawing to harvest the attached and entered rotaviruses. The total amount of rotaviruses in organoids incubated for 48 hrs were harvested by repeated freezing and thawing of entire well. (E) Volcano plots of differentially expressed genes in rotavirus infected (for 48 hrs) compared to un-infected fetal liver organoids. (F) Gene ontology (GO) enrichment analysis of differentially expressed genes. All the data represent as means ± SEM. For each organoids batch, experiments were repeated 3-6 times. Mann-Whitney test; $*P < 0.05$, $**P < 0.01$.

This is in line with the observations that naïve organoids grow and become hyaline in a spheroidal shape, whereas rotavirus-infected organoids are opaque, shriveled and disorganized (Fig. 2A; upper panel). Propidium iodide (PI) staining marked the wide-spread of dead cells in infected organoids (Fig. 2A; middle panel). Confocal analysis after immunostaining of viral VP6 protein further visualized the disruption of infected organoid cells (Fig. 2A; lower panel). Quantitative analysis demonstrated significant increase of the percentage of deteriorated biliary organoids at 12-, 24- and 48-hours post-infection of rotavirus (Fig. 2B). Thus, rotavirus infection causes severe cytopathogenesis in human biliary organoids.

Next, we evaluated a monoclonal neutralizing antibody targeting rotavirus VP7 protein (10) using three representative batches of biliary organoids. It effectively inhibited rotavirus infection in a dose-dependent manner (Fig. 2C). Finally, the effects of the known broad antiviral drugs were tested in all bathes of organoids. Similar as in HIOs (see Fig. S1D in the supplemental material), mycophenolic acid (MPA) and interferon-alpha (IFN-α) potently inhibited rotavirus in all batches of biliary organoids (Fig. 2D). Surprisingly, ribavirin is effective in intestinal (Fig. S1D) but not in biliary organoids (Fig. 2D). Therefore, antiviral drugs and neutralizing antibodies are potential therapeutics to combat rotavirus infection in the human biliary epithelium compartment.
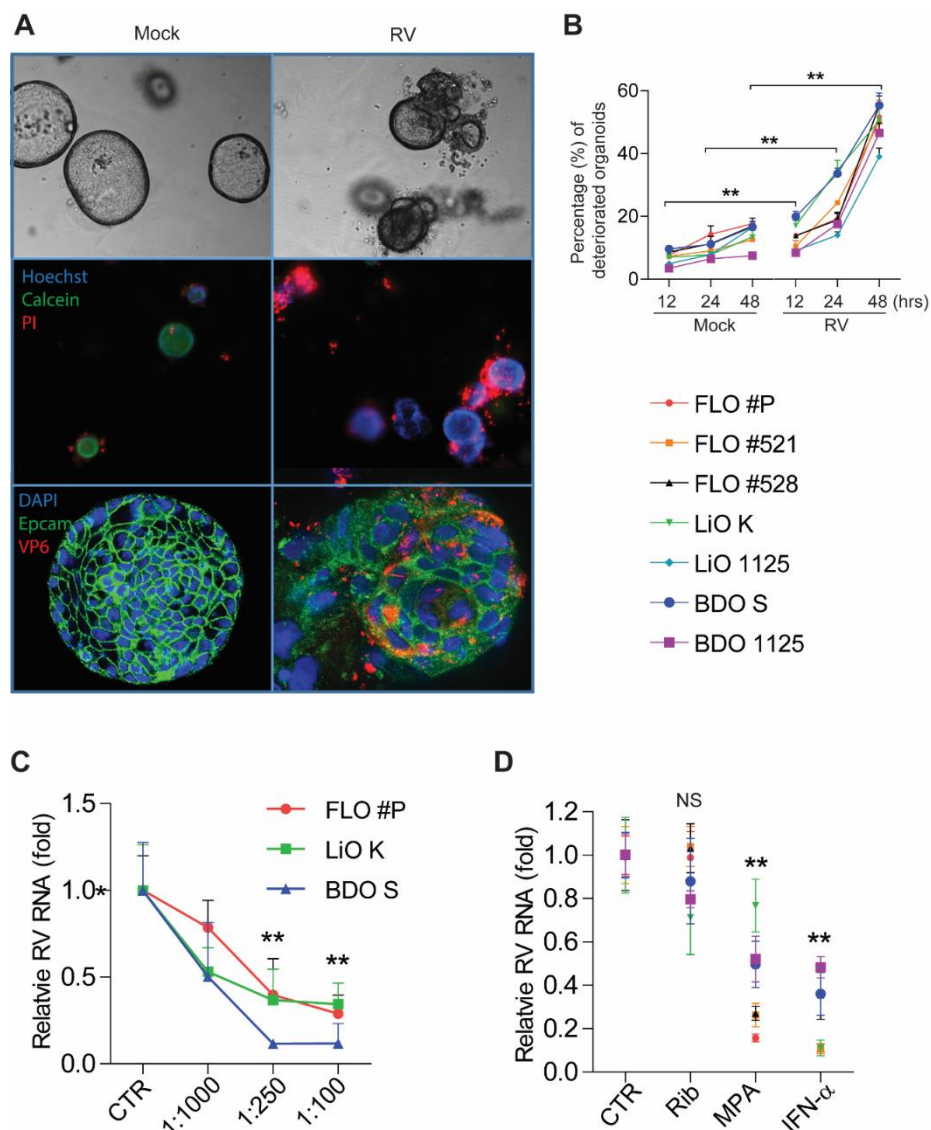
Figure 2. Cytopathogenesis of rotavirus infected human biliary organoids, and efficacy of antiviral treatment/neutralizing antibody. (A) Organoids from 50 µm -150 µm diameter were selected to capture images. Optical microscopy images of infected and un-infected organoids (upper). Fluorescence staining of dead cells (PI; red), live cells (Calcein; green) and nuclei (Hoechst; blue) (middle). Confocal immunostaining of rotavirus structural protein VP6 (red), Epcam (green) and nuclei (blue) (lower). These are representative images of one FLO batch from the tested seven biliary organoids batches. (B) Quantitative analysis of the percentage of deteriorated organoids with or without rotavirus infection at indicated time points and calculated based on the live/dead cell staining (A, middle). (C) The inhibitory activities of neutralizing monoclonal antibody HS-1 against rotavirus infection in three representative batches of biliary organoids. (D) The effects of the broad-spectrum antiviral drugs on rotavirus in biliary organoids. Ribavirin: Rib; mycophenolic acid: MPA; interferon alpha: IFN-α. All the data represent as means ± SEM. For each organoids batch, experiments were repeated 3-6 times. Mann-Whitney test; *P < 0.05, **P < 0.01.

Discussion and conclusions

Although the etiologies and pathogenesis of BA remain largely unknown, multiple pathogenic mechanisms are likely involved, including genetic mutations (11), exposure of environmental toxins (12), dysregulation of immune system, and most intriguingly, viral factors in particular rotavirus (3, 13-18). Previous studies have attempted to detect rotavirus in liver or biliary tissues and the antibody in serum of BA patients, but results are inconclusive (19). Since the wide implementation of vaccines that have substantially counteracted rotavirus-mediated diarrheal disease, more direct investigation on causality of rotavirus infection for BA has become possible. A survey of the national registry system in Taiwan found decreased incidence of BA from 2004 to 2009 mirroring the increased uptake of rotavirus vaccination (20). A nationwide population-based study in Korea has shown that rotavirus infection in neonates is a risk factor for BA, although vaccination did not impact disease incidence (21).

Unfortunately, detection of rotavirus in tissue is often not feasible, as advanced disease is usually diagnosed in children of 4-6 weeks old and the virus likely has been cleared by that time. Here we show, however, using organoid technology that the human biliary epithelium supports the full life cycle of rotavirus infection and results in cellular and morphological changes consistent with BA development, even in the absence of immune cell components in our model. Furthermore, we identify therapeutic strategies potentially useful for combating rotavirus infection in the biliary epithelium.

Interestingly, a study in mice has demonstrated that maternal vaccination can prevent rotavirus-induced BA in newborn pups (22). This is in line with our findings that neutralizing antibodies inhibit rotavirus infection in organoids. Thus, we have substantiated the causal evidence of rotavirus inducing BA in humans and provided potential strategies to combat the disease.

Materials and methods

Human fetal liver organoids (FLOs, *n*=3 batches) were initiated from 17-week-old human fetal livers collected at abortion, from adult liver (LiOs, *n*=2 batches), and from adult bile duct

(BDOs, *n*=2 batches). Human intestinal organoids (HIOs, *n*=1 batch) were cultured to serve as standard model for rotavirus infection. Detailed methods are described in the Text S1 of supplemental materials and methods.

Data availability. Details about data availability can be found in Text S1 in the supplemental material.

References

1. **Balistreri WF, Grand R, Hoofnagle JH, Suchy FJ, Ryckman FC, Perlmutter DH, Sokol RJ.** 1996. Biliary atresia: current concepts and research directions. Summary of a symposium. Hepatology **23:**1682-1692.
2. **Hartley JL, Davenport M, Kelly DA.** 2009. Biliary atresia. The Lancet **374:**1704-1713.
3. **Riepenhoff-Talty M, Gouvea V, Evans MJ, Svensson L, Hoffenberg E, Sokol RJ, Uhnoo I, Greenberg SJ, Schäkel K, Zhaori G.** 1996. Detection of group C rotavirus in infants with extrahepatic biliary atresia. Journal of Infectious Diseases **174:**8-15.
4. **Yin Y, Bijvelds M, Dang W, Xu L, van der Eijk AA, Knipping K, Tuysuz N, Dekkers JF, Wang Y, de Jonge J.** 2015. Modeling rotavirus infection and antiviral therapy using primary intestinal organoids. Antiviral research **123:**120-131.
5. **Clevers H.** 2016. Modeling development and disease with organoids. Cell **165:**1586-1597.
6. **Hu H, Gehart H, Artegiani B, LÖpez-Iglesias C, Dekkers F, Basak O, van Es J, de Sousa Lopes SMC, Begthel H, Korving J.** 2018. Long-term expansion of functional mouse and human hepatocytes as 3D organoids. Cell **175:**1591-1606. e1519.
7. **Broutier L, Andersson-Rolf A, Hindley CJ, Boj SF, Clevers H, Koo B-K, Huch M.** 2016. Culture and establishment of self-renewing human and mouse adult liver and pancreas 3D organoids and their genetic manipulation. Nature protocols **11:**1724.
8. **Shiota J, Zaki NHM, Merchant JL, Samuelson LC, Razumilava N.** 2019. Generation of Organoids from Mouse Extrahepatic Bile Ducts. JoVE (Journal of Visualized Experiments)**:**e59544.
9. **Cao W, Chen K, Bolkestein M, Yin Y, Verstegen MMA, Bijvelds MJC, Wang W, Tuysuz N, ten Berge D, Sprengers D.** 2017. Dynamics of proliferative and quiescent stem cells in liver homeostasis and injury. Gastroenterology **153:**1133-1147.
10. **Ruggeri FM, Greenberg HB.** 1991. Antibodies to the trypsin cleavage peptide VP8 neutralize rotavirus by inhibiting binding of virions to target cells in culture. Journal of virology **65:**2211-2219.
11. **Cheng G, Tang CS-M, Wong EH-M, Cheng WW-C, So M-T, Miao X, Zhang R, Cui L, Liu X, Ngan ES-W.** 2013. Common genetic variants regulating ADD3 gene expression alter biliary atresia risk. Journal of hepatology **59:**1285-1291.
12. **Walesky C, Goessling W.** 2016. Nature and nurture: Environmental toxins and biliary atresia. Hepatology **64:**717-719.
13. **Mahjoub F, Shahsiah R, Ardalan FA, Iravanloo G, Sani MN, Zarei A, Monajemzadeh M, Farahmand F, Mamishi S.** 2008. Detection of Epstein Barr Virus by Chromogenic In Situ Hybridization in cases of extra-hepatic biliary atresia. Diagnostic pathology **3:**19.
14. **Morecki R, Glaser JH, Cho S, Balistreri WF, Horwitz MS.** 1982. Biliary atresia and reovirus type 3 infection. New England Journal of Medicine **307:**481-484.
15. **Tyler KL, Sokol RJ, Oberhaus SM, Le M, Karrer FM, Narkewicz MR, Tyson RW, Murphy JR, Low R, Brown WR.** 1998. Detection of reovirus RNA in hepatobiliary tissues from patients with extrahepatic biliary atresia and choledochal cysts. Hepatology **27:**1475-1482.
16. **Fischler B, Ehrnst A, Forsgren M, Örvell C, Nemeth A.** 1998. The viral association of neonatal cholestasis in Sweden: a possible link between cytomegalovirus infection and extrahepatic biliary atresia. Journal of pediatric gastroenterology and nutrition **27:**57-64.
17. **Fischler B, Woxenius S, Nemeth A, Papadogiannakis N.** 2005. Immunoglobulin deposits in liver tissue from infants with biliary atresia and the correlation to cytomegalovirus infection. Journal of pediatric surgery **40:**541-546.
18. **Brindley SM, Lanham AM, Karrer FM, Tucker RM, Fontenot AP, Mack CL.** 2012. Cytomegalovirus-specific T-cell reactivity in biliary atresia at the time of diagnosis is associated with deficits in regulatory T cells. Hepatology **55:**1130-1138.
19. **Hertel PM, Estes MK.** 2012. Rotavirus and biliary atresia: can causation be proven? Current opinion in gastroenterology **28:**10-17.

20.   **Lin Y-C, Chang M-H, Liao S-F, Wu J-F, Ni Y-H, Tiao M-M, Lai M-W, Lee H-C, Lin C-C, Wu T-C.** 2011. Decreasing rate of biliary atresia in Taiwan: a survey, 2004–2009. Pediatrics **128:**e530-e536.
21.   **Lee JH, Ahn HS, Han S, Swan HS, Lee Y, Kim HJ.** 2019. Nationwide population-based study showed that the rotavirus vaccination had no impact on the incidence of biliary atresia in Korea. Acta Paediatrica.
22.   **Bondoc AJ, Jafri MA, Donnelly B, Mohanty SK, McNeal MM, Ward RL, Tiao GM.** 2009. Prevention of the murine model of biliary atresia after live rotavirus vaccination of dams. Journal of pediatric surgery **44:**1479-1490.

Text S1 – Supplemental Materials and Methods

Reagents

Propidium iodide (PI) (Method Detection Limit [MDL] no. MFCD00011921), calcein-AM (MDL no. MFCD05861516), ribavirin (MDL no. MFCD00058564) and mycophenolic acid (MPA) (MDL no. MFCD00036814) were purchased from Sigma. All the reagents above were dissolved in dimethyl sulfoxide (DMSO). Hoechst 33342 (Catalog number: H3570) and Type I human recombinant IFN alpha 2a (IFN-α) were purchased from Thermo Fisher, and IFN-α was dissolved in culture medium.

Viruses

Simian rotavirus SA11, a widely used laboratory strain(1), was gifted by Karen Knipping from Nutricia Research Utrecht, The Netherland. Rotavirus SA11 was prepared as previously described(2).

Cell lines and human organoids

Human colon cancer cell line Caco2 was cultured as previous study(3). Cells were analyzed by genotyping and confirmed to be mycoplasma negative.

Human primary small intestinal organoids (HIOs) were cultured as described previously(4). three batches of human fetal liver organoids (FLO P, FLO 521 and FLO 528), two adult bile duct organoids (BDO S, DD 1125) and two adult liver organoids (LiO K, DL 1125) were cultured as previously described(5). The use of human organoids was approved by the Medisch Ethische Toetsings Commissie Erasmus MC (Medical Ethical Committee of the Erasmus medical center).

Virus inoculation assay

Virus, cell line and organoids were treated as previously described (4). Briefly, the stock of SA11 rotavirus ($4.5*10^8$ TCID$_{50}$/ml) was used. MA104 cell line was inoculated with the diluted stock virus at MOI of 0.7 at 37°C with 5 μg/mL of trypsin (Gibco, Paisley, UK) and 5% CO_2 for 15 min.

For inoculating organoids, collected organoids were incubated with trypsin pre-activated rotavirus at concentration of $4.5*10^5$ $TCID_{50}$/ml for 1.5 h followed by 4 times wash with PBS. Afterwards, for RNA and protein detection assay, organoids with no Matrigel remain were spun down at 500 g for 10 min to adhered to the bottom of 24-well or 48-well plate coated with Collagen R solution (SERVA, Heidelberg, Germany). Culture medium was added gently and organoids were incubated at 37°C with 5% CO_2. Supernatant was harvested for secondary infection assay after 48 h incubation. Supernatant and organoids were harvested at different time points for RNA isolation or Western blot assay. Infected organoids for observation or staining were mixed with Matrigel and seeded back to 24-well plate for continues culturing.

For secondary infection assay, Caco2 cells were washed, suspended in T75 flask and subsequently seeded into a 48-well plate (5×10^4 cells/well). Culture medium was discarded when cell confluence was approximately 80%, and cell monolayers were washed twice with PBS. 100 μL of serum-free DMEM medium, then pretreated supernatant were added and incubated at 37°C with 5% CO_2 for 60 min for infection, followed by 4 times washing with PBS to remove un-attached viruses. Then, cells were incubated with maintenance medium with 1 μg/mL of trypsin at 37°C with 5% CO_2.

TCID50 assay

The titers of rotaviruses produced by organoids were determined by calculating the $\log_{10}TCID_{50}$/mL in Ma104 cells using the method developing by Reed and Muench in 1938(6).

RNA isolation and sequencing, cDNA synthesis and qRT-PCR

Total RNA was isolated using Macherey-Nagel NucleoSpin® RNA II kit (Bioke, Leiden, Netherlands) and quantified using a Nanodrop ND-1000 (Wilmington, DE, USA). The quality of RNA was measured by Bioanalyzer RNA 6000 Picochip as quality-control step, followed by RNA sequencing performed by Novogene with paired-end 150 bp (PE 150) sequencing strategy. qRT-PCR assay were performed and glyceraldehyde 3-phosphate dehydrogenase (GAPDH) gene was used as housekeeping gene. Relative gene expression was normalized to GAPDH using the formula $2^{-\Delta\Delta CT}$ ($\Delta\Delta CT = \Delta CTsample - \Delta CTcontrol$). Template control and reverse transcriptase control were included in all qRT-PCR experiments. Primers for SA11

rotavirus are TGGTTAAACGCAGGATCGGA as sense and AACCTTTCCGCGTCTGGTAG as antisense primer. The primers for the reference gene GAPDH are GTCTCCTCTGACTTCAACAGCG and ACCACCCTGTTGCTGTAGTAGCCAA as sense and antisense primer, respectively.

Determination of organoids cell death

The staining and scoring process was performed as previously(3). In short, minimum of 100 organoids were counted after 3 days of passaging. After 1.5 h incubation with SA11 rotavirus, organoids were cultured in Matrigel for 48 h followed by staining with propidium iodide (PI) (red, dead cells), Hoechst (blue, nuclear), and Calcein (green, live cells). Images were detected using EVOS FL cell imaging system (Thermo Fisher). Under fluorescence version, organoids in which red signal is more than green signal and also more than 50% of blue signal was counted as positive. On the contrary, organoids in which green signal is more than red signal and also more than 50% of blue signal was treated as negative or viable. Three random visions in each well have been chosen and organoids have been counted by total number and viable number. The proportion of deteriorated organoids was calculated as (viable/ total).

Western blot assay

Lysed cells were subjected to SDS-PAGE, and proteins were transferred to PVDF membrane (Immobilon-FL). SA11 rotavirus VP4 (1:1000, HS-2, mouse monoclonal; provided by professor Harry Greenberg, Stanford University School of Medicine, USA) was detected by western blot analysis and β-actin protein was detected as loading control (sc-47778, 1:1000, mouse monoclonal; Santa Cruz). The intensity of the immunoreactive bands of blotted protein was quantified by the Odyssey V3.0 software.

Immunofluorescence analysis

After rotavirus infection, organoids were harvested and fixed in 4% paraformaldehyde in PBS at 4°C for 10 min. Fixed organoids were added into the CytoSpin II Cytocentrifuge (Shandon Scientifi Ltd, Runcorn, England), then spun down at 1000 rpm for 2 min. The slides containing organoids were rinsed 3 times with PBS for 5 min each, followed by treatment

with 0.1% (vol/vol) Tritonx100 for 4 min. Subsequently, the slides were twice rinsed with PBS for 5 min, followed by incubation with milk-tween-glycine medium (0.05% tween, 0.5% skim milk and 0.15% glycine) to block background staining for 30 min. Slides were incubated in a humidity chamber with anti-rotavirus antibody (1:250, mouse monoclonal; Abcam) and anti-EpCAM antibody (1:250, rabbit polyclonal; Abcam) diluted in milk-tween-glycine medium at 4 ºC overnight. Slides were washed 3 times for 5 min each in PBS prior to 1 h incubation with 1:1000 dilutions of the anti-mouse IgG (H+L, Alexa Fluor® 594) and the anti-rabbit IgG (H+L, Alexa Fluor® 488) secondary antibodies. Nuclei were stained with DAPI (4, 6-diamidino-2-phenylindole; Invitrogen). Images were detected using Leica SP5 cell imaging system.

Neutralization assay

Neutralizing monoclonal antibody (MAb) HS-1 was gifted by Professor Harry Greenberg, Stanford University School of Medicine, USA. Neutralization assay was performed as previous study(7). Briefly, rotavirus were activated by 5 µg/mL trypsin, followed by adding Mab in series of dilution (1:1000, 1:250, 1:100), then kept neutralizing for 2 h at 37 ºC and overnight at 4 ºC. After 48 h inoculation with organoids, RNA was isolated and detected by qRT-PCR.

Statistics

The statistical significance of differences between means was assessed with the Mann-Whitney test (GraphPad Prism 5; GraphPad Software Inc., La Jolla, CA). The threshold for statistical significance was defined as $P \leq 0.05$.
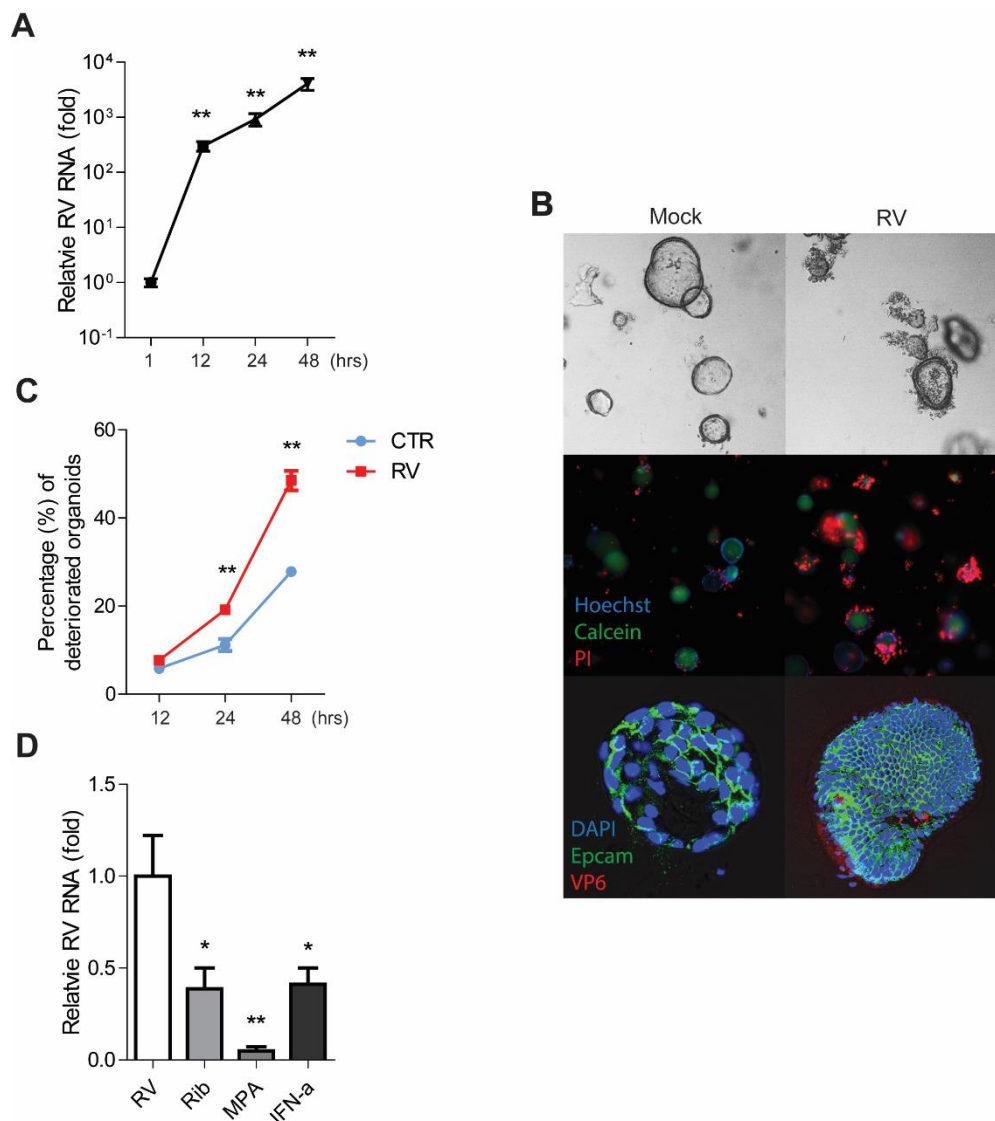
Supplementary Figures

Figure S1. Characterizing rotavirus infection in human intestinal organoids (HIOs). (A) Rotavirus RNA quantified by qRT-PCR post-inoculation. (B) Optical microscopy images of infected and un-infected organoids (upper). Fluorescence staining of dead cells (PI; red), live cells (Calcein; green) and nuclei (Hoechst; blue) (middle). Confocal immunostaining of rotavirus structural protein VP6 (red), Epcam (green) and nuclei (blue) (lower). (C) Quantitative analysis of the percentage of deteriorated organoids with or without rotavirus infection at indicated time points and calculated based on the live/dead cell staining (F, middle). (D) The effects of the broad-spectrum antiviral drugs on rotavirus in intestinal organoids. Ribavirin: Rib; mycophenolic acid: MPA; interferon alpha: IFN-α. All the data represent means ± SEM. Experiments were repeated 3-6 times. Mann-Whitney test; *P < 0.05, **P < 0.01.
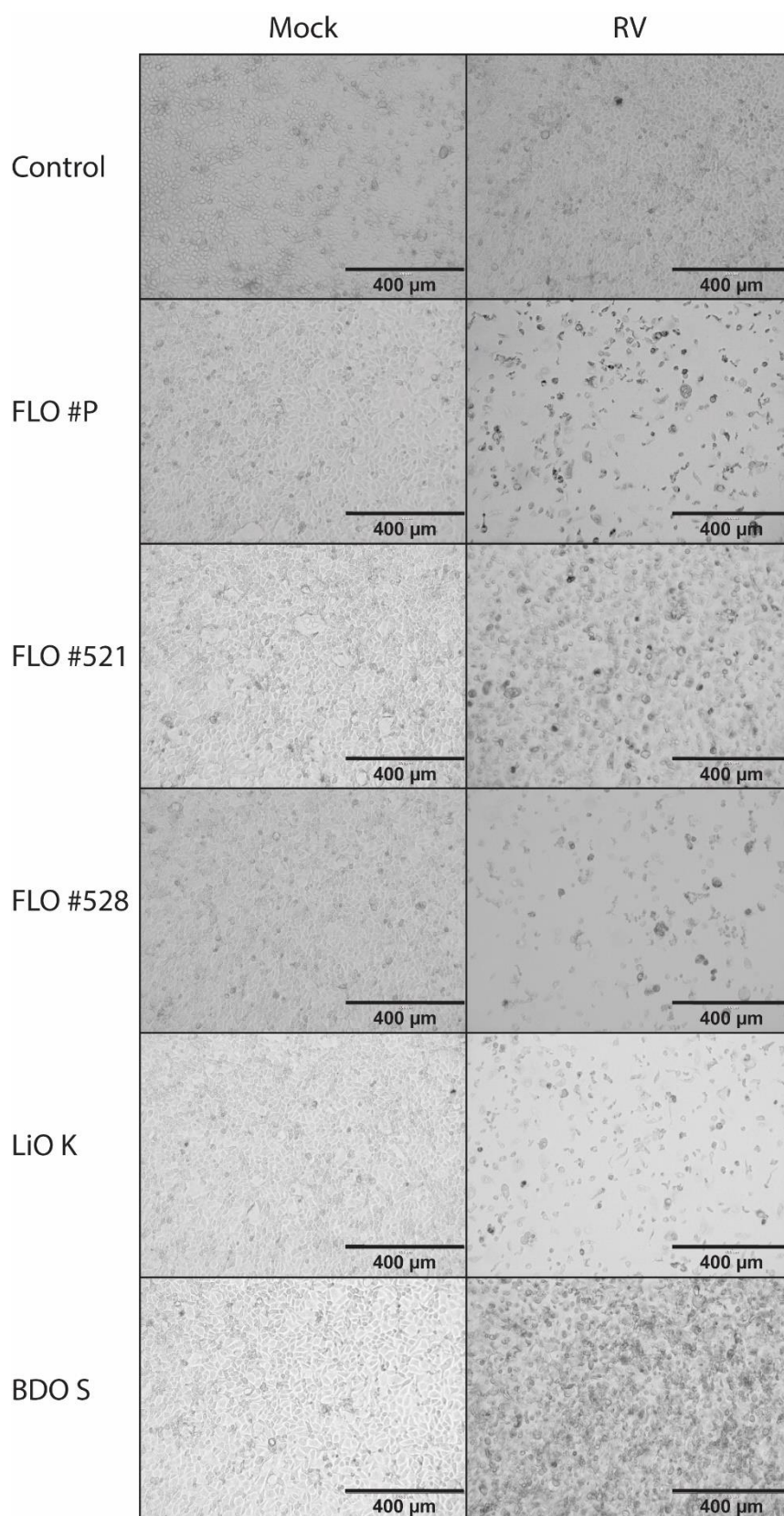
Figure S2. Optical microscopy images of Caco2 cell infected with 10^4 times diluted rotavirus stocks harvested from five batches of organoids infected with rotavirus at 48 hours post-infection with the control at baseline inoculation (See Fig. 2D in details). In mock group, cells were all hyaline and

polygonous, while the other infected groups, except the control group, cells were spindle-shaped or crimpled with large number of exfoliated cells, indicating cytopathogenesis.

References

1. **Cecílio AB, de Faria DB, de Carvalho Oliveira P, Caldas S, de Oliveira DA, Sobral MEG, Duarte MGR, de Souza Moreira CP, Silva CG, de Almeida VL.** 2012. Screening of Brazilian medicinal plants for antiviral activity against rotavirus. Journal of ethnopharmacology **141:**975-981.
2. **Knipping K, Garssen J, van't Land B.** 2012. An evaluation of the inhibitory effects against rotavirus infection of edible plant extracts. Virology journal **9:**137.
3. **Chen S, Ding S, Yin Y, Xu L, Li P, Peppelenbosch MP, Pan Q, Wang W.** 2019. Suppression of pyrimidine biosynthesis by targeting DHODH enzyme robustly inhibits rotavirus replication. Antiviral research **167:**35-44.
4. **Yin Y, Bijvelds M, Dang W, Xu L, van der Eijk AA, Knipping K, Tuysuz N, Dekkers JF, Wang Y, de Jonge J.** 2015. Modeling rotavirus infection and antiviral therapy using primary intestinal organoids. Antiviral research **123:**120-131.
5. **Huch M, Gehart H, van Boxtel R, Hamer K, Blokzijl F, Verstegen MMA, Ellis E, van Wenum M, Fuchs SA, de Ligt J.** 2015. Long-term culture of genome-stable bipotent stem cells from adult human liver. Cell **160:**299-312.
6. **Reed LJ, Muench H.** 1938. A simple method of estimating fifty per cent endpoints. American journal of epidemiology **27:**493-497.
7. **Ruggeri FM, Greenberg HB.** 1991. Antibodies to the trypsin cleavage peptide VP8 neutralize rotavirus by inhibiting binding of virions to target cells in culture. Journal of virology **65:**2211-2219.

Chapter 3

The eukaryotic translation initiation factor 4F complex restricts rotavirus infection via regulating the expression of IRF1 and IRF7

Sunrui Chen[‡], Cui Feng[‡], Yan Fang[‡] Xinying Zhou, Lei Xu, Wenshi Wang, Xiangdong Kong, Maikel P. Peppelenbosch, Qiuwei Pan and Yuebang Yin

[‡]These authors contributed equally to this work.

ABSTRACT

The eIF4F complex is a translation initiation factor that closely regulates translation in response to a multitude of environmental conditions including viral infection. How translation initiation factors regulate rotavirus infection remains poorly understood. In this study, the knockdown of the components of the eIF4F complex using shRNA and CRISPR/Cas9 was performed. We demonstrate that loss-of-function of the three components of eIF4F, including eIF4A, eIF4E and eIF4G, remarkably promotes the levels of rotavirus genomic RNA and viral protein VP4. Consistently, knockdown of the negative regulator of eIF4F and programmed cell death protein 4 (PDCD4) inhibits the expression of viral mRNA and the VP4 protein. Mechanically, we confirmed that the silence of the eIF4F complex suppressed the protein level of IRF1 and IRF7 that exert potent antiviral effects against rotavirus infection. Thus, these results demonstrate that the eIF4F complex is an essential host factor restricting rotavirus replication, revealing new targets for the development of new antiviral strategies against rotavirus infection.

KEYWORDS: Rotavirus; eIF4F complex; Translation initiation factors; IRF7; IRF7.

INTRODUCTION

Rotavirus is considered to be one of leading causative agent of severe diarrhea in infants younger than five years old [1], and it causes estimated 215,000 deaths in children each year globally [2]. Although rotavirus infection mainly occurs in low-income countries [3], it also inflicts a heavy burden in industrialized countries. For example, in the European Union, rotavirus infection causes more than 200 deaths, over 87,000 hospital admissions, and almost 700,000 outpatient visits in children younger than five years of age annually [4]. Emerging evidence indicates that rotavirus infection causes severe complications in organ transplant patients irrespective to their ages [5]. Although vaccines have been developed, no approved antiviral treatment is available.

The genome of rotavirus contains 11 segments encoding 12 proteins including six structural (VP1-4, VP6, and VP7) and six non-structural proteins (NSP1-6) [6]. Among the structural proteins, as a spike protein, rotavirus VP4 plays an essential role in both viral entry and exit [7]. VP4 was also demonstrated to be of importance in viral attachment and internalization [8], which is often used for the development of rotavirus vaccines [8]. VP4 contains two subunits including a C-terminal subunit VP5* and a N-terminal subunit VP8*, and both VP5* and VP8* help virus entry by interacting with several putative partners and cell surface receptors [7]. The rotavirus genome is a double-strand RNA containing a cap at 5' untranslated regions (UTR) synthesized by the viral transcriptase but lacks a polyadenylated tail instead having a consensus sequence at 3' UTR [9]. It has been reported that rotavirus NSP3 is able to bind to the 3' consensus sequence of viral mRNA and interact with eIF4G to aid translation of viral mRNA [10]. Rotavirus NSP3 stabilizes the eIF4E–eIF4G interaction to exert an enhanced effect on the translation of both poly (A)- and non-poly (A)-tailed mRNAs [11].

There are three phases in protein synthesis including initiation, elongation, and termination [11]. Initiation determines translation rates [12]. Most of the eukaryotic mRNAs are characterized by a m7GpppX structure (where m7Gppp is the 7-methyl-guanosine-containing and X is any nucleotide), termed as a cap, at the 5' ends and the poly (A) tail at the 3' end [13]. The mRNA containing a cap at the 5' ends is able to be more efficiently translated than that lacking this structure [14], and these mRNAs are translated in a cap-dependent manner [12]. The cap structure is bound by the eukaryotic translation initiation factor 4F (eIF4F) which is a

protein complex containing three constituent proteins: a eukaryotic translation initiation factor 4A (eIF4A), a eukaryotic translation initiation factor 4E (eIF4E), and a eukaryotic translation initiation factor 4G (eIF4G) [15]. The eIF4F complex plays a pivotal role in cap-dependent mRNA protein translation initiated by recruiting mRNA to a ribosome [13]. As an RNA helicase, eIF4A makes use of ATP hydrolysis to unwind and resolve the RNA secondary structure [16]. The eIF4E recognizes and binds to the 7-methylguanosine (m7G) cap located at the 5'-UTRs of mRNA to mediate the mRNA recruitment on ribosomes, thus initiating the translation together with other initiation factors [17]. As a scaffold protein, eIF4G plays a central role in translation initiation by assembling eIF4E and eIF4A to further form the eIF4F complex [18]. The programmed cell death protein 4 (PDCD4) is a translation suppressor of mRNAs by interacting with eIF4A to suppress its helicase activity [19]. As a downstream target of mechanistic target of the rapamycin (mTOR) pathway, the phosphorylation of protein kinase S6K1 is able to phosphorylate PDCD4 to release it from eIF4A, thus allowing eIF4A to interact with eIF4G to form the eIF4F complex, followed by initiating translation [20].

Viruses require components from the host cell to replicate, assemble viral components, and release their new synthesized virions [14]. Viral protein synthesis completely relies on the translational machinery of the host due to viruses lacking this machinery themselves [21]. Viruses are able to exploit the translational machinery, including eIF4F, to support the translation of their transcripts [15]. Certain mammalian viruses are involved in targeting the eIF4F complex to regulate both viral and host mRNA translation; while many RNA viruses inhibit host protein synthesis to initiate the translation of their own mRNAs by inhibiting eIF4F [22]. Feline calicivirus (FCV) and mouse norovirus (MNV) have been reported to be capable of directly interacting with eIF4E, and viral RNA translation requires the eIF4A, indicating that the replication of the two viruses requires eIF4F [23]. Blocking eIF4E–eIF4G interaction has been demonstrated to cause inhibition of coronavirus replication, indicating that eIF4F has a promoting effect on the virus replication [24]. Furthermore, certain members of the eIF4G family were thought to be able restrict the infection of Rice yellow mottle virus (RYMV) [25]. Thus, the eIF4F complex has different effects on distinct viruses.

The eIF4F complex plays an essential role in regulating interferon signaling which is considered to be the first line of antiviral defense [26]. The phosphorylation of eIF4E was reported to exert antiviral effect via regulating the production of type I interferon [27]. It was found that

the eIF4F complex could tightly regulate the translation of the signal transducer and activator of transcription 1 (STAT1) mRNA that plays a crucial role in type I interferon signaling [28]. Thus, in this study, we have dissected the effects of the cellular translation machinery, the eIF4F complex, on rotavirus infection, and we found that the eIF4F complex is an essential host factor in counteracting rotavirus infection through regulating the antiviral protein IRF1 and IRF7.

2.RESULTS

2.1. The eIF4A inhibits rotavirus infection

We first examined the effects of rotavirus infection on the expression of the components of the eIF4F complex, including eIF4A and eIF4E, at indicated time points (1, 2, 4, 6, 24, and 48 h). Although rotavirus infection did not affect the protein expression of the eIF4F complex (Supplementary Figure S1), it is interesting to investigate whether the components of the eIF4F complex regulate the course of the rotavirus infection. To this aim, we first detected the effects of eIF4A on rotavirus infection, by performing a lentiviral RNAi-mediated loss-of-function assay to silence the eIF4A gene. All five short hairpin RNA (shRNA) vectors showed successful knockdown (Figure 1A, B). Importantly, two shRNA vectors (No 1 and 2) resulted in a 121.7 ± 60.6 (n = 6, P < 0.01)- and 56.7 ± 29.9 (n = 6, P < 0.01)- fold increase in SA11 rotavirus mRNA, respectively (Figure 1C). All shRNA vectors showed no clear cytotoxicity determined by 3-(4,5-dimethyl-2-thiazolyl)-2,5-diphenyl-2-H-tetrazolium bromide (MTT) assay (Supplementary Figure S2A). Western blot indicated that all five shRNA vectors increased the rotavirus VP4 protein level (Figure 1D). To further verify these findings, we used CRISPR/Cas9 to knockout the eIF4A gene in Caco2 cells (Figure 1E). After eIF4A knockout, the viral mRNA and protein levels were remarkably reduced (Figure 1F, G).
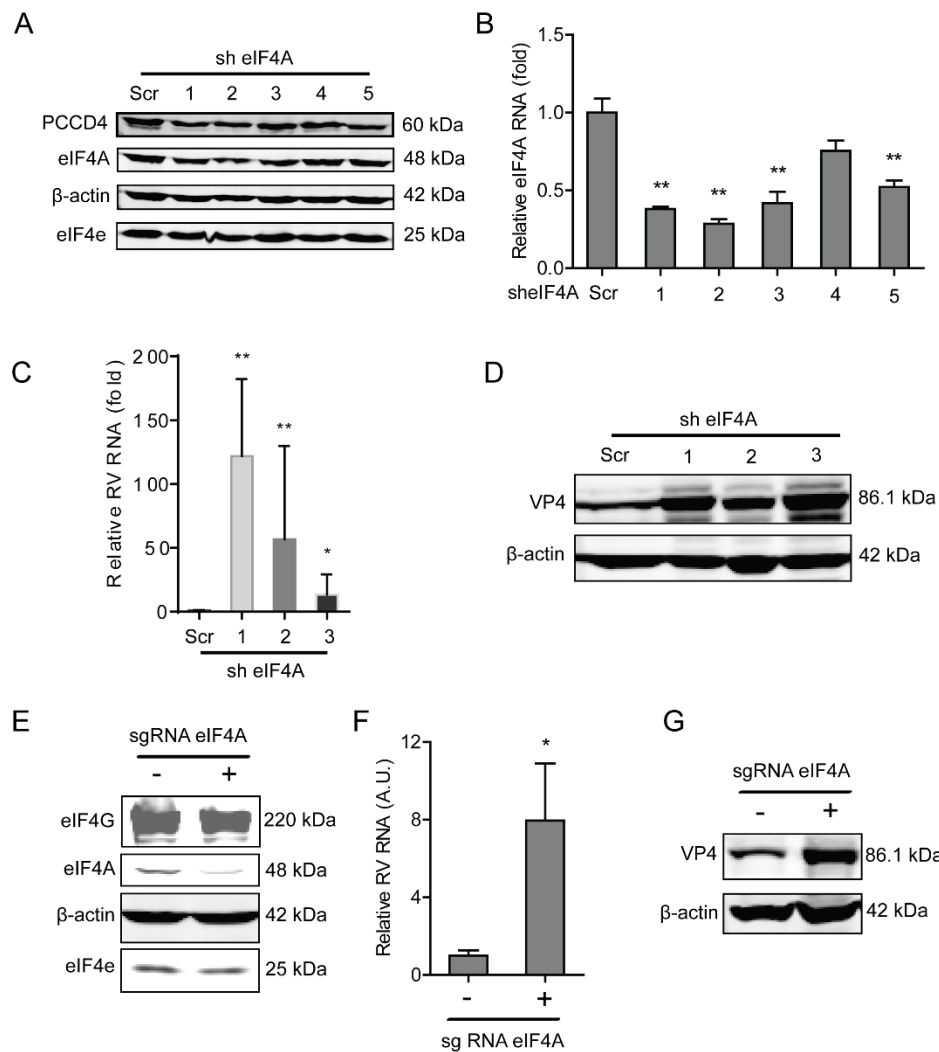
Figure 1. Knockdown of eIF4A supports rotavirus infection. (A) Western blot assay detected eIF4A in Caco2 cells transduced with lentiviral RNAi vectors against eIF4A. (B) Successful knockdown by shRNA vectors measured by RT-qPCR (n = 6, **P< 0.01, Mann-Whitney test). (C) Silence of eIF4A increased rotavirus genomic RNA level (n = 6, *P< 0.05, **P< 0.01, Mann-Whitney test). (D) Silence of eIF4A increased viral VP4 protein level in SA11 rotavirus infected Caco2 cells. (E) Western blot detected eIF4A protein level in Caco2 cells transduced with CRIPSRs against eIF4A, suggesting a successful knockout. (F) Silence of eIF4A by CRISPR/Cas9 increased rotavirus genomic RNA level (n = 6, *P< 0.05, Mann-Whitney test). (G) Silence of eIF4A by CRISPR/Cas9 increased viral VP4 protein level in SA11 rotavirus infected Caco2 cells.

2.2. Blocking eIF4E promotes rotavirus infection

Another component of the eIF4F complex, eIF4E, is responsible for binding to the cap of mRNA. Similarly, a lentiviral RNAi-mediated loss-of-function assay was performed to silence the eIF4E gene to assess its effect on rotavirus infection. One out of the four shRNAs exerted a potent knockdown effect on eIF4E (Figure 2A). Consistently, this shRNA vector resulted in a

14.5 ± 5.8 (n = 6, P < 0.01)-fold increase in SA11 rotavirus mRNA (Figure 2B). All shRNA vectors showed no clear cytotoxicity measured by MTT assay (Supplementary Figure S2B). This shRNA vector resulted in the increase in the SA11 rotavirus VP4 protein level (Figure 2C). To further verify this, we used CRISPR/Cas9 to knockout eIF4E in Caco2 cells (Figure 2D). After eIF4E gene knockout, the viral RNA and protein levels were restricted (Figure 2E, F).
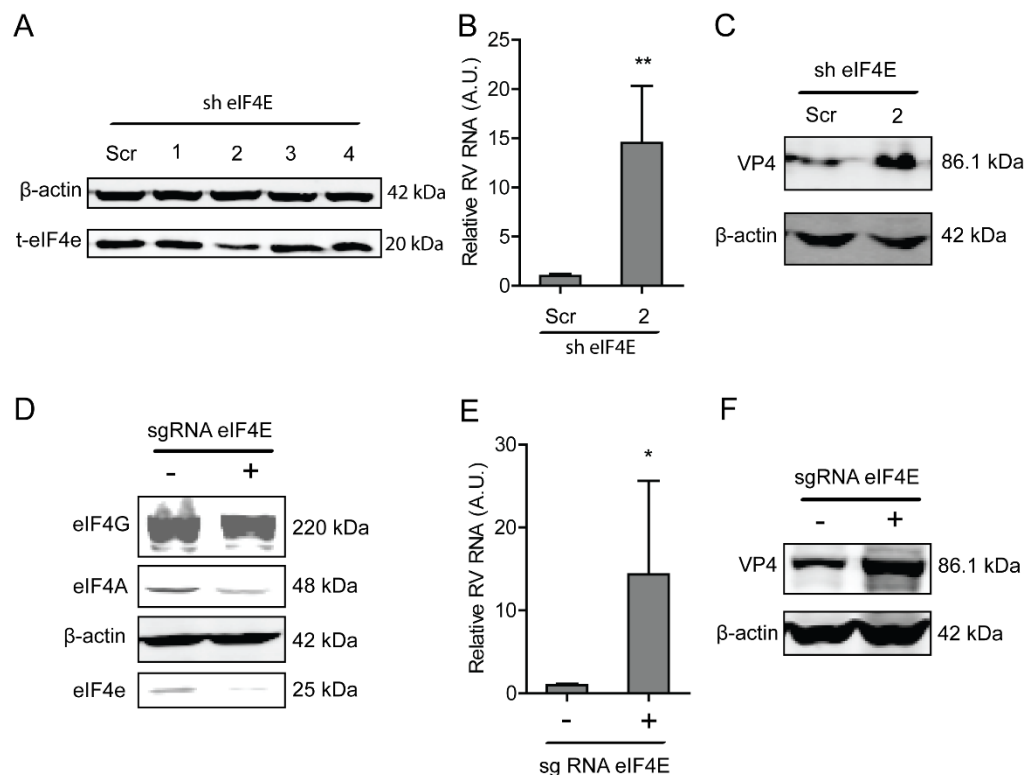

Figure 2. The eIF4E suppresses rotavirus infection. (A) Western blot assay measured eIF4E protein in Caco2 cells transduced lentiviral RNAi vectors against eIF4E, indicating that one out of three shRNA vectors showed potent knockdown. (B) The knockdown of eIF4E significantly promoted rotavirus genomic RNA (n = 6, *P< 0.05, Mann-Whitney test). (C) Western blot assay confirmed eIF4E knockdown increased rotavirus protein level. (D) The eIF4E was knockout by crispr/cas9 assay. (E) Silence of eIF4E by crispr/cas9 increased rotavirus RNA level (n = 6, *P< 0.05, Mann-Whitney test). (F) Silence of eIF4E by crispr/cas9 increased rotavirus VP4 protein level.

2.3. The eIF4G suppresses rotavirus infection

As a scaffolding protein, eIF4G protein is able to physically link mRNA and the small ribosomal subunit via protein-protein interactions. To investigate the effects of eIF4G protein on rotavirus infection, a lentiviral shRNA-mediated loss-of-function assay was conducted, which resulted in gene silence of eIF4G by all five shRNA vectors at both the mRNA and protein level

(Figure 3A,B). Importantly, all these shRNA vectors resulted in a potent increase in the viral RNA and protein level (Figure 3C, D). The vitality of cells was not affected by these shRNA vectors (Supplementary Figure S2C). To further verify these findings, we performed a Crispr/cas9 assay to knockout eIF4G in Caco2 cells (Figure 3E). After gene knockout, the viral RNA and protein levels were inhibited (Figure 3F, G).

To further verify the effect of eIF4A, eIF4E, and eIF4G on rotavirus infection, CRIPRs against eIF4A, eIF4E, and eIF4G were co-transfected in Caco2 cells. After puromycin selection, the knockout of eIF4A, eIF4E, and eIF4G was detected by western blot, indicating successful knockout of three genes (Figure 4A). The effect of eIF4A, eIF4E, and eIF4G on rotavirus infection was further detected by RT-qPCR and western blot, demonstrating that both viral genomic RNA and viral protein VP4 synthesis were promoted (Figure 4B, C).
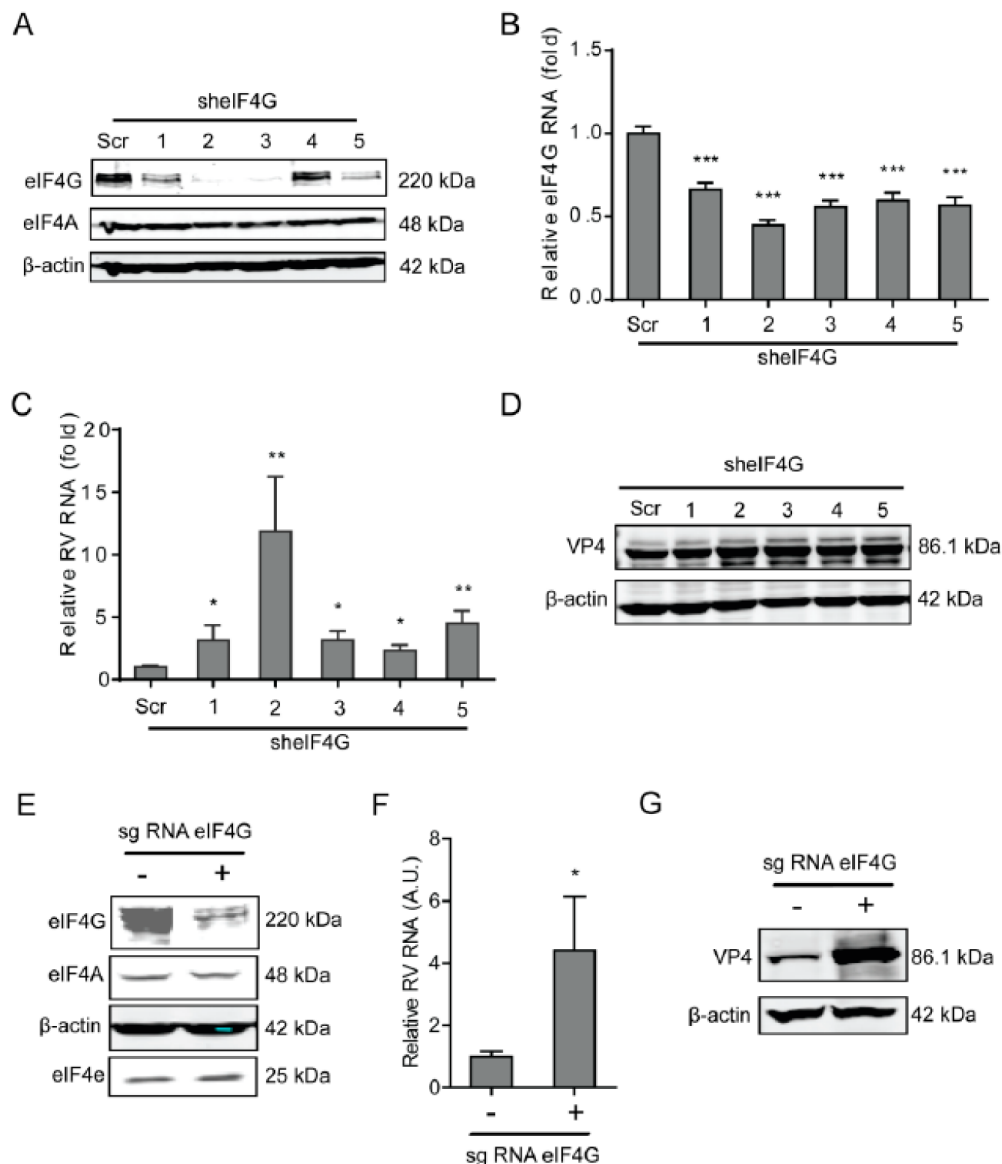
Figure 3. Silence of eIF4G promotes rotavirus infection. (A) Western blot assay detected eIF4G in Caco2 cells transduced with lentiviral RNAi vectors against eIF4G. (B) Successful knockdown by shRNA vectors detected by RT-qPCR assay (n = 6, **P< 0.01, Mann-Whitney test). (C) Silence of eIF4G showed increased rotavirus genomic RNA level (n = 6, *P< 0.05, **P< 0.01, Mann-Whitney test). (D) Silence of eIF4G promoted viral VP4 protein level in SA11 rotavirus infected Caco2 cells. (E) Western blot assay detected eIF4G in Caco2 cells transduced with CRIPSRs against eIF4G. (F) Silence of eIF4A by CRISPR/Cas9 increased rotavirus genomic RNA level (n = 6, *P< 0.05, Mann-Whitney test). (G) Silence of eIF4G by CRISPR/Cas9 increased viral VP4 protein level in SA11 rotavirus infected Caco2 cells.
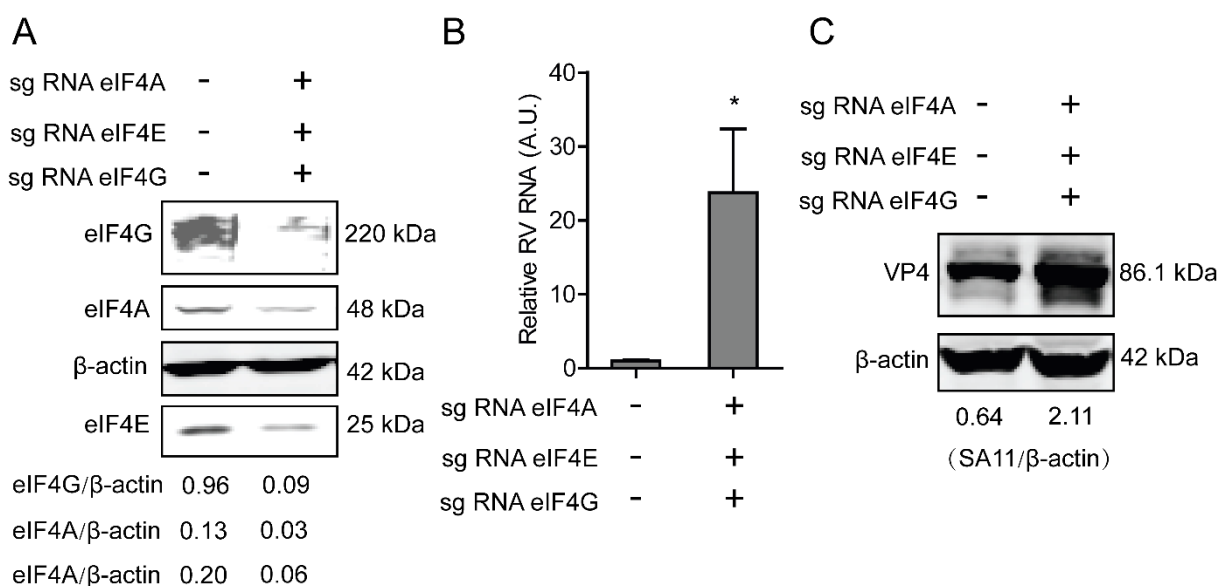

Figure 4. Silence of eIF4A/E/G promotes rotavirus infection. (A) Western blot assay detected eIF4 A/E/G in Caco2 cells transduced CRIPRs against eIF4A, eIF4E and eIF4G. (B) Silence of eIF4A/E/G promoted rotavirus genomic RNA level detected by qPCR assay (n = 6, **P< 0.01, Mann-Whitney test). (C) Silence of eIF4A/E/G showed increased rotavirus protein VP4.

2.4. Programmed cell death protein 4 (PDCD4) promotes rotavirus infection

PDCD4 functions by inhibiting the translation by directly inhibiting the helicase activity of eIF4A to competitively bind to the scaffold protein eIF4G. To further verify the effects of the eIF4F complex on rotavirus infection, a lentiviral shRNA-mediated loss-of-function assay was performed to silence PDCD4, which indicated that one out of three shRNA vectors (No 1) exerted a potent knockdown effect (Figure 5A, B). Consistently, the shRNA vector resulted in a 50 ± 12 % (n= 8, P < 0.05)-fold reduction in SA11 rotavirus mRNA (Figure 5C), and remarkable reduction in viral VP4 protein levels (Figure 5D). All shRNA vectors have no significant cytotoxicity (supplementary Figure S2D).
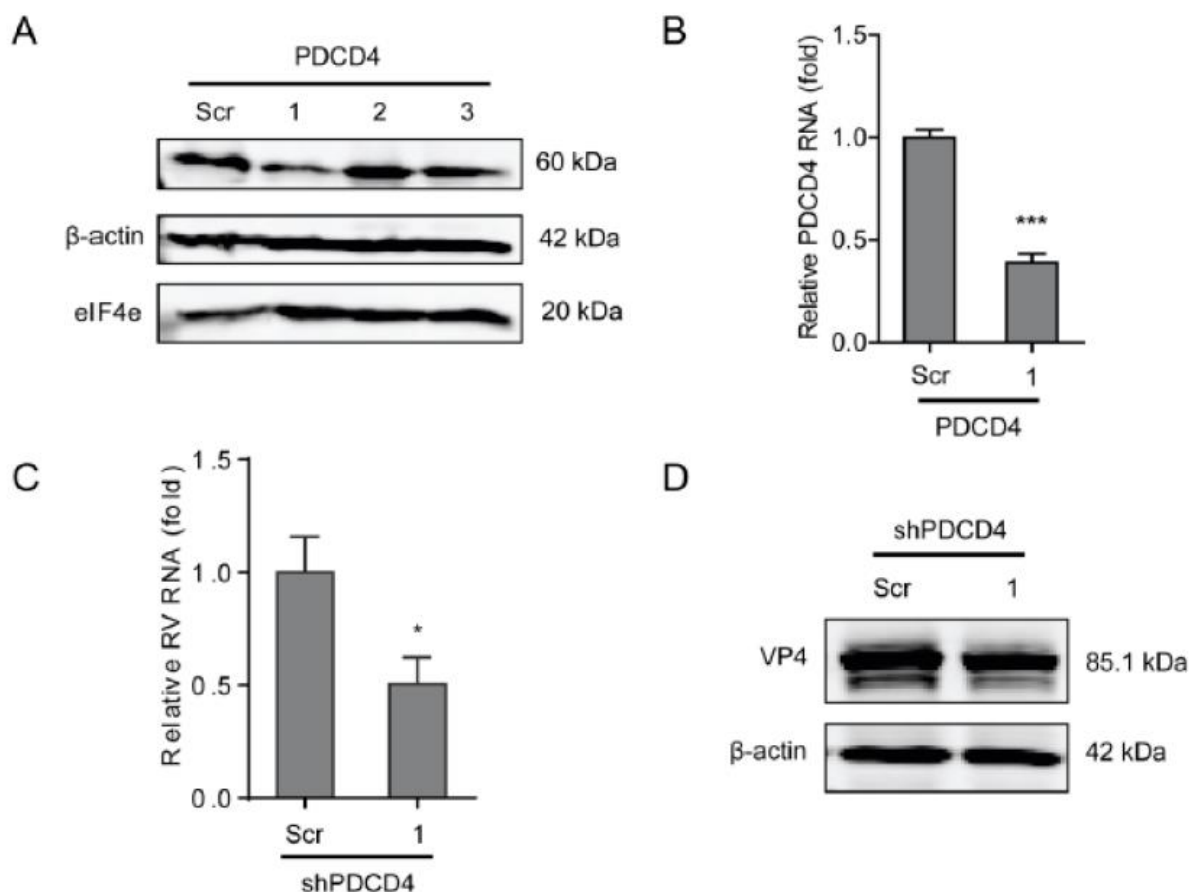
Figure 5. **PDCD4 sustains rotavirus infection**. (A) Western blot assay detected PDCD4 in Caco2 cells transduced lentiviral RNAi vectors against PDCD4. (B) One out of three shRNA vectors showed successful knockdown detected by RT-qPCR (n = 6, **P< 0.01, Mann-Whitney test). (C) Silence of PDCD4 showed inhibition of rotavirus genomic RNA level (n = 8, *P< 0.05, Mann-Whitney test). (D) Silence of PDCD4 inhibited viral VP4 protein level in SA11 rotavirus infected Caco2 cells.

2.5. The eIF4F complex inhibits the level of antiviral proteins to exert anti-rotavirus effect

To further explore the underlying molecular mechanism of the antiviral effects of the eIF4F complex on rotavirus infection, we questioned the effect of the eIF4F complex on several antiviral proteins including interferon regulatory factor 1 (IRF1), IRF7, and retinoic acid-inducible-I (RIG-I), which indicated that the knockdown of eIF4A had no obvious effect on these antiviral proteins. While the knockdown of eIF4E (shRNA No 2) was able to inhibit protein level of IRF1 and IRF7 (Figure 6B). Knockdown of eIF4G was also capable of suppressing the protein level of IRF1 and IRF7 (Figure 6C). To further verify this, the effect of IRF7 and IRF1 on rotavirus replication was detected, indicating that knockout of either IRF7 (Figure 6D) or

IRF1 (Figure 6F) could significantly reduce the genomic mRNA of SA11 rotavirus (Figure 6E, G). Thus, the antiviral effect against rotavirus of the eIF4F complex may operate through regulating the expression antiviral proteins in the host.
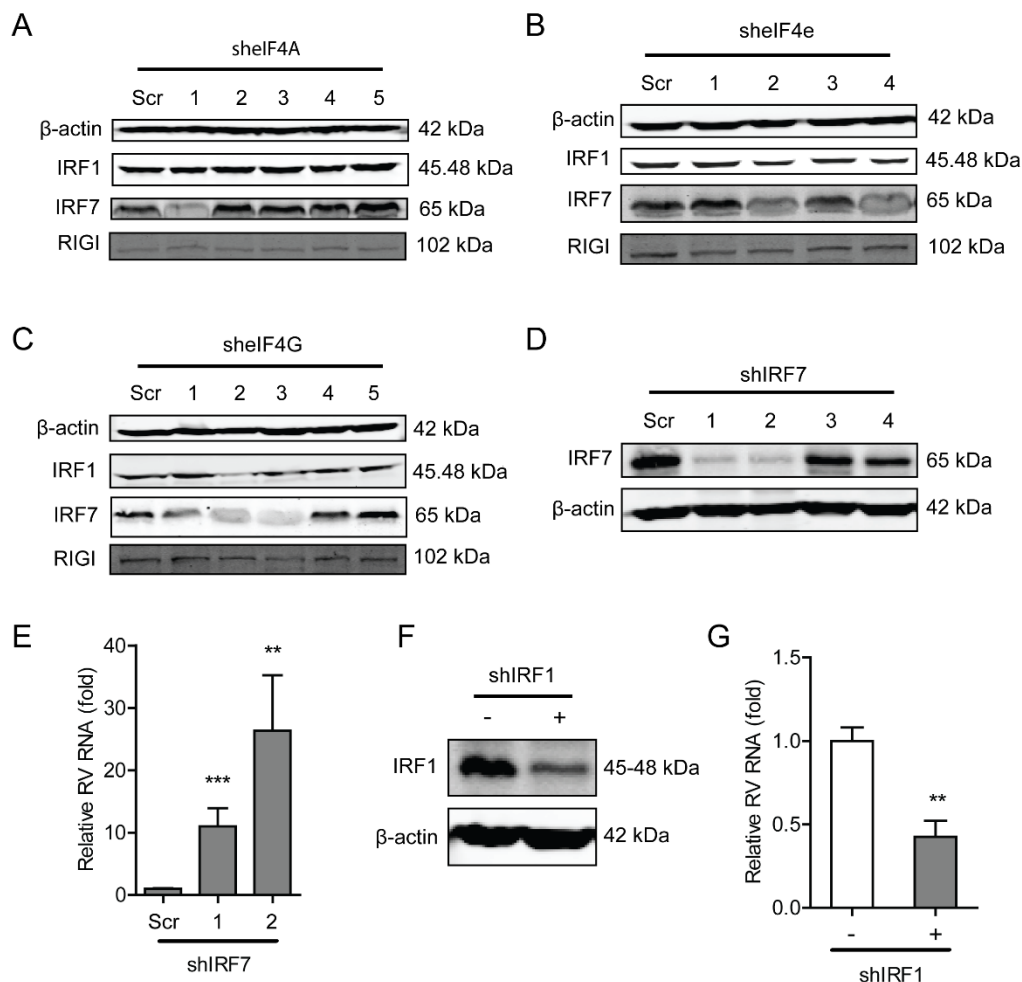

Figure 6. The eIF4F complex is required for IRF7 that exerts anti-rotavirus effect. (A) Western blot assay detected the protein level of antiviral factors including IRF1, IRF7, and RIG-I in eIF4A knockdown Caco2 cells. (B) Western blot assay detected the protein level of antiviral factors including IRF1, IRF7, and RIG-I in eIF4E knockdown Caco2 cells. (C) Western blot assay detected the protein level of antiviral factors including IRF1, IRF7, and RIG-I in eIF4G knockdown Caco2 cells. (D) Western blot assay detected the protein level of IRF7 in eIF4G knockout Caco2 cells, and two out of four shRNA vectors showed successful knockdown of IRF7 detected by western blot. (E) Silence of IRF7 increased rotavirus genomic RNA level detected by qPCR assay (n = 6, **P< 0.01, ***P< 0.001, Mann-Whitney test). (F) Western blot assay detected the protein level of IRF7 in eIF4G knockout Caco2 cells, indicating successful knockdown of IRF1 detected by western blot. (G) Silence of IRF1 increased rotavirus genomic RNA level detected by qPCR assay (n = 6, **P< 0.01, Mann-Whitney test).

3. DISCUSSION

Many viral mRNAs have acquired a variety of sophisticated strategies to compete with cellular mRNAs that are already present in the cytoplasm. This allows the selective translation of viral mRNAs, since they do not possess the required components to initiate the translation of mRNA [23,29]. The eIF4F initiation factor complex plays a vital role in initiating translation by recognizing the 5' cap structure in a cap-dependent manner [23]. As the target of numerous cellular signaling pathways, eIF4F closely controls the translation in response to a multitude of environmental conditions including viral infection [30]. In contrast, viral infections often cause dysregulation of eIF4F expression to benefit its replication. Vesicular stomatitis virus (VSV) was reported to cause modifications of the eIF4F complex to inhibit host protein synthesis [31]. Human Cytomegalovirus (HCMV) replication was demonstrated to increase the overall abundance of the eIF4F components and promote assembly of the eIF4F complexes [32]. The cellular cap-dependent protein level was reported to be rapidly inhibited by foot-and-mouth disease virus (FMDV) via inducing the cleavage of eIF4G [33]. However, we did not find remarkably altered expression levels of the components of eIF4F, including eIF4A and eIF4E, upon rotavirus infection (Supplementary Figure S1).

The eIF4F is a tripartite complex composed of three components including a cap-binding subunit (eIF4E), an RNA helicase (eIF4A), and a large molecular scaffold (eIF4G) that is associated with eIF3-bound 40S ribosome subunits [30]. These three components of the eIF4F complex were reported to closely regulate the life cycle of various viruses either promoting or restricting the infection. By treating influenza virus infected cells with Hippuristanol, a sterol, which is able to suppress RNA binding, ATPase, and helicase activities to block eIF4A-dependent translation, which demonstrated that eIF4A fully determines the translation of influenza virus mRNAs [34]; however, eIF4E does not affect influenza virus protein synthesis [29]. Hepatitis E virus (HEV) requires all three components of eIF4F to replicate in the host [35]. The protein synthesis of Junin virus (JUNV), Tacaribe virus (TCRV), and Pichinde virus (PICV) requires the participation of eIF4A and eIF4G but not eIF4E [36]. The eIF4F complex is required for maintaining translation efficiency of HCMV at the start of infection; while viral protein synthesis becomes increasingly insensitive to inhibition of eIF4F complex at late stage of virus infection [37]. Cencic et al. demonstrated that blocking the interaction between eIF4E

and eIF4G by a small molecule was capable of remarkably suppressing corovarius replication [24]. Rotavirus mRNAs are capped but not polyadenylated, and its NSP3 is capable of binding to eIF4G to stabilize the eIF4E–eIF4G interaction [10]. However, knockdown of NSP3 did not influence the synthesis of viral proteins, indicating that it is not involved in viral mRNA translation and virus replication [38]. We have previously confirmed that the PI3K-Akt-mTOR pathway sustains rotavirus infection via its downstream effector 4E-BP1 [39], which provokes us to further investigate the effect of eIF4E on rotavirus infection, since mTOR exerts the function of splitting the 4E-BP1-eIF4E dimer via phosphorylating 4E-BP1 [40]. Unexpectedly, we found that blocking the three components of the eIF4F complex promotes rotavirus infection (Figure 1, Figure 2, Figure 3, and Figure 4). This suggests that the inhibitory effect of eIF4F on rotavirus might be via another scenario other than the regulating of the capping process of viral mRNA. PDCD4 is capable of directly inhibiting the helicase activity of eIF4A by competing its binding to eIF4G to suppress the activity of the eIF4F complex [41]. Consistently, we found that blocking PDCD4 was capable of inhibiting rotavirus infection (Figure 5), which is in agreement with the effect of the eIF4F complex on rotavirus infection. Herein, our findings suggest that the eIF4F complex exerts inhibitory effects on rotavirus infection.

Mounting evidence reveals that the eIF4F complex perverts the interferon signaling pathway that exerts a pivotal role in defensing various viruses. Viruses often trigger a cascade of event to activate certain transcription factors, such as IRF3, IRF7, and NF- B, after being recognized by pattern-recognition receptors (e.g., Toll-like receptors), which eventually enhances interferon-β (IFN-β) to exert antiviral effects [27]. It was confirmed that the dephosphorylation of eIF4E was able to stimulate the NF-κB pathway to promote the production of type I interferon [27]. The eIF4F complex was demonstrated to closely regulate the translation of STAT1 mRNA [28]. In 4E-BP1-/- and 4E-BP2-/- double knockout mouse embryonic fibroblasts (MEF), it was found that type-I IFN was strongly promoted through enhancing the expression of IRF7 mRNA [26]. The binding of eIF4E to eIF4G may be involved in the translation of IRF7 mRNA [42]. Consistently, we demonstrated that knockdown and knockout of eIF4E and eIF4G were capable of suppressing the protein level of IRF1 and IRF7 (Figure 6). Importantly, we confirmed that IRF1 and IRF7 per se were able to significantly inhibit rotavirus replication (Figure 6). Thus, we have provided a possible novel insight into how the eIF4F complex regulates rotavirus replication.

In summary, this study has demonstrated that the three components of the eIF4F complex can remarkably inhibit rotavirus infection. The negative regulator of the eIF4F complex, PDCD4, inhibits rotavirus replication. The effect of eIF4F complex on rotavirus replication is through regulating the protein level of certain antiviral proteins including IRF1 and IRF7 that exerting remarkable antiviral effect against rotavirus. Hereto, this study revealed new insight in the regulation of eIF4F on rotavirus replication, and the eIF4F complex may represent as important targets for the development of new antivirals and antiviral therapies against rotavirus infection.

4. MATERIALS AND METHODS

4.1. Cell culture and Virus

All cells used in the study were grown in Dulbecco's Modified Eagle Medium (DMEM, Lonza, Verviers, Belguim) containing 20% (v/v) heat-inactivated fetal calve serum (FCS) (Hyclone, Lonan, Utah) and penicillin (100 IU/mL)/ streptomycin (100 mg/mL) (P/S) Invitrogen-Gibco) at 37°C in a humidified 5% CO2 incubator.

Simian rotavirus SA11 was used and prepared as described previously [39,43].

4.2. Inoculation of SA11 Rotavirus in cells

The inoculation method of SA11 rotavirus was described previously [6,44]. Briefly, cell monolayers were incubated with SA11 rotavirus (MOI = 0.7) at 37°C with 5% CO2 for 60 min for infection, followed by removing unbound viral particles by washing with cold PBS three times, followed by adding culture medium (FCS free) containing 5 µg/mL of trypsin and indicative drugs. Thereafter, cells were incubated at 37oC in a humidified 5% CO2 incubator. Viral titer was detected by RT-qPCR after 48 h inoculation.

4.3. Real-time quantitative reverse transcription PCR (RT-qPCR) analyses

Total RNA was isolated using NucleoSpin® RNA kit (MACHEREY-NAGEL, Düren, Germany) according to the manufacturer's instructions. The extracted RNA was dissolved in diethylpyrocarbonate (DEPC)-treated water, and its concentration was measured using a

Nanodrop ND-1000 (Wilmington, DE, USA). The 500 ng of total RNA was used for cDNA synthesis using the reverse transcription system from TAKARA (TAKARA BIO INC) according to manufacturer's instructions. The resultant cDNA was diluted and used for evaluating gene expression with corresponding primers. All RT-qPCR experiments were performed by SYBR-Green-based (Applied Biosystems SYBR Green PCR Master Mix; Thermo Fisher Scientific Life Scienc; Carlsbad, CA, USA) real-time PCR with the StepOnePlus System (Thermo Fisher Scientific Life Sciences). The expression of target mRNAs was normalized to the glyceraldehyde 3-phosphate dehydrogenase (GAPDH) mRNA. The relative mRNA levels of target genes were expressed as 2-ΔΔCt, in which ΔΔCt = (ΔCtTarget - ΔCtGAPDH) treatment - (ΔCtTarget - ΔCtGAPDH) control. Gene primers for RT-qPCR were listed in supplementary Table S1.

4.4. Gene knockdown by shRNA

Lentiviral shRNA vectors, targeting eIF4A, eIF4E, eIF4B, and PDCD4 or non-targeted control lentivirus was prepared in 293T cells in a 6-well-plate using a standard third-generation packaging system (All shRNA primers were listed in supplementary Table S2).

Cell monolayers were transfected with lentiviral vectors for three days, followed by screening by puromycin (8 µg/mL) to obtain stable clones, and the knockdown effect was detected by western blot.

4.5. Gene knockout by clustered regularly interspaced short palindromic repeats (CRISPR/Cas9) assay

The sgRNAs against eIF4A, eIF4E, eIF4G (primers were listed in supplementary Table S3) were designed using freely available online tools (https://www.genscript.com/gRNA-database.html). Oligos were annealed according to the manufacturer's protocol (37°C for 30 min; 95°C for 5 min and then ramp down to 25°C at 5°C/min). Subsequently, annealed oligos were ligated into Lenti CRISPR v2, followed by transforming 10 µL of electrocomp™cells (ThermoFisher SCIENTIFIC, Carlsbad, USA) with 5 µL of annealed oligos, and then incubated at 37°C for overnight. 2–3 colonies were picked up and cultured in LB medium, followed by performing a sequence verification. The verified colony was expanded in a LB containing

Ampicillin culture (100 μg/mL, SIGMA-ALDRICH, Saint Louis, USA) and DNA was isolated by using DNA extraction kit (ThermoFisher SCIENTIFIC) according to manufacturer's protocol. CRISPR DNA was co-transfected with packaging plasmids including pVSV-G, pMD, and pREV into HEK293T cells and lentiviral vectors were harvested.

Cell monolayers were transfected with lentiviral vectors for three days, followed by screening by puromycin (8 μg/mL) to obtain stable clones, and the knockdown effect was detected by western blot.

4.6. The 3-(4, 5)-dimethylthiahiazo (-z-y1)-3, 5-di- phenytetrazoliumromide (MTT) assay

MTT assay was used to evaluate cell viability, and the cells were seeded into 96-well plates (5000 cells/well). Then, the viable cells were quantified at indicated time points by adding 10 μL 5 mg/mL MTT per well, and the cells were incubated for an aditional 3 h in a humidified incubator. Thereafter, medium containing MTT was removed, and a total of 100 μL dimethyl sulfoxide (DMSO) was added, followed by measuring the absorbance (490 nm) after 50 min inoculation.

4.7. Western blot

Western blot was described previously [6]. Briefly, cells were lysed using Laemmli buffer containing 10% dithiothreitol (DTT, Thermo Fisher Scientific, Carlsbad, USA), and then denatured by heating at $95^{\circ}C$ for 5 min. Proteins were detected with antibodies against eIF4A (Cell Signaling Technology, Danvers, USA), eIF4E (Cell Signaling Technology), eIF4G (Cell Signaling Technology), PDCD4 (Cell Signaling Technology), and SA11 rotavirus VP4 (provided by professor Harry Greenberg, Stanford University School of Medicine, USA). The bound antibodies were visualized with Odyssey (LI-COR Biosciences, USA). The β-actin (Santa Cruz) was used as a loading control.

4.8. Statistics

All numerical results are reported as Mean ± Standard Error of Mean (SEM). The statistical significance of differences between means was assessed with the Mann–Whitney test using

GraphPad Prism 5 (stationary-pc/mac version; GraphPad Software Inc., La Jolla, CA, USA). The statistical significance was defined as P $\leqslant$ 0.05.

REFERENCE

1. Tate, J. E.; Burton, A. H.; Boschi-Pinto, C.; Steele, A. D.; Duque, J.; Parashar, U. D., 2008 estimate of worldwide rotavirus-associated mortality in children younger than 5 years before the introduction of universal rotavirus vaccination programmes: a systematic review and meta-analysis. *Lancet Infect Dis* **2012,** 12, (2), 136-41.

2. Tate, J. E.; Burton, A. H.; Boschi-Pinto, C.; Parashar, U. D., Global, Regional, and National Estimates of Rotavirus Mortality in Children <5 Years of Age, 2000-2013. *Clin Infect Dis* **2016,** 62 Suppl 2, S96-S105.

3. Bines, J. E.; Danchin, M.; Jackson, P.; Handley, A.; Watts, E.; Lee, K. J.; West, A.; Cowley, D.; Chen, M. Y.; Barnes, G. L.; Justice, F.; Buttery, J. P.; Carlin, J. B.; Bishop, R. F.; Taylor, B.; Kirkwood, C. D., Safety and immunogenicity of RV3-BB human neonatal rotavirus vaccine administered at birth or in infancy: a randomised, double-blind, placebo-controlled trial. *Lancet Infect Dis* **2015,** 15, (12), 1389-97.

4. Vesikari, T.; Karvonen, A.; Prymula, R.; Schuster, V.; Tejedor, J. C.; Cohen, R.; Meurice, F.; Han, H. H.; Damaso, S.; Bouckenooghe, A., Efficacy of human rotavirus vaccine against rotavirus gastroenteritis during the first 2 years of life in European infants: randomised, double-blind controlled study. *Lancet* **2007,** 370, (9601), 1757-63.

5. Yin, Y.; Metselaar, H. J.; Sprengers, D.; Peppelenbosch, M. P.; Pan, Q., Rotavirus in organ transplantation: drug-virus-host interactions. *Am J Transplant* **2015,** 15, (3), 585-93.

6. Yin, Y.; Bijvelds, M.; Dang, W.; Xu, L.; van der Eijk, A. A.; Knipping, K.; Tuysuz, N.; Dekkers, J. F.; Wang, Y.; de Jonge, J.; Sprengers, D.; van der Laan, L. J.; Beekman, J. M.; Ten Berge, D.; Metselaar, H. J.; de Jonge, H.; Koopmans, M. P.; Peppelenbosch, M. P.; Pan, Q., Modeling rotavirus infection and antiviral therapy using primary intestinal organoids. *Antiviral Res* **2015,** 123, 120-31.

7. Condemine, W.; Eguether, T.; Courousse, N.; Etchebest, C.; Gardet, A.; Trugnan, G.; Chwetzoff, S., The C-terminus of rotavirus VP4 protein contains an actin binding domain which requires co-operation with the coiled-coil domain for actin remodeling. *J Virol* **2018**.

8. Li, Y.; Xue, M.; Yu, L.; Luo, G.; Yang, H.; Jia, L.; Zeng, Y.; Li, T.; Ge, S.; Xia, N., Expression and characterization of a novel truncated rotavirus VP4 for the development of a recombinant rotavirus vaccine. *Vaccine* **2018,** 36, (16), 2086-2092.

9. Imai, M.; Akatani, K.; Ikegami, N.; Furuichi, Y., Capped and conserved terminal structures in human rotavirus genome double-stranded RNA segments. *J Virol* **1983,** 47, (1), 125-36.

10. Vende, P.; Piron, M.; Castagne, N.; Poncet, D., Efficient translation of rotavirus mRNA requires simultaneous interaction of NSP3 with the eukaryotic translation initiation factor eIF4G and the mRNA 3' end. *J Virol* **2000,** 74, (15), 7064-71.

11. Gratia, M.; Sarot, E.; Vende, P.; Charpilienne, A.; Baron, C. H.; Duarte, M.; Pyronnet, S.; Poncet, D., Rotavirus NSP3 Is a Translational Surrogate of the Poly(A) Binding Protein-Poly(A) Complex. *J Virol* **2015,** 89, (17), 8773-82.

12. Mamane, Y.; Petroulakis, E.; LeBacquer, O.; Sonenberg, N., mTOR, translation initiation and cancer. *Oncogene* **2006,** 25, (48), 6416-22.

13. Gingras, A. C.; Raught, B.; Sonenberg, N., eIF4 initiation factors: effectors of mRNA recruitment to ribosomes and regulators of translation. *Annu Rev Biochem* **1999,** 68, 913-63.

14. Zan-Kowalczewska, M.; Bretner, M.; Sierakowska, H.; Szczesna, E.; Filipowicz, W.; Shatkin, A. J., Removal of 5'-terminal m7G from eukaryotic mRNAs by potato nucleotide pyrophosphatase and its effect on translation. *Nucleic Acids Res* **1977,** 4, (9), 3065-81.

15. Montero, H.; Garcia-Roman, R.; Mora, S. I., eIF4E as a control target for viruses. *Viruses* **2015,** 7, (2), 739-50.

16. Malka-Mahieu, H.; Newman, M.; Desaubry, L.; Robert, C.; Vagner, S., Molecular Pathways: The eIF4F Translation Initiation Complex-New Opportunities for Cancer Treatment. *Clin Cancer Res* **2017,** 23, (1), 21-25.

17.   Pisera, A.; Campo, A.; Campo, S., Structure and functions of the translation initiation factor eIF4E and its role in cancer development and treatment. *J Genet Genomics* **2018,** 45, (1), 13-24.

18.   Chang, Y.; Huh, W. K., Ksp1-dependent phosphorylation of eIF4G modulates post-transcriptional regulation of specific mRNAs under glucose deprivation conditions. *Nucleic Acids Res* **2018,** 46, (6), 3047-3060.

19.   Biyanee, A.; Ohnheiser, J.; Singh, P.; Klempnauer, K. H., A novel mechanism for the control of translation of specific mRNAs by tumor suppressor protein Pdcd4: inhibition of translation elongation. *Oncogene* **2015,** 34, (11), 1384-92.

20.   Dennis, M. D.; Jefferson, L. S.; Kimball, S. R., Role of p70S6K1-mediated phosphorylation of eIF4B and PDCD4 proteins in the regulation of protein synthesis. *J Biol Chem* **2012,** 287, (51), 42890-9.

21.   Gale, M., Jr.; Tan, S. L.; Katze, M. G., Translational control of viral gene expression in eukaryotes. *Microbiol Mol Biol Rev* **2000,** 64, (2), 239-80.

22.   Walsh, D., Manipulation of the host translation initiation complex eIF4F by DNA viruses. *Biochem Soc Trans* **2010,** 38, (6), 1511-6.

23.   Chaudhry, Y.; Nayak, A.; Bordeleau, M. E.; Tanaka, J.; Pelletier, J.; Belsham, G. J.; Roberts, L. O.; Goodfellow, I. G., Caliciviruses differ in their functional requirements for eIF4F components. *J Biol Chem* **2006,** 281, (35), 25315-25.

24.   Cencic, R.; Desforges, M.; Hall, D. R.; Kozakov, D.; Du, Y.; Min, J.; Dingledine, R.; Fu, H.; Vajda, S.; Talbot, P. J.; Pelletier, J., Blocking eIF4E-eIF4G interaction as a strategy to impair coronavirus replication. *J Virol* **2011,** 85, (13), 6381-9.

25.   Boisnard, A.; Albar, L.; Thiemele, D.; Rondeau, M.; Ghesquiere, A., Evaluation of genes from eIF4E and eIF4G multigenic families as potential candidates for partial resistance QTLs to Rice yellow mottle virus in rice. *Theor Appl Genet* **2007,** 116, (1), 53-62.

26.   Colina, R.; Costa-Mattioli, M.; Dowling, R. J.; Jaramillo, M.; Tai, L. H.; Breitbach, C. J.; Martineau, Y.; Larsson, O.; Rong, L.; Svitkin, Y. V.; Makrigiannis, A. P.; Bell, J. C.; Sonenberg, N., Translational control of the innate immune response through IRF-7. *Nature* **2008,** 452, (7185), 323-8.

27.   Herdy, B.; Jaramillo, M.; Svitkin, Y. V.; Rosenfeld, A. B.; Kobayashi, M.; Walsh, D.; Alain, T.; Sean, P.; Robichaud, N.; Topisirovic, I.; Furic, L.; Dowling, R. J. O.; Sylvestre, A.; Rong, L.; Colina, R.; Costa-Mattioli, M.; Fritz, J. H.; Olivier, M.; Brown, E.; Mohr, I.; Sonenberg, N., Translational control of the activation of transcription factor NF-kappaB and production of type I interferon by phosphorylation of the translation factor eIF4E. *Nat Immunol* **2012,** 13, (6), 543-550.

28.   Cerezo, M.; Guemiri, R.; Druillennec, S.; Girault, I.; Malka-Mahieu, H.; Shen, S.; Allard, D.; Martineau, S.; Welsch, C.; Agoussi, S.; Estrada, C.; Adam, J.; Libenciuc, C.; Routier, E.; Roy, S.; Desaubry, L.; Eggermont, A. M.; Sonenberg, N.; Scoazec, J. Y.; Eychene, A.; Vagner, S.; Robert, C., Translational control of tumor immune escape via the eIF4F-STAT1-PD-L1 axis in melanoma. *Nat Med* **2018**.

29.   Burgui, I.; Yanguez, E.; Sonenberg, N.; Nieto, A., Influenza virus mRNA translation revisited: is the eIF4E cap-binding factor required for viral mRNA translation? *J Virol* **2007,** 81, (22), 12427-38.

30.   Walsh, D.; Arias, C.; Perez, C.; Halladin, D.; Escandon, M.; Ueda, T.; Watanabe-Fukunaga, R.; Fukunaga, R.; Mohr, I., Eukaryotic translation initiation factor 4F architectural alterations accompany translation initiation factor redistribution in poxvirus-infected cells. *Mol Cell Biol* **2008,** 28, (8), 2648-58.

31.   Connor, J. H.; Lyles, D. S., Vesicular stomatitis virus infection alters the eIF4F translation initiation complex and causes dephosphorylation of the eIF4E binding protein 4E-BP1. *J Virol* **2002,** 76, (20), 10177-87.

32.   Walsh, D.; Perez, C.; Notary, J.; Mohr, I., Regulation of the translation initiation factor eIF4F by multiple mechanisms in human cytomegalovirus-infected cells. *J Virol* **2005,** 79, (13), 8057-64.

33. Strong, R.; Belsham, G. J., Sequential modification of translation initiation factor eIF4GI by two different foot-and-mouth disease virus proteases within infected baby hamster kidney cells: identification of the 3Cpro cleavage site. *J Gen Virol* **2004,** 85, (Pt 10), 2953-62.

34. Yanguez, E.; Castello, A.; Welnowska, E.; Carrasco, L.; Goodfellow, I.; Nieto, A., Functional impairment of eIF4A and eIF4G factors correlates with inhibition of influenza virus mRNA translation. *Virology* **2011,** 413, (1), 93-102.

35. Zhou, X.; Xu, L.; Wang, Y.; Wang, W.; Sprengers, D.; Metselaar, H. J.; Peppelenbosch, M. P.; Pan, Q., Requirement of the eukaryotic translation initiation factor 4F complex in hepatitis E virus replication. *Antiviral Res* **2015,** 124, 11-9.

36. Linero, F.; Welnowska, E.; Carrasco, L.; Scolaro, L., Participation of eIF4F complex in Junin virus infection: blockage of eIF4E does not impair virus replication. *Cell Microbiol* **2013,** 15, (10), 1766-82.

37. Lenarcic, E. M.; Ziehr, B.; De Leon, G.; Mitchell, D.; Moorman, N. J., Differential role for host translation factors in host and viral protein synthesis during human cytomegalovirus infection. *J Virol* **2014,** 88, (3), 1473-83.

38. Montero, H.; Arias, C. F.; Lopez, S., Rotavirus Nonstructural Protein NSP3 is not required for viral protein synthesis. *J Virol* **2006,** 80, (18), 9031-8.

39. Yin, Y.; Dang, W.; Zhou, X.; Xu, L.; Wang, W.; Cao, W.; Chen, S.; Su, J.; Cai, X.; Xiao, S.; Peppelenbosch, M. P.; Pan, Q., PI3K-Akt-mTOR axis sustains rotavirus infection via the 4E-BP1 mediated autophagy pathway and represents an antiviral target. *Virulence* **2018,** 9, (1), 83-98.

40. Ruoff, R.; Katsara, O.; Kolupaeva, V., Cell type-specific control of protein synthesis and proliferation by FGF-dependent signaling to the translation repressor 4E-BP. *Proc Natl Acad Sci U S A* **2016,** 113, (27), 7545-50.

41. Wei, N. A.; Liu, S. S.; Leung, T. H.; Tam, K. F.; Liao, X. Y.; Cheung, A. N.; Chan, K. K.; Ngan, H. Y., Loss of Programmed cell death 4 (Pdcd4) associates with the progression of ovarian cancer. *Mol Cancer* **2009,** 8, 70.

42. Petersson, J.; Ageberg, M.; Sanden, C.; Olofsson, T.; Gullberg, U.; Drott, K., The p53 target gene TRIM22 directly or indirectly interacts with the translation initiation factor eIF4E and inhibits the binding of eIF4E to eIF4G. *Biol Cell* **2012,** 104, (8), 462-75.

43. Yin, Y.; Chen, S.; Hakim, M. S.; Wang, W.; Xu, L.; Dang, W.; Qu, C.; Verhaar, A. P.; Su, J.; Fuhler, G. M.; Peppelenbosch, M. P.; Pan, Q., 6-Thioguanine inhibits rotavirus replication through suppression of Rac1 GDP/GTP cycling. *Antiviral Res* **2018,** 156, 92-101.

44. Yin, Y.; Wang, Y.; Dang, W.; Xu, L.; Su, J.; Zhou, X.; Wang, W.; Felczak, K.; van der Laan, L. J.; Pankiewicz, K. W.; van der Eijk, A. A.; Bijvelds, M.; Sprengers, D.; de Jonge, H.; Koopmans, M. P.; Metselaar, H. J.; Peppelenbosch, M. P.; Pan, Q., Mycophenolic acid potently inhibits rotavirus infection with a high barrier to resistance development. Antiviral Res 2016, 133, 41-9.

Supplementary Information

Supplementary table 1. qRT-PCR primers (human gene) used in the study, from 5' to 3'.

| Gene name	Sense primer	Antisense primer
eIF4A	AAGCCGTGGATTCAAGGACCAG	CACCTCAAGCACATCAGAAGGC
eIF4E	ATGCCTGGCTGTGACTACTCAC	GAGGTCACTTCGTCTCTGCTGT
eIF4G	GCCATTTCAGAGCCCAACTTCTC	CGGAAGTTCACAGTCACTGTTGG
PDCD4	ACTGTGCCAACCAGTCCAAAGG	CCTCCACATCATACACCTGTCC
GAPDH	TGTCCCCACCCCCAATGTATC	CTCCGATGCCTGCTTCACTACCTT

Supplementary table 2. shRNA target sequences.

ShRNA	Sequence
sheIF4A-1	CCGGGCCGTGTGTTTGATATGCTTACTCGAGTAAGCATATCAAACACACGGCTTTTTG
sheIF4A-2	CCGGGCCGTAAAGGTGTGGCTATTACTCGAGTAATAGCCACACCTTTACGGCTTTTTG
sheIF4A-3	CCGGCCTTGTATCAAGGGTTATGATCTCGAGATCATAACCCTTGATACAAGGTTTTTG
sheIF4A-4	CCGGCGAAATGTTAAGCCGTGGATTCTCGAGAATCCACGGCTTAACATTTCGTTTTTG
sheIF4E-1	CCGGCCACTCTGTAATAGTTCAGTACTCGAGTACTGAACTATTACAGAGTGGTTTTTG
sheIF4E-2	CCGGCCAAAGATAGTGATTGGTTATCTCGAGATAACCAATCACTATCTTTGGTTTTTG
sheIF4E-3	CCGGCCGACTACAGAAGAGGAGAAACTCGAGTTTCTCCTCTTCTGTAGTCGGTTTTTG
sheIF4E-4	CCGGCGGCTGATCTCCAAGTTTGATCTCGAGATCAAACTTGGAGATCAGCCGTTTTTG
sheIF4G-1	CCGGCCCTACAGAATTTGGGACCTACTCGAGTAGGTCCCAAATTCTGTAGGGTTTTTG
sheIF4G-2	CCGGGCCCTTGTAGTGACCTTAGAACTCGAGTTCTAAGGTCACTACAAGGGCTTTTTG
sheIF4G-3	CCGGGCAGATAGTATCCAACACGTTCTCGAGAACGTGTTGGATACTATCTGCTTTTTG
sheIF4G-4	CCGGCCCAAGTAATGATGATCCCTTCTCGAGAAGGGATCATCATTACTTGGGTTTTTG
shPDCD4-1	CCGGGCGGTTTGTAGAAGAATGTTTCTCGAGAAACATTCTTCTACAAACCGCTTTTTG
shPDCD4-2	CCGGCTGACCTTTGTGGGACAGTAACTCGAGTTACTGTCCCACAAAGGTCAGTTTTTG
shPDCD4-3	CCGGCTACCATTACTGTAGACCAAACTCGAGTTTGGTCTACAGTAATGGTAGTTTTTG

**Supplementary table 3**. Sg RNA Primers (human gene) used in the study, from 5' to 3'.

Sg RNA	Sense primer	Antisense primer
eIF4A	CACCGCCCCCGATACAGGCGTGAC	CGGGGGCTATGTCCGCACTGCAAA
eIF4E	CACCGGGACGTCCCCACTTGTCCG	CCCTGCAGGGGTGAACAGGCCAAA
eIF4G	CACCGCTATCCAGTCGAACACCCGC	CGATAGGTCAGCTTGTGGGCGCAAA

Supplementary Figures:
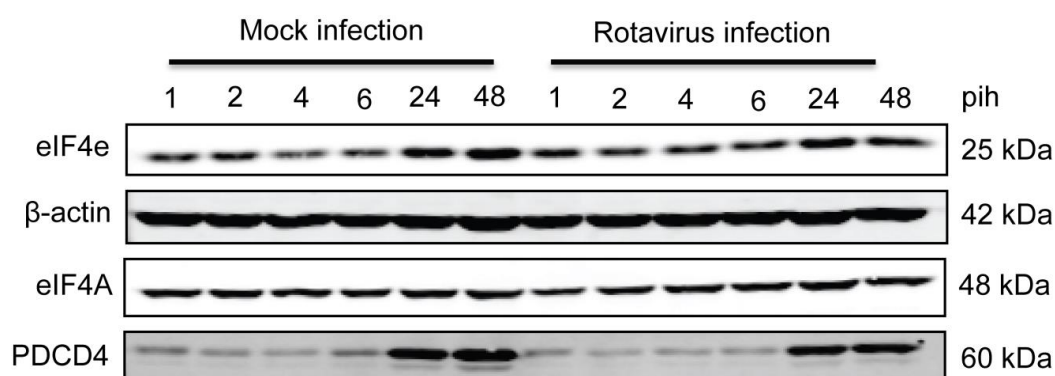
Supplementary Fig. 1. The effect of rotavirus and mock infection (1, 2, 4, 6, 24 and 48 hr) on the expression level of eIF4E, eIF4A and PDCD4. Western blot assay detected the expression of eIF4E, eIF4A and PDCD4 after 1, 2, 4, 6, 24 and 48 hr post-infection by rotavirus and mock infection in Caco2 cells.
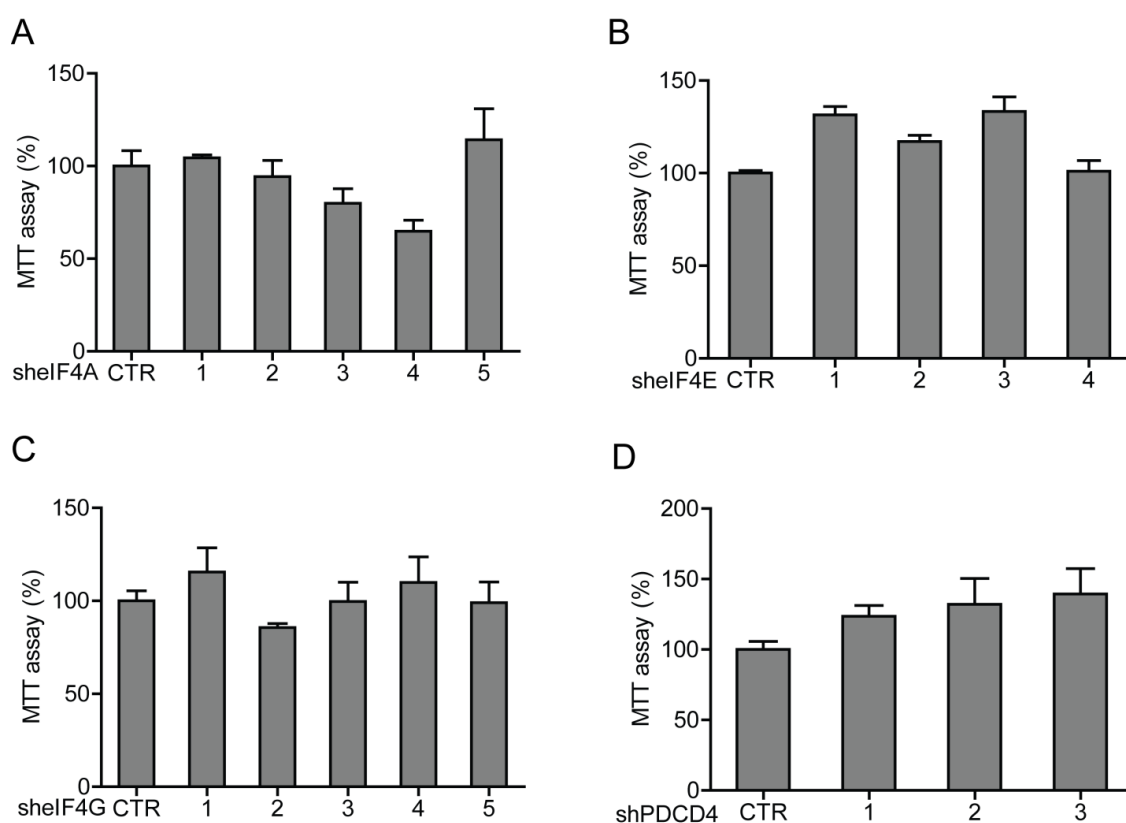
Supplementary Fig. 2. Effect of shRNA against eIF4A (A), eIF4E (B), eIF4G (C) and PDCD4 (D) on host cell viability determined by MTT assays.

Chapter 4

Basal interferon signaling and therapeutic use of interferons in controlling rotavirus infection in human intestinal cells and organoids

Mohamad S. Hakim, **<u>Sunrui Chen</u>**, Shihao Ding, Yuebang Yin, Aqsa Ikram, Xiao-xia Ma, Wenshi Wang, Maikel P. Peppelenbosch, Qiuwei Pan

Abstract

Rotavirus (RV) primarily infects enterocytes and results in severe diarrhea, particularly in children. It is known that the host immune responses determine the outcome of viral infections. Following infections, interferons (IFNs) are produced as the first and the main anti-viral cytokines to combat the virus. Here we showed that RV predominantly induced type III IFNs (IFN-λ1), and to a less extent, type I IFNs (IFN-α and IFN-β) in human intestinal cells. However, it did not produce detectable IFN proteins and thus, was not sufficient to inhibit RV replication. In contrast, we revealed the essential roles of the basal IFN signaling in limiting RV replication by silencing *STAT1, STAT2* and *IRF9* genes. In addition, exogenous IFN treatment demonstrated that RV replication was able to be inhibited by all types of IFNs, both in human intestinal Caco2 cell line and in primary intestinal organoids. In these models, IFNs significantly upregulated a panel of well-known anti-viral IFN-stimulated genes (ISGs). Importantly, inhibition of the JAK-STAT cascade abrogated ISG induction and the anti-RV effects of IFNs. Thus, our study shall contribute to better understanding of the complex RV-host interactions and provide rationale for therapeutic development of IFN-based treatment against RV infection.

Keywords: immune responses; interferons; interferon-stimulated genes; JAK-STAT pathway; rotavirus

Introduction

Rotavirus (RV) is a member of the *Reoviridae* family that primarily infects mature enterocytes of the small intestinal villi. However, it can spread systemically to cause viremia and infection of multiple organs[1]. RV is the most frequent agent of severe dehydrating diarrhea episodes in children under five years of age[2]. Before introduction of RV vaccines, RV caused 9.8 billion of severe diarrhea episodes and 1.9 billion diarrhea-related deaths worldwide, with the highest burden in southeast Asian and African countries[3]. The incidence is lower especially in countries that have introduced oral RV vaccination[4].

Intestinal innate immune responses are the first line of defense to battle RV infection[5]. Recognition of RV viral proteins and double-stranded RNA by the host induces the production of cytokines, including interferons (IFNs)[6]. IFNs are potent anti-viral cytokines classified into three different groups, type I (IFN-α, IFN-β, IFN-δ, and others), type II (IFN-γ) and type III (IFN-λ1, IFN-λ2 and IFN-λ3) IFNs[7,8]. Some members are widely used in the clinic for treating viral infections or malignancy, whereas others are at stages of clinical development. Even though they bind to distinct receptors, they signal through a common, classical Janus kinase signal transducer and activator of transcription (JAK-STAT) pathway[8,9].

Once activated, STAT1 and STAT2 are phosphorylated and bind IFN regulatory factor 9 (IRF9) to form IFN stimulated gene factor 3 complex (ISGF3). ISGF3 subsequently translocates to the nuclues, inducing transcription of hundreds IFN-stimulated genes (ISGs) which cooperatively establish an anti-viral state that protects against various types of viruses[10]. Furthermore, IFN induction following RV recognition is essential to promote the development of adaptive, B-cell-mediated immune responses[11]. On the other hand, however, RV has developed effective strategies to evade the host immune response[12]. RV can inhibit IFN production in the infected cells[13] and also block the action of STAT1 and STAT2 proteins[14]. Viral nonstructural protein NSP1-mediated IFN inhibition has been shown to be associated with different levels of RV replication in primary mouse cells[15].

Detectable levels of IFN-α[16] and IFN-γ[17,18] were documented in chidlren with acute RV diarrhea, suggesting a role for these INFs in disease pathogenesis. Indeed, early *in vitro*[19-21] and animal studies in calves[22] and piglets[23] demonstrated anti-RV effects of both type I and II IFNs.

However, in the murine models of homologous RV infection, administration of type I (IFN-α and IFN-β) and II (IFN-γ) IFNs failed to protect the mice against RV infection[24]. In addition, mice deficient in type I or II IFN receptor signaling controlled RV infection as well as wild-type mice[24,25]. These results suggest a minor role of type I and II IFNs in controlling RV infection in mice. Interestingly, a more prominent function of type III IFNs in constraining viral infection was suggested by experimentation in mouse models[25,26]. Administration of IFN-λ conferred better protection against RV infection than IFN-α/β[25].

Because animal models do not always recapitulate the responsiveness in human, we therefore comprehensively assessed the role of endogenous and the therapeutic IFNs on RV infection in human intestinal cell line and primary intestinal organoids. We found that the basal JAK-STAT cascade is effective in restraining RV infection. Furthermore, RV is sensitive to inhibition by all three types of IFNs in both models. Our results strengthen the evidence of essential roles of IFN pathway in protecting the host against viral infection.

Results

RV infection modulates *IFN* gene expression

First, we investigated whether RV SA11 modulates the expression of the three types of *IFN* genes. Human intestinal Caco2 cells were infected with RV SA11 for 48 hours. An effective replication was shown by an increase in intracellular RNA level as well as secreted rotavirus in culture medium (Supplementary Fig. S1). In addition, immunofluorescence staining showed VP6-positive Caco2 cells at 48 hours after infection, indicating productive replications (Supplementary Fig. S2).

Relative RNA levels of *ifna, ifnb, ifng, il29* (IFN-λ1) and *il28* (IFN-λ2/IFN-λ3) genes were examined and compared to uninfected cells at 6, 24, 36 and 48 hours post infection. As shown in Fig. 1, RV infection had no major effect on the gene expression at 6 and 24 hours post-infection. At 36 hours after infection, only *il29* gene expression was notably increased by 3.4 ± 1.0 ($P < 0.05$) fold. Importantly, at 48 hours after infection, the expression of *ifna* and *ifnb* genes were significantly increased by 2.8 ± 0.6 ($P < 0.001$) and 2.8 ± 0.5 ($P < 0.01$) fold, respectively. A profound upregulation was observed on *il29* by 29.6 ± 10.7 fold ($P < 0.001$). No difference was found on *il28* gene expression. The expression level of *ifng* gene was

undetectable (data not shown). Together, our findings showed that RV SA11 infection preferentially induced *il29* (IFN-λ1) gene expression in Caco2 cells.
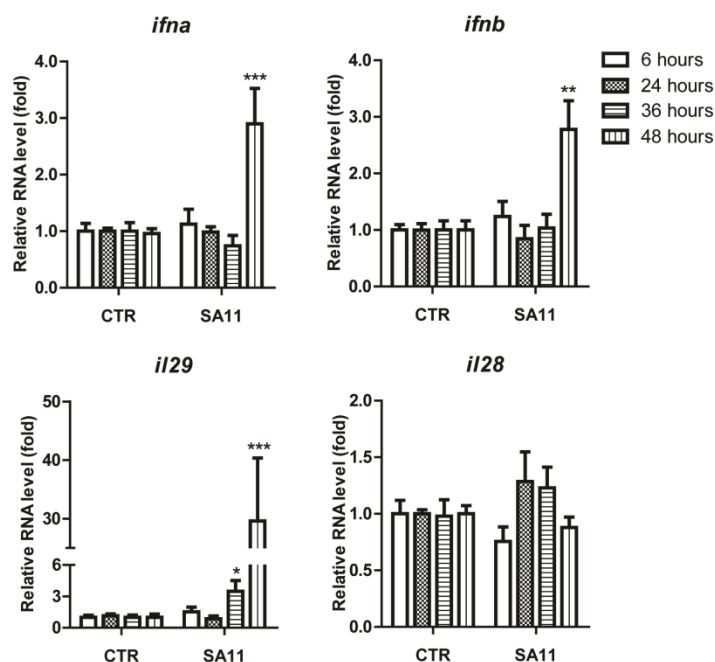

Figure 1. RV infection modulates IFN gene expression in Caco2 cells. Caco2 cells were infected with RV SA11. Relative RNA levels of *ifna, ifnb, il29* (IFN-λ1) and *il28* (IFN-λ2 and IFN-λ3) genes were examined at 6, 24, 36 and 48 hours post infection as compared to uninfected cells. Data were normalized to GAPDH and presented as means ± SEM. (n = 3 independent experiments with each of 3-4 replicates; **$P < 0.01$; ***$P < 0.0001$)

The increased expression of IFN genes does not result in production of detectable IFN protein and was not sufficient to limit RV SA11 replication

To examine whether the increased expression of IFN genes result in IFN production in our cell culture system, we collected the conditioned medium (supernatant) derived from control and SA11-infected Caco2 cells at 48 hours post-infection. Then, we performed IFN production bioassay by adding the conditioned medium into two highly IFN sensitive cell lines, Huh7-based ISRE-luciferase and HCV-luciferase reporter cell lines. As shown in Fig. 2A, the supernatant from SA11-infected Caco2 cells was not capable of stimulating ISRE reporter, while as low as 1 U/mL of IFN-α significantly induced ISRE-luc by 1.8 ± 0.2 fold ($P < 0.001$). Consistently, it was not able to diminish HCV replication, although as low as 0.1 IU/mL of IFN-α considerably reduced HCV-luc by 40 ± 7% fold ($P < 0.001$) (Fig. 2B).

The induced expression of IFN-α and IFN-λ1 proteins can signal via autocrine and paracrine manner to stimulate ISGs expression. Therefore, to confirm our previous findings from ISRE-luciferase cell lines, we also examined ISG expression in SA11-infected Caco2 cells. Despite a clear induction of IFN genes, we observed no upregulation of ISGs, both at 24 and 48 hours post-infection. At 48 hours, some ISGs were significantly downregulated by SA11 infection, including IRF1, IRF9, MX1 and IFIT3 (Fig. 2C).

To rule out the possibility that endogenous IFN produced (if any) following RV infection is sufficient to restrict RV replication, we investigated whether the inhibition of JAK proteins, the downstream elements of IFN receptor, influences RV replication. Treatment of JAK I inhibitor at 5 and 10 μM had no effect on RV replication (Fig. 2D). At those concentrations, the drug did not influence the cell viability as determined by MTT assay (Fig. 2E). Collectively, our results demonstrate that the increased expression of IFN genes during RV infection does not result in IFN production and consequently appears relatively unimportant for constraining RV replication in intestinal epithelial cells.

Basal IFN signaling is necessary to restrict RV replication

As no functional production of IFN is observed following RV infection, we investigated the possibility that constitutive ligand independent IFN signal transduction defends intestinal epithelial cells against RV replication. ISGF3 that consists of STAT1, STAT2 and IRF9 is a central complex in IFN signal transduction. We have previously reported that in the absence of IFN stimulation, unphosphorylated ISGF3 drives constitutive ISG expression in homeostatic conditions and is critical to provide immunity against hepatitis C (HCV) and E (HEV) virus infections[27]. It is thus possible that constitutive IFN signal transduction is important for counteracting RV in intestinal cells as well.

To test this possibility, we first transduced Caco2 cells with a lentiviral vector expressing STAT1- and STAT2-specific shRNA. A successful knockdown is shown in Fig. 3A and 3C. Supplementary Fig. S3 shows the quantification of knockdown efficiency. Importantly, shRNA-mediated STAT1 and STAT2 knockdown resulted in an increased RV replication by 3.8 ± 0.6 fold ($P < 0.01$) (Fig. 3B) and 13 ± 4.6 ($P < 0.001$) (Fig. 3D), respectively.

Next we investigated the role of IRF9. Two of three tested IRF9-specific shRNA (sh-2 and sh-3) exert a potent gene silencing capacity (Fig. 3E and Supplementary Fig. S3). Consistently, IRF9 KD led to 4.8 ± 1.0 fold elevation of RV replication as compared to sh-CTR transfected cells (P < 0.001) (Fig. 3F). Altogether, these results indicate that the integrity of ISGF3 complex is required to provide basal immunity against RV infections.
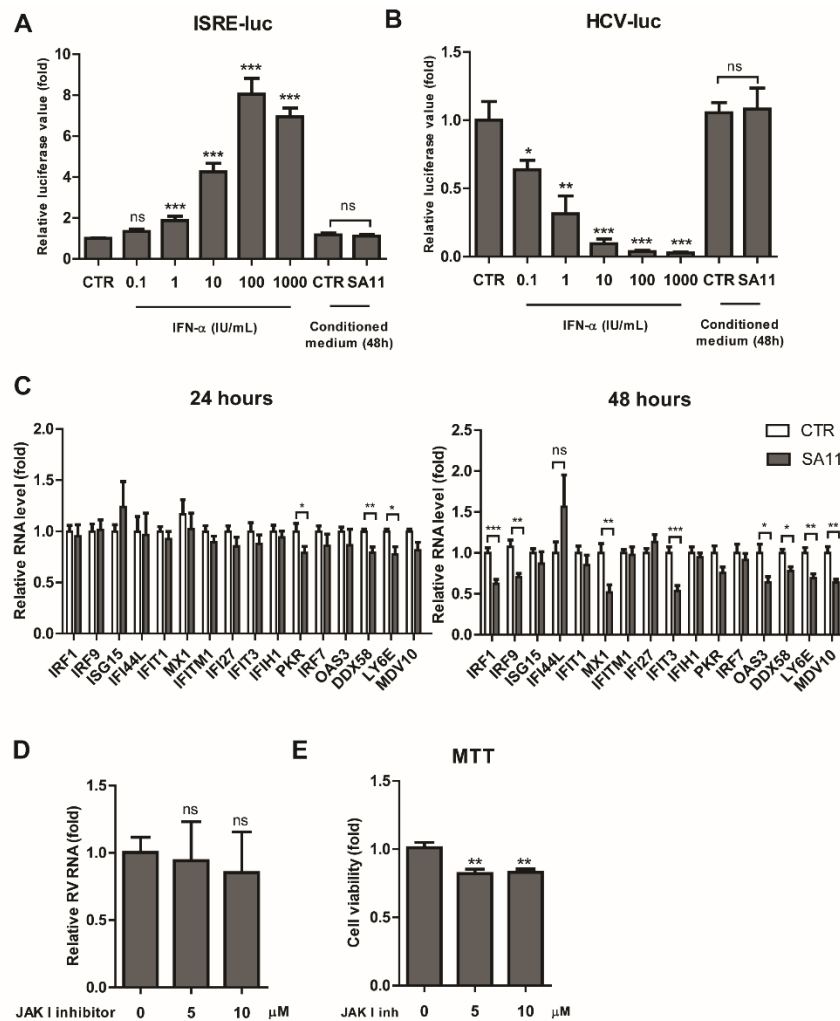

Figure 2. The increased expression of IFN genes does not result in production of detectable IFN protein and was not sufficient to limit RV SA11 replication. IFN production bioassay was performed in ISRE-luciferase **(A)** and HCV-luciferase **(B)** cell lines which are highly sensitive to IFN treatment. Conditioned medium derived from 48 hours post-RV infection on Caco2 cells was used (n = 3 independent experiments with each 2-3 replicates). **(C)** Caco2 cells were infected with RV SA11. Relative RNA levels of IFN-stimulated genes (ISGs) were examined at 24 and 48 hours post-infection as compared to uninfected cells (n = 3 independent experiments with each 2-3 replicates). **(D)** *Pan*-JAK I inhibitor had no effects on RV replication (n = 3 independent experiments with each 2-3 replicates). **(E)** *Pan*-JAK I inhibitor did not affect cell viability

as determined by MTT assay (OD_{490} value) at 48 hours of treatment (n = 3 independent experiments with each 2 replicates). Data were presented as means ± SEM., **$P < 0.01$; ***$P < 0.001$; ns, not significant.
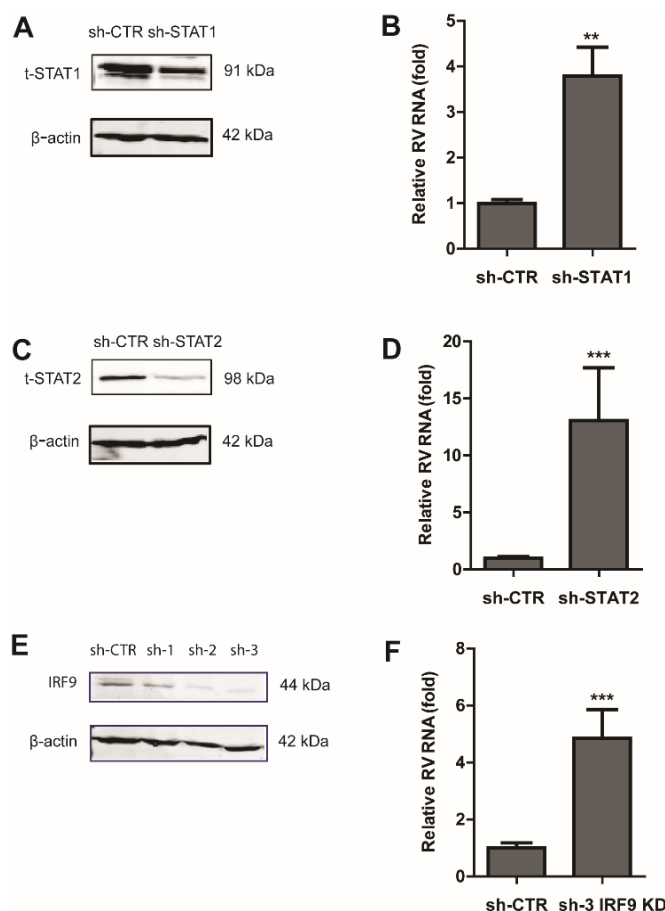

Figure 3. The key component of ISGF3 complex is necessary to restrict RV replication. (A) STAT1 knockdown by lentiviral shRNA vectors. Western blot analysis confirms a successful knockdown of total STAT1 protein. **(B)** Correspondingly, knockdown of STAT1 led to a significant increase of RV replication (n = 3 independent experiments with 3-4 replicates each). **(C)** Knockdwon of STAT2 by lentiviral shRNA vectors. Western blot analysis shows a potent decrease of total STAT2 protein level. **(D)** Similarly, silencing of STAT2 resulted in a prominent increase of RV RNA level (n = 3 independent experiments with 3-4 replicates each). **(E)** IRF9 knockdwon by lentiviral shRNA vectors. Western blot analysis shows a potent decrease of IRF9 protein level. **(F)** Knockdown of IRF9 led to a notable increase of RV replication (n = 3 independent experiments with 3-4 replicates each). Data were presented as means ± SEM., **$P < 0.01$; ***$P < 0.001$.

RV SA11 is sensitive to IFN treatment in human intestinal Caco2 cells and primary intestinal organoids

Since we did not find a significant role of endogenous IFN in restricting RV replication, we then investigated whether RV was sensitive to exogenous IFN treatment (Fig. 4A). Treatment of SA11-infected Caco2 cells with 100 and 1000 IU/mL of IFNα resulted in a potent inhibition of RV replication by 79 ± 4% ($P < 0.001$) and 98 ± 0.7% ($P < 0.001$) as measured in total RNA levels. Similarly, IFNβ treatment at 100 and 1000 IU/mL dose-dependently inhibited total viral RNA

levels by 60 ± 9% ($P < 0.01$) and 73 ± 7% ($P < 0.001$). Type II IFNs also strongly reduced RV replication, although the effects were not dose-dependent. At concentration of 100 and 1000 ng/mL, IFNγ restricted RV replication by 81 ± 6% ($P < 0.001$) and 68 ± 7% ($P < 0.01$). Analysis of intra and extracellular RNA levels also demonstrated the inhibition of RV replication by type I and II IFNs in Caco2 cells (Supplementary Fig. S4).

Next, we investigated anti-RV effects of type III IFNs. Treatment of SA11-infected Caco2 cells with 100 and 1000 ng/mL of IFNλ1 resulted in a notable restriction of RV replication by 76 ± 11% ($P < 0.01$) and 65 ± 6% ($P < 0.001$). Inhibition of RV replication was also observed with IFNλ2 treatment. At a concentration of 100 and 1000 ng/mL, IFNλ2 decreased RV replication by 61 ± 17% ($P < 0.01$) and 50 ± 7% ($P < 0.05$), respectively. At a similar concentration, IFNλ3 significantly dimished RV replication by 52 ± 7% ($P < 0.05$) and 62 ± 6% ($P < 0.01$). Analysis of intra and extracellular RNA levels also demonstrated the effects of type III IFNs in limiting rotavirus replication in Caco2 cells (Supplementary Fig. S4).

To further confirm the effects of various types of IFNs that we observed in the conventional 2D cell culture system, we employed a 3D culture model of primary intestinal organoids derived from one individual (P1) to more closely mimic the physiological situation *in vivo* (Fig. 4B). Treatment of SA11-infected organoid with 1000 IU/mL of IFNα and IFNβ led to a significant reduction of intracellular viral RNA levels by 73.9 ± 7.5% ($P < 0.05$) and 57.8 ± 7.7% ($P < 0.05$), respectively. Surprisingly, the inhibition by IFNγ was more pronounced. Treatment of SA11-infected organoid with 1000 ng/mL of IFNγ significantly reduced intracellular viral RNA levels by 99.5 ± 0.1% ($P < 0.01$) (Fig. 4C). Similarly, treatment with 1000 ng/mL of IFNλ1, IFNλ2 or IFNλ3 significantly diminished intracellular viral RNA levels by 70.2 ± 7.6% ($P < 0.01$), 78.2 ± 4.2% ($P < 0.01$) and 79.6 ± 3.6% ($P < 0.01$), respectively (Fig. 4C). Quantification of extracellular (secreted) RNA levels also showed a notable reduction of viral production (Supplementary Fig. S5). To confirm these findings, we obtained primary intestinal organoids from the second individual (P2). Similarly, treatment of SA11-infected organoid with IFNα (1000 IU/mL), IFNγ (1000 ng/mL) and IFNλ1 (1000 ng/mL) significantly reduced total viral RNA levels by 74.6 ± 5.1% ($P < 0.01$), 85.5 ± 4.4% ($P < 0.01$) and 71.4 ± 10.5% ($P < 0.01$), respectively (Supplementary Fig. S6A). Collectively, these results suggest that all type of IFNs effectively inhibit RV replication, both in 2D and 3D culture model system.

Sensitivity of patient-derived RV strains to type I, II and III IFNs

Next, we evaluated the sensitivity of patient-derived RV strains against different types of IFNs. We treated human RV (G1P[8]) with IFNα 100 IU/mL (as representative of type I IFN), IFNγ 100 ng/mL (type II IFN), IFNλ1 and IFNλ3 100 ng/mL (as representative of type III IFN) for 48 hours. Three out of four samples were sensitive to the inhibition by IFNα and all samples were inhibited by IFNγ (Fig. 5). Interestingly, only one sample which is sensitive to type III IFN treatment. Collectively, our data suggest that type I and II IFN more efficiently inhibit the replication of human RV strains as compared to type III IFN.

Figure 4. Exogenous treatment of type I, II and III IFNs inhibits RV SA11 infection. Antiviral activity of IFNα, IFNβ, IFNγ, IFNλ1, IFNλ2 and IFNλ3 treatment against RV SA11 infection on **(A)** Caco2 cells (n = 2-3 independent experiments with each of 3-4 replicates) and **(C)** organoids (n = 3 independent experiments with each of 2-3 replicates) at 48 hours after infection. Data were presented as means ± SEM., *P < 0.05; **P < 0.01; ***P < 0.001. **(B)** A representative picture of the morphology of human small intestinal organoid at day 4 post embedding in Matrigel. The organoid used in this experiment was derived from one individual (P1).
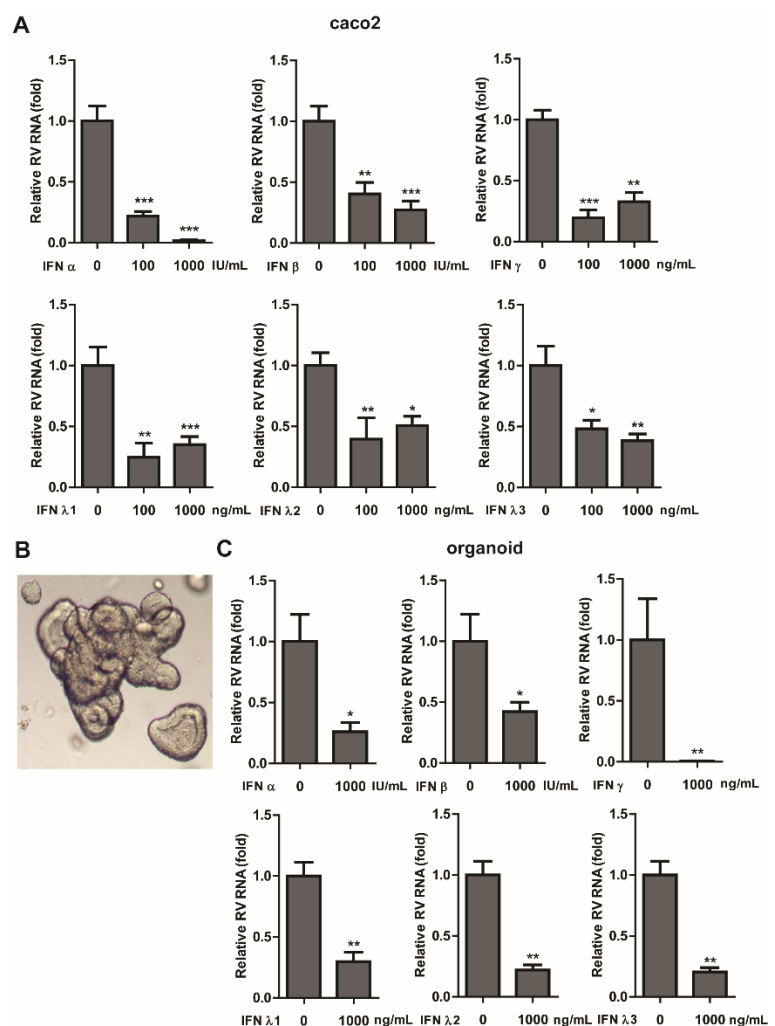
Induction of the known antiviral ISGs by all three types of IFNs

The observed anti-RV activity of type I, II and III IFNs prompted us to investigate whether all types of IFNs effectively induce the expression of known anti-viral ISGs in Caco2 cells and organoid. Although there are hundreds of ISGs, only a subset have broad or targeted antiviral effects[28]. We have selectively investigated the expression of those known antiviral ISGs. Indeed, treatment of Caco2 cells with recombinant human IFN-α (1000 IU/mL), IFN-γ (1000 ng/mL) and IFN-λ1 (1000 ng/mL) for 24 hours induced the expression a panel of ISGs (Fig. 6A). Similarly, they also efficiently induced ISGs in organoids derived from both P1 (Fig. 6B) and P2 (Supplementary Fig. S6B). Interestingly, we observed a variation of the type and extent of ISG induction with different IFN treatment. For example, IRF1 and RTP4 were more induced by IFN-γ as compared to IFN-α in Caco2 cells. In contrast, DDX60 and IFI6 were more induced by IFN-α as compared to IFN-γ (Fig. 6A). In organoid (P1), several ISGs were more efficiently induced by IFN-λ1 as compared to IFN-α and IFN-γ, including OASL, ISG15 and OAS1 (Fig. 6B).
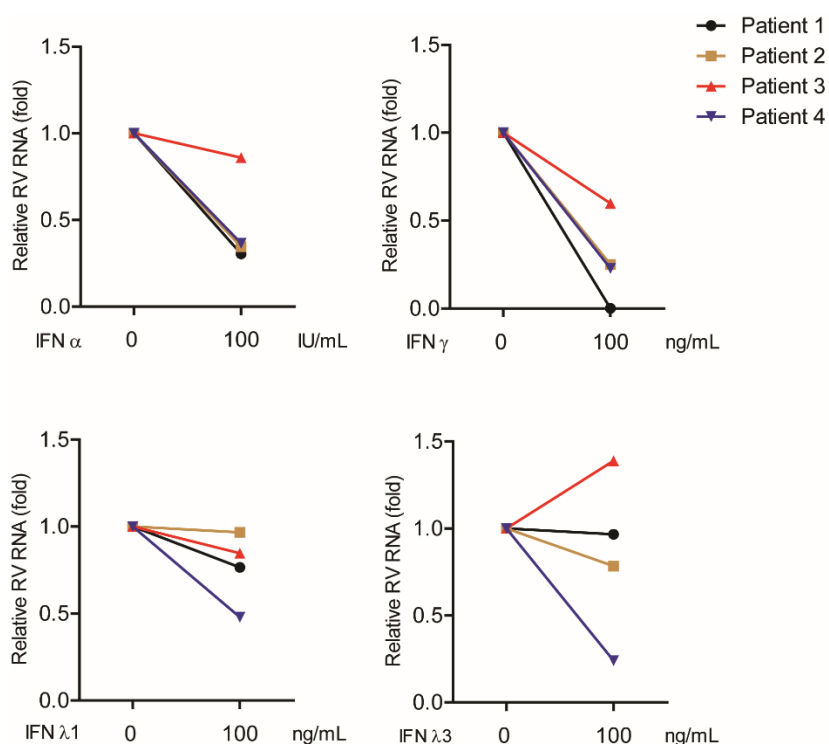
Figure 5. Sensitivity of patient-derived RV strains to type I, II and III IFNs. Caco2 cells were infected with four different patient-derived RV strains (G1P[8]) and treated with IFNα 100 IU/mL (as representative of type I IFN), IFNγ 100 ng/mL (type II IFN), IFNλ1 and IFNλ3 100 ng/mL (as representative of type III IFN). Distinct sensitivity was observed among these patient-derived RV samples. Human RV RNA levels were quantified by qRT-PCR at 48 hours post-infection and normalized to a reference gene GAPDH. The data are derived from an experiment for multiple patient-derived RV strains.

Inhibition of JAK-STAT signaling abrogates the anti-RV activity of IFN-α as well as IFN-γ

The ISG induction by type I and III IFNs is mediated via a similar pathway involving ISGF3 complex. For type II IFN, its signaling pathway involves phosphorylation and dimerization of STAT1 to form IFNγ activation factor (GAF)[9]. To investigate the role of JAK-STAT signaling pathway in the anti-RV effects of IFNs, we used JAK I inhibitor that predominantly inhibit JAK1 protein, the upstream element that is responsible for STAT1 and STAT2 phosphorylation. As expected, JAK I inhibitor (10 µM) efficiently blocked IFNα- and IFNγ-induced ISG expression in Caco2 cells (Supplementary Fig. S7 and S8). Consistently, JAK I inhibitor treatment abolished the anti-RV effects of IFN-α and IFNγ in Caco2 cell lines (Fig. 7A and 7B, repectively). These data clearly indicate an important role of JAK-STAT pathway in mediating the anti-RV effects of IFNs.
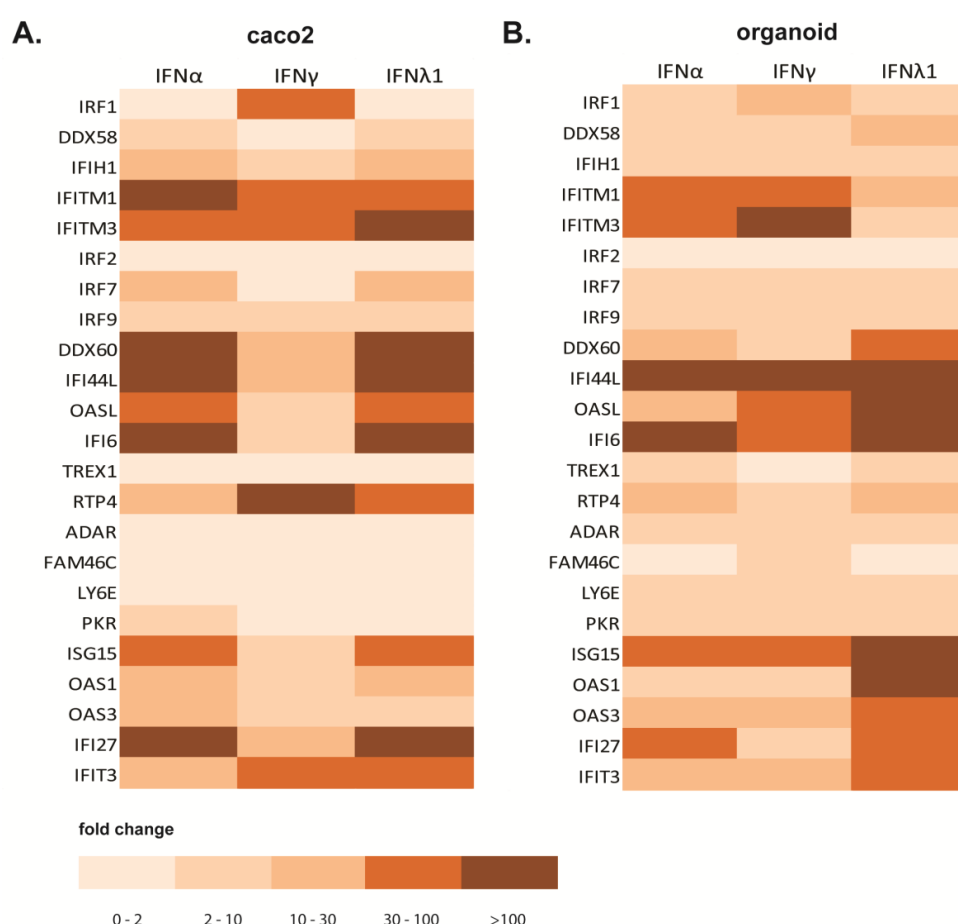
Figure 6. ISG induction by type I, II and III IFNs on Caco2 cells and organoids. Caco2 cells **(A)** and organoids **(B)** were stimulated with IFNα 1000 IU/mL (as representative of type I IFN), IFNγ 1000 ng/mL (type II IFN) and IFNλ1 1000 ng/mL (as representative of type III IFN) for 24 hours. The expression levels of several ISGs were measured by qRT-PCR. The organoid used in this experiment was derived from one individual (P1).
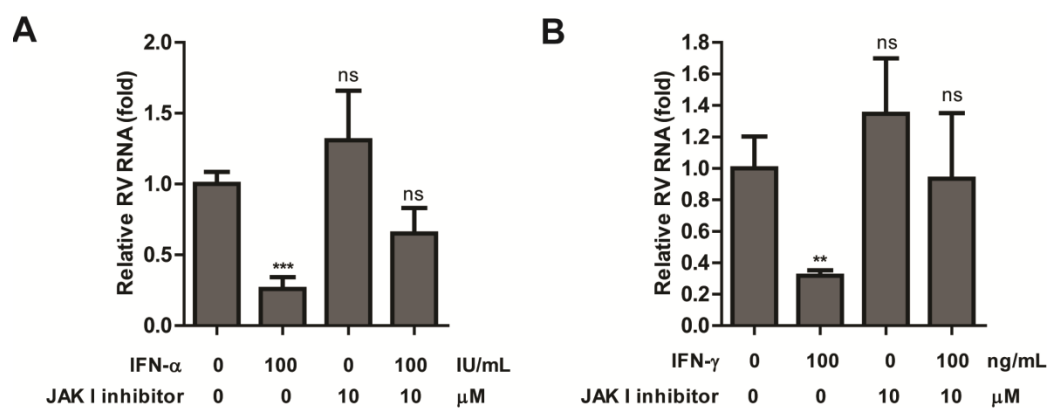
Figure 7. JAK I inhibitor blocks the anti-RV effects of IFNα and IFNγ. Caco2 cells were first infected with RV SA11 for 60 minutes. After four times washing, IFNα or IFNγ and *Pan*-JAK I inhibitor were added simultaneously to SA11-infected Caco2 cells and then cultured for 48 hours. *Pan*-JAK I inhibitor (10 μM) can block the anti-RV effects of IFNα 100 IU/mL **(A)** and IFNγ 100 ng/mL **(B)** in Caco2 cells. (n = 3 independent experiments with 2-4 replicates each) Data were presented as means ± SEM., *$P < 0.05$; **$P < 0.01$; ns, not significant.

Discussion

The *in vitro* study of RV biology had mainly been based on the conventional two-dimensional (2D) cell culture system of intestinal carcinoma-derived cell lines, including Caco2 and HT29 cell lines[14,29-31]. They are homogenous immortalized cell lines that can functionally reflect the real biological processes in the humans intestinal epithelium However, they are lacking three-dimensional (3D) higher order organisation present in the human intestine *in vivo*[32]. Recently, 3D models of primary intestinal organoids were developed for studying RV biology which better recapitulate the architecture and cellular composition of the human intestine[33-35]. Intestinal organoids contain heterogenous and non-transformed cell types, including enterocytes, enteroendocrine cells, goblet cells, Paneth cells and stem cells[35]. Therefore, they enable us to investigate individual-specific response associated with histo-blood group antigen (HBGAs) profiles and microbiome diversity[35].

Transcriptional analysis of SA11-infected Caco2 cells revealed that RV predominantly induced type III (IFNλ1) rather than type I (IFNα and IFNβ) IFN responses. In other intestinal epithelial cells, such as HT29, RV infection induces type I IFN response (IFNβ) and subsequently regulates ISG expression[29,30,36]. However, our findings are consistent with previous studies in human intestinal enteroids (organoids) infected with human RV strains in which predominant type III

IFN responses (IFNλ1 and IFNλ2) were observed[34]. The relatively low induction of type I IFNs in these human epithelial cells is also consistent with studies in murine RV[37]. Following murine RV infection, type I IFN response was mainly produced by immune (hematopoietic) cells, not epithelial cells[37]. A predominant type III IFN response was also observed in hepatocytes upon HCV[38] and HEV infection[39]. However, both type I and III IFN were similarly induced following influenza virus infection in lung epithelial cells[40]. Thus, all these findings suggest that preferential induction of type I and/or type III IFN response is virus- and cell type-specific and reflects the complex regulation of type I and III IFN induction following viral infections.

Despite a clear induction of type III IFN responses, our IFN production bioassay found undetectable levels of IFN proteins in the (conditioned) culture medium from SA11-infected Caco2 cells (Fig. 2A and 2B). Consistently, we did not observe ISG upregulation in SA11-infected Caco2 cells (Fig. 2C), indicating an absence of secreted IFN to stimulate ISG expression in an autocrine and/or paracrine manner. Further analysis by inhibiting downstream IFN signaling using JAK inhibitors demonstrated that RV replication levels were not altered. In human intestinal enteroids (organoids) infected with human RV strains, type III IFN induction was followed by stimulation of type III-dependent ISGs[34]. These discrepancies may be due to different RV strains as well as the different cellular composition of both models. However, despite this ISG induction, blockade of type I and III IFN receptor had no effects on RV replication[34]. Altogether, these findings indicate that endogenously produced IFNs (if any) were not sufficient to limit RV replication, even though they were able to induce ISGs in intestinal organoid models. These findings also suggest the ability of RV to subvert innate immune responses. It is known that RV have multiple ways to blunt innate IFN responses[12]. It has been shown that RV nonstructural protein 1 (NSP1) interacts with IRF3 to promote its degradation, leading to attenuation of IFN induction[41].

While previous studies mainly focused on the role of STAT1 in RV replication[15,42], here we highlighted the role of basal IFN signaling in constraining RV infection. Individual knockdown of ISGF3 component, i.e. STAT1, STAT2 and IRF9, led to an elevated level of RV replication. Similarly, STAT1 knockout (KO) mice shed a significantly higher titer of RV than wild-type (WT) controls[42]. STAT1 is also shown to protect against lethal challenge of murine norovirus infection in mice[43]. In dengue virus (DENV)-infected mice, STAT2 was essentially required to protect against DENV-mediated diseases independently of STAT1[44]. Our findings are also

consistent with our previous *in vitro* studies demonstrating that unphosphorylated ISGF3 complex is responsible for maintaining basal transcription of ISGs in the absence of IFN stimulation to provide a "combat-ready" antiviral state in the susceptible host[27]. Thus, constitutive IFN signaling, ligand independent but maintained by background expression of its essential component, including STAT1, STAT2 and IRF9, are pivotal to restrict RV replication in the intestinal epithelium.

While endogenous IFN response was not able to reduce RV replication, exogenous IFN treatment was effective to limit RV replication. We demonstrated that all three types of IFNs have notable antiviral effects against simian RV SA11 both in Caco2 cells and human organoids. Patient-specific organoid lines have promising implications for personalized medicine. Noteworthy, our study employed organoids derived from only two individuals. In this aspect, using organoids derived from several numbers of patients would be much better in recapitulating inter-individual variations, including HBGAs profiles, microbime diversity and genetic background[32,35].

We have also successfully cultivated four human-derived RV strains from acute diarrhea patients. Treatment with representative type I (IFNα), II (IFNγ) and III (IFNλ1 and IFNλ3) IFNs showed various sensitivity of human RV to IFNs, in which more pronounced inhibition was observed with type I and II rather than type III IFN treatment. In previous studies using human organoid models, type I IFN was more effective than type III IFN to suppress human RV replication[34]. However, conflicting results were found from *in vivo* studies about the relative contributions of type I and III IFNs during RV infections[25,26,45]. Type I IFN response plays a functional role to limit extra-intestinal spread in the mesenteric lymph node (MLN)[45]. On the other hand, RV has the capacity to attenuate the antiviral actions of IFNs[14]. Our study therefore suggests that human RV may differentially adapt in homologous host.

While many previous studies mainly focused on the effects of type I and III IFNs, our study highlights the role of type II IFN (IFNγ) in limiting RV replication. Previous studies showed that IFNγ level in the serum was significantly higher in children with RV diarrhea than those of control children[17]. In our study, transcriptional analysis showed that IFNγ mRNA level was not detectable from SA11-infected Caco2 cells (data not shown). However, it has been shown that IFNγ was produced from human peripheral blood mononuclear cells (PBMCs) stimulated with

RV[46]. Consistently, the level of IFNγ gene expression as well as secreted level in the supernatant of PBMCs were significantly elevated in children with RV diarrhea as compared with controls[18,47]. These findings suggest that immune cells, and not epithelial Caco2 cells, were responsible for IFNγ production upon RV infection.

RV-specific CD4+ and CD8+ IFNγ+ T cells were detected in the peripheral blood of RV-infected children and adults[48,49]. IFNγ producing T cells were also observed following experimental vaccines in animals and associated with disease protection[21,50,51]. It was previously shown that IFNγ inhibit RV entry into Caco2 cells[20]. In our study, we found that human IFNγ significantly reduces RV replication, suggesting that IFNγ can inhibit RV infection at various steps of the life cycle in the infected cells. In apparent agreement, it was suggested that IFNγ responses critically determine the severity of RV diseases in children[52].

ISGs are the ultimate effectors of IFN-mediated antiviral responses. Based on our findings, all three types of IFNs effectively induced a panel of well-known anti-viral ISGs both in Caco2 cells and in human organoids. However, further studies are needed to identify specific anti-RV ISGs to improve our understanding of immunity against RV infections. In conclusions, our study describes the role of both endogenous and exogenous IFN in RV infection, as well as the role of both basal and activated IFN signaling in limiting RV infection. These knowledge shall contribute to the better understanding of RV-host interactions and therapeutic development.

Material and Methods

Reagents

Type I human recombinant IFN alpha 2a (IFNα; Thermo Scientific) and IFN beta 1a (IFNβ; Sigma-Aldrich; Catalog Number 14151); Type II IFN gamma (IFNγ; BioLegend; Catalog# 570202), and Type III IFNs IL29 (IFNλ1; Abnova), IL28A (IFNλ2; Abnova) and IL28B (IFNλ3; Abnova) were dissolved in culture medium. Stocks of Jak inhibitor I (Santa Cruz Biotech, CA) was dissolved in DMSO (Sigma-Aldrich, St Louis, MO, USA) with a final concentration of 5 mg/mL. Anti-STAT1 antibody (#9172) was purchased from Cell Signaling Technology. IRF9 antibody was obtained from LSBio (Life Span BioSciences, Inc). β-actin and STAT2 (sc-476) antibodies were purchased from Santa Cruz Biotechnology. Anti-rabbit or anti-mouse IRDye-conjugated antibodies were used as secondary antibodies for western blotting (Stressgen, Victoria, BC, Canada).

Viruses

Simian RV SA11, a broadly used laboratory strain, was employed. SA11 RV used in this study was prepared as described previously[53]. RV genome copy numbers were determined by quantitative real-time polymerase chain reaction (qRT-PCR). A plasmid template was used to generate a standard curve by plotting the log copy number versus the cycle threshold (C_T) as previously described [33].

Human-derived RV strains (G1P[8]) were obtained from fecal samples of four RV patients and stored at -80 °C freezer (the Erasmus MC Biobank, Department of Viroscience, Erasmus Medical Center, Rotterdam). These samples were collected during diarrhea period and tested negative for enterovirus, parechovirus, norovirus genogroup I and II, adenovirus, astrovirus and sapovirus by qRT-PCR. The patient characteristics were shown in Supplementary Table S1.

Cell and human primary intestinal organoid culture

Caco2 cell line (human caucasian colon adenocarcinoma ECACC) was cultured in Dulbecco's modified Eagles's medium (DMEM; Lonza, Verviers, Belgium) containing 20% (vol/vol) heat-inactivated fetal calf serum (FCS; Sigma-Aldrich, St. Louis USA), 100 U/mL penicillin and

streptomycin (Gibco, Grand Island, USA). The cells were maintained in 5% CO_2 at 37 $^{\circ}$C in a humidified incubator.

Organoid culture was performed as described previously[33]. Briefly, intestinal tissues taken from biopsy were vigorously shaken in 8 mM EDTA for 15 min at 4 $^{\circ}$C. The EDTA solution was then discarded. Loosened crypts were collected by pipetting the solution up and down for 8-10 times through a 10 mL pipette and transferred into a 50 mL tube (Greiner Bioone, the Netherlands). The biopsies were repeatedly used for crypts collection (2-3 times). Crypt suspensions were pooled and centrifuged at 300 g for 5 min. The crypt pellets were resuspended in 2 mL complete medium containing growth factors CMGF-: advanced DMEM/F12 supplemented with 1% (vol/vol) GlutaMAX™ Supplement (Gibco, Grand island, USA), 10 mM HEPES. The crypts were collected by centrifugation at 130g for 5 min at 4 $^{\circ}$C, suspended in matrigel (Corning, Bedford, USA) and placed in the center of a 24-well plate (40 µL per well). After the matrigel had solidified (15 min at 37 $^{\circ}$C), organoids were maintained in culture medium at 37 $^{\circ}$C, 5% CO_2. Culture medium was refreshed every 2-3 days, and organoids were passaged every 6-7 days.

Inoculation of SA11 and human-derived RV strains and treatment

Caco2 cells cultured in T75 flask were suspended and subsequently seeded into 48-well plate (5 * 10^4 cells/well) in DMEM complemented with 20% (vol/vol) FCS and 100 IU/mL penicillin-streptomycin. After 2-3 days of culture, culture medium was removed when the cell confluence was about 80%. The cell layers were then washed twice with 500 µL PBS. Serum-free DMEM medium (100 µL) containing 5 µg/mL of trypsin (Gibco, Paisley, UK) and SA11 RV were added and incubated for 60 min at 37 $^{\circ}$C with 5% CO_2 to allow efficient infection, followed by four times washing with PBS (500 µL each) to remove free virus particles. Subsequently, culture medium containing 5 µg/mL of trypsin (and indicated treatments) were added to the infected cells and incubated for 24 or 48 hours at 37 $^{\circ}$C with 5% CO_2.

For organoid infection, SA11 RV (contain 5000 genome copies) was first activated with 5 µg/mL of trypsin at 37 $^{\circ}$C with 5% CO_2 for 30 minutes. Subsequently, organoids were infected with the activated SA11 for 60 minutes at 37 $^{\circ}$C with 5% CO_2, followed by four times washing with PBS to discard the free viruses. Organoids were then aliquoted into 48-well plates that

have been coated with 20% (vol/vol) Collagen R Solution (SERVA, Heidelberg, Germany) and maintained in culture medium containing indicated treatments at 37 °C with 5% CO_2.

Quantitative real-time polymerase chain reaction (qRT-PCR)

Total, intracellular or extracellular (secreted) RNA was isolated by using the Machery-NucleoSpin RNA II kit (Bioke, Leiden, The Netherlands) and quantified by a Nanodrop ND-1000 spectrophotometer (Wilmington, DE, USA). cDNA was made from total RNA using a cDNA Synthesis Kit (Takara Bio Inc, Shiga, Japan) with random hexamer primers. qRT-PCR of RV RNA and genes of interest were performed with a SYBRGreen-based real-time PCR (MJ Research Opticon, Hercules, CA, USA) according to the manufacturer's instructions with the StepOnePlus System (Thermo Fisher Scientific Life Sciences). Glyceraldehyde-3-phosphate dehydrogenase (GAPDH) gene was used as a housekeeping gene to normalize (relative) gene expression using the $2^{-\Delta\Delta CT}$ formula. All primers used in this study are listed in Supplementary Table S2.

Lentiviral vector production and transfection assays

Lentiviral pLKO knockdown vectors (Sigma–Aldrich) targeting STAT1, STAT2 and IRF9 or scrambled control, were obtained from the Erasmus Center of Biomics. All shRNA sequences are listed in Supplementary Table S3. The lentiviral vectors were produced in human embryonic kidney epithelial cell line HEK 293T cells as previously described[54]. The shRNA vectors exerting optimal gene knockdown were selected. To generate the gene knockdown cells, Caco2 cells were transduced with the lentiviral vectors and subsequently selected by adding puromycin (8 µg/mL; Sigma) to the culture medium. Knockdown and control Caco2 cells were infected with RV as previously described.

IFN production bioassay

The IFN production bioassay was performed to detect secreted IFN proteins in the culture medium as described previously[55]. Briefly, the culture (conditioned) medium derived from control and SA11-infected Caco2 cells (48 hours) were collected and filtered through 0.45 µm pore size membrane. Two luciferase reporter models which are extremely sensitive to IFN treatments were employed. Huh7.5-ET-Luc luciferase model is a hepatitis C virus (HCV)

replicon (I389/NS3-3V/LucUbiNeo-ET) in which the HCV-related firefly luciferase activity (HCV-luc) can be potently inhibited by a low concentration of IFN-α treatments. Huh7-ISRE-luc is a luciferase reporter model in which the firefly luciferase gene was driven by multiple IFN-stimulated response elements (ISRE) promoter. In this model, the firefly luciferase activity can be potently stimulated by a low concentration of IFN-α treatment. Therefore, these two luciferase models can be employed to sensitively detect the presence of IFN proteins in the conditioned medium. Huh7 HCV-luc and ISRE-luc cells were cultured in DMEM supplemented with 10% FCS (vol/vol), 100 U/mL penicillin and streptomycin. For Huh7 HCV-luc, 250 µg/mL G418 (Sigma-Aldrich) was added to the culture medium.

Western blot assay

Cultured cells were lysed in Laemmli sample buffer containing 0.1 M dithiothreitol (DTT) and heated for 5 min at 95°C. Cell lysates were subjected to 10% sodium dodecyl sulfate polyacrylamide gel electrophoresis (SDS-PAGE) for 100 min running at 110 V. The proteins were transferred onto polyvinylidene difluoride (PVDF) membrane (Immobilon-FL) for 1.5 hours with an electric current of 250 mA. Subsequently, the membrane was blocked with a mixture of 2.5 ml of blocking buffer (Odyssey) and 2.5 ml of PBS containing 0.05% Tween 20 for 1 hour at room temperature. This was followed by an overnight incubation with the indicated primary antibody (1:1000 dilution) at 4°C. The membrane was then washed three times, followed by incubation for 1 hour with IRDye-conjugated secondary antibody (1:5000 dilution) at room temperature. After washing three times, the protein bands were detected with the Odyssey 3.0 Infrared Imaging System. The intensity of the immunoreactive bands of blotted proteins was quantified by the Odyssey V3.0 software.

Immunofluorescence microscope assay

Caco2 cells were seeded on glass coverslips. After SA11 infection for 48 hours, cells were washed with PBS, fixed in 4% PBS-buffered formalin for 10 mins and blocked with tween-milk-glycine medium (PBS, 0.05% tween, 5g/L skim milk and 1.5g/L glycine). Samples were incubated with anti-rotavirus (ab181695) antibody (Abcam) overnight at 4 °C. Subsequently, samples were incubated with 1:1000 dilutions of Alexa Fluor™ 594 goat anti-mouse secondary

antibodies (Invitrogen). Nuclei were stained with DAPI (4,6-diamidino-2-phenylindole; Invitrogen). Images were detected using immunofluorescence microscope.

MTT assay

10 mM 3-(4,5-dimethylthiazol-2-yl)-2,5-diphenyltetrazolium bromide (MTT) (Sigma) was added to Caco2 cells seeded in 96-well plates at indicated time points. The cells were incubated at 37 ^{0}C with 5% CO_2 for 3 hours. The culture medium was then removed and 100 µl of dimethyl sulfoxide (DMSO) was added to each well. The absorbance of each well was read on the microplate absorbance readers (BIO-RAD) at wavelength of 490 nm.

Study Approval

Human intestinal tissue were obtained during surgical resection. A written informed consent was signed by the volunteers or patients who agreed to participate. The study was approved by the Medical Ethical Committee of the Erasmus Medical Center (Medisch Ethische Toetsings Commissie Erasmus MC), and all experiments were performed in accordance with relevant guidelines and regulations.

Statistical Analysis

Statistical analysis was performed using the nonpaired, nonparametric test (Mann-Whitney test; GraphPad Prism software, GraphPad Software Inc., La Jolla, CA). *P* values <0.05 were considered statistically significant.

References

1   Greenberg, H. B. & Estes, M. K. Rotaviruses: from pathogenesis to vaccination. *Gastroenterology* **136**, 1939-1951, doi:10.1053/j.gastro.2009.02.076 (2009).

2   Lanata, C. F. *et al.* Global causes of diarrheal disease mortality in children <5 years of age: a systematic review. *PLoS One* **8**, e72788, doi:10.1371/journal.pone.0072788 (2013).

3   Walker, C. L. *et al.* Global burden of childhood pneumonia and diarrhoea. *Lancet* **381**, 1405-1416, doi:10.1016/S0140-6736(13)60222-6 (2013).

4   Desai, R. *et al.* Reduction in morbidity and mortality from childhood diarrhoeal disease after species A rotavirus vaccine introduction in Latin America - a review. *Mem Inst Oswaldo Cruz* **106**, 907-911, doi:S0074-02762011000800002 (2011).

5   Holloway, G. & Coulson, B. S. Innate cellular responses to rotavirus infection. *J Gen Virol* **94**, 1151-1160, doi:10.1099/vir.0.051276-0 (2013).

6   Deal, E. M., Jaimes, M. C., Crawford, S. E., Estes, M. K. & Greenberg, H. B. Rotavirus structural proteins and dsRNA are required for the human primary plasmacytoid dendritic cell IFNalpha response. *PLoS Pathog* **6**, e1000931, doi:10.1371/journal.ppat.1000931 (2010).

7   Randall, R. E. & Goodbourn, S. Interferons and viruses: an interplay between induction, signalling, antiviral responses and virus countermeasures. *J Gen Virol* **89**, 1-47, doi:10.1099/vir.0.83391-0 (2008).

8   Donnelly, R. P. & Kotenko, S. V. Interferon-lambda: a new addition to an old family. *J Interferon Cytokine Res* **30**, 555-564, doi:10.1089/jir.2010.0078 (2010).

9   Platanias, L. C. Mechanisms of type-I- and type-II-interferon-mediated signalling. *Nat Rev Immunol* **5**, 375-386, doi:10.1038/nri1604 (2005).

10   Schneider, W. M., Chevillotte, M. D. & Rice, C. M. Interferon-stimulated genes: a complex web of host defenses. *Annu Rev Immunol* **32**, 513-545, doi:10.1146/annurev-immunol-032713-120231 (2014).

11   Deal, E. M., Lahl, K., Narvaez, C. F., Butcher, E. C. & Greenberg, H. B. Plasmacytoid dendritic cells promote rotavirus-induced human and murine B cell responses. *J Clin Invest* **123**, 2464-2474, doi:10.1172/JCI60945 (2013).

12   Arnold, M. M., Sen, A., Greenberg, H. B. & Patton, J. T. The battle between rotavirus and its host for control of the interferon signaling pathway. *PLoS Pathog* **9**, e1003064, doi:10.1371/journal.ppat.1003064 (2013).

13   Graff, J. W., Ettayebi, K. & Hardy, M. E. Rotavirus NSP1 inhibits NFkappaB activation by inducing proteasome-dependent degradation of beta-TrCP: a novel mechanism of IFN antagonism. *PLoS Pathog* **5**, e1000280, doi:10.1371/journal.ppat.1000280 (2009).

14   Holloway, G., Truong, T. T. & Coulson, B. S. Rotavirus antagonizes cellular antiviral responses by inhibiting the nuclear accumulation of STAT1, STAT2, and NF-kappaB. *J Virol* **83**, 4942-4951, doi:10.1128/JVI.01450-08 (2009).

15   Feng, N. *et al.* Variation in antagonism of the interferon response to rotavirus NSP1 results in differential infectivity in mouse embryonic fibroblasts. *J Virol* **83**, 6987-6994, doi:10.1128/JVI.00585-09 (2009).

16   De Boissieu, D., Lebon, P., Badoual, J., Bompard, Y. & Dupont, C. Rotavirus induces alpha-interferon release in children with gastroenteritis. *J Pediatr Gastroenterol Nutr* **16**, 29-32 (1993).

17   Jiang, B. *et al.* Cytokines as mediators for or effectors against rotavirus disease in children. *Clin Diagn Lab Immunol* **10**, 995-1001 (2003).

18   Azim, T. *et al.* Rotavirus-specific subclass antibody and cytokine responses in Bangladeshi children with rotavirus diarrhoea. *J Med Virol* **69**, 286-295, doi:10.1002/jmv.10280 (2003).

19   Dagenais, L., Pastoret, P. P., Van den Broecke, C. & Werenne, J. Susceptibility of bovine rotavirus to interferon. Brief report. *Arch Virol* **70**, 377-379 (1981).

20   Bass, D. M. Interferon gamma and interleukin 1, but not interferon alfa, inhibit rotavirus entry into human intestinal cell lines. *Gastroenterology* **113**, 81-89, doi:S0016508597003144 (1997).

21 McNeal, M. M. *et al.* IFN-gamma is the only anti-rotavirus cytokine found after in vitro stimulation of memory CD4+ T cells from mice immunized with a chimeric VP6 protein. *Viral Immunol* **20**, 571-584, doi:10.1089/vim.2007.0055 (2007).

22 Schwers, A. *et al.* Experimental rotavirus diarrhoea in colostrum-deprived newborn calves: assay of treatment by administration of bacterially produced human interferon (Hu-IFN alpha 2). *Ann Rech Vet* **16**, 213-218 (1985).

23 Lecce, J. G., Cummins, J. M. & Richards, A. B. Treatment of rotavirus infection in neonate and weanling pigs using natural human interferon alpha. *Mol Biother* **2**, 211-216 (1990).

24 Angel, J., Franco, M. A., Greenberg, H. B. & Bass, D. Lack of a role for type I and type II interferons in the resolution of rotavirus-induced diarrhea and infection in mice. *J Interferon Cytokine Res* **19**, 655-659, doi:10.1089/107999099313802 (1999).

25 Pott, J. *et al.* IFN-lambda determines the intestinal epithelial antiviral host defense. *Proc Natl Acad Sci U S A* **108**, 7944-7949, doi:10.1073/pnas.1100552108 (2011).

26 Hernandez, P. P. *et al.* Interferon-lambda and interleukin 22 act synergistically for the induction of interferon-stimulated genes and control of rotavirus infection. *Nat Immunol* **16**, 698-707, doi:10.1038/ni.3180 (2015).

27 Wang, W. *et al.* Unphosphorylated ISGF3 drives constitutive expression of interferon-stimulated genes to protect against viral infections. *Sci Signal* **10**, doi:10.1126/scisignal.aah4248 (2017).

28 Schoggins, J. W. & Rice, C. M. Interferon-stimulated genes and their antiviral effector functions. *Curr Opin Virol* **1**, 519-525, doi:10.1016/j.coviro.2011.10.008 (2011).

29 Frias, A. H. *et al.* Intestinal epithelia activate anti-viral signaling via intracellular sensing of rotavirus structural components. *Mucosal Immunol* **3**, 622-632, doi:10.1038/mi.2010.39 (2010).

30 Frias, A. H., Jones, R. M., Fifadara, N. H., Vijay-Kumar, M. & Gewirtz, A. T. Rotavirus-induced IFN-beta promotes anti-viral signaling and apoptosis that modulate viral replication in intestinal epithelial cells. *Innate Immun* **18**, 294-306, doi:10.1177/1753425911401930 (2012).

31 Cuadras, M. A., Feigelstock, D. A., An, S. & Greenberg, H. B. Gene expression pattern in Caco-2 cells following rotavirus infection. *J Virol* **76**, 4467-4482 (2002).

32 Dutta, D. & Clevers, H. Organoid culture systems to study host-pathogen interactions. *Curr Opin Immunol* **48**, 15-22, doi:10.1016/j.coi.2017.07.012 (2017).

33 Yin, Y. *et al.* Modeling rotavirus infection and antiviral therapy using primary intestinal organoids. *Antiviral Res* **123**, 120-131, doi:10.1016/j.antiviral.2015.09.010 (2015).

34 Saxena, K. *et al.* A paradox of transcriptional and functional innate interferon responses of human intestinal enteroids to enteric virus infection. *Proc Natl Acad Sci U S A* **114**, E570-E579, doi:10.1073/pnas.1615422114 (2017).

35 Saxena, K. *et al.* Human Intestinal Enteroids: a New Model To Study Human Rotavirus Infection, Host Restriction, and Pathophysiology. *J Virol* **90**, 43-56, doi:10.1128/JVI.01930-15 (2015).

36 Hirata, Y., Broquet, A. H., Menchen, L. & Kagnoff, M. F. Activation of innate immune defense mechanisms by signaling through RIG-I/IPS-1 in intestinal epithelial cells. *J Immunol* **179**, 5425-5432, doi:179/8/5425 (2007).

37 Sen, A. *et al.* Innate immune response to homologous rotavirus infection in the small intestinal villous epithelium at single-cell resolution. *Proc Natl Acad Sci U S A* **109**, 20667-20672, doi:10.1073/pnas.1212188109 (2012).

38 Park, H. *et al.* IL-29 is the dominant type III interferon produced by hepatocytes during acute hepatitis C virus infection. *Hepatology* **56**, 2060-2070, doi:10.1002/hep.25897 (2012).

39 Yin, X. *et al.* Hepatitis E virus persists in the presence of a type III interferon response. *PLoS Pathog* **13**, e1006417, doi:10.1371/journal.ppat.1006417 (2017).

40 Crotta, S. *et al.* Type I and type III interferons drive redundant amplification loops to induce a transcriptional signature in influenza-infected airway epithelia. *PLoS Pathog* **9**, e1003773, doi:10.1371/journal.ppat.1003773 (2013).

41 Barro, M. & Patton, J. T. Rotavirus nonstructural protein 1 subverts innate immune response by inducing degradation of IFN regulatory factor 3. *Proc Natl Acad Sci U S A* **102**, 4114-4119, doi:10.1073/pnas.0408376102 (2005).

42   Vancott, J. L., McNeal, M. M., Choi, A. H. & Ward, R. L. The role of interferons in rotavirus infections and protection. *J Interferon Cytokine Res* **23**, 163-170, doi:10.1089/107999003321532501 (2003).

43   Karst, S. M., Wobus, C. E., Lay, M., Davidson, J. & Virgin, H. W. t. STAT1-dependent innate immunity to a Norwalk-like virus. *Science* **299**, 1575-1578, doi:10.1126/science.1077905 (2003).

44   Perry, S. T., Buck, M. D., Lada, S. M., Schindler, C. & Shresta, S. STAT2 mediates innate immunity to Dengue virus in the absence of STAT1 via the type I interferon receptor. *PLoS Pathog* **7**, e1001297, doi:10.1371/journal.ppat.1001297 (2011).

45   Lin, J. D. *et al.* Distinct Roles of Type I and Type III Interferons in Intestinal Immunity to Homologous and Heterologous Rotavirus Infections. *PLoS Pathog* **12**, e1005600, doi:10.1371/journal.ppat.1005600 (2016).

46   Yasukawa, M., Nakagomi, O. & Kobayashi, Y. Rotavirus induces proliferative response and augments non-specific cytotoxic activity of lymphocytes in humans. *Clin Exp Immunol* **80**, 49-55 (1990).

47   Xu, J. *et al.* Expression of Toll-like receptors and their association with cytokine responses in peripheral blood mononuclear cells of children with acute rotavirus diarrhoea. *Clin Exp Immunol* **144**, 376-381, doi:10.1111/j.1365-2249.2006.03079.x (2006).

48   Jaimes, M. C. *et al.* Frequencies of virus-specific CD4(+) and CD8(+) T lymphocytes secreting gamma interferon after acute natural rotavirus infection in children and adults. *J Virol* **76**, 4741-4749 (2002).

49   Rojas, O. L. *et al.* Human rotavirus specific T cells: quantification by ELISPOT and expression of homing receptors on CD4+ T cells. *Virology* **314**, 671-679, doi:S0042682203005075 (2003).

50   Yuan, L. *et al.* Virus-specific intestinal IFN-gamma producing T cell responses induced by human rotavirus infection and vaccines are correlated with protection against rotavirus diarrhea in gnotobiotic pigs. *Vaccine* **26**, 3322-3331, doi:10.1016/j.vaccine.2008.03.085 (2008).

51   Smiley, K. L. *et al.* Association of gamma interferon and interleukin-17 production in intestinal CD4+ T cells with protection against rotavirus shedding in mice intranasally immunized with VP6 and the adjuvant LT(R192G). *J Virol* **81**, 3740-3748, doi:10.1128/JVI.01877-06 (2007).

52   Mormile, R. Severe gastroenteritis and acute pancreatitis following rotavirus infection in children: The age-related failure of IFN-gamma? *Immunol Lett* **175**, 58-59, doi:10.1016/j.imlet.2016.04.017 (2016).

53   Knipping, K., Garssen, J. & van't Land, B. An evaluation of the inhibitory effects against rotavirus infection of edible plant extracts. *Virol J* **9**, 137, doi:10.1186/1743-422X-9-137 (2012).

54   Pan, Q. *et al.* Combined antiviral activity of interferon-alpha and RNA interference directed against hepatitis C without affecting vector delivery and gene silencing. *J Mol Med (Berl)* **87**, 713-722, doi:10.1007/s00109-009-0470-3 (2009).

55   Xu, L. *et al.* IFN regulatory factor 1 restricts hepatitis E virus replication by activating STAT1 to induce antiviral IFN-stimulated genes. *FASEB J* **30**, 3352-3367, doi:10.1096/fj.201600356R (2016).

Supplementary Information
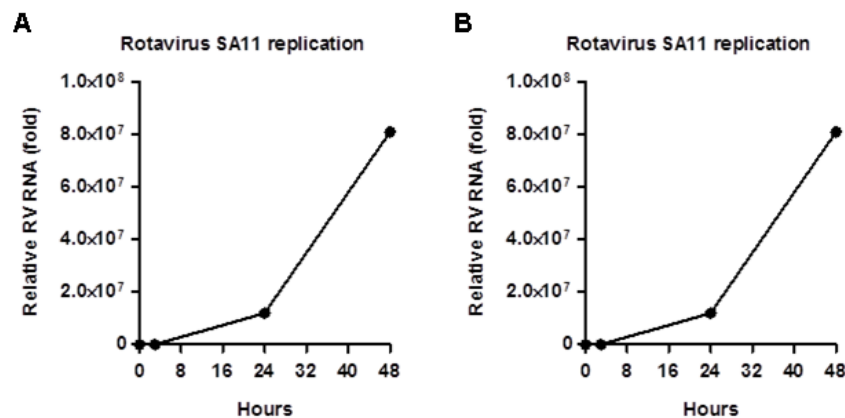
Supplementary Figure S1. Efficient replication of rotavirus SA11 in Caco2 cells as demonstrated by qRT-PCR. Intracellular **(A)** and secreted (extracellular) levels **(B)** of rotavirus SA11 were detected and quantified by qRT-PCR at 0 (before virus inoculation) as well as at 1, 24 and 48 hours after inoculation. For intracellular RNA quantification **(A)**, RV RNA levels were shown as fold increases relative to 1 hour post infection. GAPDH was used as the housekeeping gene.
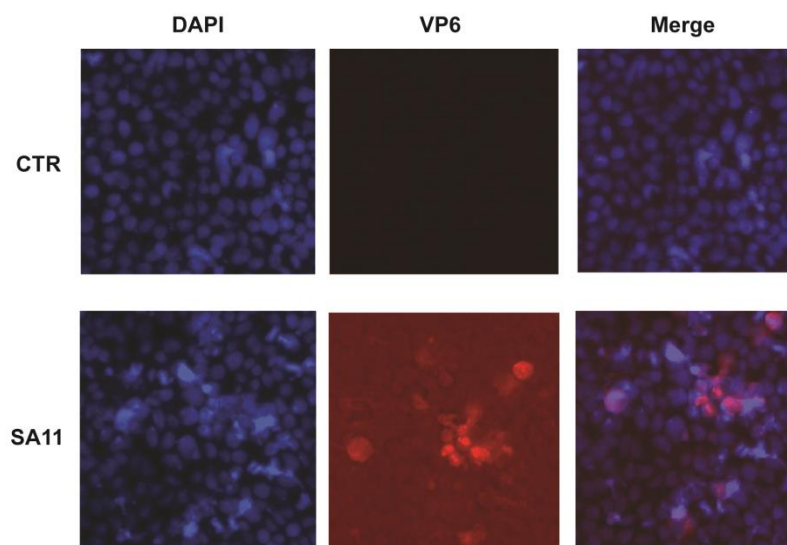
**Supplementary Figure S2. Efficient replication of rotavirus SA11 in Caco2 cells as demonstrated by immunofluorescence stainings.** Representrative immunofluorescence stainings of ab181695 (targeting VP6 rotavirus protein) (red) after 48 hours infection of Caco2 cells with rotavirus SA11. Nuclei were visualized by DAPI (blue).
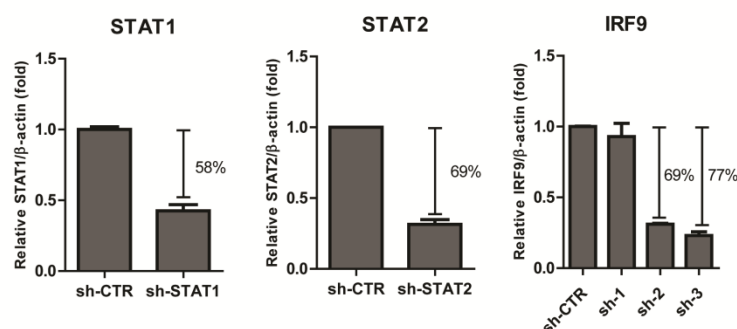
Supplementary Figure S3. Western blot assays showed a successful knockdown of STAT1 (58% reduction), STAT2 (69% reduction) and IRF9 proteins (69% and 77% reduction). β-actin served as an internal reference. (means ± SEM, n = 3).
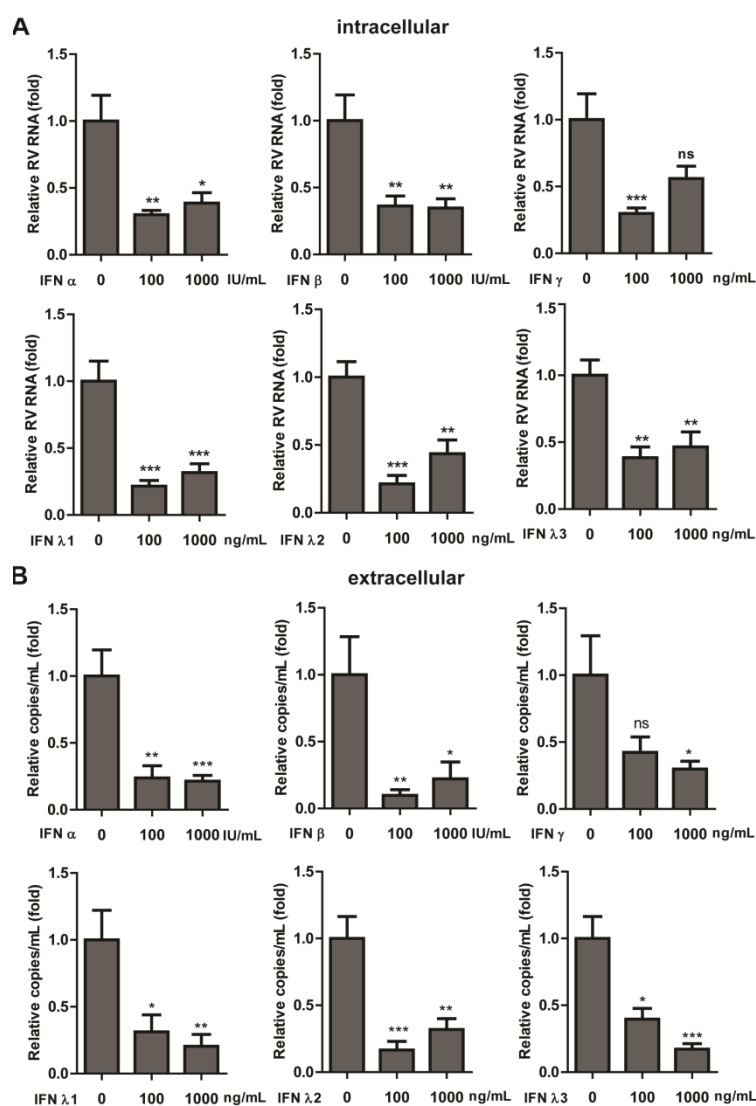
Supplementary Figure S4. The effects of exogenous treatment of type I, II and III IFNs on RV SA11 replication in Caco2 cells. Antiviral activities of IFNα, IFNβ, IFNγ, IFNλ1, IFNλ2 and IFNλ3 treatments against RV SA11 infection on Caco2 cells were determined by quantifying intracellular **(A)** and extracellular (secreted) **(B)** RNA levels at 48 hours post-infection. (n = 2-3 independent experiment with each of 3 replicates) Data were presented as means ± SEM., *$P < 0.05$; **$P < 0.01$; ***$P < 0.001$; ns, not significant.
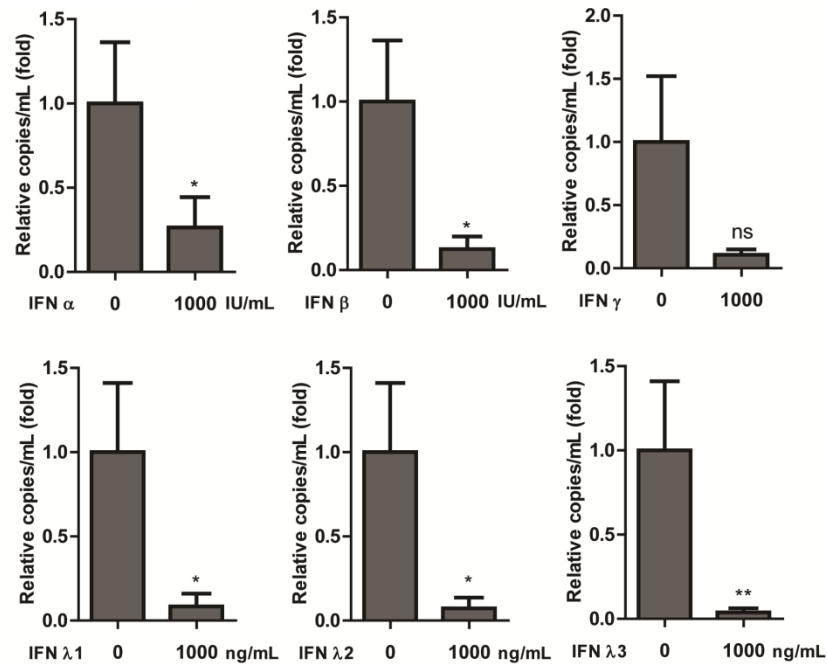
Supplementary Figure S5. The effects of type I, II and III IFNs on the extracellular level of RV SA11 in human organoids. Antiviral effects of IFNα, IFNβ, IFNγ, IFNλ1, IFNλ2 or IFNλ3 treatment against RV SA11 infection in organoids were determined by quantifying extracellular (secreted) RNA levels at 48 hours post-infection. The organoids were derived from one individual (P1). Data were presented as means ± SEM., *$P < 0.05$; **$P < 0.01$; ns, not significant. (n = 3 independent experiments with each of 2-3 replicates).
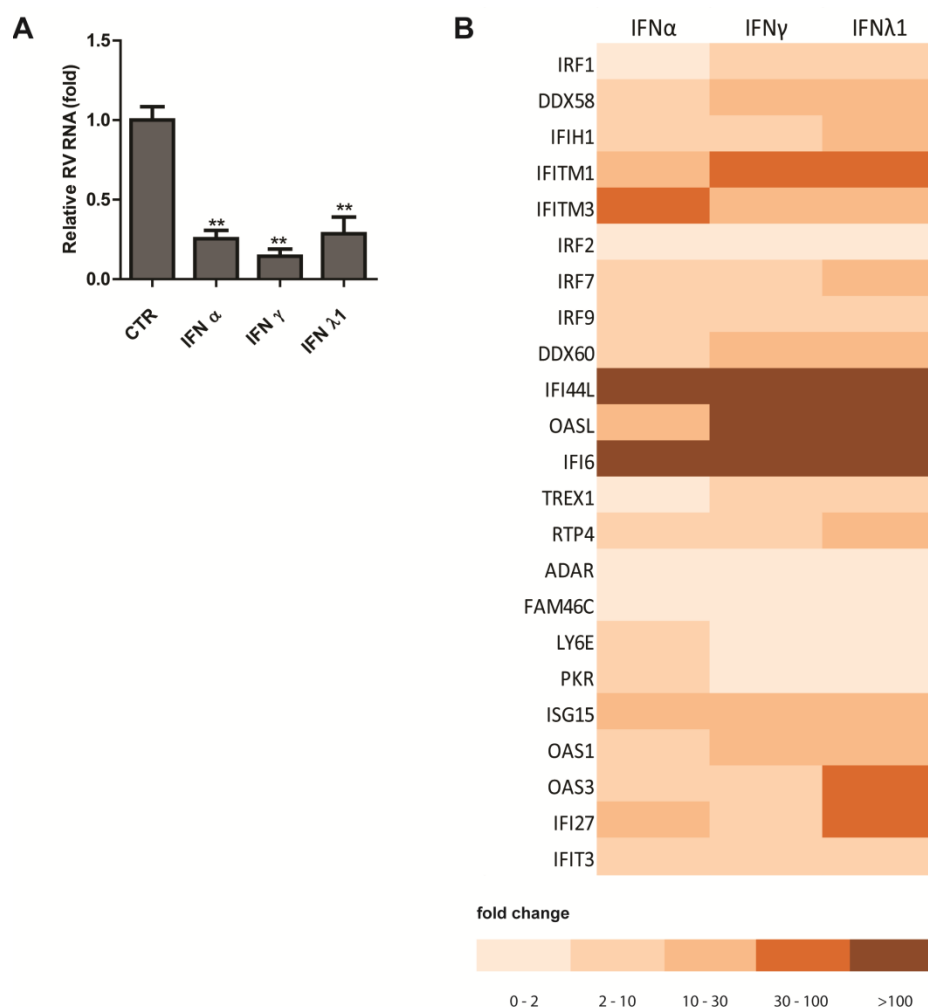
Supplementary Figure S6. (A) Antiviral effects of representative type I (IFNα, 1000 IU/mL), type II (IFNγ, 1000 ng/mL), and type III (IFNλ1, 1000 ng/mL) treatment against RV SA11 infection in organoids were determined by quantifying total RV RNA levels at 48 hours post-infection. The organoid was derived from individual 2 (P2). Data were presented as means ± SEM, **$P < 0.01$. (n = 3 independent experiments with each of 1-2 replicates). **(B)** Organoids (P2) were stimulated with IFNα 1000 IU/mL, IFNγ 1000 ng/mL and IFNλ1 1000 ng/mL for 24 hours. The expression levels of several ISGs were measured by qRT-PCR.
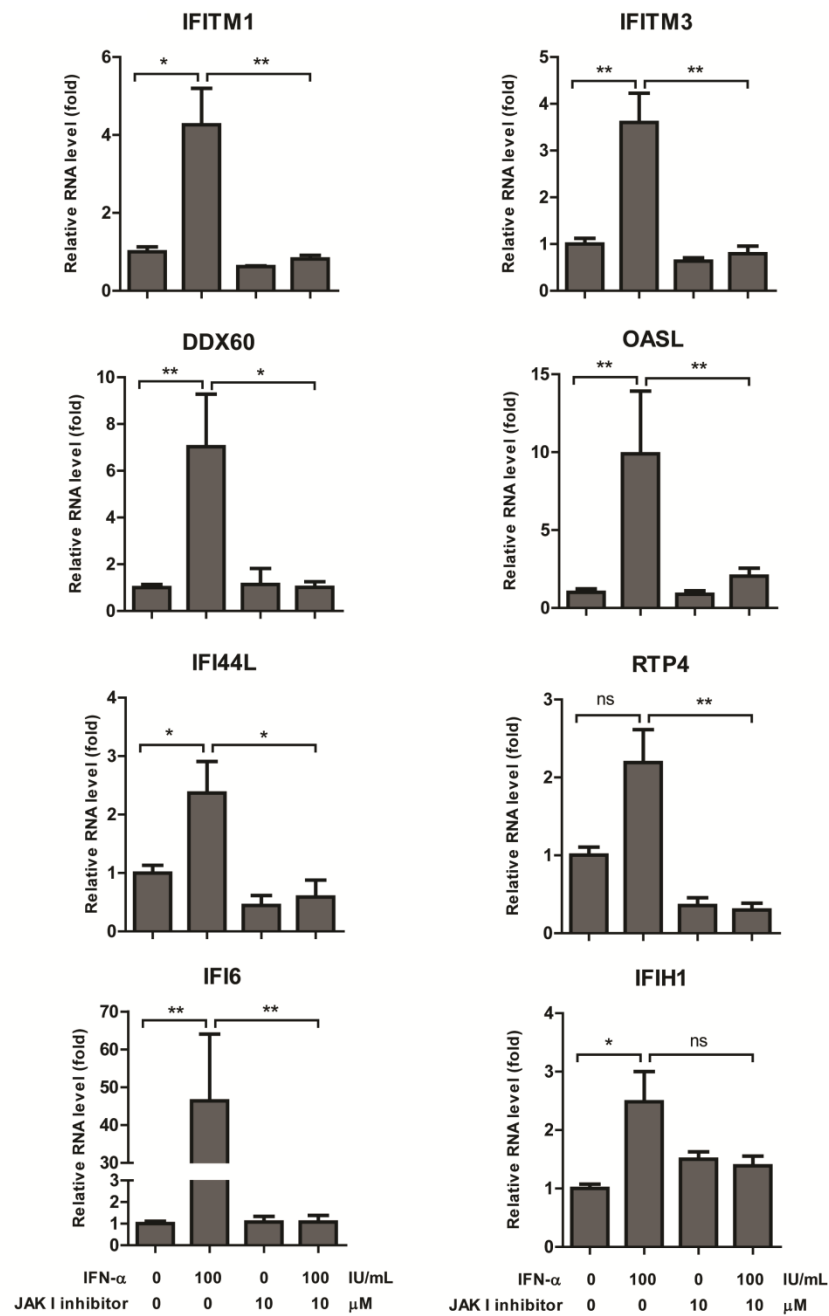
Supplementary Figure S7. JAK I inhibitor blocks IFNα-induced ISGs in Caco2 cells. JAK I inhibitor (10 µM) abrogated IFNα- (100 IU/mL) induced ISG expression as measured by qRT-PCR. Data were presented as means ± SEM., *P < 0.05; **P < 0.01; ns, not significant. (n = 3 independent experiments with each of 2-3 replicates)
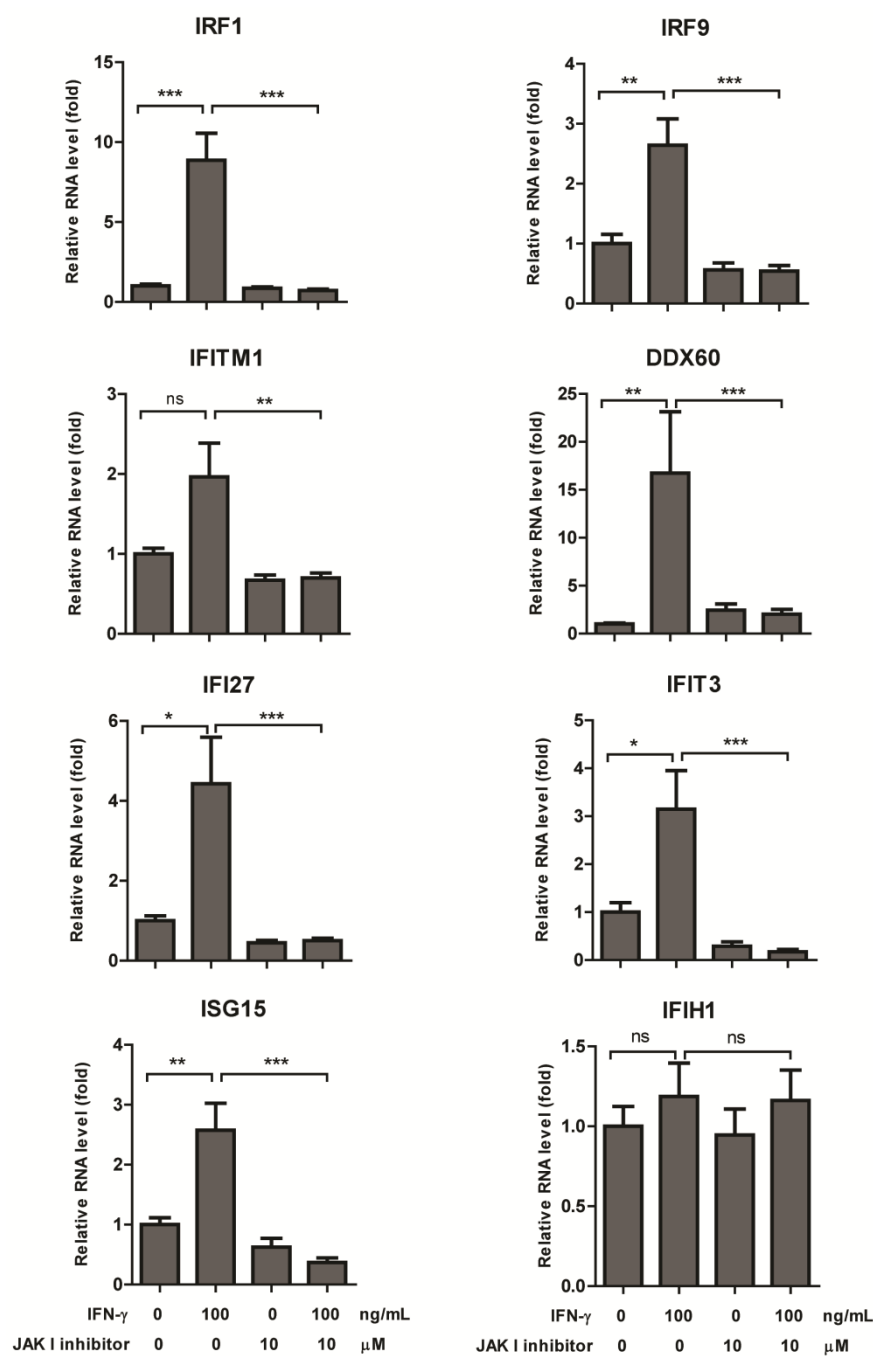
Supplementary Figure S8. JAK I inhibitor abolishes IFNγ-induced expression of ISGs in Caco2 cells. JAK I inhibitor (10 µM) abrogated IFNγ- (100 ng/mL) induced ISG expression as measured by qRT-PCR. Data were presented as means ± SEM., *$P < 0.05$; **$P < 0.01$; ***$P < 0.001$; ns, not significant. (n = 3 independent experiments with each of 2-3 replicates)

Supplementary Table S1. Patient characteristics.

Patient	Age (years)	Gender	Clinical symptoms	Virus Detection							
				Enterovirus	Parechovirus	Norovirus genogroups I	Norovirus genogroups II	Adenovirus	Astrovirus	Sapovirus	Rotavirus
1	74	Female	Congestive heart failure, myocarditis	No	No	No	No	No	No	No	Yes
2	27	Female	Fever, diarrhea, nausea, vomiting	No	No	No	No	No	No	No	Yes
3	67	Male	Fever, stomachache, watery diarrhea (Kidney transplant)	No	No	No	No	No	No	No	Yes
4	1.5	Female	Vomiting, watery diarrhea	No	No	No	No	No	No	Yes	Yes

Supplementary Table S2. Primers used in this study.

Target Genes	Sequences (5' - 3')
Viruses	
RV SA11-F	TGGTTAAACGCAGGATCGGA
RV SA11-R	AACCTTTCCGCGTCTGGTAG
Human RV-F	ACCATCTACACATGACCCTC
Human RV-R	CACATAACGCCCCTATAGCC
Human Genes	
IRF1-F	GAGGAGGTGAAAGACCAGAGCA
IRF1-R	TAGCATCTCGGCTGGACTTCGA
DDX58-F	CACCTCAGTTGCTGATGAAGGC
DDX58-R	GTCAGAAGGAAGCACTTGCTACC
IFIH1(MDA5)-F	GCTGAAGTAGGAGTCAAAGCCC
IFIH1(MDA5)-R	CCACTGTGGTAGCGATAAGCAG
IFITM1-F	GGCTTCATAGCATTCGCCTACTC
IFITM1-R	AGATGTTCAGGCACTTGGCGGT
IFITM3-F	CTGGGCTTCATAGCATTCGCCT
IFITM3-R	AGATGTTCAGGCACTTGGCGGT
IRF2-F	TAGAGGTGACCACTGAGAGCGA
IRF2-R	CTCTTCATCGCTGGGCACACTA
IRF7-F	CCACGCTATACCATCTACCTGG
IRF7-R	GCTGCTATCCAGGGAAGACACA
IRF9-F	CCACCGAAGTTCCAGGTAACAC
IRF9-R	AGTCTGCTCCAGCAAGTATCGG
DDX60-F	GGTGTTTTCACCAGGGAGTATCG
DDX60-R	CCAGTTTTGGCGATGAGGAGCA
IFI44L-F	TGCACTGAGGCAGATGCTGCG
IFI44L-R	TCATTGCGGCACACCAGTACAG
OASL-F	GTGCCTGAAACAGGACTGTTGC
OASL-R	CCTCTGCTCCACTGTCAAGTGG
IFI6-F	TGATGAGCTGGTCTGCGATCCT
IFI6-R	GTAGCCCATCAGGGCACCAATA
TREX-F	GCATCTGTCAGTGGAGACCACA
TREX-R	CAGTGGTTGTGACAGCAGATGG
RTP4-F	GACGCTGAAGTTGGATGGCAAC
RTP4-R	GTGGCACAGAATCTGCACTTGG
ADAR-F	TCCGTCTCCTGTCCAAAGAAGG
ADAR-R	TTCTTGCTGGGAGCACTCACAC
FAM46C-F	CCTTGAACAGCAGAGGAAGTTGG
FAM46C-R	GGAGATGAGGTTCAGAGTCTGC
LY6E-F	GACCAGGACAACTACTGCGTGA
LY6E-R	AAGCCACACCAACATTGACGCC
PKR-F	GAAGTGGACCTCTACGCTTTGG
PKR-R	TGATGCCATCCCGTAGGTCTGT
ISG15-F	CTCTGAGCATCCTGGTGAGGAA
ISG15-R	AAGGTCAGCCAGAACAGGTCGT
OAS1-F	AGGAAAGGTGCTTCCGAGGTAG

OAS1-R	GGACTGAGGAAGACAACCAGGT
OAS3-F	CCTGATTCTGCTGGTGAAGCAC
OAS3-R	TCCCAGGCAAAGATGGTGAGGA
IFI27-F	CGTCCTCCATAGCAGCCAAGAT
IFI27-R	ACCCAATGGAGCCCAGGATGAA
IFIT3-F	CCTGGAATGCTTACGGCAAGCT
IFIT3-R	GAGCATCTGAGAGTCTGCCCAA
IFNαR1-F	CGCCTGTGATCCAGGATTATCC
IFNαR1-R	TGGTGTGTGCTCTGGCTTTCAC
IFNλR1-F	CAGCAAGTTCTCTAAGCCCACC
IFNλR1-R	GTCATTCACGGACTCTGGTCTG
IFNα-F	GACTCCATCTTGGCTGTGA
IFNα-R	TGATTTCTGCTCTGACAACCT
IFNβ1-F	CTTGGATTCCTACAAAGAAGCAGC
IFNβ1-R	TCCTCCTTCTGGAACTGCTGCA
IFN-γ-F	GAGTGTGGAGACCATCAAGGAAG
IFN-γ-R	TGCTTTGCGTTGGACATTCAAGTC
IFNλ1 (IL-29)-F	GGAAGACAGGAGAGCTGCAACT
IFNλ1 (IL-29)-R	AACTGGGAAGGGCTGCCACATT
IFNλ2/3 (IL-28)-F	TCGCTTCTGCTGAAGGACTGCA
IFNλ2/3 (IL-28)-R	CCTCCAGAACCTTCAGCGTCAG
GAPDH-F	TGTCCCCACCCCCAATGTATC
GAPDH-R	CTCCGATGCCTGCTTCACTACCTT

Supplementary Table S3. Lentiviral sh-RNA sequences used in this study.

Name	Oligo Sequences (5' - 3')
shSTAT1	CCGGCGACAGTATGATGAACACAGTCTCGAGACTGTGTTCATCATACTGTCGTTTTT
shSTAT2	CCGGGCTGAGCCATAGGTCTAAATACTCGAGTATTTAGACCTATGGCTCAGCTTTTT
shIRF9-1	CCGGTTCAAGGCCTGGGCAATATTTCTCGAGAAATATTGCCCAGGCCTTGAATTTTTG
shIRF9-2	CCGGGAGACTTGGTCAGGTACTTTCCTCGAGGAAAGTACCTGACCAAGTCTCTTTTTG
shIRF9-3	CCGGCTCAGTAGTTGTCCGTGATAACTCGAGTTATCACGGACAACTACTGAGTTTTTG

Chapter 5

Suppression of Pyrimidine biosynthesis by targeting DHODH enzyme robustly inhibits rotavirus replication

Sunrui Chen, Shihao Ding, Yuebang Yin, Lei Xu, Pengfei Li, Maikel P. Peppelenbosch, Qiuwei Pan and Wenshi Wang

Abstract

Rotavirus infection remains a great health burden worldwide, especially in various developing countries. It causes severe dehydrating diarrhea in infants, young children, as well as in immunocompromised and organ-transplanted patients. Viral replication heavily relies on the host to supply nucleosides. Thus, host enzymes involved in nucleotide biosynthesis represent potential targets for antiviral development. Dihydroorotate dehydrogenase (DHODH) is the rate-limiting enzyme in the *de novo* biosynthesis pathway of pyrimidines. In this study, we demonstrated that two specific DHODH enzyme inhibitors, brequinar (BQR) and leflunomide (LFM) robustly inhibited rotavirus replication in the conventional human intestinal Caco2 cell line model as well as in human primary intestinal organoids. The antiviral effect is conserved between both the laboratory strain SA11 and the rotavirus strain 2011K, isolated from clinical sample. Mechanistic study indicated that BQR and LFM exerted their anti-rotavirus effect through targeting DHODH to deplete pyrimidine nucleotide pool. Therefore, targeting pyrimidine biosynthesis represents a potential approach for developing antiviral strategies against rotavirus.

1. Introduction

Rotavirus (RV), a member of *Reoviridae* family, is a non-enveloped virus which has a double-stranded RNA genome of 11 segments surrounded by three concentric protein layers. It has been reported to cause estimated 25% of moderate-to-severe illnesses (Kotloff et al., 2013) and 30% of total diarrheal deaths during the first 2 years from birth (Wang et al., 2016a). The development and deployment of rotavirus vaccines was a breakthrough in the fight against diarrheal diseases. Two rotavirus vaccines, Rotarix[TM] and Rotateq, are licensed and widely available in several countries (Yin et al., 2018). Nevertheless, due to limited resources, developing countries including India, Nigeria, Pakistan, Ethiopia and the Democratic Republic of the Congo bear the major burden of mortality (Groome et al., 2014). In addition, immunocompromised patients are also under the risk of RV infection which causes remarkable morbidity and mortality (Lee and Ison, 2014; Sugata et al., 2012; Yin et al., 2015c). For the treatment of rotavirus gastroenteritis, intravenous fluid supply has been used for treatment of dehydration from diarrhea. However, in the severe case of inpatients and immunocompromised patients who are suffering from prolonged diarrhea and fever, virus-specific treatment is urgently required. In fact, there is still no FDA-approved medication available against rotavirus disease. Therefore, to ensure that the remaining burden of mortality and morbidity can be fully addressed in the future, research on the development of novel antiviral strategies is highly needed.

Cellular nucleotides, composed of purines and pyrimidines, play a vital role in constituting nucleic acids RNA and DNA. *De novo* synthesis and salvage pathway are the two pathways for nucleic acid synthesis *in vivo* (Evans and Guy, 2004). Viral replication heavily relies on host supply of nucleoside biosynthesis. Therefore, host enzymes involved in nucleoside biosynthesis represent potential targets for antiviral development. Ribavirin, the most well-known antiviral drug, is such an inhibitor that suppresses guanine biosynthesis via inhibition of cellular IMP dehydrogenase (IMPDH). Several studies have indicated that depletion of cellular GTP pool is the primary mechanism by which ribavirin inhibits virus replication (e.g. flaviviruses and hepatitis E virus) (García et al., 2018; Nicolini et al., 2018). Along this line, we aim to investigate whether inhibitors of the pyrimidine biosynthesis pathway could be targeted for potential antiviral development against rotavirus.

Dihydroorotate dehydrogenase (DHODH) is sequentially the fourth and the rate-limiting enzyme in the *de novo* biosynthesis pathway of pyrimidines. It is located in the inner membrane of mitochondria, where it plays a role of converting dihydroorotate to orotate(Munier-Lehmann et al., 2013). Then, the multifunctional UMP synthase uses orotate to produce UMP, one of the essential precursors for synthesis of all other pyrimidine nucleotides. Several studies have reported that inhibition of DHODH enzyme suppresses a range of different viruses replication (Hoffmann et al., 2011; Luthra et al., 2018; Tan et al., 2005; Wang et al., 2011; Wang et al., 2016b).

In this study, we report that brequinar (BQR) and leflunomide (LFM), two DHODH inhibitors, potently inhibit rotavirus replication in human intestinal cell line as well as three dimensional (3D) cultured primary intestinal organoids. Mode-of-action studies demonstrate that their antiviral activity is mainly achieved via the inhibition of DHODH, resulting in the depletion of intracellular pyrimidine pools. Collectively, our study has stressed the concept that targeting pyrimidine biosynthesis represents a potential approach for antiviral development against rotavirus.

2. Materials and methods

2.1 Reagents

Brequinar (BQR) sodium salt hydrate (Method Detection Limit [MDL] no. MFCD21363375), leflunomide (LFM) (Chemical Abstracts Service [CAS] no. 75706-12-6) ，6-azauracil (6-AU) (MDL no. MFCD00006456) and uridine (CAS no. 58-96-8), were purchased from Sigma. All the reagents were dissolved in dimethyl sulfoxide (DMSO).

2.2. Viruses

Simian rotavirus SA11, a broadly used and well-studied laboratory strain (Cecílio et al., 2012), was a gift from Karen Knipping from Nutricia Research Utrecht, The Netherland. In the study, rotavirus SA11 was prepared as described (Knipping et al., 2012). Stool sample collected from rotavirus infected patient was obtained from the Erasmus MC biobank, Department of Viroscience, Erasmus Medical Center, Rotterdam. This stool sample 2011K was taken during patient diarrhea period and tested for enterovirus, parechovirus, norovirus genogroups I and

II, rotavirus, adenovirus, astrovirus and sapovirus by PCR. Sample 2011K is only positive to rotavirus and negative to other virus mentioned above. Sample information was also described in previous studies (Corless et al., 2002; Hoek et al., 2013; van Maarseveen et al., 2010).

2.3. Cell lines and human primary intestinal organoids

The human colon cancer cell line Caco2 and the human embryonic kidney cell line 293T (HEK 293T) were cultured in Dulbecco's modified Eagle's medium (DMEM; Lonza, Verviers, Belgium) containing 20% (vol/ vol) heat-inactivated fetal calf serum (FCS, Sigma–Aldrich, St. Louis USA) and 100 U/ml Penicillin/ Streptomycin (P/S, Gibco, Grand Island, USA) solution. A humidified incubator was used for cells culturing at 37°C in 5% CO_2. Cells were analyzed by genotyping and confirmed to be mycoplasma negative.

Human primary small intestinal organoids culture was performed as described previously (Yin et al., 2015a). Fragments of intestinal biopsies or surgically resected intestinal tissues were treated with complete chelating solution (CCS, MilliQ H_2O was supplemented with 1.0 g/L of Na_2HPO_4-$2H_2O$, 1.08 g/L of KH_2PO_4, 5.6 g/L of NaCl, 0.12 g/L of KCl, 15 g/L of Sucrose, 10 g/L of D-Sorbitol and 80 µg/L of DL-dithiothreitol) followed by 8 mM EDTA. Crypts were finally collected and suspended in 40 µL growth factor reduced phenol-red free Matrigel (Corning, Bedford, USA). Then, they were incubated at 37°C with 5% CO_2 with culture medium containing CMGF, 2% (vol/vol) of B-27® Supplements (Gibco, Grand Island, USA), 1% (vol/vol) of N2® Supplements (Gibco, Grand Island, USA), 500 pg/mL of EGF, 1 mM n-Acetyl Cysteine, 10 mM Nicotinamide, 0.5 µM A83-01 (TGF-b inhibitor), 3 µM SB202190 (p38 inhibitor), 20% (vol/vol) of R-Spondin 1 (conditioned medium), 10% (vol/vol) of Noggin (conditioned medium) and 50% (vol/vol) of Wnt3a (conditioned medium). Culture medium was refreshed every 2-3 days, and HIOs were passaged every 6–7 days.

2.4. Inoculation of SA11 rotavirus and clinical derived strain 2011K

Caco2 cells were washed, suspended in a T75 flask and subsequently seeded into a 48-well plate (5×10^4 cells/well). Culture medium was discarded when cell confluence was approximately 80%, and cell monolayers were washed twice with PBS. 100 µL of serum-free DMEM medium, then rotavirus (MOI=0.7) with 5 µg/mL of trypsin (Gibco, Paisley, UK) were

added and incubated at 37°C with 5% CO_2 for 60 min for infection, followed by 4 times washing with PBS to remove un-attached viruses Then, cells were incubated with culture medium containing 5 μg/ml of trypsin at 37°C with 5% CO_2.

2.5. Virus production assay

Virus, cell line and HIOs were treated as described in previous work (Yin et al., 2015b). In short, caco2 cells were inoculated with SA11 rotavirus (MOI=0.7) then harvested after 48h incubation with serum-free medium to perform assays as followed. In parallel, human primary intestinal organoids were infected with 10 times higher concentration of SA11 rotavirus than cell infection for 1.5h followed by 4 times washing with PBS. Afterwards, HIOs with no Matrigel remain were spun down at 500g for 10 min to adhered to the bottom of 24-well plate coated with Collagen R solution (SERVA, Heidelberg, Germany). Organoids culture medium was added gently and HIOs were incubated at 37°C with 5% CO_2. Culture medium and HIOs were harvested respectively after 48h to detect and enumerate rotavirus. Virus titers from supernatants were determined by calculating the $\log_{10}TCID_{50}$/mL in Ma104 cells using the method developed by Reed and Muench(Reed and Muench, 1938).

2.6. RNA isolation, cDNA synthesis and qRT-PCR

Total RNA was isolated using Macherey-Nagel NucleoSpin® RNA II kit (Bioke, Leiden, Netherlands) and quantified using a Nanodrop ND-1000 (Wilmington, DE, USA). Total RNA reverse transcription was performed by using a cDNA Synthesis kit (TAKARA BIO INC.) with random hexamer primers. Real-time PCR reactions (50°C for 2 min, 95°C for 10 min, followed by 50 or 60 cycles of 95°C for 15 s and 58°C for 30 s and 72°C for 10 min) were performed with SYBRGreen-based real-time PCR (Applied Biosystems®, Austin, USA) according to the manufacturer's instruction. Glyceraldehyde 3-phosphate dehydrogenase (GAPDH) gene was used as housekeeping gene. Relative gene expressions were normalized to GAPDH using the formula $2^{-\Delta\Delta CT}$ (ΔΔCT = ΔCTsample - ΔCTcontrol). Template control and reverse transcriptase control were included in all RT-qPCR experiments. All qRT-PCR primers are listed in Supplementary table 1.

2.7. Quantification of rotavirus genome copy numbers

An amplicon of the SA11 (a fragment of VP6 gene from 564-718) was cloned into the pCR2.1-TOPO vector (Invitrogen, San Diego, CA) to generate a template for quantifying rotavirus genome copy number. The plasmid was extracted by Quick Plasmid Miniprep Kit (Invitrogen, Lohne, Germany) following manufacturer's instructions. A series of dilutions (from 10^{-2} to 10^{-10}) were prepared and then were amplified and quantified by qRT-PCR to generate a standard curve. This standard curve was generated by plotting the log copy number versus the cycle threshold (CT) value (Fig. S1). Copy numbers were calculated by using the following equation:

Copy number (molecules/µl) = [concentration (ng/µl) × 6.022× 10^{23} (molecules/mol)]/[length of amplicon× 640 (g=/mol) × 10^9 (ng/g).

2.8. Determination of compromised organoids scoring

The scoring process was performed as previously(Grabinger et al., 2014). In short, a minimum of 100 organoids were counted after 3 days following passaging. After a 1.5h incubation with SA11 rotavirus, HIOs were cultured in matrigel and treated with different agents for 48h, and HIOs were counted and defined as viable or dead via their morphological appearance in the optimal microscope (Axiovert 40 CFL, Zeiss, Oberkochen, Germany) in at least three random visions in different parallel wells, the description of this scoring system is showed in Fig. S3. The proportion of deteriorated organoids was calculated as (viable/ total) %.

2.9. Gene knockdown assays

Lentiviral shRNA vectors, targeting dihydroorotate dehydrogenase (DHODH) gene or non-targeted control lentivirus were produced in 293T cells as previous work (Qu et al., 2018). Caco2 cells were inoculated with lentivirus to generate stable gene knockdown cells. Cells were subsequently selected with 5 µg/mL puromycin (Sigma). After pilot study, two shRNA vectors exerting optimal gene knockdown were selected. Knockdown and control Caco2 cells were incubated with rotavirus as described above. All shRNA primers were listed in supplementary table 2.

2.10. Western blot assay

Lysed cells were subjected to SDS-PAGE, and proteins were transferred to PVDF membrane (Immobilon-FL). DHODH (ab 54621, 1:1000, mouse monoclonal, Abcam), SA11 rotavirus VP4

(1:1000, HS-2, mouse monoclonal; provided by professor Harry Greenberg, Stanford University School of Medicine, USA) was detected by western blot analysis and β-actin protein was detected as loading control (sc-47778, 1:1000, mouse monoclonal; Santa Cruz). The intensity of the immunoreactive bands of blotted protein was quantified by the Odyssey V3.0 software.

2.11. Immunofluorescence analysis

After rotavirus infection and BQR treatment, HIOs were harvested and fixed in 4% paraformaldehyde in PBS at 4°C for 10 min. Fixed HIOs were added into the CytoSpin II Cytocentrifuge (Shandon Scientifi Ltd, Runcorn, England), then spined down at 1000 rpm for 2 min. The slides containing HIOs were rinsed 3 times with PBS for 5 min each, followed by treatment with 0.1% (vol/vol) Tritonx100 for 4 min. Subsequently, the slides were twice rinsed with PBS for 5 min, followed by incubation with milk-tween-glycine medium (0.05% tween, 0.5% skim milk and 0.15% glycine) to block background staining for 30 min. Slides were incubated in a humidity chamber with anti-rotavirus antibodies (1:250, mouse monoclonal; Abcam) diluted in milk-tween-glycine medium at 4 ºC overnight. Slides were washed 3 times for 5 min each in PBS prior to 1h incubation with 1:1000 dilutions of the anti-mouse IgG (H+L, Alexa Fluor® 594) secondary antibody. Nuclei were stained with DAPI (4, 6-diamidino-2-phenylindole; Invitrogen). Images were detected using EVOS FL cell imaging system (Thermo Fisher).

2.12. MTT assay

The CC_{50} values of BQR and LFM (1613μM for BQR and 372μM for LFM) were determined by MTT assay (Fig. 1C) as previous study (Qu et al., 2018). Approximately 1×10^4 Caco2 cells were seeded per well in 96-well plate. After 48h, cells were incubated with 10 μL 5 mg/ml MTT for 3 h, then replaced with 100 ml dimethyl sulfoxide (DMSO) medium (Sigma). Absorbance (490 nm) was analyzed accordingly.

2.13. Statistics

All numerical results reported represent at least two technical replicates obtained in two independent biological replicates and are reported as Mean ± SEM. The statistical significance

of differences between means was assessed with the Mann-Whitney test (GraphPad Prism 5; GraphPad Software Inc., La Jolla, CA). The threshold for statistical significance was defined as $P \leq 0.05$.

3. Result

3.1. BQR and LFM potently inhibit the replication of SA11 and patient-derived rotavirus strain 2011K.

BQR is an immunosuppressive and anti-proliferative compound which has been evaluated in multiple clinical trials as a potential treatment for cancer (Madak et al., 2017; Makowka et al., 1993). Similarly, LFM is also an immunosuppressive drug used in active moderate-to-severe rheumatoid arthritis and psoriatic arthritis (Davis et al., 1996). So we tried to investigate whether these two inhibitors of the pyrimidine biosynthesis pathway have potential anti-rotavirus effect. After infection by simian rotavirus SA11, Caco2 cells were treated with various concentrations of BQR and LFM for 48h. BQR and LFM potently inhibited SA11 rotavirus replication in a dose-dependent manner as measured in both RNA and protein levels (Fig. 1A and B), while cell viability was not affected (Fig. 1C). The IC_{50} values of BQR and LFM are 0.04917 µM and 48.98 µM respectively, while the CC_{50} values are 1613 µM and 372 µM, indicating a high specificity of these two compounds on rotavirus (Fig. 1C and Fig. S2). Consistently, SA11 rotavirus titer was also significantly decreased by BQR and LFM treatment (Fig. 1D). Indirect fluorescence microscopy analysis further confirmed that BQR and LFM could inhibit rotavirus replication (Fig. 2A and B). 3D cultured primary human intestinal organoids (HIO) represent a state-of-art model for investigating intestinal physiology and pathology. Therefore, we further tested the antiviral activity of BQR and LFM in the HIO model. Importantly, BQR and LFM reduced the levels of cellular viral RNA and inhibited virus production significantly, while no cytotoxicity effects were observed (Fig. 3A and B, Fig. S3A). For instance, with 5µM of BQR, cellular viral RNA was decreased by 65% (n=6, p<0.01), and virus production was inhibited by 76% (n=6, p<0.01). Since rotavirus infection causes pathological and morphological changes on organoids, we randomly selected three scopes and quantified the proportion of compromised organoids upon different treatments. Both BQR and LFM could strongly decrease the proportion of compromised organoids (Fig. 4 A-C). This notion was further supported by the evidence that BQR and LFM treatment led to decreased levels of rotavirus VP6 protein (Fig. 4D). Next, we expand our study to patient-derived rotavirus strain 2011K. Consistently, BQR and LFM profoundly inhibited virus

replication of this rotavirus strain (Fig. 5). Collectively, these results demonstrated that BQR and LFM could potently inhibit rotavirus replication.
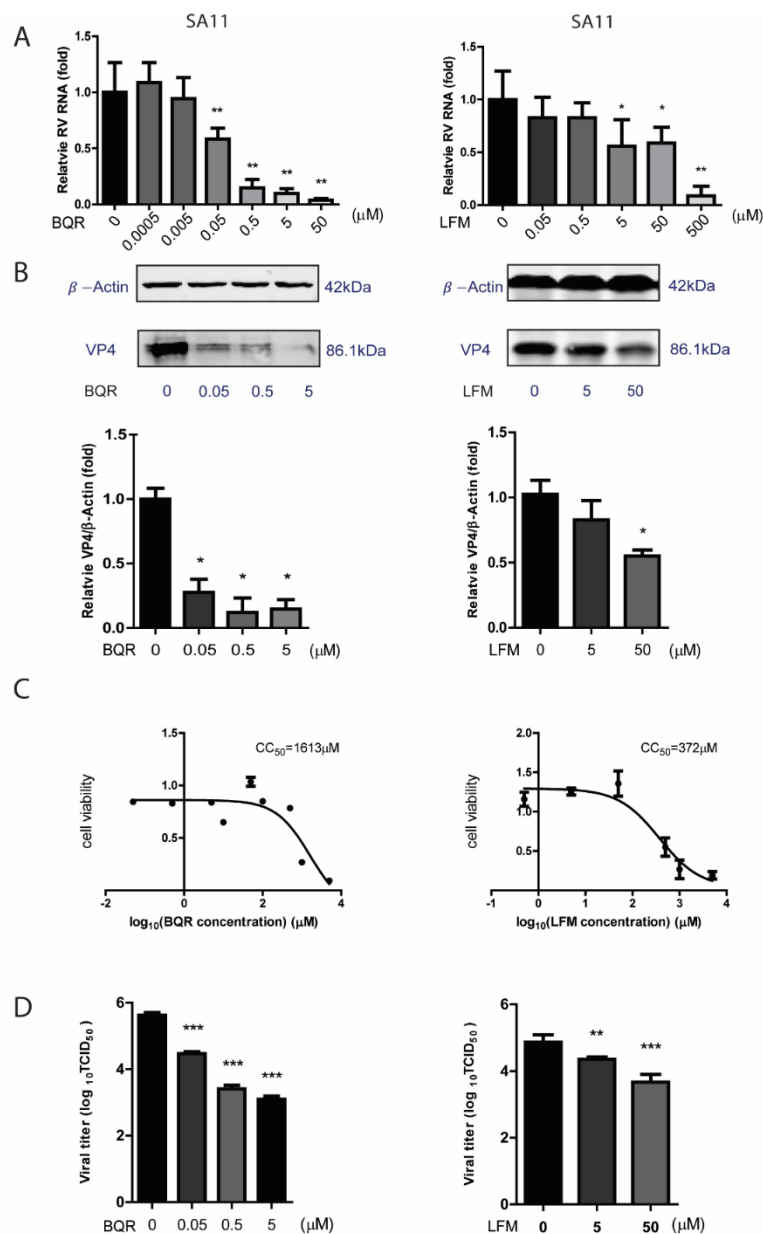

Figure 1. BQR and LFM exert potent antiviral activity against rotavirus SA11 on Caco2 cells. Caco2 cells were infected with SA11 rotavirus. After infection, cells were treated with various concentrations of BQR or LFM. (A) qRT-PCR analysis indicated that BQR (n=6) and LFM (n=6) exerted potent antiviral effect against rotavirus replication. Data were normalized to housekeeping genes *GAPDH* and presented relative to the control (CTR) (set as 1). Data represent means ± SEM. *, $P < 0.05$; **, $P < 0.01$. (B) Western blot analysis showed that BQR (n=4, 0.05 to 5 µM) and LFM (n=4, 50 µM) inhibited rotavirus replication. Data represent means ± SEM. *, $P < 0.05$. (C) 50% cytotoxic concentration (CC_{50}) curves of BQR (left panel) and LFM (right panel) were determined by MTT assays. (D) The supernatant of each well was harvested after freeze and

thaw for three times, virus titer from different groups was measured (n=4. Data represent means ± SEM. ***, $P < 0.001$).
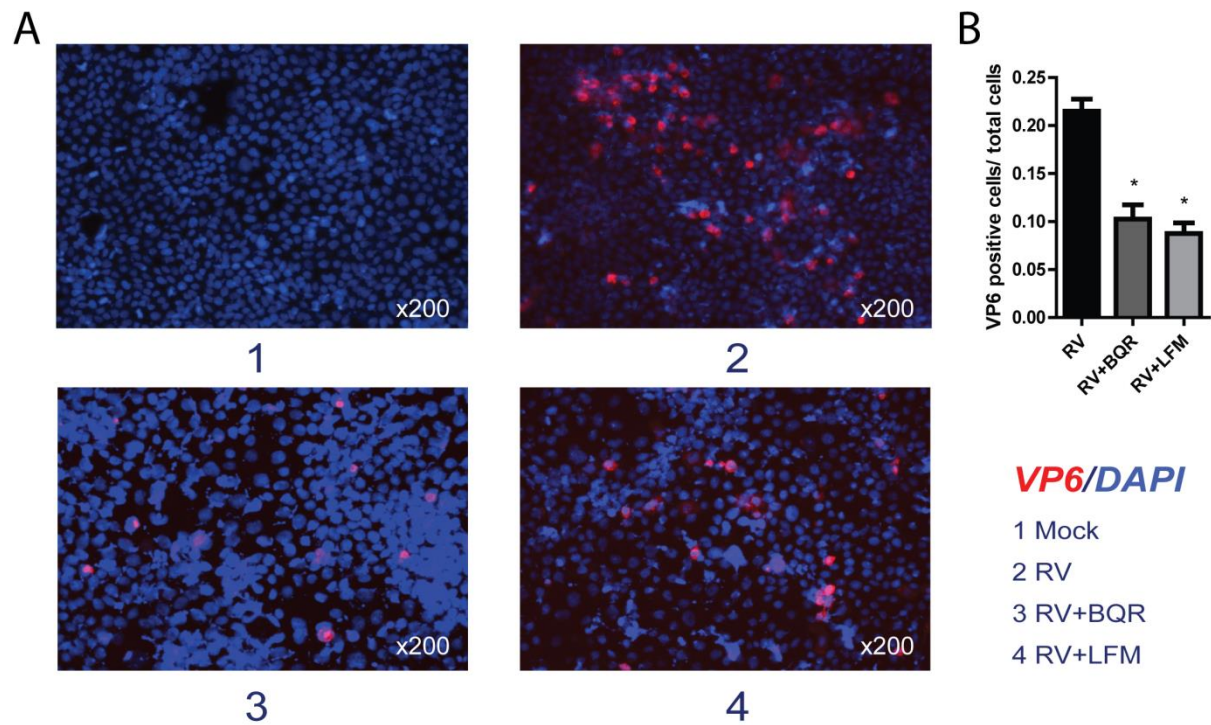

Figure 2. BQR and LFM inhibit the expression of rotavirus VP6 protein. (A)Indirect fluorescence microscope analysis of viral structural protein VP6 (red) upon treatment with BQR (0.05 µM) and LFM (5 µM). Nuclei were visualized by DAPI (blue). (B) The ratio of VP6 positive cells/ total cell number was quantified (n=4). Data represent means ± SEM. *, $P < 0.05$.

A

B
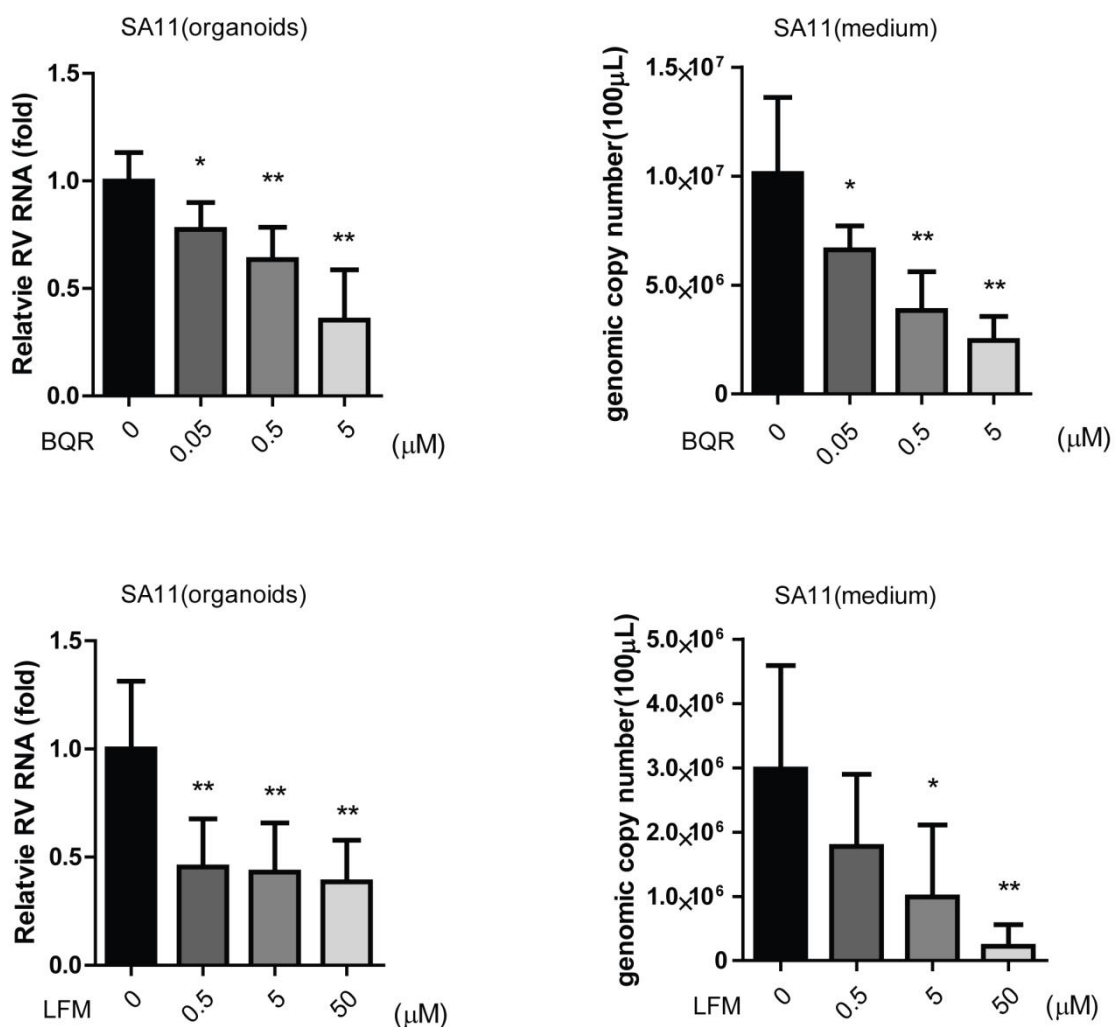
Figure 3. BQR and LFM exert potent antiviral activity against rotavirus SA11 on human intestinal organoids. (A) Representative microscopy of cultured human small intestinal organoids. (B) BQR (n=6) as well as LFM (n=6) inhibit SA11 replication and virus production after 48h incubation. The relative rotavirus

RNA and genomic copy number were analyzed by qRT-PCR. Data represent means ± SEM. *, $P < 0.05$; **, $P < 0.01$. (Data of standard curve is in Supplementary Fig. S1)

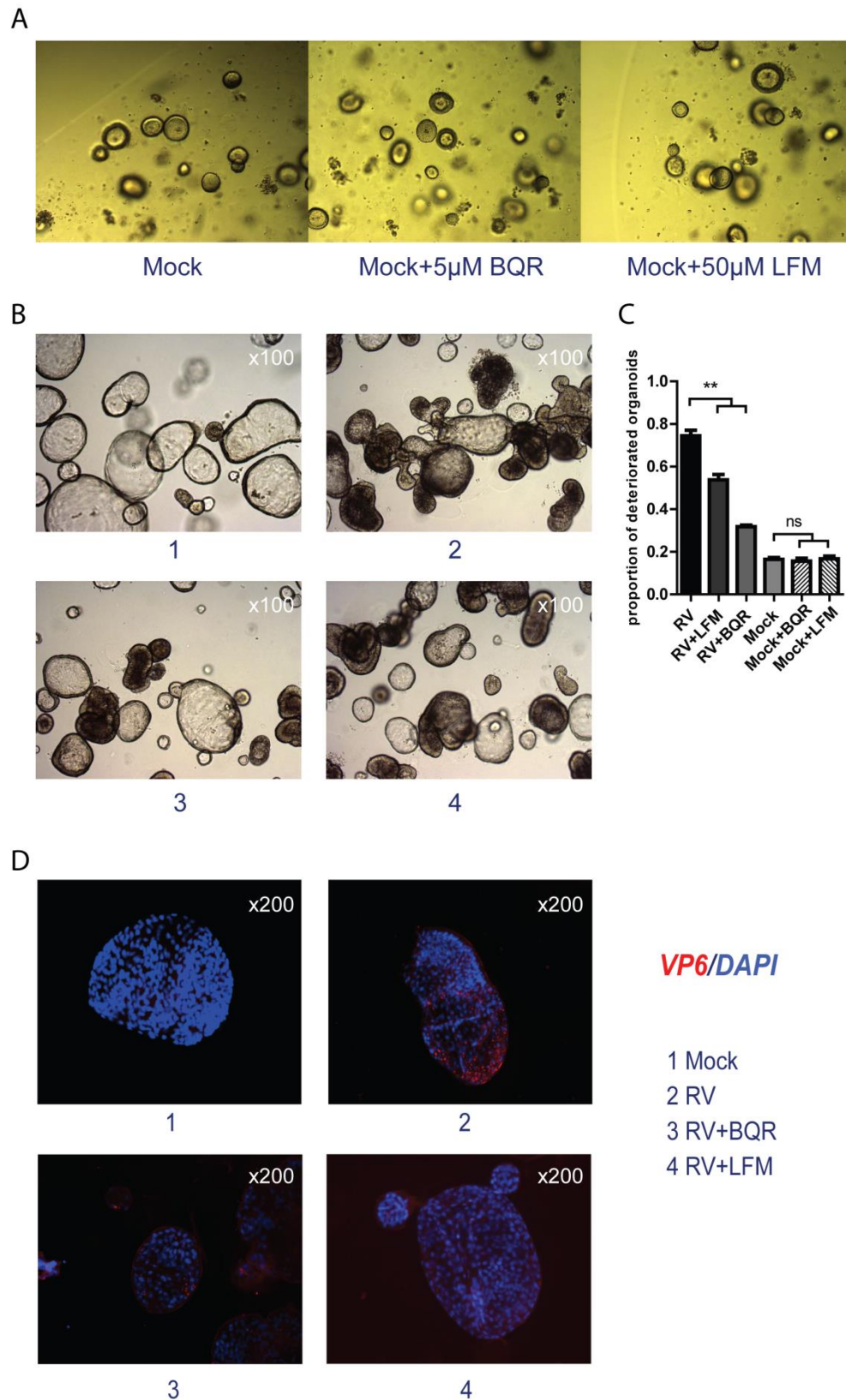**Figure 4. Microscopy image analysis indicated that BQR and LFM exert potent antiviral activity against rotavirus SA11 on human intestinal organoids (HIOs).** (A) Microscopy image analysis of HIOs treated with 5μM BQR and 50μM LFM. (B) Microscopy image analysis of HIOs infected by rotavirus SA11 and treated with CTR, 5μM BQR or 50μM LFM. (C) Scoring of proportion of deteriorated HIOs in different random visions, n=6. Data represent means ± SEM. **, $P < 0.01$. (D) 5μM BQR and 50μM LFM inhibited rotavirus SA11 replication on HIOs. Rotavirus structural protein VP6 (red). Nuclei were visualized by DAPI (blue).
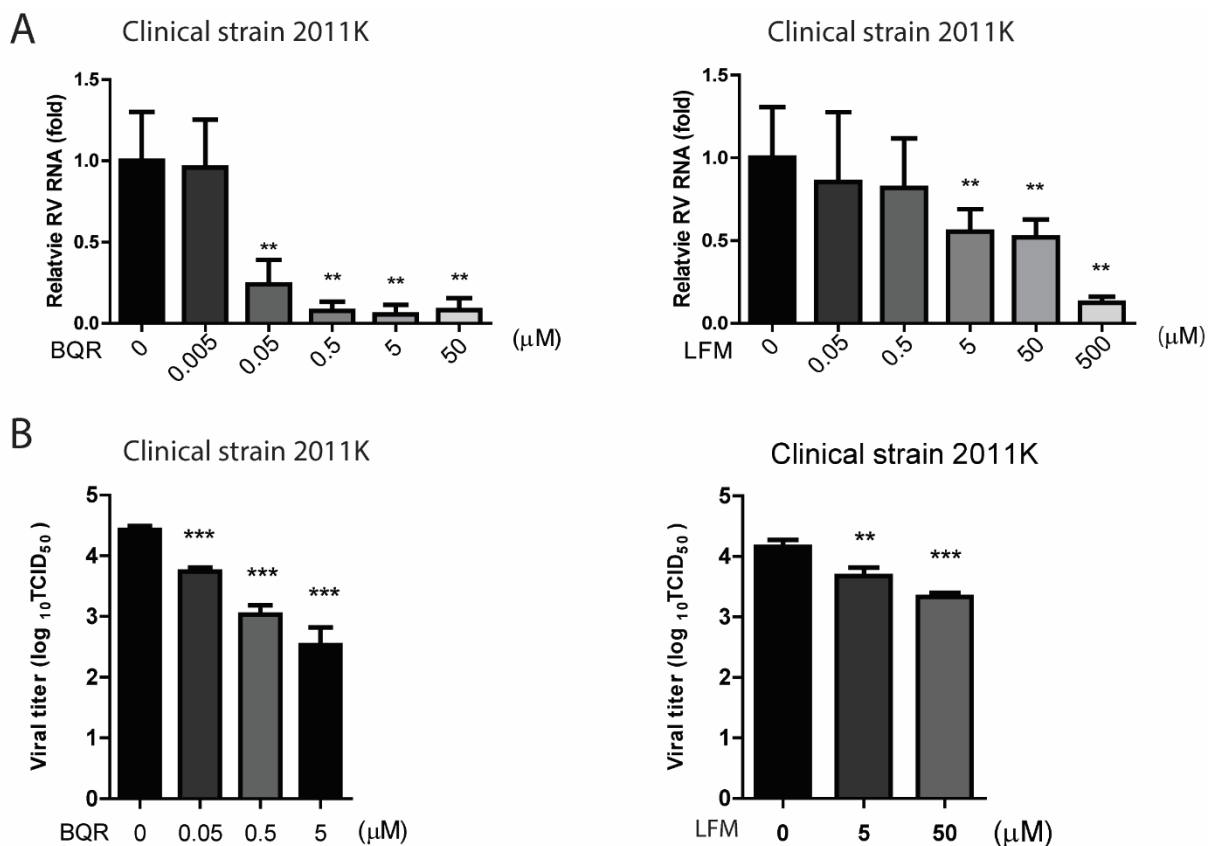
Figure 5. BQR and LFM showed antiviral effect against clinical-derived rotavirus strains. (A) qRT-PCR analysis indicated that BQR (n=6) and LFM (n=6) exerted strong antiviral effect against rotavirus 2011K. Data were normalized to housekeeping genes *GAPDH* and are presented relative to the control (CTR) (set as 1). Data represent means ± SEM. *, $P < 0.05$; **, $P < 0.01$. (B) Virus titer of rotavirus 2011K were measured upon BQR and LFM treatment respectively (n=4). Data represent means ± SEM. ***, $P < 0.001$.

3.2 BQR and LFM, two DHODH inhibitors, inhibit rotavirus replication through depletion of the cellular pyrimidine nucleotide pool

Classically, BQR and LFM are two well-established DHODH inhibitors. Upon inhibition of DHODH, cellular pyrimidine biosynthesis pathway will be blocked, resulting in the depletion

of pyrimidine nucleotide pool. To investigate whether these two compounds exert a similar mode-of-action against rotavirus, we employed both BQR and LFM for further mechanistic study. We first used an RNAi-based loss-of-function assay to study the role of DHODH. Two successful knock-down clones were confirmed by both qRT-PCR and western blot (Fig. 6A). Silencing of DHODH resulted in compromised rotavirus replication (Fig. 6B). The specificity of the effect was further confirmed when we added BQR and LFM to DHODH knockdown or control cell lines infected with SA11. Knockdown of DHODH abrogated the anti-rotavirus effect rate of BQR from 53% to 37% and 38% respectively. As for LFM, the effect decreased from 72% to 50% in both knockdown cell lines (Fig. 6C). To further validate whether the antiviral effect of BQR and LFM was achieved via the depletion of pyrimidine pool, exogenous uridine was supplemented to cell culture medium. Of note, supplementation of pyrimidine dose-dependently abolished the anti-rotavirus effect of BQR and LFM. At the concentration of 2000μM, the BQR and LFM-provoked anti-rotavirus effect was totally abolished (Fig. 6D). Taken together, these results indicated that BQR and LFM exerts their anti-rotavirus effect through targeting DHODH to deplete pyrimidine nucleotide pool. Orotidine 5'-monophosphate decarboxylase (ODCase) serves as the downstream enzyme of DHODH, which catalyzes OMP to UMP. 6-azauracil (6-AU), a potent inhibitor of ODCase, was evaluated for its potential effect on rotavirus replication. Consistently, 6-AU also inhibits rotavirus replication (Fig. 7A). Conceptually, targeting pyrimidine biosynthesis represents a potential approach for antiviral development against rotavirus.
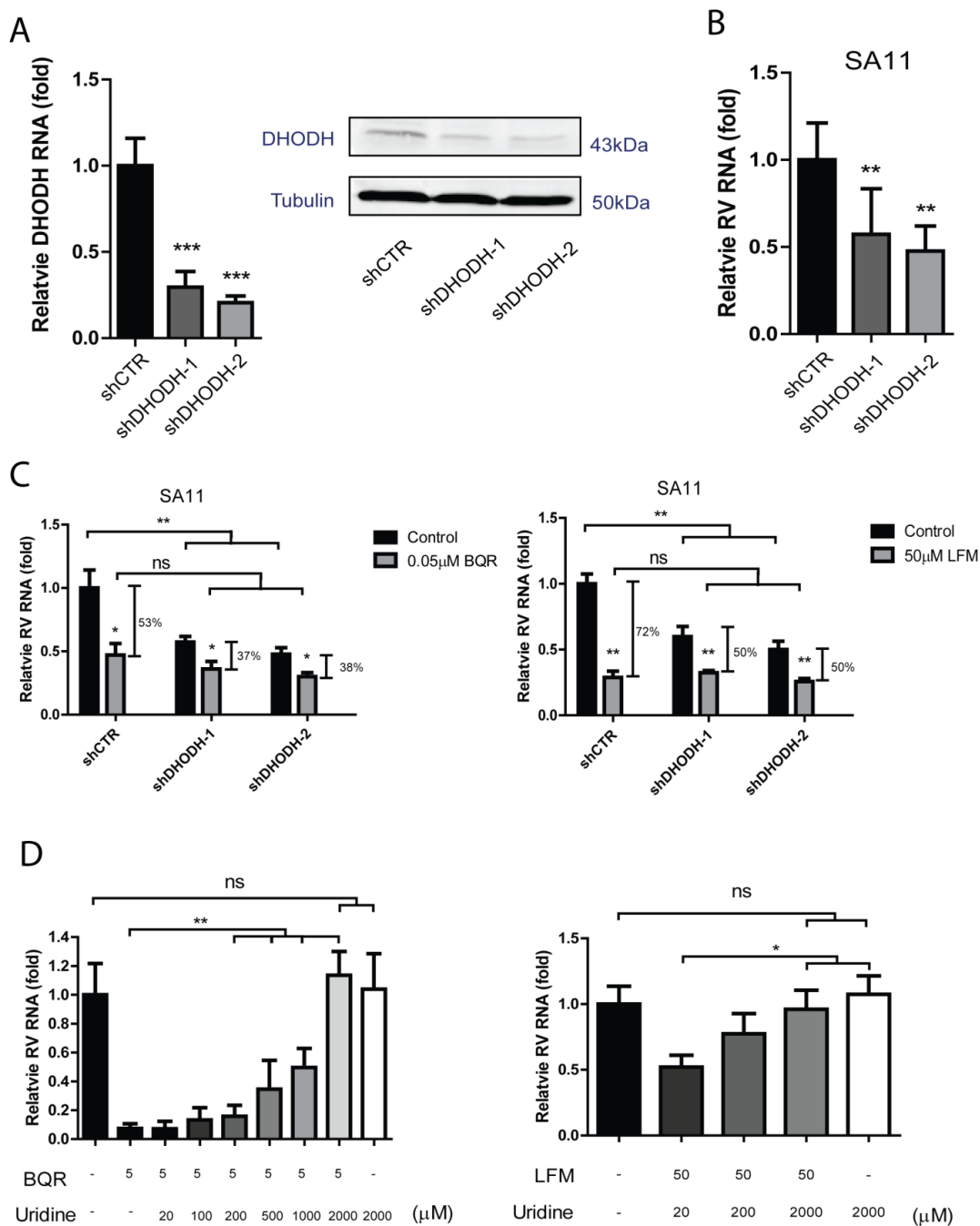
Figure 6. BQR and LFM exert its anti-rotavirus effect through targeting DHODH to deplete pyrimidine nucleotide pool. (A) qRT-PCR and western blot analysis confirmed the knockdown of DHODH in Caco2 cells (n=9). Data represent means ± SEM. ***, $P < 0.001$. (B) Knockdown of DHODH significantly inhibits SA11 rotavirus replication in Caco2 cells (n=6). Data represent means ± SEM. **, $P < 0.01$. (C) Anti-rotavirus effect of BQR and LFM was partially blocked in two clones of DHODH knockdown cells (n=6). Data represent means ± SEM. *, $P < 0.05$. (D) Supplementation of exogenous uridine attenuates the anti-rotavirus effect of BQR and LFM in Caco2 cells (n=6). Data represent means ± SEM. **, $P < 0.01$.
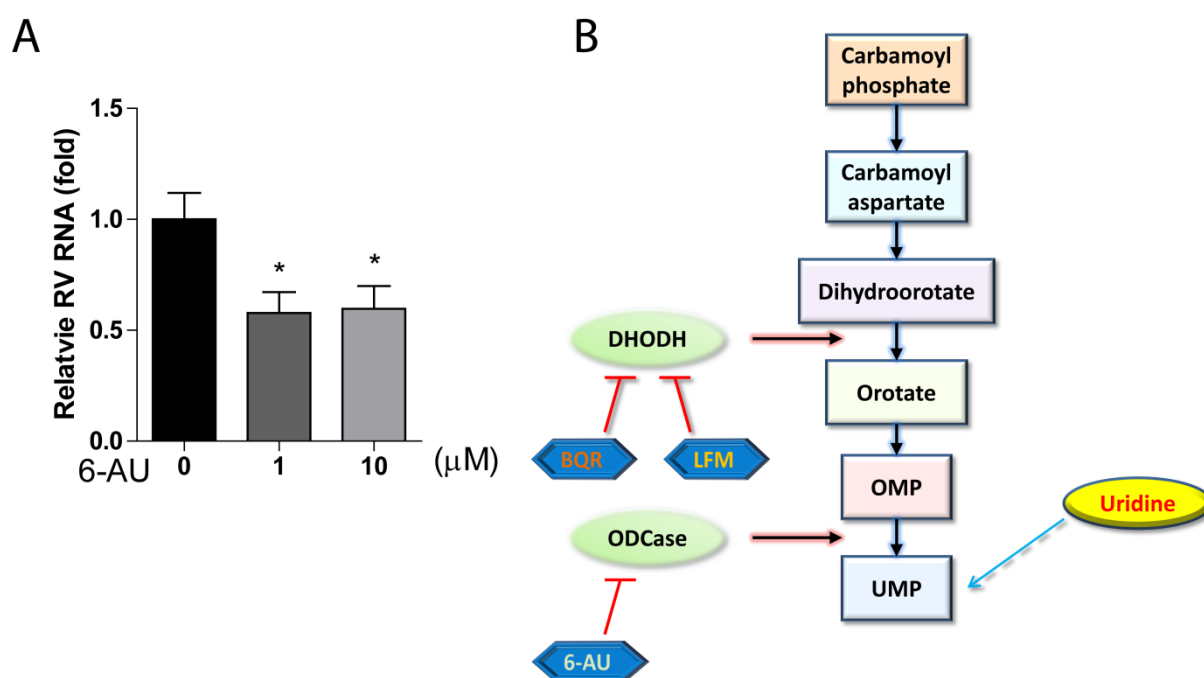
Figure 7. Depleting pyrimidine nucleotide pool inhibits rotavirus replication. (A) qRT-PCR analysis showed that 6-AU, a specific inhibitor of ODCase, inhibited rotavirus replication (n=6). Data represent means ± SEM. *, $P < 0.05$. (B) Schematic overview of *de novo* pyrimidine biosynthesis pathway.

4. Discussion

Though rotavirus vaccines have been introduced, and the vaccines remarkably reduced the burden of rotavirus gastroenteritis in many developed countries, due to prevalence and diversity of the virus, one third to half of the children is subject to vaccination failure in some developing countries (Macartney et al., 2000). Antiviral treatment may serve as complement to vaccination. A drug repurposing approach offers many advantages for the identification of new antiviral strategies over the development of new drugs, since safety and pharmacology in humans are already well known. Therefore, if a drug, currently in clinical use, demonstrates considerable antiviral activity against rotavirus, there should be great potential to expand its application to combating rotavirus infection.

Of note, BRQ and LFM are two well-known immunosuppressive agents (Batt, 1999). As for LFM, it was reported as immunosuppressive therapy for bone marrow (Avery et al., 2004) and renal (Chon and Josephson, 2011) transplantation. Accumulating evidence indicates that organ transplant patients, irrespective of their age, are more vulnerable to rotavirus infection. Thus, the potential clinical prospects of BQR and LFM or their analogues may be to achieve a "one stone two birds" effect: exerting immunosuppressive function and anti-rotavirus effect at the same time. Of note, BQR was reported to have some side effects, such as leukocytopenia ,thrombocytopenia, reduced body weight gain or body weight loss, thymic atrophy, cellular depletion of bone marrow and splenic white pulp, and villous atrophy in jejunum (Pally et al., 1998). Similarly, LFM also has side effects, including gastrointestinal symptoms, rash or allergic reactions and alopecia (Emery et al., 2000; Mladenovic et al., 1995; Smolen et al., 1999; Strand et al., 1999). These kinds of clinical observations should be seen in the light of that all drugs come with side effects. Importantly, the drug dosages of both drugs used in our study for inhibition of rotavirus are much lower than their previous clinical trial dosages (Maroun et al., 1993; Natale et al., 1992; Smolen et al., 1999). This might make BQR or LFM a preferable option for treating rotavirus infection, achieving high efficacy with less side effects. In addition, pyrimidine biosynthesis (Figure 7B) represents a potential host pathway for novel antiviral drug development. These specific inhibitors of this pathway may represent as a starting point for the development of efficient anti-rotavirus drugs with more broad applications.

Intestinal carcinoma-derived cell lines such as Caco2 cell line are widely used as *in vitro* models to investigate rotavirus infection (Cuadras et al., 2002; Frias et al., 2012). Compared to such two-dimensional (2D) single cell type culture systems, the three-dimensional (3D) model of human primary intestinal organoids surpasses 2D models in cell diversity and spatial structure for mimicking rotavirus infection (Yin et al., 2015a). Specifically, these primary intestinal organoids consist of many undifferentiated and heterogeneous cell types with similar functions as in the organ/tissue of origin (Sato and Clevers, 2012, 2013; Sato et al., 2011; Sato et al., 2009), including enterocytes, enteroendocrine cells, goblet cells, Paneth cells and stem cells (Saxena et al., 2015). We have validated our results observed in conventional cell culture model also in the primary human organoids. Moreover, the use of rotavirus strains isolated

from clinical samples leads our study one step closer to eventual improved clinical therapy for rotavirus infection.

Nucleotides play an important role in host cell metabolism and are essential for virus infection. Many inhibitors targeting *de novo* pyrimidine biosynthesis (Fig. 7B) have been well studied on dengue virus, HBV, HEV and other virus infection models (Beardsley et al., 1989; Greene et al., 1995; Hoppe-Seyler et al., 2012; Nelson et al., 1975; Qing et al., 2010; Silva et al., 1997; Wang et al., 2011; Wang et al., 2016b). In this study, we demonstrated that both BQR and LFM, inhibitors of DHODH enzyme, have potent antiviral activity against rotavirus infection. Mechanistic study demonstrated that BQR and LFM exert their anti-rotavirus effect through targeting DHODH to deplete pyrimidine nucleotide pool. Therefore, targeting pyrimidine biosynthesis represents a potential approach for developing antivirals against rotavirus.

References

Avery, R.K., Bolwell, B.J., Yen-Lieberman, B., Lurain, N., Waldman, W.J., Longworth, D.L., Taege, A.J., Mossad, S.B., Kohn, D., Long, J.R., 2004. Use of leflunomide in an allogeneic bone marrow transplant recipient with refractory cytomegalovirus infection. Bone marrow transplantation 34, 1071.

Batt, D.G., 1999. Inhibitors of dihydroorotate dehydrogenase. Expert Opinion on Therapeutic Patents 9, 41-54.

Beardsley, G.P., Moroson, B.A., Taylor, E.C., Moran, R.G., 1989. A new folate antimetabolite, 5, 10-dideaza-5, 6, 7, 8-tetrahydrofolate is a potent inhibitor of de novo purine synthesis. Journal of Biological Chemistry 264, 328-333.

Bonavia, A., Franti, M., Keaney, E.P., Kuhen, K., Seepersaud, M., Radetich, B., Shao, J., Honda, A., Dewhurst, J., Balabanis, K., 2011. Identification of broad-spectrum antiviral compounds and assessment of the druggability of their target for efficacy against respiratory syncytial virus (RSV). Proceedings of the National Academy of Sciences 108, 6739-6744.

Cecílio, A.B., de Faria, D.B., de Carvalho Oliveira, P., Caldas, S., de Oliveira, D.A., Sobral, M.E.G., Duarte, M.G.R., de Souza Moreira, C.P., Silva, C.G., de Almeida, V.L., 2012. Screening of Brazilian medicinal plants for antiviral activity against rotavirus. Journal of ethnopharmacology 141, 975-981.

Cheung, N.N., Lai, K.K., Dai, J., Kok, K.H., Chen, H., Chan, K.-H., Yuen, K.-Y., Kao, R.Y.T., 2017. Broad-spectrum inhibition of common respiratory RNA viruses by a pyrimidine synthesis inhibitor with involvement of the host antiviral response. Journal of General Virology 98, 946-954.

Chon, W.J., Josephson, M.A., 2011. Leflunomide in renal transplantation. Expert review of clinical immunology 7, 273-281.

Corless, C.E., Guiver, M., Borrow, R., Edwards-Jones, V., Fox, A.J., Kaczmarski, E.B., Mutton, K.J., 2002. Development and evaluation of a 'real-time'RT-PCR for the detection of enterovirus and parechovirus RNA in CSF and throat swab samples. Journal of medical virology 67, 555-562.

Cuadras, M.A., Feigelstock, D.A., An, S., Greenberg, H.B., 2002. Gene expression pattern in Caco-2 cells following rotavirus infection. Journal of virology 76, 4467-4482.

Davis, J.P., Cain, G.A., Pitts, W.J., Magolda, R.L., Copeland, R.A., 1996. The immunosuppressive metabolite of leflunomide is a potent inhibitor of human dihydroorotate dehydrogenase. Biochemistry 35, 1270-1273.

Dunn, M.C.C., Knight, D.A., Waldman, W.J., 2011. Inhibition of respiratory syncytial virus in vitro and in vivo by the immunosuppressive agent leflunomide. Antiviral therapy 16, 309.

Emery, P., Breedveld, F., Lemmel, E., Kaltwasser, J., Dawes, P., Gömör, B., Van den Bosch, F., Nordström, D., Bjørneboe, O., Dahl, R.J.R., 2000. A comparison of the efficacy and safety of leflunomide and methotrexate for the treatment of rheumatoid arthritis. 39, 655-665.

Evans, D.R., Guy, H.I., 2004. Mammalian pyrimidine biosynthesis: fresh insights into an ancient pathway. Journal of Biological Chemistry 279, 33035-33038.

Frias, A.H., Jones, R.M., Fifadara, N.H., Vijay-Kumar, M., Gewirtz, A.T., 2012. Rotavirus-induced IFN-β promotes anti-viral signaling and apoptosis that modulate viral replication in intestinal epithelial cells. Innate immunity 18, 294-306.

García, C.C., Quintana, V.M., Castilla, V., Damonte, E.B., 2018. Towards Host Cell-Targeting Therapies to Treat Dengue Virus Infections. Frontiers in Anti-Infective Drug Discovery: Volume 7 7, 45.

Grabinger, T., Luks, L., Kostadinova, F., Zimberlin, C., Medema, J.P., Leist, M., Brunner, T., 2014. Ex vivo culture of intestinal crypt organoids as a model system for assessing cell death induction in intestinal epithelial cells and enteropathy. Cell death & disease 5, e1228.

Grandin, C., Hourani, M.-L., Janin, Y.L., Dauzonne, D., Munier-Lehmann, H., Paturet, A., Taborik, F., Vabret, A., Contamin, H., Tangy, F., 2016. Respiratory syncytial virus infection in macaques is not suppressed by intranasal sprays of pyrimidine biosynthesis inhibitors. Antiviral research 125, 58-62.

Greene, S., Watanabe, K., Braatz-Trulson, J., Lou, L., 1995. Inhibition of dihydroorotate dehydrogenase by the immunosuppressive agent leflunomide. Biochemical pharmacology 50, 861-867.

Groome, M.J., Moon, S.-S., Velasquez, D., Jones, S., Koen, A., Niekerk, N.v., Jiang, B., Parashar, U.D., Madhi, S.A., 2014. Effect of breastfeeding on immunogenicity of oral live-attenuated human

rotavirus vaccine: a randomized trial in HIV-uninfected infants in Soweto, South Africa. Bulletin of the World Health Organization 92, 238-245.

Hoek, R.A.S., Paats, M.S., Pas, S.D., Bakker, M., Hoogsteden, H.C., Boucher, C.A.B., van der Eerden, M.M., 2013. Incidence of viral respiratory pathogens causing exacerbations in adult cystic fibrosis patients. Scandinavian journal of infectious diseases 45, 65-69.

Hoffmann, H.-H., Kunz, A., Simon, V.A., Palese, P., Shaw, M.L., 2011. Broad-spectrum antiviral that interferes with de novo pyrimidine biosynthesis. Proceedings of the National Academy of Sciences 108, 5777-5782.

Hoppe-Seyler, K., Sauer, P., Lohrey, C., Hoppe-Seyler, F., 2012. The inhibitors of nucleotide biosynthesis leflunomide, FK778, and mycophenolic acid activate hepatitis B virus replication in vitro. Hepatology 56, 9-16.

Knipping, K., Garssen, J., van't Land, B., 2012. An evaluation of the inhibitory effects against rotavirus infection of edible plant extracts. Virology journal 9, 1.

Kotloff, K.L., Nataro, J.P., Blackwelder, W.C., Nasrin, D., Farag, T.H., Panchalingam, S., Wu, Y., Sow, S.O., Sur, D., Breiman, R.F., 2013. Burden and aetiology of diarrhoeal disease in infants and young children in developing countries (the Global Enteric Multicenter Study, GEMS): a prospective, case-control study. The Lancet 382, 209-222.

Lee, L.Y., Ison, M.G., 2014. Diarrhea caused by viruses in transplant recipients. Transplant Infectious Disease 16, 347-358.

Luthra, P., Naidoo, J., Pietzsch, C.A., De, S., Khadka, S., Anantpadma, M., Williams, C.G., Edwards, M.R., Davey, R.A., Bukreyev, A., 2018. Inhibiting pyrimidine biosynthesis impairs Ebola virus replication through depletion of nucleoside pools and activation of innate immune responses. Antiviral research 158, 288-302.

Macartney, K.K., Baumgart, D.C., Carding, S.R., Brubaker, J.O., Offit, P.A., 2000. Primary murine small intestinal epithelial cells, maintained in long-term culture, are susceptible to rotavirus infection. Journal of virology 74, 5597-5603.

Madak, J.T., Cuthbertson, C.R., Chen, W., Showalter, H.D., Neamati, N., 2017. Design, synthesis, and characterization of brequinar conjugates as probes to study DHODH inhibition. Chemistry–A European Journal 23, 13875-13878.

Makowka, L., Sher, L.S., Cramer, D.V., 1993. The development of brequinar as an immunosuppressive drug for transplantation. Immunological reviews 136, 51-70.

Maroun, J., Ruckdeschel, J., Natale, R., Morgan, R., Dallaire, B., Sisk, R., Gyves, J.J.C.c., pharmacology, 1993. Multicenter phase II study of brequinar sodium in patients with advanced lung cancer. 32, 64-66.

Marschall, M., Niemann, I., Kosulin, K., Bootz, A., Wagner, S., Dobner, T., Herz, T., Kramer, B., Leban, J., Vitt, D., 2013. Assessment of drug candidates for broad-spectrum antiviral therapy targeting cellular pyrimidine biosynthesis. Antiviral research 100, 640-648.

Mladenovic, V., Domljan, Z., Rozman, B., Jajic, I., Mihajlovic, D., Dordevic, J., Popovic, M., Dimitrijevic, M., Zivkovic, M., Campion, G.J.A., Rheumatology, R.O.J.o.t.A.C.o., 1995. Safety and effectiveness of leflunomide in the treatment of patients with active rheumatoid arthritis. 38, 1595-1603.

Munier-Lehmann, H.l.n., Vidalain, P.-O., Tangy, F.d.r., Janin, Y.L., 2013. On dihydroorotate dehydrogenases and their inhibitors and uses. Journal of medicinal chemistry 56, 3148-3167.

Natale, R., Wheeler, R., Moore, M., Dallaire, B., Lynch, W., Carlson, R., Grillo-Lopez, A., Gyves, L.J.A.o.o., 1992. Multicenter phase II trial of brequinar sodium in patients with advanced melanoma. 3, 659-660.

Nelson, J.A., Carpenter, J.W., Rose, L.M., Adamson, D.J., 1975. Mechanisms of action of 6-thioguanine, 6-mercaptopurine, and 8-azaguanine. Cancer Research 35, 2872-2878.

Nicolini, L.A., Zappulo, E., Viscoli, C., Mikulska, M., 2018. Management of chronic viral hepatitis in the hematological patient. Expert review of anti-infective therapy 16, 227-241.

Pally, C., Smith, D., Jaffee, B., Magolda, R., Zehender, H., Dorobek, B., Donatsch, P., Papageorgiou, C., Schuurman, H.-J.J.T., 1998. Side effects of brequinar and brequinar analogues, in combination with cyclosporine, in the rat. 127, 207-222.

Qing, M., Zou, G., Wang, Q.-Y., Xu, H.Y., Dong, H., Yuan, Z., Shi, P.-Y., 2010. Characterization of dengue virus resistance to brequinar in cell culture. Antimicrobial agents and chemotherapy 54, 3686-3695.

Qu, C., Zhang, S., Wang, W., Li, M., Wang, Y., van der Heijde-Mulder, M., Shokrollahi, E., Hakim, M.S., Raat, N.J., Peppelenbosch, M.P.J.T.F.J., 2018. Mitochondrial electron transport chain complex III sustains hepatitis E virus replication and represents an antiviral target. 33, 1008-1019.

Reed, L.J., Muench, H.J.A.j.o.e., 1938. A simple method of estimating fifty per cent endpoints. 27, 493-497.

Sato, T., Clevers, H., 2012. Primary mouse small intestinal epithelial cell cultures, Epithelial Cell Culture Protocols. Springer, pp. 319-328.

Sato, T., Clevers, H., 2013. Growing self-organizing mini-guts from a single intestinal stem cell: mechanism and applications. Science 340, 1190-1194.

Sato, T., Stange, D.E., Ferrante, M., Vries, R.G.J., Van Es, J.H., Van Den Brink, S., Van Houdt, W.J., Pronk, A., Van Gorp, J., Siersema, P.D., 2011. Long-term expansion of epithelial organoids from human colon, adenoma, adenocarcinoma, and Barrett's epithelium. Gastroenterology 141, 1762-1772.

Sato, T., Vries, R.G., Snippert, H.J., Van De Wetering, M., Barker, N., Stange, D.E., Van Es, J.H., Abo, A., Kujala, P., Peters, P.J., 2009. Single Lgr5 stem cells build crypt–villus structures in vitro without a mesenchymal niche. Nature 459, 262.

Saxena, K., Blutt, S.E., Ettayebi, K., Zeng, X.-L., Broughman, J.R., Crawford, S.E., Karandikar, U., Sastri, N.P., Conner, M.E., Opekun, A., 2015. Human intestinal enteroids: a new model to study human rotavirus infection, host restriction and pathophysiology. Journal of virology, JVI. 01930-01915.

Silva, H.T., Cao, W., Shorthouse, R.A., Loffler, M., Morris, R.E., 1997. In vitro and in vivo effects of leflunomide, brequinar, and cyclosporine on pyrimidine biosynthesis, Transplantation proceedings. Elsevier Science Publishing Company, Inc., pp. 1292-1293.

Smee, D.F., Hurst, B.L., Day, C.W., 2012. D282, a non-nucleoside inhibitor of influenza virus infection that interferes with de novo pyrimidine biosynthesis. Antiviral chemistry and chemotherapy 22, 263-272.

Smolen, J.S., Kalden, J.R., Scott, D.L., Rozman, B., Kvien, T.K., Larsen, A., Loew-Friedrich, I., Oed, C., Rosenburg, R., Lancet, E.L.S.G.J.T., 1999. Efficacy and safety of leflunomide compared with placebo and sulphasalazine in active rheumatoid arthritis: a double-blind, randomised, multicentre trial. 353, 259-266.

Strand, V., Cohen, S., Schiff, M., Weaver, A., Fleischmann, R., Cannon, G., Fox, R., Moreland, L., Olsen, N., Furst, D.J.A.o.i.m., 1999. Treatment of active rheumatoid arthritis with leflunomide compared with placebo and methotrexate. 159, 2542-2550.

Sugata, K., Taniguchi, K., Yui, A., Nakai, H., Asano, Y., Hashimoto, S., Ihira, M., Yagasaki, H., Takahashi, Y., Kojima, S., 2012. Analysis of rotavirus antigenemia in hematopoietic stem cell transplant recipients. Transplant Infectious Disease 14, 49-56.

Tan, Y.H., Driscoll, J.S., Mui, S.M., 2005. Dihydroorotate dehydrogenase inhibitors for the treatment of viral-mediated diseases. Patent No: US 6841561 B1.

van Maarseveen, N.M., Wessels, E., de Brouwer, C.S., Vossen, A.C.T.M., Claas, E.C.J., 2010. Diagnosis of viral gastroenteritis by simultaneous detection of Adenovirus group F, Astrovirus, Rotavirus group A, Norovirus genogroups I and II, and Sapovirus in two internally controlled multiplex real-time PCR assays. Journal of Clinical Virology 49, 205-210.

Waldman, W.J., Knight, D.A., Blinder, L., Shen, J., Lurain, N.S., Miller, D.M., Sedmak, D.D., Williams, J.W., Chong, A.S.F., 1999. Inhibition of cytomegalovirus in vitro and in vivo by the experimental immunosuppressive agent leflunomide. Intervirology 42, 412-418.

Wang, H., Naghavi, M., Allen, C., Barber, R.M., Bhutta, Z.A., Carter, A., Casey, D.C., Charlson, F.J., Chen, A.Z., Coates, M.M., 2016a. Global, regional, and national life expectancy, all-cause mortality,

and cause-specific mortality for 249 causes of death, 1980–2015: a systematic analysis for the Global Burden of Disease Study 2015. The lancet 388, 1459-1544.

Wang, Q.-Y., Bushell, S., Qing, M., Xu, H.Y., Bonavia, A., Nunes, S., Zhou, J., Poh, M.K., de Sessions, P.F., Niyomrattanakit, P., 2011. Inhibition of dengue virus through suppression of host pyrimidine biosynthesis. Journal of virology, JVI. 02510-02510.

Wang, Y., Wang, W., Xu, L., Zhou, X., Shokrollahi, E., Felczak, K., Van Der Laan, L.J.W., Pankiewicz, K.W., Sprengers, D., Raat, N.J.H., 2016b. Crosstalk between nucleotide synthesis pathways with cellular immunity in constraining hepatitis E virus replication. Antimicrobial agents and chemotherapy, AAC. 02700-02715.

Yin, Y., Bijvelds, M., Dang, W., Xu, L., van der Eijk, A.A., Knipping, K., Tuysuz, N., Dekkers, J.F., Wang, Y., de Jonge, J., 2015a. Modeling rotavirus infection and antiviral therapy using primary intestinal organoids. Antiviral research 123, 120-131.

Yin, Y., Bijvelds, M., Dang, W., Xu, L., van der Eijk, A.A., Knipping, K., Tuysuz, N., Dekkers, J.F., Wang, Y., de Jonge, J.J.A.r., 2015b. Modeling rotavirus infection and antiviral therapy using primary intestinal organoids. 123, 120-131.

Yin, Y., Dang, W., Zhou, X., Xu, L., Wang, W., Cao, W., Chen, S., Su, J., Cai, X., Xiao, S., 2018. PI3K-Akt-mTOR axis sustains rotavirus infection via the 4E-BP1 mediated autophagy pathway and represents an antiviral target. Virulence 9, 83-98.

Yin, Y., Metselaar, H.J., Sprengers, D., Peppelenbosch, M.P., Pan, Q., 2015c. Rotavirus in Organ Transplantation: Drug-Virus-Host Interactions. American Journal of Transplantation 15, 585-593.

Supplementary information

Supplementary table 2. qRT-PCR primers (human gene) used in the study, from 5' to 3'.

Gene name	Sense primer	Antisense primer
SA11 Rotavirus	TGGTTAAACGCAGGATCGGA	AACCTTTCCGCGTCTGGTAG
Human Patient Rotavirus	ACCATCTACACATGACCCTC	CACATAACGCCCCTATAGCC
Human GAPDH	GTCTCCTCTGACTTCAACAGCG	ACCACCCTGTTGCTGTAGTAGCCAA

Supplementary table 2. shRNA target sequences.

ShRNA	Sequence
shDHODH-1	CCGGCGATGGGCTGATTGTTACGAACTCGAGTTCGTAACAATCAGCCCATCGTTTTT
shDHODH-2	CCGGGTGAGAGTTCTGGGCCATAAACTCGAGTTTATGGCCCAGAACTCTCACTTTTT

$y = -0.2993x + 11.39 \ R^2 = 0.9986 \ P < 0.0001$
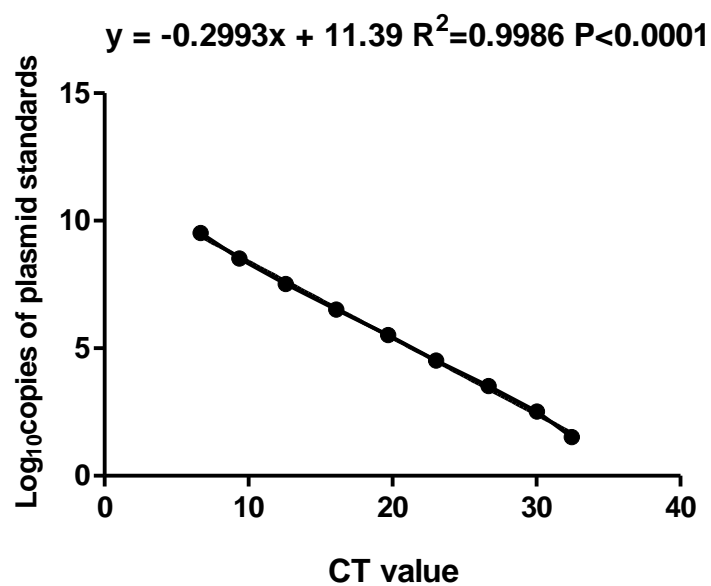
Supplementary Fig. S1. Standard curve for quantifying rotavirus genome copy numbers. An amplicon of the SA11 was cloned into the pCR2.1-TOPO vector. The plasmid was extracted, followed by a series of dilutions, from 10^{-2} to 10^{-10}, were prepared and then were amplified and quantified by qRT-PCR. Standard curve was generated by plotting the cycle threshold (CT) value regarding the log copy number.
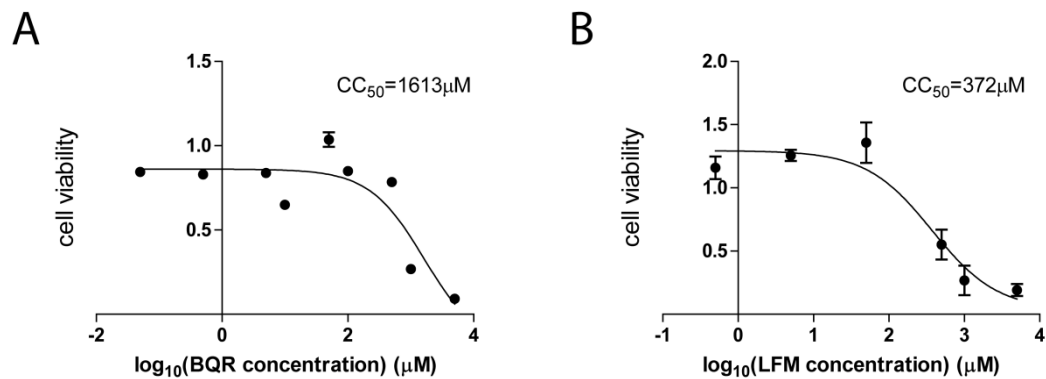
Supplementary Fig. S2. 50% cytotoxic concentration (CC_{50}) curves of BQR (A) and LFM (B) determined by MTT assays. Caco2 cells treated with two agents for 48h respectively.
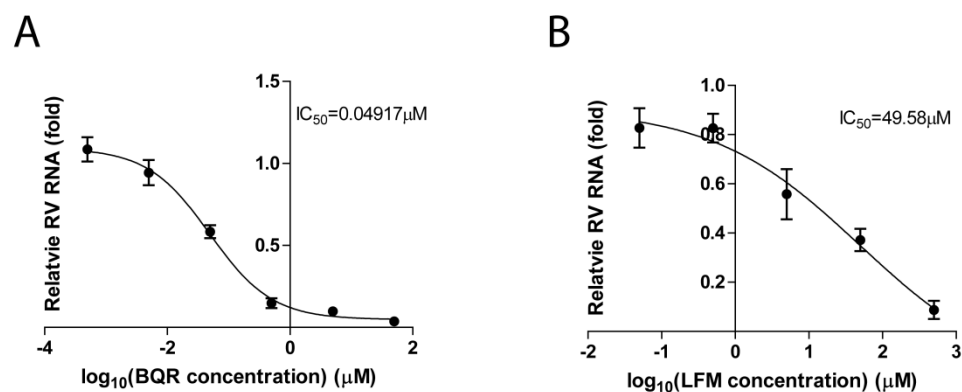
Supplementary Fig. S3. 50% inhibitory concentration (IC_{50}) curves of BQR (A) and LFM (B) against SA11 rotavirus on Caco2 cell line.

A

B

positive(defined as dead HIO)

negative(defined as live HIO)

PI/*Hoechst*/*Calcein*

1 Mock
2 Mock+0,5µM BQR
3 Mock+50µM LFM
4 Mock+1% DMSO
5 Mock+2% DMSO
6 Mock+5% DMSO
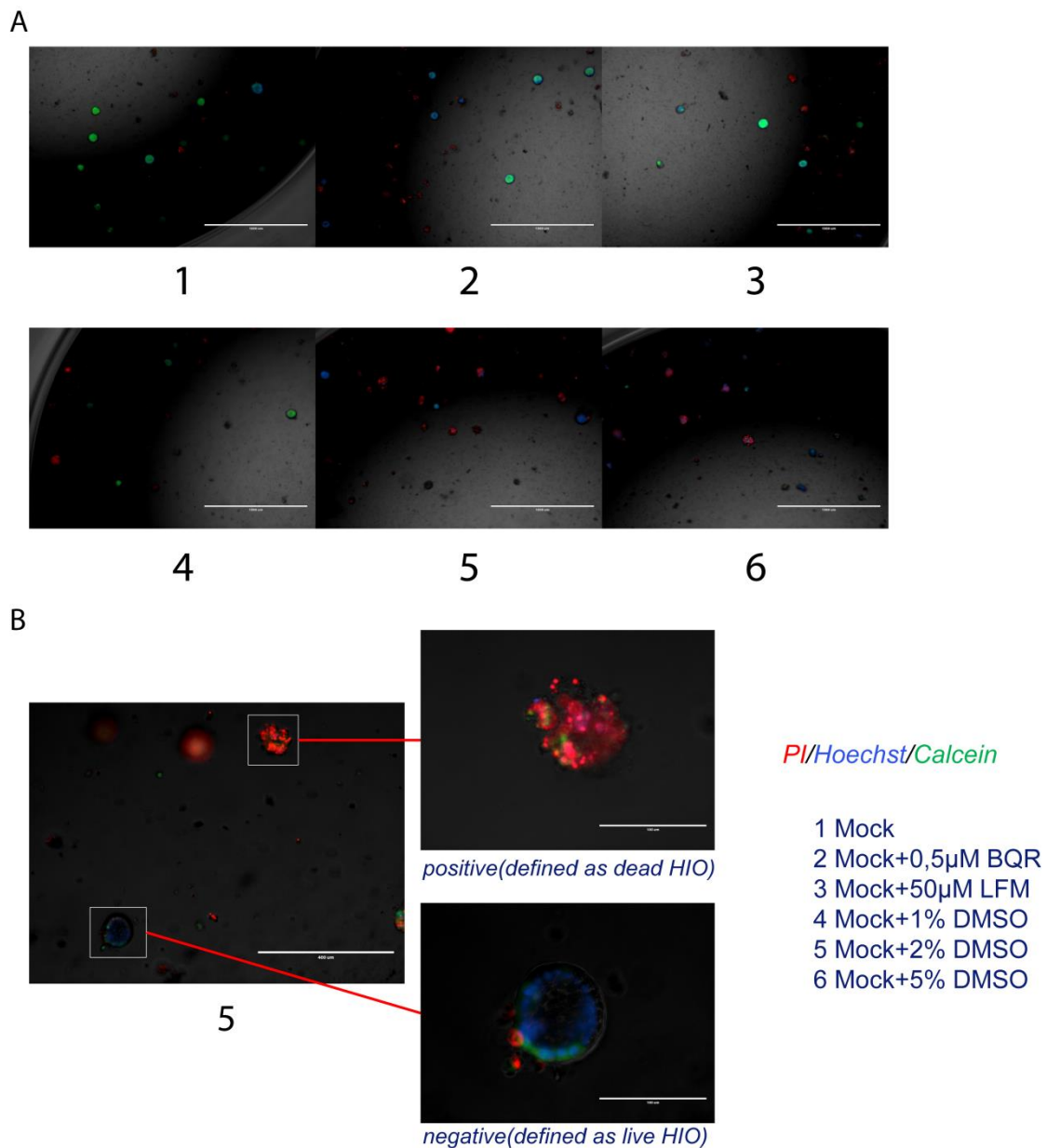
Supplementary Fig. S4. Description of the organoid scoring system. (A) Fluorescence microscopy images analysis of HIOs treated with BQR, LFM and various concentration of DMSO after 48h incubation and then stained by PI(red) which represented as dead cell, Hoechst(blue) which represented as nuclear, and Calcein(green) which represented as live cell. (B) After 48h, in 2% DMSO group, we define the upper right HIO(which red signal is more than green signal and also more than 50% of blue signal) as positive HIO, on the contrary, HIOs like lower left one, will be counted as negative HIO, in optimal microscopy image, positive HIOs were opaque and disorganized while negative HIOs were hyaline and in a spheroidal shape.

Chapter 6

6-thioguanine inhibits rotavirus replication through suppression of Rac1 GDP/GTP cycling

Yuebang Yin[‡], **Sunrui Chen[‡]**, Mohamad S. Hakim[‡], Wenshi Wang, Lei Xu, Wen Dang, Changbo Qu, Auke P. Verhaar, Junhong Su, Gwenny M. Fuhler, Maikel P. Peppelenbosch, and Qiuwei Pan

ABSTRACT

Rotavirus infection has emerged as an important cause of complications in organ transplantation recipients and might play a role in the pathogenesis of inflammatory bowel disease (IBD). 6-thioguanine (6-TG) has been widely used as an immunosuppressive drug for organ recipients and treatment of IBD in the clinic. This study aims to investigate the effects and mode-of-action of 6-TG on rotavirus replication. Human intestinal Caco2 cell line, 3D model of human primary intestinal organoids, laboratory rotavirus strain (SA11) and patient-derived rotavirus isolates were used. We have demonstrated that 6-TG significantly inhibits rotavirus replication in these intestinal epithelium models. Importantly, gene knockdown or knockout of Rac1, the cellular target of 6-TG, significantly inhibited rotavirus replication, indicating the supportive role of Rac1 for rotavirus infection. We have further demonstrated that 6-TG can effectively inhibit the active form of Rac1 (GTP-Rac1), which essentially mediates the anti-rotavirus effect of 6-TG. Consistently, ectopic over-expression of GTP-Rac1 facilitates but an inactive Rac1 (N17) or a specific Rac1 inhibitor (NSC23766) inhibits rotavirus replication. In conclusion, we have identified 6-TG as an effective inhibitor of rotavirus replication via the inhibition of Rac1 activation. Thus, for transplantation patients or IBD patients infected with rotavirus or at risk of rotavirus infection, the choice of 6-TG as a treatment appears rational.

Keywords: Rotavirus; 6-thioguanine; Rac1; intestinal organoids

INTRODUCTION

Rotavirus, a double stranded RNA (dsRNA) virus in the *Reoviridae* family, is a major cause of gastroenteritis, particularly in children younger than 5 years of age. As a major global health problem, this virus causes 114 million diarrhea episodes, 2.4 million hospitalizations, and an estimated 215,000 deaths worldwide annually (Grimwood and Buttery, 2007; Tate et al., 2016). Although rotavirus infection mainly occurs in developing countries, it also results in over 200 deaths and more than 87,000 hospital admissions in infants in European Union (Vesikari et al., 2007). Besides young children, organ transplantation patients are also susceptible to rotavirus infection irrespective of their age, causing long-term diarrhea and even death due to graft failure (Yin et al., 2015b). Although two global licensed rotavirus vaccines have been launched, no specific antiviral treatment is available.

A thio analogue of the naturally occurring purine base guanine, 6-thioguanine (6-TG), has been used in the clinic since the early 1950s (Munshi et al., 2014). 6-TG was initially developed to treat cancer; whereas currently it is widely used as an immunosuppressive agent in organ transplantation. It is also used as treatment for acute lymphoblastic leukemia in children and for autoimmune diseases (Bourgine et al., 2011). In particular, 6-TG is often used to treat inflammatory bowel disease (IBD) (de Boer et al., 2006). IBD including Crohn's disease (CD), ulcerative colitis (UC) and indeterminate colitis (IC) represent a heavy burden in Western countries (Kolho et al., 2012). Although the causes of exacerbations of IBD remain poorly characterized, gastrointestinal infections including rotavirus might induce flares in IBD (Masclee et al., 2013). Thus, preventing or treating rotavirus infection in these patients is of importance.

Upon ingestion, 6-TG is first metabolized into 6-thioguanosine monophosphate (6-TGMP), and subsequently into 6-thioguanosine diphosphate (6-TGDP), and finally into 6-thioguanosine triphosphate (6-TGTP) (Chouchana et al., 2012). Among these metabolites, 6-TGDP and 6-TGTP are able to compete with endogenous guanosine phosphates for Rac1 binding and to form 6-TGNP•Rac1 complexes. These complexes are in turn incapable to support the formation of the active configuration of Rac1, a process that Rac1 interacts with GTP. Thus, 6-TG indirectly

provokes inhibition of Rac1-dependent signaling (Shin et al., 2016), which has substantial consequences for cellular physiology. As a member of the Ras superfamily of Rho GTPases, GTP-bound Rac1 mediates a myriad of cellular processes including actin reorganization and gene transcription. Intriguingly, IBD is characterized by hyperactivation of Rac1 in the phagocyte compartment. This is associated with reduced effector function of Rac1, which is sensitive to 6-TG treatment (Parikh et al., 2014). The inhibition of Rac1 resulting from 6-TG treatment restores innate immune functionality of phagocytes in IBD patients, contributing to disease remission (Parikh et al., 2014). Thus, Rac1 hyperactivation appears an important immunosuppressive effector in human pathophysiology, at least in the phagocyte compartment.

Given the clinical relevance and the potential in revealing mechanistic insight, we have investigated the effects and mechanism-of-action of 6-TG on rotavirus replication. To this end, we have demonstrated that 6-TG effectively combats rotavirus replication through inhibition of Rac1 activation.

MATERIALS AND METHODS

Viruses and reagents

Simian rotavirus SA11 strain and patient-derived rotavirus isolates (G1P[8]) were prepared as previously described (Yin et al., 2015a; Yin et al., 2016).

Stocks (0.1 mg/mL) of 6-TG (Sigma-Aldrich) were dissolved in alkali solution (1 M NaOH, 50 mg/ml), and NSC23766 (Merck Millipore) was dissolved in H_2O (2 mM). All chemicals were stored in 25 µL aliquots and frozen at -80 ºC.

Conventional enterocyte culture and human primary intestinal organoid culture

Human colon cancer cell line Caco2 and human embryonic kidney cell line 293T (HEK 293T) cells were grown in Dulbecco's modified Eagle medium (DMEM) (Invitrogen-Gibco, Breda, The Netherlands) supplemented with 20% (vol/vol) heat-inactivated fetal calve serum (FCS) (Hyclone, Lonan, Utah) and Penicillin (100 IU/mL)/streptomycin (100 mg/mL) (Invitrogen-Gibco) at 37°C in

a humidified 5% CO2 incubator. Rac1 knockout mouse embryonic fibroblast (MEF) cells were cultured in DMEM supplemented with 10% FCS, Penicillin (100 IU/mL)/streptomycin (100 mg/mL), L-Glutamine (Gibco® by Life Technologies), non-essential amino acids (Gibco® by Life Technologies) and sodium-pyruvate (Gibco® by Life Technologies). Caco2 cells with stable knockdown of Rac1 were generated by transduction of lentiviral shRNA (produced in HEK293T cells) targeting Rac1 and selected with puromycin (6 µg/mL) as described previously (Yin et al., 2016). The shRNA targeting sequences used in this study were listed in Table S1.

Rotavirus inoculation and drug treatment

Inoculation and treatment of Caco2 cells and human intestinal organoids with SA11 and patient-derived rotavirus were performed as previously described (Yin et al., 2016).

Viability assay of cells or organoids

The viability of cells or organoids was determined by 3-(4, 5-Dimethylthiazol-2-yl)-2,5-diphenyl-tetrazolium bromide (MTT) assay. Briefly, Caco2 cells ($1x10^4$ cells/well) or organoids were seeded into a 96-well culture plate and incubated with various concentrations of 6-TG or NSC23766 for 48 h, followed by adding 500 µg/mL of MTT (solution to each well and incubation at 37 °C for 3 hrs. Subsequently, the medium was removed, and replaced with 100 µL DMSO and incubated at 37 °C for 50 min. Then, the absorbance was measured at 490 nm in an enzyme-linked immunosorbent assay reader (BIO-RAD). The effects of 6-TG, NSC294002, IFNα and ribavirin on host cell viability were determined by MTT assay (Fig. S1).

Transfection of plasmids

A constitutively active Rac1V12 and dominant inactive Rac1N17 plasmids were prepared as previously described (Apolloni et al., 2013). HEK 293 cells were seeded into 6-well plates for Rac activation assay or 48-well plates for infection assay with ~70% confluence. The cells were washed with PBS, followed by adding 500 µL of Opti-MEM® reduced serum medium with 2 µg Rac1V12 or Rac1N17 plasmids and 10 µg polyethylenimine (PEI) per well of a 6-well plate, or 100 µL of Opti-MEM® reduced serum medium (Thermo Fisher Scientific) with 0.25 µg Rac1V12 or Rac1N17

plasmids and 1.25 µg polyethylenimine (PEI) (Sigma-Aldrich) per well of a 48-well plate. After 4 to 5 hrs of incubation, 2 mL or 0.5 mL of DMEM containing 10% FCS was added to each well of 6-well plate or 48-well plate, respectively. Transfected cells were infected with rotavirus for 24 hrs.

Quantitative real-time PCR (qRT-PCR)

Total cellular RNA was isolated using a NucleoSpin® RNA kit (MACHEREY-NAGEL, Düren, Germany) following the manufacturer's protocol, and quantified with a Nanodrop ND-1000 (Wilmington, DE, USA). cDNA was synthesized using the reverse transcription system from TAKARA according to manufacturer's instructions (TAKARA BIO INC). The resulting cDNA was diluted 1:10, and 2 µL of the diluted cDNA was used for qRT-PCR with primers listed in Table S1. All qRT-PCR experiments were performed by SYBR-Green-based (Applied Biosystems SYBR Green PCR Master Mix; Thermo Fisher Scientific Life Science) real-time PCR with the StepOnePlus System (Thermo Fisher Scientific Life Sciences). The expression of target mRNA was normalized to the glyceraldehyde 3-phosphate dehydrogenase (GAPDH) mRNA. Gene expression analysis was performed by the $\Delta\Delta C_T$ method (Yin et al., 2015a; Yin et al., 2016).

Rac activation assay

The levels of Rac1-bound GTP were detected using Rac interactive binding (CRIB) domain of PAK (aa56-272) as described previously (Fuhler et al., 2008). In brief, GST-PAKcrib protein was pre-coupled to glutathione-Sepharose beads (Sigma-Aldrich) for 45 min at 4 °C. Caco2 cells treated with various concentrations of 6-TG or NSC23766 (48 h, seeded in 6-well-plate) were lysed for 10 min in lysis buffer (50 mM Tris, pH 7.4, 10% glycerol, 200mM NaCl, 1% NP-40, 2mM MgCl$_2$, 2 mM sodium orthovanadate, and protease inhibitors). Cell lysates were incubated with pre-coupled beads for 45 min. Then, agarose beads were washed 3 times with 1x lysis buffer, followed by boiling in Laemmli buffer, and sodium dodecyl sulfate-polyacrylamide gel electrophoresis (SDS-PAGE, 15%) analysis.

Western blotting

Cell lysates were subjected to SDS-PAGE, and proteins were transferred to PVDF membrane (Immobilon-FL). Rac1 monoclonal antibody (1:1000, rabbit; cell signaling) and SA11 rotavirus VP4 [1:1000, HS-2, a mouse monoclonal antibody (provided by Professor Harry Greenberg, Stanford University School of Medicine, USA)] were detected by Western blotting analysis. Detection of β-actin was served as loading control (1:1000, mouse monoclonal; Santa Cruz) as previously described (Versteeg et al., 2002).

Serial passaging of rotavirus with 6-TG treatment

To investigate whether rotavirus can develop resistance to 6-TG treatment, viruses were passaged in both MA104 and Caco2 cells in the absence of drug (vehicle control) or in the presence of gradually increasing concentrations of the drug (1000 ng/mL of 6-TG for passage 1-10 and 2000 ng/mL of 6-TG for passage 11-20). In brief, MA104 or Caco2 cells in 24-well plate were inoculated with 200 μL virus (MOI=0.7) at 37 °C for 1 hr, followed by adding 6-TG or without drug (as control). After 48 hrs, both cells and supernatant were harvested, subsequently frozen, thawed once, and centrifuged. The supernatant containing passaged viruses was stored at -80 °C until used for the next passage. Viruses were serially passaged by using 1 aliquot of viral stock from the preceding passage to infect fresh MA104 or Caco2 cells. The effect of each passage of virus (same titer) was quantified by qRT-PCR.

IC50 and CC50 calculation

IC50 and CC50 calculation were described previously (Yin et al., 2016).

Statistics

Data are presented as means, and statistical comparison between different groups was performed by Mann-Whitney test (two-tailed) using GraphPad Prism 5. Error bars represent the SEM, and P value <0.05 was considered statistically significant.

RESULTS

6-TG remarkably inhibits rotavirus replication

To assess the effects of 6-TG on rotavirus replication, we treated SA11 rotavirus-infected Caco2 cells with various concentrations (0.001 – 10000 ng/mL) of 6-TG for 48 hrs. This resulted in dose-dependent inhibition of rotavirus RNA replication (Fig. 1A, n = 3-17, *P<0.05, ***P<0.001). The IC$_{50}$ value of 6-TG against SA11 rotavirus was 3.0×10^{-13} M, which is substantially below the concentrations reached in patients undergoing 6-TG or azathioprine therapy. CC$_{50}$ of 6-TG to Caco2 cells was 9.8×10^{-6} M and selectivity index (SI, CC$_{50}$/IC$_{50}$) was 3.3×10^{7} (Table S2). This was further confirmed at the infectious virus production levels and protein levels of the rotavirus VP4 protein (Fig. 1B and 1C). To further verify the effect of 6-TG on rotavirus replication, SA11 rotavirus-infected Caco2 cells were treated with 6-TG at different time points (6, 12, 24 and 48 hrs), indicating that 6-TG significantly inhibited rotavirus RNA replication in time-dependent Manner (Fig. 1D, n = 4-8, *P<0.05, ***P<0.01). These results were substantiated by experiments in human primary intestinal organoids, a model system that recapitulates many aspects of the intestinal epithelium, including the presence of a villus domain and a crypt domain (Fig. 1E) (Sato and Clevers, 2013). 6-TG significantly inhibited SA11 rotavirus replication and virus production in these organoids (Fig. 1F and G, n = 6, *P<0.05, **P<0.01). Our results were essentially repeated using five patient-derived rotavirus isolates in Caco2 cells but also in human intestinal organoids (Table S3). Treatment with 100 ng/mL 6-TG inhibited patient-derived isolates in both Caco2 cells (Fig.1H) and human intestinal organoids (Fig.1I). Hence, 6-TG significantly counteracts rotavirus replication at clinically relevant concentrations.

Development of resistance to 6-TG is uncommon for rotavirus

Rotavirus was serially passaged in the presence of escalating concentrations of 6-TG to assess the potential of drug resistance development. As a control, wild-type SA11 rotavirus was passaged in the absence of the drug. During the initial ten passages, infected cultures were exposed to 1000 ng/mL of 6-TG; whereas the drug concentration was increased to 2000 ng/mL at the subsequent later passages. After 20 passages, the effects of 6-TG (100 ng/mL) on each representative passage (both drug treated and untreated) of rotavirus was quantified by qRT-PCR. Our results indicate that rotavirus remains sensitive to 6-TG treatment in MA104 cells (Fig. 2A) and Caco2 cells (Fig.

2B). Therefore, rotavirus does not easily develop 6-TG resistance, suggesting that the antiviral effects of 6-TG likely depend on a cellular target but not a direct interaction with the virus itself.
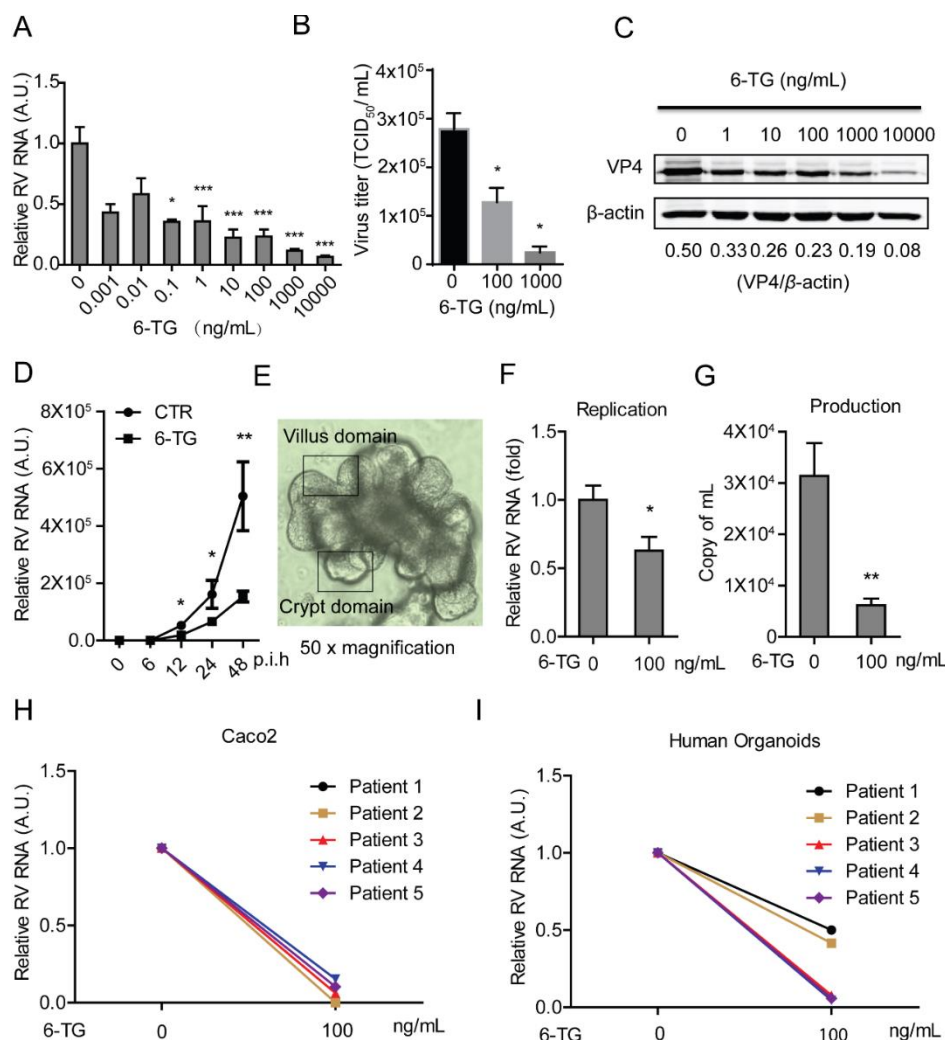

Fig. 1. 6-TG effectively inhibits rotavirus replication. (A) Treatment with 6-TG (48 hrs) significantly inhibited viral genomic RNA in SA11 rotavirus infected Caco2 cells (MOI = 0.7) in a dose-dependent manner (n = 6-17, means ± SEM, *$P < 0.05$, ***$P < 0.001$, Mann-Whitney test, A.U. denotes artificial unit). (B) Effects of 6-TG on the production of infectious viral particles determined by TCID50 method. Each bar represents the $TCID_{50}$/mL (mean ± SEM) (n = 3, $P < 0.05$, Mann-Whitney test). (C) Treatment with 6-TG (48 h) significantly inhibited viral VP4 protein in SA11 rotavirus infected Caco2 cells in a dose-dependent manner (the densitometric analysis of immunoreactive bans in western bots was quantified by ImageJ software, and the ratio of VP4/β-actin was expressed in arbitrary units). (D) Treatment with 6-TG (6 - 48 hrs) significantly inhibited viral genomic RNA in SA11 rotavirus infected Caco2 cells (MOI = 0.7) in a time-dependent manner (n = 4-8, means ± SEM, *$P < 0.05$, ***$P < 0.01$, Mann-Whitney test, p.i.h denotes hour of post infection). (E) The morphology of human primary

small intestinal organoids with clear villus domain and crypt domain. (F) Treatment with 6-TG (48 hrs) significantly inhibited genomic RNA in SA11 rotavirus (MOI = 7) infected human intestinal organoids (n = 6, means ± SEM, *$P < 0.05$, Mann-Whitney test). (G) Treatment with 6-TG (48 hrs) significantly inhibited viral production in SA11 rotavirus infected human intestinal organoids (n = 6, means ± SEM, **$P < 0.01$, Mann-Whitney test). (H) Treatment with 100 ng/mL of 6-TG (48 hrs) inhibited viral RNA of patient-derived rotavirus isolates in Caco2 cells. (I) Treatment with 100 ng/mL of 6-TG (48 hrs) inhibited viral RNA of patient-derived rotavirus isolates in human intestinal organoids.

Rac1, the cellular target of 6-TG, sustains rotavirus replication

Although initially characterized as a nucleotide synthesis inhibitor, in the last decade it has become clear that many of the effects of 6-TG, at least in gastrointestinal pathophysiology, depend on its potency to inhibit Rac1 (Shin et al., 2016). Thus, we investigated the potential role of Rac1 on rotavirus replication. To this end, we performed a lentiviral RNAi-mediated loss-of-function assay to silence the Rac1 gene. Two (no. 9689 and 9691) out of five RNAi vectors showed potent knockdown of the target gene (Fig. 3A). Importantly, these two RNAi vectors resulted in 65.0 ± 0.1% (n = 10, P < 0.001) and 61.8 ± 0.2% (n = 6, P < 0.05) reduction of SA11 rotavirus viral RNA, respectively (Fig. 3B). In apparent agreement, we obtained Rac1 knockout mouse embryonic fibroblasts cells (MEFs), and their status as a *bona fide* knockout was confirmed by western blot assay (Fig. 3C). Rotavirus replication in Rac1 knockout MEFs (-/-) was significantly less efficient (62.4 ± 0.2%; n = 4; P < 0.05), compared with the replication in wild type MEF (lf/lf) (Fig. 3D). Thus, decreased Rac1 levels correlate with increased resistance towards rotavirus replication.

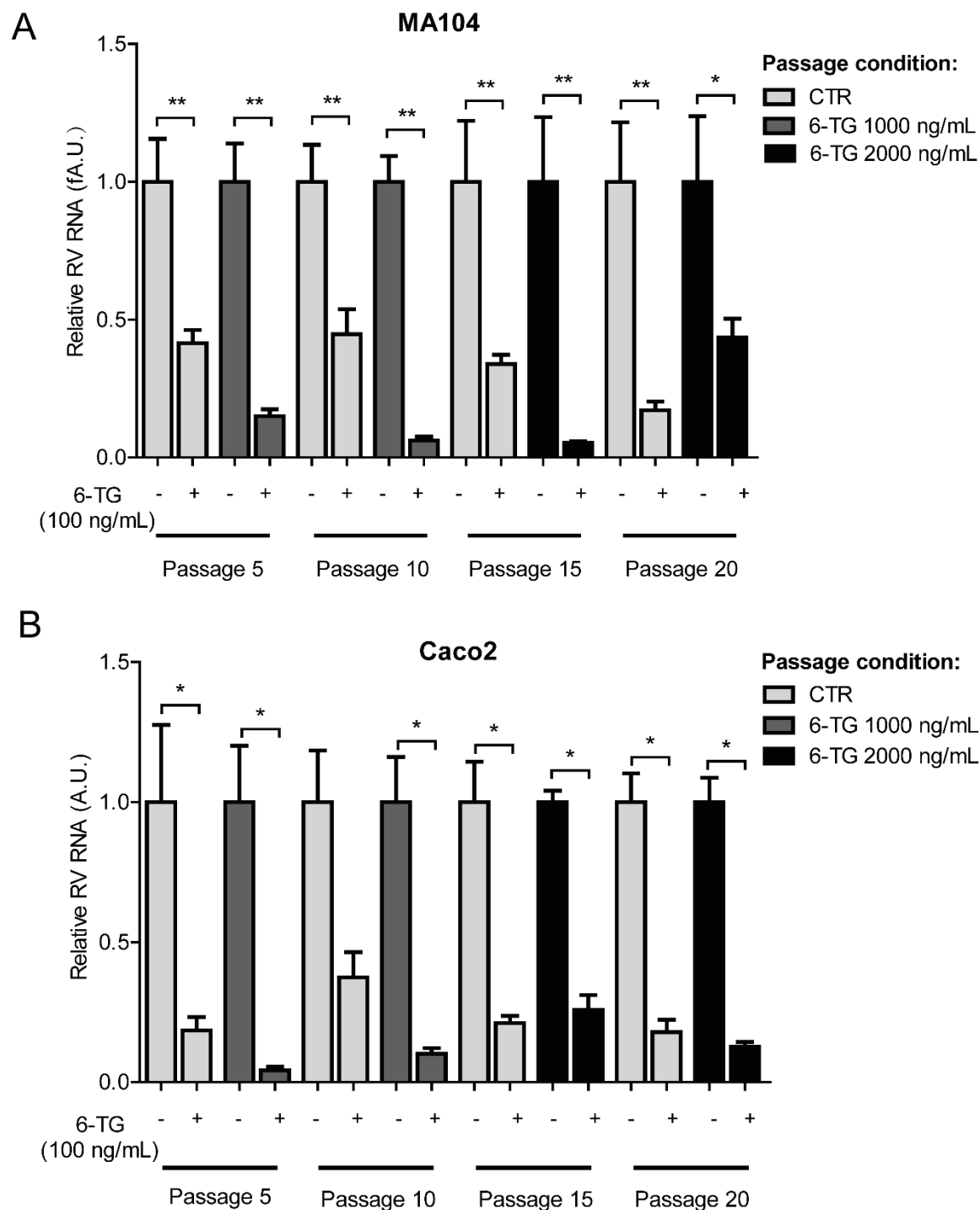**Fig. 2.** 6-TG has a high barrier to drug resistance development. Rotavirus was serially passaged in MA104 or Caco2 cells exposed to no 6-TG (as control) and increasing concentrations of 6-TG until 20 passages (infected cultures were exposed to 1000 ng/mL of 6-TG in passage 1-10; whereas the drug concentration was increased to 2000 ng/mL at the subsequent later passages). The effect of 6-TG (100 ng/mL) on passage 5, 10, 15 and 20

(the drug treated and untreated) of rotavirus was quantified using qRT-PCR. 6-TG retained its anti-rotavirus activity even with continuous exposure to 6-TG for 20 passages in MA104 cells (A) and Caco2 cells (B).

Efficient rotavirus replication requires Rac1 activation

Rac1 acts as binary switch in cellular biochemistry, and it is only capable of provoking signaling in the active GTP-bound form (Shin et al., 2016). NSC23766, a specific GTP-Rac1 inhibitor was able to effectively inhibit GTP-Rac1 accumulation in Caco2 cells, as evident when tested in GTP-Rac1 specific pull-down assay (Fig. 4A and B). Importantly, treatment with either 5 or 25 µM NSC23766 for 48 hrs resulted in 58.8 ± 0.1% (n = 8; P < 0.05) and 77.48 ± 0.1% (n = 10; P < 0.001) reduction on viral RNA levels, respectively (Fig. 4C). The IC_{50} value of NSC23766 against SA11 rotavirus was $1.1×10^{-8}$ M, the CC_{50} of NSC23766 to Caco2 cells was $3.1×10^{-4}$ M, and the SI was $2.8 ×10^4$ (Table. S2). The inhibitory effect of NSC23766 on the rotavirus infectious was further verified by a western blot assay, revealing that treatment with either 1, 5 or 25 µM NSC23766 significantly inhibits rotavirus VP4 protein synthesis in Caco2 cells (Fig. 4D). The effect of this drug was further confirmed by experiments in human primary intestinal organoids, which indicated 91.1 ± 0.1% (n = 6; P < 0.05) reduction of viral RNA in the organoids (Fig. 4E) following treatment with NSC23766.

Next, we tested the effects of constitutively active and dominant negative forms of Rac1 on rotavirus replication. This was done by transfection of the active Rac1V12 plasmid or the dominant negative Rac1N17 plasmid. Expression of both plasmids was successful when tested by flow cytometry (Fig. 4F). Accordingly, Rac1V12-transfected cells displayed abundant GTP-Rac1, which in contrast is low in Rac1N17-transfected cells, as determined in a Rac pull-down assay (Fig. 4G). These results were confirmed by analyzing abundance of phospho-PAK2 status (Fig. 4H). Importantly, Rac1V12 promoted, but Rac1N17 inhibited rotavirus replication (Fig. 4I). Taken together, activation of Rac1 supports rotavirus replication.
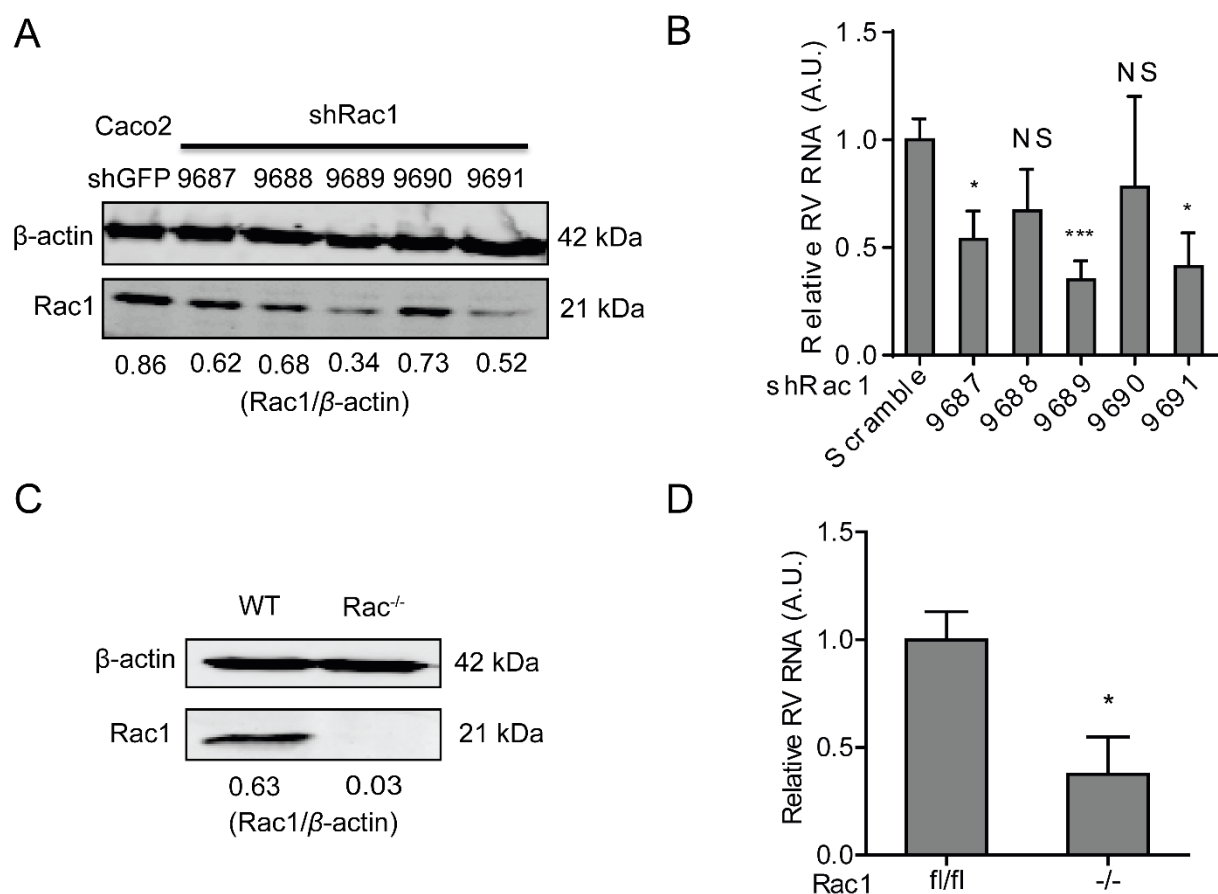
Fig. 3. Rac1, the drug target of 6-TG, sustains rotavirus replication. (A) Western blot assay detected Rac1 in transduced Caco2 cells transduced lentiviral RNAi vectors against Rac1 (The ratio of Rac1/β-actin was expressed in arbitrary units). (B) Three (No. 9687, 9689 and 9690) out of five lentiviral shRNA vectors inhibited rotavirus genomic RNA (n = 6-10, means ± SEM, *P < 0.05, ***P < 0.001, Mann-Whitney test). (C) Western blot assay confirmed knockout of Rac1 in Rac1 knockout (-/-) MEF cells. (D) SA11 rotavirus replication was significantly attenuated in Rac1 knockout (-/-) MEF cells (n = 4, means ± SEM, *P < 0.05, Mann-Whitney test).

Figure 4
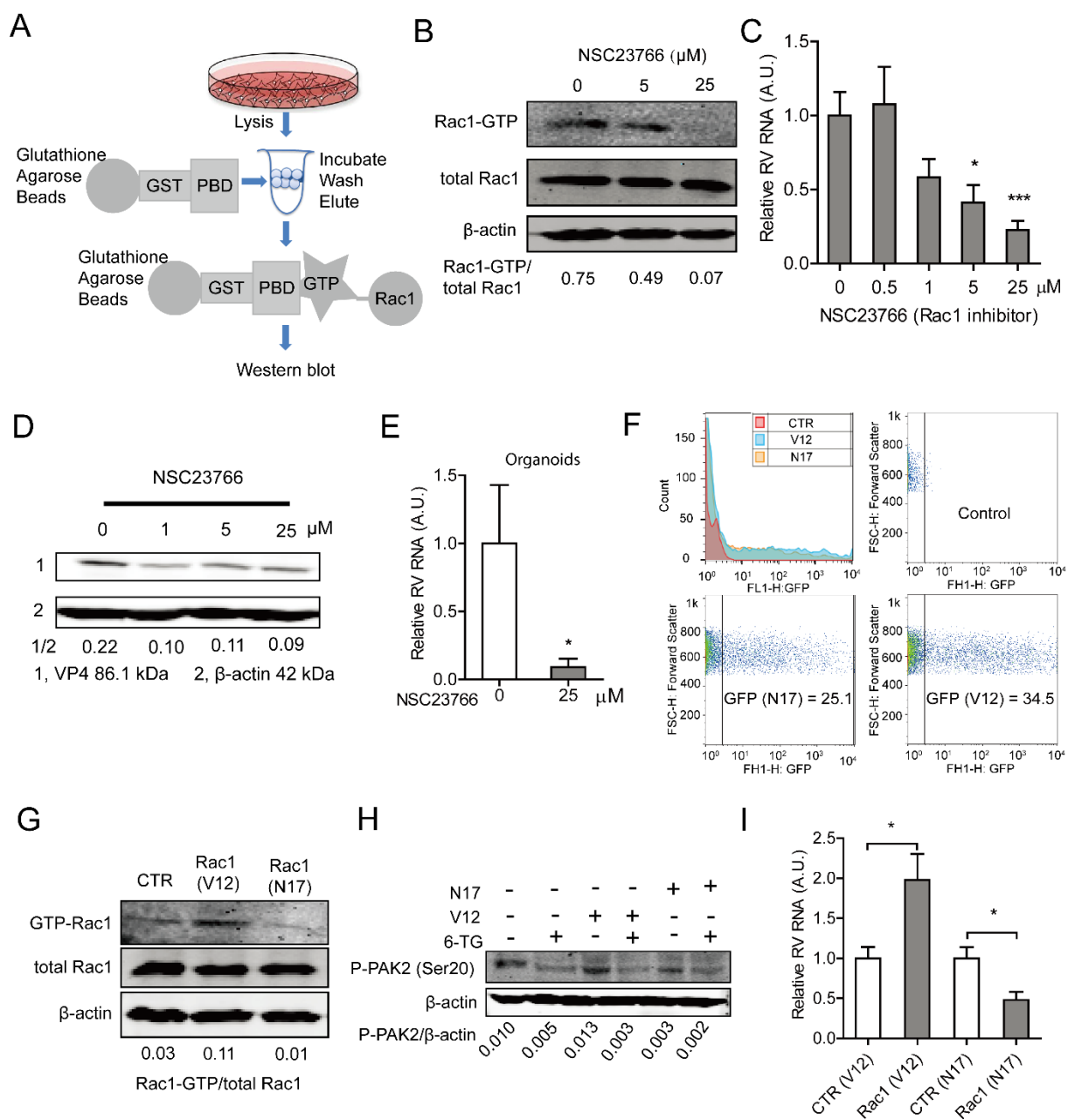
Fig. 4. The activation form of Rac1 is required for supporting rotavirus replication. (A) Schematic depicting the pull-down assay. (B) NSC23766 inhibited GTP-Rac1 detected by pulldown assay (The ratio of GTP-Rac1/Rac was expressed in arbitrary units). (C) Treatment with NSC23766 (48 hrs) significantly inhibited viral genomic RNA in SA11 rotavirus infected Caco2 cells in a dose-dependent manner (n = 8-10, means ± SEM, *$P < 0.05$, ***$P < 0.001$, Mann-Whitney test). (D) Treatment with NSC23766 (48 hrs) significantly inhibited viral VP4 protein in SA11 rotavirus infected Caco2 cells in a dose-dependent manner (The ratio of VP4/β-actin was expressed in arbitrary units). (E) Treatment with NSC23766 (48 hrs) significantly inhibited viral RNA in SA11 rotavirus infected

human intestinal organoids (n = 6, means ± SEM, *$P < 0.05$, Mann-Whitney test). (F) Flow cytometric analysis of green fluorescence indicated the percentages of transduced cells with Rac1V12 and Rac1N17 plasmids. Median fluorescence identity (MFIs) of control, N17 and V12 are 3.43, 35.5 and 84.3, respectively. (G) Pull-down and western blot assays showed higher level of GTP-Rac1 with transduction of Rac1V12 but lower level of GTP-Rac1 with Rac1N17 plasmids (The ratio of GTP-Rac1/Rac was expressed in arbitrary units). (H) Detection of phospho-PAK2 indicated successful transduction of Rac1V12 and Rac1N17 plasmids. (I) Rac1V12 transduction facilitates but Rac1N17 inhibits rotavirus replication (n = 10, means ± SEM, *$P < 0.05$, Mann-Whitney test).

6-TG inhibits rotavirus via suppression of Rac1 GDP/GTP cycling

The inhibition of the activation of Rac1 by 6-TG was reported in many cell types (Fuhler et al., 2008; Shin et al., 2016; Tiede et al., 2003). Employing the Rac1 pull-down assay (Fig. 4A), we observed that 6-TG potently inhibited GTP-Rac1 accumulation; whereas corresponding western blots did not show reduced overall Rac1 levels in Caco2 cells following 6-TG treatment (Fig. 5A). Functional studies using Rac1 knockdown Caco2 cells (Fig. 5B and 5C) were performed to demonstrate that both 6-TG and NSC23766 require Rac1 to combat rotavirus replication. In agreement, pharmacological Rac1 inhibitors did not inhibit rotavirus replication in Rac1 knockout MEF cells (Fig. 5D). Thus 6-TG inhibits rotavirus via suppression of Rac1 activation.

6-TG has no combination effect with IFNα, but moderately antagonistic effect with ribavirin on rotavirus replication

Interferon-alpha (IFNα) and ribavirin are widely used as general antivirals, being confirmed to significantly inhibit rotavirus replication *in vitro* (Yin et al., 2015a). Consistently, we again demonstrated the inhibitory effects of IFNα and ribavirin on rotavirus RNA (Fig. 6A, and 6E) and viral protein (Fig. 6B and 6F) in a dose-dependent manner. The IC_{50} value of IFNα against SA11 rotavirus was 3.1×10^{-5} IU, CC_{50} of IFNα to Caco2 cells was 18706 IU, and SI was 6.0×10^8 (Table S2). The IC_{50} value of ribavirin against SA11 rotavirus was 1.6×10^{-7} M, CC_{50} of ribavirin to Caco2 cells was 3.02×10^{-2} M and SI was 1.9×10^5 (Table S2). Next, we assessed the combinatory antiviral effects of 6-TG with IFNα or ribavirin. The combination of 6-TG and IFNα resulted in no combination (no synergy or antagonism) antiviral effect, with a synergy volume of -2.8 μM^2% (Fig.

6C and 6D). However, the combination of 6-TG and ribavirin resulted in moderately antagonistic antiviral effect, with a synergy volume of -26.02 μM²% (Fig. 6G and 6H).
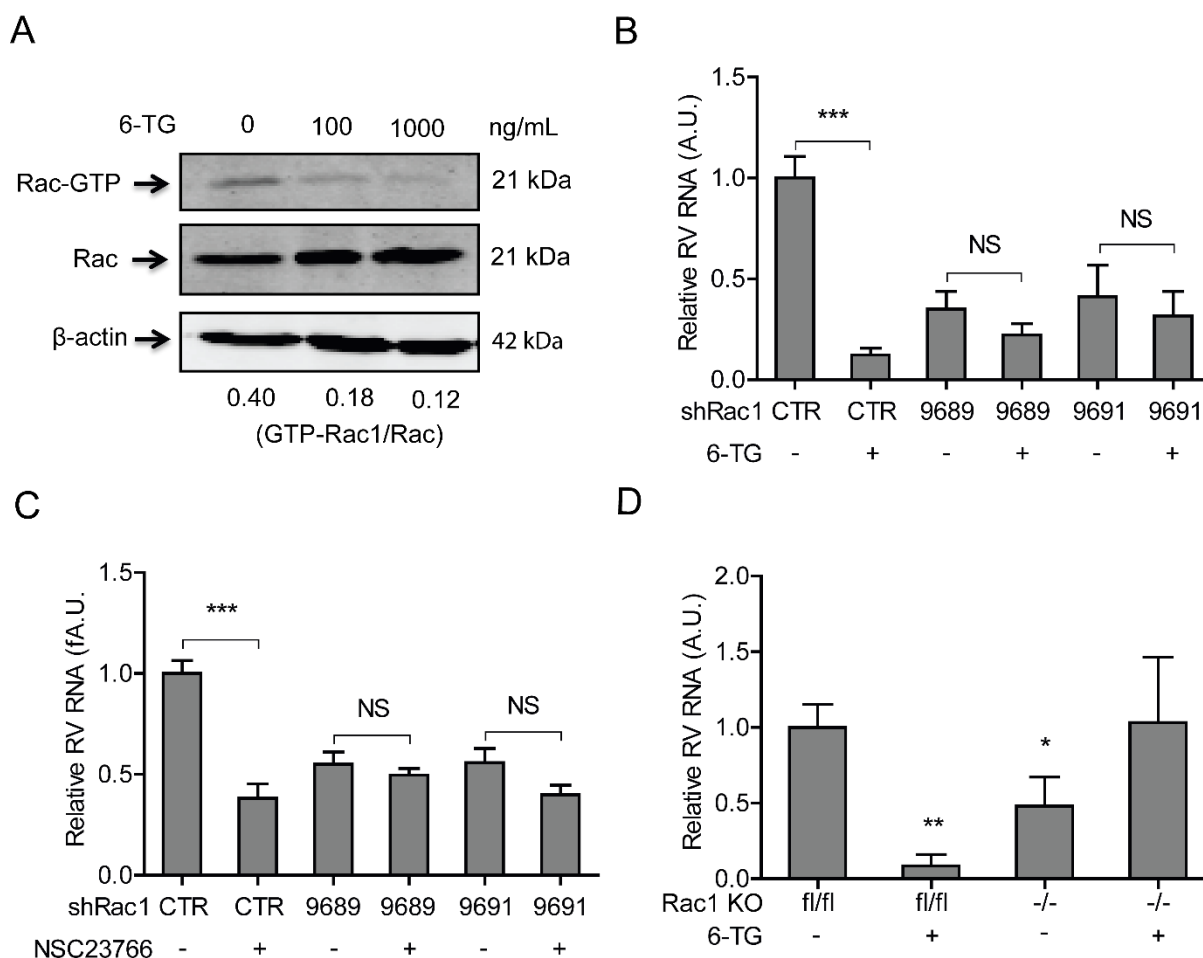
Fig. 5. 6-TG inhibits rotavirus via suppression of Rac1 activation. (A) Anti-rotavirus effect of 6-TG (100 ng/mL) was attenuated in Rac1 knockdown Caco2 cells (The ratio of VP4/β-actin was expressed in arbitrary units). (B) 6-TG inhibited GTP-Rac1 detected by pull-down assay. (C) Anti-rotavirus effect of NSC23766 (25 μg ng/mL) was attenuated in Rac1 knockdown Caco2 cells. (D) The anti-rotavirus effect of 6-TG (100 ng/mL) was attenuated in Rac1 knockout (-/-) MEF cells (n = 6-8, means ± SEM, *P < 0.05, **P < 0.01, Mann-Whitney test).
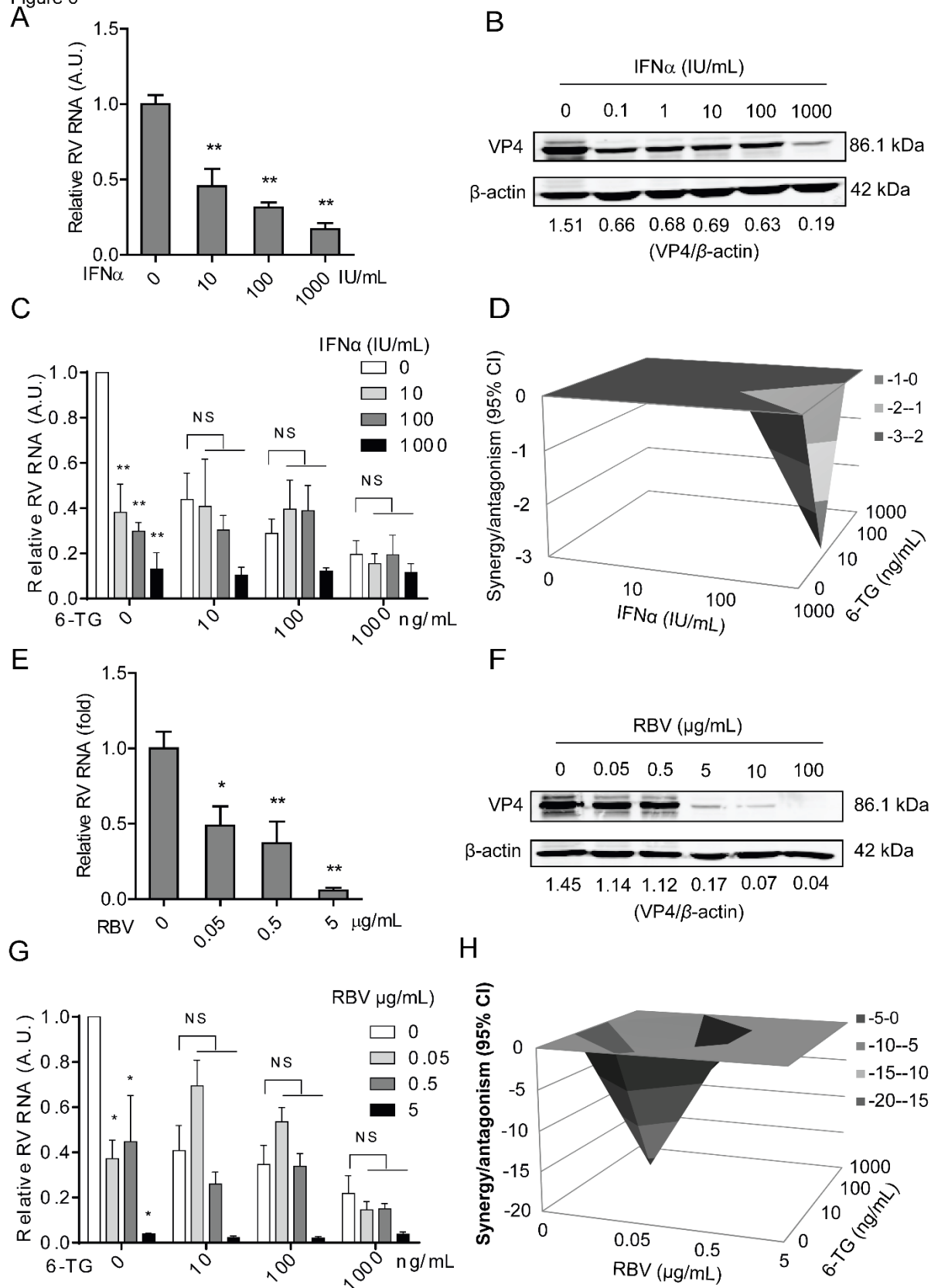
Figure 6

Fig. 6. The effects of the combination of 6-TG with IFNα, or ribavirin on rotavirus replication. (A) Treatment with IFNα (48 hrs) significantly inhibited viral genomic RNA in SA11 rotavirus infected Caco2 cells in a dose-dependent manner (n = 4, means ± SEM, **$P < 0.01$, Mann-Whitney test). (B) Treatment with IFNα (48 hrs) remarkably inhibited viral VP4 protein in SA11 rotavirus infected Caco2 cells in a dose-dependent manner (The ratio of VP4/β-actin was expressed in arbitrary units). (C) Effect of the combination of various concentrations of 6-TG and IFNα on rotavirus replication in Caco2 cells. (D) Synergy plot representing the percentage of antiviral activity above/below the expected activity for the 6-TG-IFNα combination based on the data shown in C. (E) Treatment with ribavirin (48 hrs) significantly inhibited viral genomic RNA in SA11 rotavirus infected Caco2 cells in a dose-dependent manner (n = 4-7, means ± SEM, *$P < 0.05$, **$P < 0.01$, Mann-Whitney test). (F) Treatment with ribavirin (48 hrs) remarkably inhibited viral VP4 protein in SA11 rotavirus infected Caco2 cells in a dose-dependent manner (The ratio of VP4/β-actin was expressed in arbitrary units). (G) Effect of the combination of various concentrations of 6-TG and ribavirin on rotavirus replication in Caco2 cells. (H) Synergy plot representing the percentage of antiviral activity above/below the expected activity for the 6-TG-ribavirin combination based on the data shown in G.

DISCUSSION

In this study, we have demonstrated that 6-TG effectively inhibits rotavirus replication via inhibition of the Rac1 activity. This is particularly interesting in view that rotavirus replication is especially an issue in organ transplantation recipients and in patients with IBD. 6-TG is a therapeutic option for both groups of patients. Based on the findings presented in the current study, the choice of 6-TG for these patients appears rational, in particular when they are at risk of rotavirus infection (Yin et al., 2015b).

Our results fit well with the momentum of studies that document antiviral activity of 6-TG. For instance, it has been reported that 6-TG can combat Middle East respiratory syndrome coronavirus infection by augmenting interferon responses (Cheng et al., 2015) and it has also reported that Simian virus 40 DNA replication is antagonized by 6-TG (Maybaum et al., 1987). Interestingly, it was reported that vaccinated IBD patients had lower titers of hepatitis B surface antibody (HBsAb), which might be influenced by the use of immunosuppressants including 6-TG (Watts et al., 2017).

As a 6-thiopurine (6-TP) prodrug, 6-TG is converted into pharmacologically active deoxy-6-thioguanosine phosphate (also called 6-thioguanine nucleotide) and 6-thioguanosine phosphate

(6-TGNP). 6-TGNP can bind to Rac1 to form the 6-TGNP•Rac1 complex inactivating Rac1 (Shin et al., 2016). As a major player of the Rho family of small GTPases, Rac1 plays a vital role in various cellular signaling pathways to regulate a wide variety of cell functions including gene transcription, cell proliferation, apoptosis, motility, and redox signaling (D'Ambrosi et al., 2014). The expression of Rac1 is ubiquitous, but it has two conformational states including an inactive GDP-bound form and an active GTP-bound form (Bosco et al., 2009). It exerts biological functions mainly through activation of Rac1 (i.e. GTP-bound form) (Bosco et al., 2009). Many viruses interfere with or employ the conformational states of Rac1 to regulate their infection. At early stages of African swine fever virus (ASFV) infection, Rac1 is activated, and inhibition of Rac1 is able to suppress production of this virus (Quetglas et al., 2012). Rac1 is found to be activated during intracellular mature virus (MV) of Vaccinia virus entry (Mercer and Helenius, 2008).

Although rotavirus replication *per se* does not affect the activation of Rac1 (Fig. S4), we have demonstrated that the loss-of-function of Rac1 by gene knockdown or knockout significantly impairs rotavirus replication, which is in line with the previous finding that knockdown Rac1 could significantly inhibit Enterovirus 1 (EV1) infection (Karjalainen et al., 2008). More specifically, the activation of Rac1 is required as shown by the opposing effects of ectopic over-expression of the active or inactive forms of Rac1 on rotavirus replication. This mechanistically explains the potent anti-rotavirus effects of the GTP-Rac1 inhibitors, 6-TG and NSC23766. Of note, NSC23766 has been shown to inhibit the replication of several influenza viruses including a human virus strain from the 2009 pandemic and highly pathogenic avian virus strains (Dierkes et al., 2014).

Despite the absence of approved medications for treating rotavirus, the widely used general antivirals including ribavirin and IFNα have been studied on rotavirus in experimental models (Yin et al., 2015a). Here, we have evaluated the combinatory effects of 6-TG with IFNα or ribavirin. Consistently, we confirmed that ribavirin and IFNα inhibit rotavirus replication at both RNA and protein levels (Fig. 6A and 6B). We found increased potency of IFNα in the presence of 6-TG. However, whether the combination of IFNα and 6-TG could be used to treat rotavirus infected patients remains to be further investigated.

In conclusion, this study has demonstrated that 6-TG effectively inhibits rotavirus replication with a high barrier to drug resistance development. We further identified the active form of Rac1 as

an important host factor supporting rotavirus replication. 6-TG exerts its anti-rotavirus effects via the specific inhibition of Rac1 activation. Herein, this study provided important references for clinicians to optimize medications for organ recipients or IBD patients who are infected with rotavirus or at risk of rotavirus replication. These results may also help the development of new anti-rotavirus therapies.

REFERENCE

Apolloni, S., Parisi, C., Pesaresi, M.G., Rossi, S., Carri, M.T., Cozzolino, M., Volonte, C., D'Ambrosi, N., 2013. The NADPH oxidase pathway is dysregulated by the P2X7 receptor in the SOD1-G93A microglia model of amyotrophic lateral sclerosis. J Immunol 190, 5187-5195.

Bosco, E.E., Mulloy, J.C., Zheng, Y., 2009. Rac1 GTPase: a "Rac" of all trades. Cell Mol Life Sci 66, 370-374.

Bourgine, J., Garat, A., Allorge, D., Crunelle-Thibaut, A., Lo-Guidice, J.M., Colombel, J.F., Broly, F., Billaut-Laden, I., 2011. Evidence for a functional genetic polymorphism of the Rho-GTPase Rac1. Implication in azathioprine response? Pharmacogenet Genomics 21, 313-324.

Cheng, K.W., Cheng, S.C., Chen, W.Y., Lin, M.H., Chuang, S.J., Cheng, I.H., Sun, C.Y., Chou, C.Y., 2015. Thiopurine analogs and mycophenolic acid synergistically inhibit the papain-like protease of Middle East respiratory syndrome coronavirus. Antiviral Res 115, 9-16.

Chouchana, L., Narjoz, C., Beaune, P., Loriot, M.A., Roblin, X., 2012. Review article: the benefits of pharmacogenetics for improving thiopurine therapy in inflammatory bowel disease. Aliment Pharmacol Ther 35, 15-36.

D'Ambrosi, N., Rossi, S., Gerbino, V., Cozzolino, M., 2014. Rac1 at the crossroad of actin dynamics and neuroinflammation in Amyotrophic Lateral Sclerosis. Front Cell Neurosci 8, 279.

de Boer, N.K., Reinisch, W., Teml, A., van Bodegraven, A.A., Schwab, M., Lukas, M., Ochsenkuhn, T., Petritsch, W., Knoflach, P., Almer, S., van der Merwe, S.W., Herrlinger, K.R., Seiderer, J., Vogelsang, H., Mulder, C.J., Dutch, T.G.w.g., 2006. 6-Thioguanine treatment in inflammatory bowel disease: a critical appraisal by a European 6-TG working party. Digestion 73, 25-31.

Dierkes, R., Warnking, K., Liedmann, S., Seyer, R., Ludwig, S., Ehrhardt, C., 2014. The Rac1 inhibitor NSC23766 exerts anti-influenza virus properties by affecting the viral polymerase complex activity. PLoS One 9, e88520.

Fuhler, G.M., Drayer, A.L., Olthof, S.G., Schuringa, J.J., Coffer, P.J., Vellenga, E., 2008. Reduced activation of protein kinase B, Rac, and F-actin polymerization contributes to an impairment of stromal cell derived factor-1 induced migration of CD34+ cells from patients with myelodysplasia. Blood 111, 359-368.

Grimwood, K., Buttery, J.P., 2007. Clinical update: rotavirus gastroenteritis and its prevention. Lancet 370, 302-304.

Karjalainen, M., Kakkonen, E., Upla, P., Paloranta, H., Kankaanpaa, P., Liberali, P., Renkema, G.H., Hyypia, T., Heino, J., Marjomaki, V., 2008. A Raft-derived, Pak1-regulated entry participates in alpha2beta1 integrin-dependent sorting to caveosomes. Molecular biology of the cell 19, 2857-2869.

Kolho, K.L., Klemola, P., Simonen-Tikka, M.L., Ollonen, M.L., Roivainen, M., 2012. Enteric viral pathogens in children with inflammatory bowel disease. J Med Virol 84, 345-347.

Masclee, G.M., Penders, J., Pierik, M., Wolffs, P., Jonkers, D., 2013. Enteropathogenic viruses: triggers for exacerbation in IBD? A prospective cohort study using real-time quantitative polymerase chain reaction. Inflamm Bowel Dis 19, 124-131.

Maybaum, J., Bainnson, A.N., Roethel, W.M., Ajmera, S., Iwaniec, L.M., TerBush, D.R., Kroll, J.J., 1987. Effects of incorporation of 6-thioguanine into SV40 DNA. Mol Pharmacol 32, 606-614.

Mercer, J., Helenius, A., 2008. Vaccinia virus uses macropinocytosis and apoptotic mimicry to enter host cells. Science 320, 531-535.

Munshi, P.N., Lubin, M., Bertino, J.R., 2014. 6-thioguanine: a drug with unrealized potential for cancer therapy. Oncologist 19, 760-765.

Parikh, K., Zhou, L., Somasundaram, R., Fuhler, G.M., Deuring, J.J., Blokzijl, T., Regeling, A., Kuipers, E.J., Weersma, R.K., Nuij, V.J., Alves, M., Vogelaar, L., Visser, L., de Haar, C., Krishnadath, K.K., van der Woude, C.J., Dijkstra, G., Faber, K.N., Peppelenbosch, M.P., 2014. Suppression of p21Rac signaling and increased innate immunity mediate remission in Crohn's disease. Sci Transl Med 6, 233ra253.

Quetglas, J.I., Hernaez, B., Galindo, I., Munoz-Moreno, R., Cuesta-Geijo, M.A., Alonso, C., 2012. Small rho GTPases and cholesterol biosynthetic pathway intermediates in African swine fever virus infection. J Virol 86, 1758-1767.

Sato, T., Clevers, H., 2013. Growing self-organizing mini-guts from a single intestinal stem cell: mechanism and applications. Science 340, 1190-1194.

Shin, J.Y., Wey, M., Umutesi, H.G., Sun, X., Simecka, J., Heo, J., 2016. Thiopurine Prodrugs Mediate Immunosuppressive Effects by Interfering with Rac1 Protein Function. J Biol Chem 291, 13699-13714.

Tate, J.E., Burton, A.H., Boschi-Pinto, C., Parashar, U.D., 2016. Global, Regional, and National Estimates of Rotavirus Mortality in Children <5 Years of Age, 2000-2013. Clin Infect Dis 62 Suppl 2, S96-S105.

Tiede, I., Fritz, G., Strand, S., Poppe, D., Dvorsky, R., Strand, D., Lehr, H.A., Wirtz, S., Becker, C., Atreya, R., Mudter, J., Hildner, K., Bartsch, B., Holtmann, M., Blumberg, R., Walczak, H., Iven, H., Galle, P.R., Ahmadian, M.R., Neurath, M.F., 2003. CD28-dependent Rac1 activation is the molecular target of azathioprine in primary human CD4+ T lymphocytes. J Clin Invest 111, 1133-1145.

Versteeg, H.H., Sorensen, B.B., Slofstra, S.H., Van den Brande, J.H., Stam, J.C., van Bergen en Henegouwen, P.M., Richel, D.J., Petersen, L.C., Peppelenbosch, M.P., 2002. VIIa/tissue factor interaction results in a tissue factor cytoplasmic domain-independent activation of protein synthesis, p70, and p90 S6 kinase phosphorylation. J Biol Chem 277, 27065-27072.

Vesikari, T., Karvonen, A., Prymula, R., Schuster, V., Tejedor, J.C., Cohen, R., Meurice, F., Han, H.H., Damaso, S., Bouckenooghe, A., 2007. Efficacy of human rotavirus vaccine against rotavirus gastroenteritis during the first 2 years of life in European infants: randomised, double-blind controlled study. Lancet 370, 1757-1763.

Watts, A., Bennett, W.E., Molleston, J.P., Gupta, S.K., Croffie, J.M., Waseem, S., McFerron, B.A., Steiner, S.J., Kumar, S., Vanderpool, C.P., Hon, E.C., Bozic, M.A., Subbarao, G.C., Pfefferkorn, M.D., 2017. The Incidence of Low Seroimmunity to Hepatitis B Virus in Children with Inflammatory Bowel Disease. J Pediatr Gastroenterol Nutr.

Yin, Y., Bijvelds, M., Dang, W., Xu, L., van der Eijk, A.A., Knipping, K., Tuysuz, N., Dekkers, J.F., Wang, Y., de Jonge, J., Sprengers, D., van der Laan, L.J., Beekman, J.M., Ten Berge, D., Metselaar, H.J., de Jonge, H., Koopmans, M.P., Peppelenbosch, M.P., Pan, Q., 2015a. Modeling rotavirus infection and antiviral therapy using primary intestinal organoids. Antiviral Res 123, 120-131.

Yin, Y., Metselaar, H.J., Sprengers, D., Peppelenbosch, M.P., Pan, Q., 2015b. Rotavirus in organ transplantation: drug-virus-host interactions. Am J Transplant 15, 585-593.

Yin, Y., Wang, Y., Dang, W., Xu, L., Su, J., Zhou, X., Wang, W., Felczak, K., van der Laan, L.J., Pankiewicz, K.W., van der Eijk, A.A., Bijvelds, M., Sprengers, D., de Jonge, H., Koopmans, M.P., Metselaar, H.J., Peppelenbosch, M.P., Pan, Q., 2016. Mycophenolic acid potently inhibits rotavirus infection with a high barrier to resistance development. Antiviral Res 133, 41-49.

Supplementary Information

Table S1. Primers and shRNA sequences used in the study

Sequence of rotavirus primers

	SA11 Rotavirus	Human Patient Rotavirus
Sense	TGGTTAAACGCAGGATCGGA	ACCATCTACACATGACCCTC
Anti-sense	AACCTTTCCGCGTCTGGTAG	CACATAACGCCCCTATAGCC

Primer sequences of GAPDH

Primers	Human	Mouse
GAPDH-F	GTCTCCTCTGACTTCAACAGCG	TTCCAGTATGACTCCACTCACGG
GAPDH-R	ACCACCCTGTTGCTGTAGTAGCCAA	TGAAGACACCAGTAGACTCCACGAC

shRNA targeting sequences of Rac1

No.	Sequence
9687	CCTTCTTAACATCACTGTCTT
9688	GCTAAGGAGATTGGTGCTGTA
9689	CGCAAACAGATGTGTTCTTAA
9690	CGTGAAGAAGAGGAAGAGAAA
9691	CCCTACTGTCTTTGACAATTA

Table S2. 50% inhibition concentration (IC50) of 6-TG, NSC23766, IFNα and ribavirin against SA11 rotavirus, 50% cytotoxic (CC50) of against Caco2 cells, and corresponding selectivity index (SI, CC50/IC50).

Drugs	IC50 against SA11 rotavirus (M)	CC50 against Caco2 cells (M)	selectivity index (SI, CC50/IC50)
6-TG	3.0×10^{-13} M	9.8×10^{-6} M	3.3×10^{7}
NSC23766	1.1×10^{-8} M	3.1×10^{-4} M	2.8×10^{4}
IFNα	3.1×10^{-5} IU	18706 IU	6.0×10^{8}
Ribavirin	1.6×10^{-7} M	3.02×10^{-2} M	1.9×10^{5}

Table S3. Patient characteristics.

Patient	Age (yrs)	Gender	Symptoms	Virus Detection							
				Enterovirus	Parechovirus	Norovirus genegroups I	Norovirus genegroups II	Adenovirus	Astrovirus	Sapovirus	Rotavirus
1	3.5	Female	Fever	No	No	No	No	No	No	No	Yes
2	74	Female	Congestive heart failure, myocarditis	No	No	No	No	No	No	No	Yes
3	27	Female	Fever, diarrhea, nausea, vomiting	No	No	No	No	No	No	No	Yes
4	67	Male	Fever, stomachache, watery diarrhea (Kidney transplant)	No	No	No	No	No	No	No	Yes
5	28	Female	Nausea, stomachache, watery diarrhea, fever, headache, vomiting	No	No	No	No	Yes	No	No	Yes

Supplementary Figures
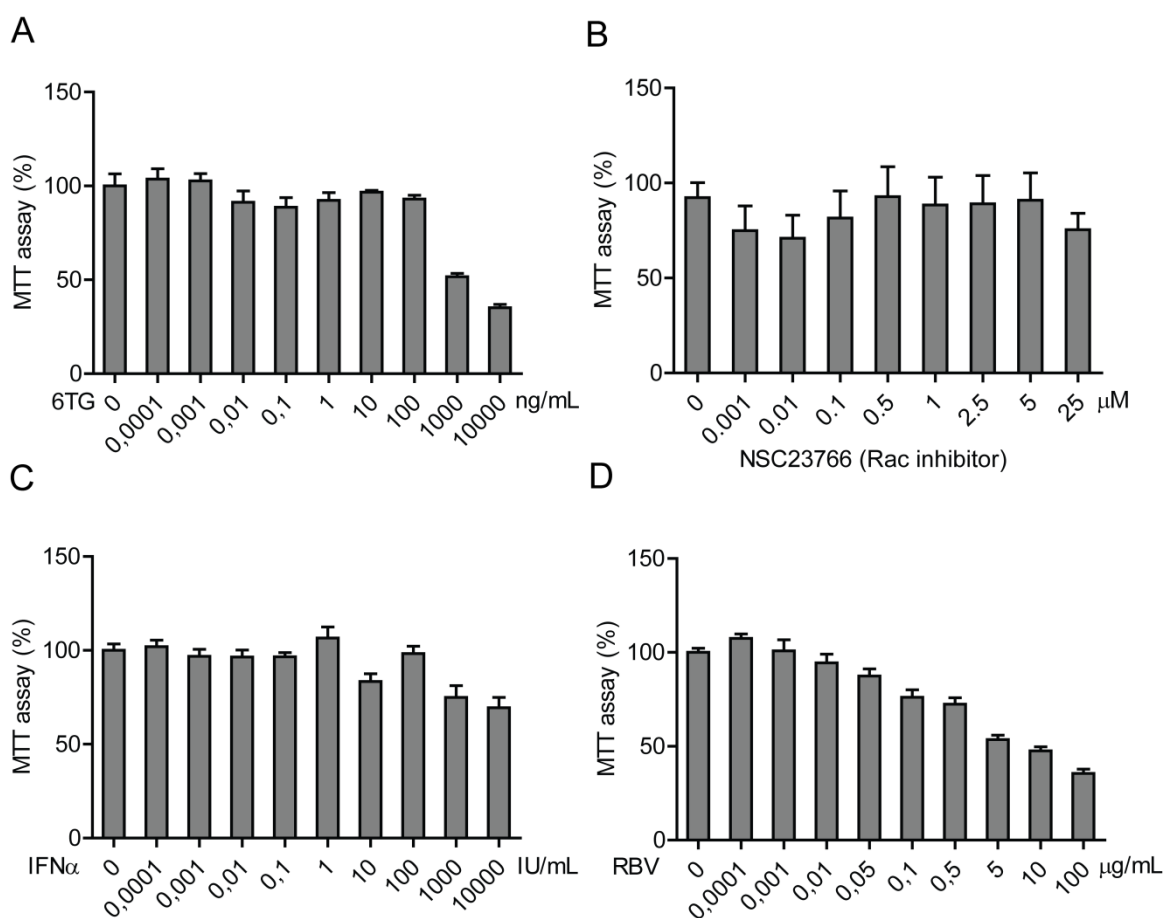
Fig. S1. Effect of 6-TG (A), NSC23766 (B), IFNα (C) and ribavirin (D) on host cell viability determined by MTT assays. Caco2 cells treated with all four drugs for 48 h.
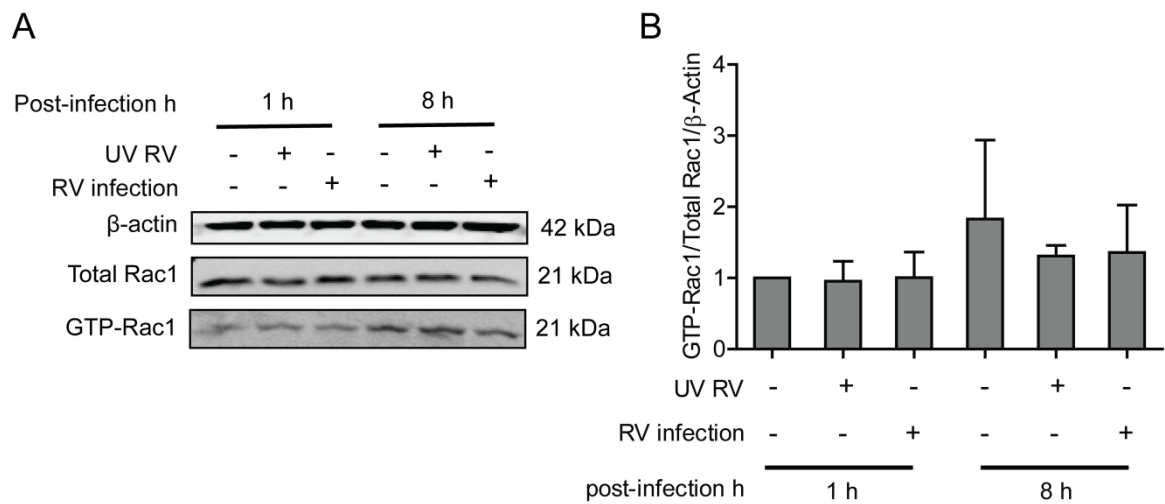
Fig. S2. The effect of inactive rotavirus by UV treatment, rotavirus and mock infection (1 and 8 h) on the expression of GTP-Rac1. (A) Western blot assay detected the expression of GTP-Rac1 after 1 and 8 h post-infection by inactive rotavirus (UV treatment), rotavirus and mock infection in Caco2 cells. (B) Quantification of the intensity of the immunoreactive bands of Rac1 (n = 4, means ± SEM, Mann-Whitney test) using Odyssey V 3.0 software.

Chapter 7

Drug screening identifies gemcitabine as inhibiting rotavirus through alteration of pyrimidine nucleotide synthesis pathway

Sunrui Chen, Yining Wang, Pengfei Li, Yuebang Yin, Marcel Bijvelds, Hugo de Jonge, Maikel P. Peppelenbosch, Denis Kainov, Qiuwei Pan

ABSTRACT

Although rotavirus infection is usually acute and self-limiting, it can cause chronic infection with severe disease phenotypes in immunocompromised patients, including organ transplantation recipients and cancer patients and irrespective of whether this concerns pediatric or adult patients. Clinical management is complicated by the absence of approved medication against rotavirus infection. Here we screened a library of safe-in-man broad-spectrum antivirals. We identified gemcitabine, a widely used anti-cancer drug, as a potent inhibitor of rotavirus infection. We confirmed this effect in 2D cell cultures and 3D cultured human intestinal organoids with both laboratory-adapted rotavirus strains and five clinical isolates. Supplementation of UTP or uridine largely abolished the anti-rotavirus activity of gemcitabine, suggesting its function through inhibition of pyrimidine biosynthesis pathway. Our results support repurposing gemcitabine for treating cancer patients at risk for rotavirus infection.

Rotavirus infection is the leading cause of severe dehydrating gastroenteritis among children under five-year-old (Greenberg and Estes, 2009). Although rotavirus infection is usually acute and self-limiting, it can cause chronic infection with severe diseases in immunocompromised patients, in particular organ transplantation recipients irrespective of whether these are pediatric or adult patients (Yin et al., 2015b). In addition, cancer patients have compromised immune system especially when undergoing chemotherapy or radiotherapy treatment, which make them prone to infections with worse outcomes (Hotchkiss and Moldawer, 2014). Rotavirus infections have been widely reported in pediatric or adult cancer patients causing prolonged diarrhea (Akhtar et al., 2018; Ghosh et al., 2017). Therefore, specific and effective antiviral treatment is urgently needed for these special populations when infected with rotavirus. Unfortunately no FDA-approved medications against rotavirus infection are available.

Developing new drugs usually takes more than ten years with enormous investment and high risk of failure. Given that only the specific population with rotavirus infection require antiviral treatment, the pharmaceutical industry will likely not develop new anti-rotavirus drugs. We propose that repurposing existing drugs represents a cost-effective approach to identify antiviral treatment that can readily benefit patients (Qu et al., 2019). In this study, we screened a library of safe-in-man broad-spectrum antiviral agents (BSAAs, https://drugvirus.info) (Andersen et al., 2020; Ianevski et al., 2018) on rotavirus infection in experimental models. These compounds are known to target viruses belonging to two or more viral families and have passed phase 1 clinical trials. This greatly enhances the probability of identifying novel activities of some of these agents against rotavirus infection and facilitates their clinical translation.

We first screened 94 BSAAs in the human intestinal Caco2 cell line infected with simian rotavirus SA11 strain (**Table S1**). To minimize non-specific effects on host cells, we used low concentration of 1 µM and treated for 48 hours. By qRT-PCR (primers listed in **Table S2**) quantification of rotavirus genomic RNA, we identified 43 candidates exerting over 50% inhibitory effects, and 17 with inhibition over 70% (**Fig. 1A**). Among these, gemcitabine was one of the most effective candidates (**Fig. 1A**). It is a cytidine analog that has been widely used for cancer treatment (Cerqueira et al., 2007; Zhang et al., 2019). It has been shown to inhibit a broad range of RNA viruses including severe acute respiratory syndrome coronavirus (SARS-

CoV), Middle East respiratory syndrome coronavirus (MERS-CoV), Zika virus and hepatitis C virus (HCV) in experimental models (Beran et al., 2012; Dyall et al., 2014; Kuivanen et al., 2017). Nucleotide and nucleoside analogues are excellent examples of BSAAs that have been widely used in the clinic for treating infections of RNA and DNA viruses (Ianevski et al., 2018). We have previously demonstrated that nucleotides, including purine and pyrimidine, biosynthesis pathways are essential in the rotavirus infection process and can be pharmacologically targeted (Chen et al., 2019; Yin et al., 2018a; Yin et al., 2016). As a cytidine analog, gemcitabine has been reported to inhibit pyrimidine biosynthesis, resulting in nucleotide depletion (Lee et al., 2017). Therefore, we focused on the effects and mode-of-action of gemcitabine on rotavirus infection in this study.

We next tested a series of gemcitabine concentrations (0.01-10 µM) in the Caco2 cell model to assess both antiviral and cytotoxic effects. We confirmed the potent anti-rotavirus effect and observed a large therapeutic window between cytotoxic and antiviral activities, as shown the CC_{50} value of 13.58 mM and IC_{50} value of 0.12 µM (**Fig. 1B, 1C**). We performed same experiments in the monkey MA104 cell line that is widely used for propagating rotavirus in laboratory. Similar trends were observed with CC_{50} value of 0.36 mM and IC_{50} value of 3.98 µM (**Supplementary Fig. S1**). By harvesting supernatant of Caco2 cells at 48-hour post-treatment, we performed TCID50 assay to determine the titers of secreted viruses. Consistently, the titers of produced rotavirus with infectivity were significantly reduced by gemcitabine treatment (**Fig. 1D**). At the protein level, we found potent inhibition of viral protein 4 (VP4) expression determined by Western blotting (**Fig. 1E**). Furthermore, immunofluorescent staining of viral capsid protein (VP6) showed significant reduction of the number of infected Caco2 cells by gemcitabine treatment (**Fig. 1F, 1G, Supplementary Fig. S2**).
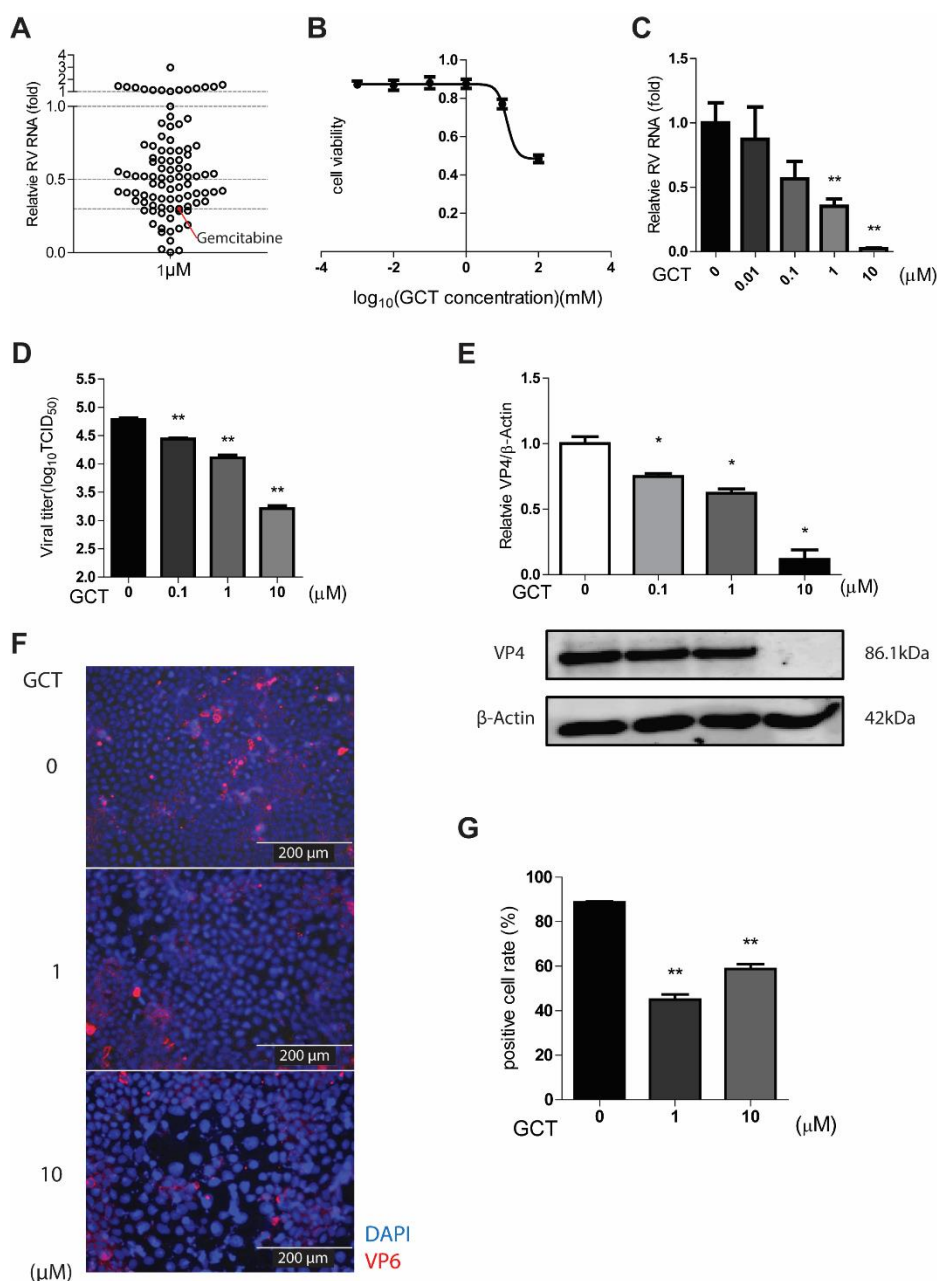
Figure 1. Screening BSAAs identified gemcitabine as a potent inhibitor of rotavirus infection. (A) Human intestinal Caco2 cells were infected with SA11 rotavirus. After infection, cells were treated with 94 BSAAs at 1 µM for 48 hours. qRT-PCR analysis of viral RNA revealed that 43 reagents exerted ≥ 50% inhibitory activity, and 17 of them exerted ≥ 70% inhibitory activity against rotavirus replication. Gemcitabine (GCT) inhibited rotavirus replication by 70%. (B) 50% cytotoxic concentration (CC_{50}) curves of GCT were determined by MTT assays on Caco2 cell line. (C) Dose-dependent inhibitory activity of GCT on rotavirus infected Caco2 cell line. qRT-PCR data were normalized to housekeeping gene *GAPDH* and presented relative to the control (CTR) (set as 1) (n = 6). (D) The supernatant of each well under GCT treatment was harvested after freezing and thawing for three times, virus titer from different groups was measured by $TCID_{50}$ assay (n = 6). (E) Rotavirus infected Caco2 cells were treated by different concentrations of GCT, and

protein samples were harvested after 48 hours. The expression of viral structural protein VP4 was stained and quantified by western blot assay (n = 4). (F) Indirect fluorescence microscope analysis of viral structural protein VP6 (red) upon treatment with GCT. Nuclei were visualized by DAPI (blue). (G) The ratio of VP6 positive cells/ total cell number was quantified under 40* vision field (Supplementary Fig. S2) (n = 6). Data represent means ± SEM. *$P < 0.05$; **$P < 0.01$; ***$P < 0.001$.

The responsiveness to antiviral therapy can vary dramatically in patients. This mainly attributes to host and viral factors. The nucleoside analog ribavirin has been used for treating HCV infection for decades. Reduced cellular uptake by the host and mutagenesis of the viral genome have been linked to treatment resistance in chronic HCV patients (Ibarra et al., 2011). As recently repositioned for treating chronic hepatitis E virus (HEV) infection (Kamar et al., 2017), viral mutagenesis during ribavirin treatment or pre-deposition of resistance mutations are thought to contribute to treatment failure (Ikram et al., 2018). Our previous studies have evaluated the effects of the nucleoside analog ribavirin and mycophenolic acid (MPA), and the antiviral cytokine interferon alpha (IFN-α) on rotavirus in cell culture models. We found the responsiveness to these agents dramatically vary among different clinical isolates from potent, moderate, minimal to even pro-viral effects (Yin et al., 2015a; Yin et al., 2016). This imposes major challenges for clinical application as how to personalize the selection of potential responders. Thus, we extended our evaluation of gemcitabine to different rotavirus strains/isolates. We found that gemcitabine significantly inhibits the replication of rhesus rotavirus RRV strain (**Fig. 2A**) and five clinical isolates (**Fig. 2B-2F**). Based on these results, we postulate that the response to gemcitabine in rotavirus patients could be universally effective.
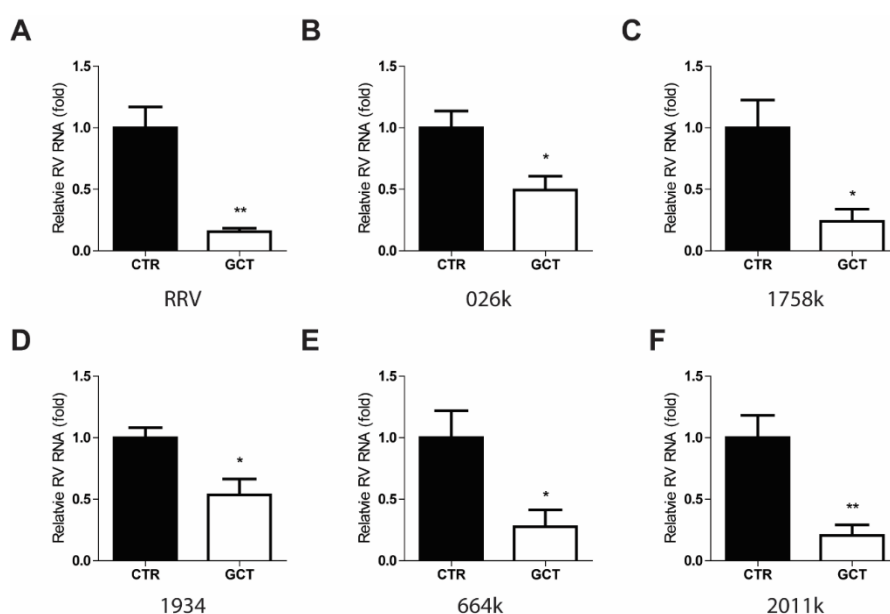
Figure 2. Antiviral effect of gemcitabine against RRV rotavirus strain and clinical isolates. qRT-PCR analysis of rotavirus RNA upon treatment of gemcitabine (GCT) at 1 μM for 48 hours in laboratory rotavirus strain RRV (A), clinically isolated rotavirus strain 026k (B), 1758k (C), 1934 (D), 664k (E), and 2011k (F). Data were normalized to housekeeping gene *GAPDH* and are presented relative to the control (CTR) (set as 1). Data represent means ± SEM; n = 6; *$P < 0.05$; **$P < 0.01$.

We have previously established that modeling of rotavirus infection in intestinal organoids allows the study of virus-host interactions and assessment of antiviral drugs efficacy (Yin et al., 2015a; Yin et al., 2018a; Yin et al., 2018b; Yin et al., 2016). Intestinal organoids, also called mini-guts, are stem cell-derived epithelial 3D cultures. These organoids are much better in recapitulating the architecture, composition, diversity, organization and functionality of cell types of the intestine when compared to more conventional model systems. Treatment with gemcitabine in rotavirus inoculated human intestinal organoids potently inhibited viral RNA synthesis and secretion of rotaviruses with approximately 80% inhibitory effects for both at 1 μM concentration treated for 48 hours (**Fig. 3A; Supplementary Fig. S3**). This effect was further confirmed at the VP4 protein level by western blot assay (**Fig. 3B**). Importantly, rotavirus infection led to morphological and pathological changes in organoids. Based on optical imaging, we observed that rotavirus infected organoids without gemcitabine treatment showed opaque, wizened and disorganized morphology. In contrast, gemcitabine treated groups, in particular with 1 μM concentration, most of the organoids were hyaline and in a spheroidal shape (**Fig. 3C upper panel**). In confocal immunostaining, VP6 protein was detected in all groups, but the intensity and frequency of the viral protein were lower in treatment groups (**Fig. 3C middle panel**). Fluorescence staining of cell viability by Propidium Iodide (PI) showed that cell death (determined as described in **Supplementary Fig. S4**) in un-treated group is more obvious, and dead cells were diffused in almost all organoids (**Fig. 3C lower panel**). This is consistent with the percentage of organoids in a deteriorated condition (**Fig. 3D**). Thus, inhibition of rotavirus replication by gemcitabine can protect organoids from rotavirus induced cytopathogenesis.
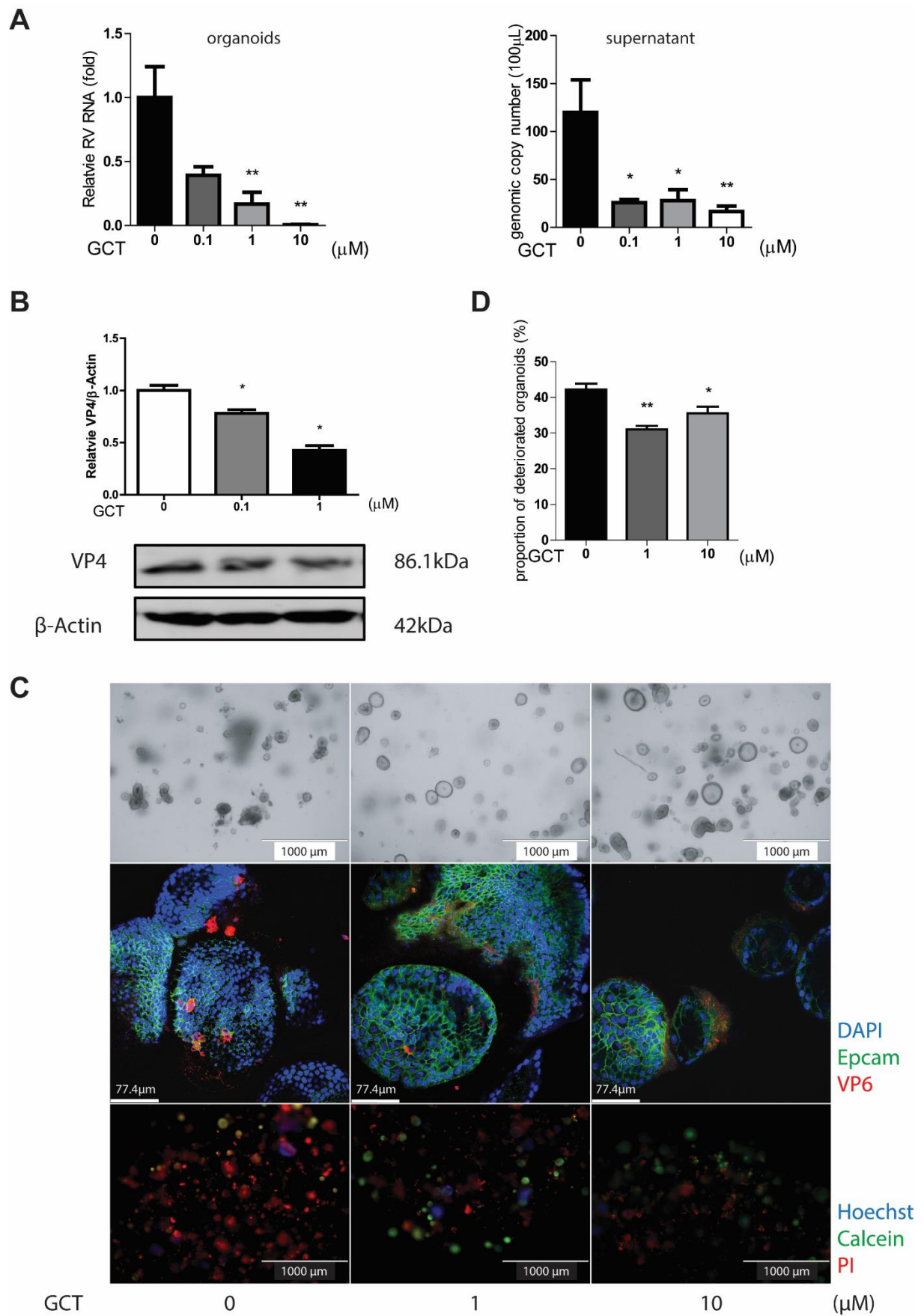
Figure 3. Antiviral activity of gemcitabine against rotavirus SA11 in human intestinal organoids. (A) Human intestinal organoids (HIOs) were inoculated with SA11 rotavirus strain and treated with gemcitabine (GCT) for 48 hours. The relative cellular rotavirus RNA and secreted viruses calculated as genomic copy number were analyzed by qRT-PCR (n = 6). Standard curve for calculation of genomic copy number is included in Supplementary Fig. S3. (B) The expression of viral structural protein VP4 was stained and quantified by western blot assay (n = 4). (C) Optical microscopy images, confocal images and indirect fluorescence microscope images of HIOs from mock group and GCT treated groups. In confocal images, VP6 protein was stained in red, green signal represents Epcam, and nuclei were visualized by DAPI (blue). In fluorescence microscope images, HIOs were stained by PI (red) indicating dead cells, Hoechst (blue) for nuclear, and Calcein (green) as live cells. (D) Rate of deteriorated HIOs was calculated as dead organoids/ total organoids (n = 6). Data represent means ± SEM; *$P < 0.05$; **, $P < 0.01$.

The antiviral activity of gemcitabine has been linked to the inhibition of pyrimidine biosynthesis pathway, especially the salvage pathway (Lee et al., 2017). We thus supplemented UTP or uridine to rotavirus infected Caco2 cell model when treated with gemcitabine. We found that exogenous supplementation of pyrimidine dose-dependently abolished the anti-rotavirus effect of gemcitabine. The anti-rotavirus effect was almost completely abolished by addition of 1000 µM UTP or uridine (**Fig. 4A, 4B**). Hence, the anti-rotavirus activity of gemcitabine was largely dependent on the salvage pyrimidine biosynthesis pathway. Combination approaches are often used in clinic to achieve optimal antiviral efficacy and avoid resistance development. We finally assessed the combinatory effects of gemcitabine with ribavirin, MPA or IFN-α, as we previously have demonstrated the anti-rotavirus effects of these three agents (Yin et al., 2015a; Yin et al., 2016). We found enhanced anti-rotavirus activity when combined with ribavirin or IFN-α, but not MPA (**Fig. 4C**).
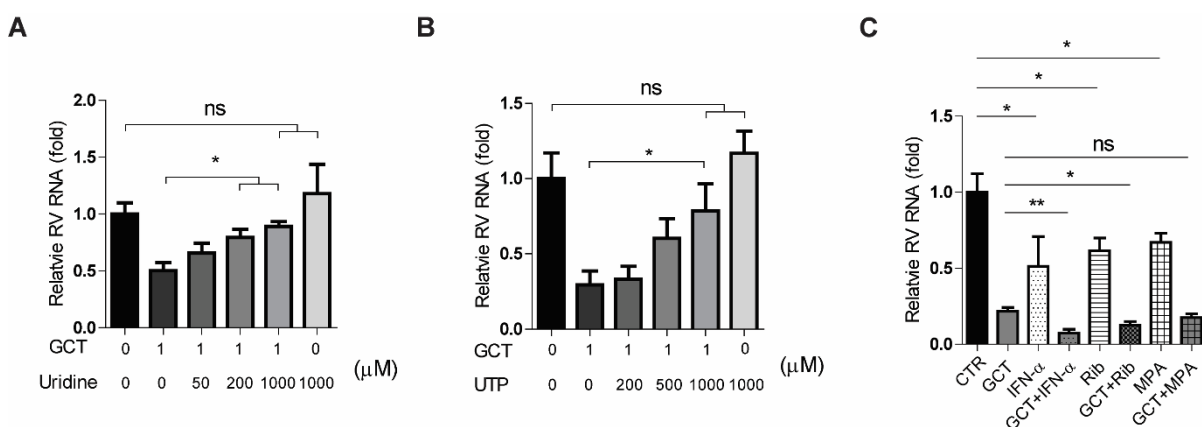
Figure 4. The effects of nucleotide supplementation and combination with other antivirals on the anti-rotavirus activity of gemcitabine. Supplementation of exogenous uridine (A) and UTP (B) attenuates the anti-rotavirus effect of gemcitabine (GCT) in Caco2 cell model (n = 6). (C) The combinatory effects of 1 μM GCT with 1000 U IFN-α, 1 μg/ml ribavirin (Rib) or 0.1 μg/ml mycophenolic acid (MPA), respectively (n = 6). Data represent means ± SEM; *$P < 0.05$; **$P < 0.01$.

In summary, we have identified gemcitabine as a potent inhibitor against rotavirus infection through screening of a BSAA library. The antiviral activity was largely dependent on the pyrimidine biosynthesis pathway. Because gemcitabine has been widely used as chemotherapy for cancer patients, and these patients are at risk of infections (Hotchkiss and Moldawer, 2014), the use of gemcitabine in cancer patients as chemotherapeutic drug probably mitigates the risk of viral infections in general. Our results support a repositioning of gemcitabine for treating rotavirus infection, especially in infected cancer patients. Furthermore, the approach of discovering new antiviral therapy from BSAAs bears essential implications in combating emerging viral pathogens, such as the ongoing coronavirus disease COVID-19 pandemic (Mahase, 2020).

References

Akhtar, T., Cargill, J., Gerrard, C., Shaw, F., Cunliffe, N.A., Cooke, R.P.D., Pizer, B., 2018. Detection of rotavirus in paediatric oncology patients with diarrhoea: the impact of rotavirus vaccine. J Hosp Infect 99, 185-187.

Andersen, P.I., Ianevski, A., Lysvand, H., Vitkauskiene, A., Oksenych, V., Bjoras, M., Telling, K., Lutsar, I., Dampis, U., Irie, Y., Tenson, T., Kantele, A., Kainov, D.E., 2020. Discovery and development of safe-in-man broad-spectrum antiviral agents. Int J Infect Dis.

Beran, R.K., Sharma, R., Corsa, A.C., Tian, Y., Golde, J., Lundgaard, G., Delaney, W.E.t., Zhong, W., Greenstein, A.E., 2012. Cellular growth kinetics distinguish a cyclophilin inhibitor from an HSP90 inhibitor as a selective inhibitor of hepatitis C virus. PLoS One 7, e30286.

Cerqueira, N.M., Fernandes, P.A., Ramos, M.J., 2007. Understanding ribonucleotide reductase inactivation by gemcitabine. Chemistry 13, 8507-8515.

Chen, S., Ding, S., Yin, Y., Xu, L., Li, P., Peppelenbosch, M.P., Pan, Q., Wang, W., 2019. Suppression of pyrimidine biosynthesis by targeting DHODH enzyme robustly inhibits rotavirus replication. Antiviral Res 167, 35-44.

Dyall, J., Coleman, C.M., Hart, B.J., Venkataraman, T., Holbrook, M.R., Kindrachuk, J., Johnson, R.F., Olinger, G.G., Jr., Jahrling, P.B., Laidlaw, M., Johansen, L.M., Lear-Rooney, C.M., Glass, P.J., Hensley, L.E., Frieman, M.B., 2014. Repurposing of clinically developed drugs for treatment of Middle East respiratory syndrome coronavirus infection. Antimicrob Agents Chemother 58, 4885-4893.

Ghosh, N., Malik, F.A., Daver, R.G., Vanichanan, J., Okhuysen, P.C., 2017. Viral associated diarrhea in immunocompromised and cancer patients at a large comprehensive cancer center: a 10-year retrospective study. Infect Dis (Lond) 49, 113-119.

Greenberg, H.B., Estes, M.K., 2009. Rotaviruses: from pathogenesis to vaccination. Gastroenterology 136, 1939-1951.

Hotchkiss, R.S., Moldawer, L.L., 2014. Parallels between cancer and infectious disease. N Engl J Med 371, 380-383.

Ianevski, A., Zusinaite, E., Kuivanen, S., Strand, M., Lysvand, H., Teppor, M., Kakkola, L., Paavilainen, H., Laajala, M., Kallio-Kokko, H., Valkonen, M., Kantele, A., Telling, K., Lutsar, I., Letjuka, P., Metelitsa, N., Oksenych, V., Bjoras, M., Nordbo, S.A., Dumpis, U., Vitkauskiene, A., Ohrmalm, C., Bondeson, K., Bergqvist, A., Aittokallio, T., Cox, R.J., Evander, M., Hukkanen, V., Marjomaki, V., Julkunen, I., Vapalahti, O., Tenson, T., Merits, A., Kainov, D., 2018. Novel activities of safe-in-human broad-spectrum antiviral agents. Antiviral Res 154, 174-182.

Ibarra, K.D., Jain, M.K., Pfeiffer, J.K., 2011. Host-based ribavirin resistance influences hepatitis C virus replication and treatment response. J Virol 85, 7273-7283.

Ikram, A., Hakim, M.S., Zhou, J.H., Wang, W., Peppelenbosch, M.P., Pan, Q., 2018. Genotype-specific acquisition, evolution and adaptation of characteristic mutations in hepatitis E virus. Virulence 9, 121-132.

Kamar, N., Wang, W., Dalton, H.R., Pan, Q., 2017. Direct-acting antiviral therapy for hepatitis E virus? Lancet Gastroenterol Hepatol 2, 154-155.

Kuivanen, S., Bespalov, M.M., Nandania, J., Ianevski, A., Velagapudi, V., De Brabander, J.K., Kainov, D.E., Vapalahti, O., 2017. Obatoclax, saliphenylhalamide and gemcitabine inhibit Zika virus infection in vitro and differentially affect cellular signaling, transcription and metabolism. Antiviral Res 139, 117-128.

Lee, K., Kim, D.E., Jang, K.S., Kim, S.J., Cho, S., Kim, C., 2017. Gemcitabine, a broad-spectrum antiviral drug, suppresses enterovirus infections through innate immunity induced by the inhibition of pyrimidine biosynthesis and nucleotide depletion. Oncotarget 8, 115315-115325.

Mahase, E., 2020. Covid-19: WHO declares pandemic because of "alarming levels" of spread, severity, and inaction. BMJ 368, m1036.

Qu, C., Li, Y., Li, Y., Yu, P., Li, P., Donkers, J.M., van de Graaf, S.F.J., de Man, R.A., Peppelenbosch, M.P., Pan, Q., 2019. FDA-drug screening identifies deptropine inhibiting hepatitis E virus involving the NF-kappaB-RIPK1-caspase axis. Antiviral Res 170, 104588.

Yin, Y., Bijvelds, M., Dang, W., Xu, L., van der Eijk, A.A., Knipping, K., Tuysuz, N., Dekkers, J.F., Wang, Y., de Jonge, J., Sprengers, D., van der Laan, L.J., Beekman, J.M., Ten Berge, D., Metselaar, H.J., de Jonge, H., Koopmans, M.P., Peppelenbosch, M.P., Pan, Q., 2015a. Modeling rotavirus infection and antiviral therapy using primary intestinal organoids. Antiviral Res 123, 120-131.

Yin, Y., Chen, S., Hakim, M.S., Wang, W., Xu, L., Dang, W., Qu, C., Verhaar, A.P., Su, J., Fuhler, G.M., Peppelenbosch, M.P., Pan, Q., 2018a. 6-Thioguanine inhibits rotavirus replication through suppression of Rac1 GDP/GTP cycling. Antiviral Res 156, 92-101.

Yin, Y., Dang, W., Zhou, X., Xu, L., Wang, W., Cao, W., Chen, S., Su, J., Cai, X., Xiao, S., Peppelenbosch, M.P., Pan, Q., 2018b. PI3K-Akt-mTOR axis sustains rotavirus infection via the 4E-BP1 mediated autophagy pathway and represents an antiviral target. Virulence 9, 83-98.

Yin, Y., Metselaar, H.J., Sprengers, D., Peppelenbosch, M.P., Pan, Q., 2015b. Rotavirus in organ transplantation: drug-virus-host interactions. Am J Transplant 15, 585-593.

Yin, Y., Wang, Y., Dang, W., Xu, L., Su, J., Zhou, X., Wang, W., Felczak, K., van der Laan, L.J., Pankiewicz, K.W., van der Eijk, A.A., Bijvelds, M., Sprengers, D., de Jonge, H., Koopmans, M.P., Metselaar, H.J., Peppelenbosch, M.P., Pan, Q., 2016. Mycophenolic acid potently inhibits rotavirus infection with a high barrier to resistance development. Antiviral Res 133, 41-49.

Zhang, Y., Chen, L., Hu, G.Q., Zhang, N., Zhu, X.D., Yang, K.Y., Jin, F., Shi, M., Chen, Y.P., Hu, W.H., Cheng, Z.B., Wang, S.Y., Tian, Y., Wang, X.C., Sun, Y., Li, J.G., Li, W.F., Li, Y.H., Tang, L.L., Mao, Y.P., Zhou, G.Q., Sun, R., Liu, X., Guo, R., Long, G.X., Liang, S.Q., Li, L., Huang, J., Long, J.H., Zang, J., Liu, Q.D., Zou, L., Su, Q.F., Zheng, B.M., Xiao, Y., Guo, Y., Han, F., Mo, H.Y., Lv, J.W., Du, X.J., Xu, C., Liu, N., Li, Y.Q., Chua, M.L.K., Xie, F.Y., Sun, Y., Ma, J., 2019. Gemcitabine and Cisplatin Induction Chemotherapy in Nasopharyngeal Carcinoma. N Engl J Med 381, 1124-1135.

Supplementary information

Materials and methods

Reagents

All the compounds used in this study were from broad-spectrum antiviral agents (BSAs) library. Names of all BSAs are listed in **Supplementary table 1**. All the reagents were dissolved in dimethyl sulfoxide (DMSO) or milli-Q water.

Viruses

Simian rotavirus SA11 and rhesus rotavirus RRV were gifted by Karen Knipping from Nutricia Research Utrecht, The Netherland. Stool samples collected from rotavirus infected patient were obtained from the Erasmus MC biobank, Department of Viroscience, Erasmus Medical Center, Rotterdam.

Cell lines and human primary intestinal organoids

Human colon cancer cell line Caco2 and African green monkey kidney cell line MA104 were cultured in Dulbecco's modified Eagle's medium (DMEM; Lonza, Verviers, Belgium) containing 20% or 10% (vol/ vol) heat-inactivated fetal calf serum (FCS, Sigma–Aldrich, St. Louis USA) respectively and 100 U/ml Penicillin/ Streptomycin (P/S, Gibco, Grand Island, USA) solution. A humidified incubator was used for cells culturing at 37° C in 5% CO_2. Cells were analyzed by genotyping and confirmed to be mycoplasma negative.

Human intestinal organoids culture was performed as described previously (Yin et al., 2015). Culture medium was refreshed every 2-3 days, and HIOs were passaged every 5–7 days.

Virus inoculation and production assay

Virus, cell line and human intestinal organoids (HIOs) were maintained and treated as in previous work (Chen et al., 2019; Yin et al., 2015; Yin et al., 2018a; Yin et al., 2018b; Yin et al., 2016). In short, Caco2 cells and MA104 cells seeded into a multi-well plate (5×10^4 cells/well). Culture medium was discarded when cell confluence was approximately 80%, followed by

twice PBS washing. Then 100 μL of serum-free DMEM medium, rotavirus (MOI=0.7) with 5 μg/mL of trypsin (Gibco, Paisley, UK) were added and incubated at 37°C with 5% CO_2 for 60 min for infection, followed by 3 times washing with PBS to remove un-attached viruses. Then, cells were incubated with culture medium containing 5 μg/ml of trypsin at 37°C with 5% CO_2. In parallel, human primary intestinal organoids were infected with 10 times higher concentration of SA11 rotavirus than cell infection for 1.5 h followed by 4 times washing with PBS. Afterwards, HIOs with no Matrigel remain were spun down at 500g for 10 min to adhered to the bottom of 24-well plate coated with Collagen R solution (SERVA, Heidelberg, Germany). Organoids culture medium was added gently and HIOs were incubated at 37°C with 5% CO_2. Culture medium and HIOs were harvested respectively after 48h to detect and enumerate rotavirus. Virus titers from supernatants were determined by calculating the $log_{10}TCID_{50}/mL$ method.

RNA isolation, cDNA synthesis and qRT-PCR

Total RNA was isolated using Macherey-Nagel NucleoSpin® RNA II kit (Bioke, Leiden, Netherlands) and quantified using a Nanodrop ND-1000 (Wilmington, DE, USA). Total RNA reverse transcription was performed by using a cDNA Synthesis kit (TAKARA BIO INC.) with random hexamer primers. Real-time PCR reactions (50°C for 2 min, 95°C for 10 min, followed by 50 or 60 cycles of 95°C for 15 s and 58°C for 30 s and 72°C for 10 min) were performed with SYBRGreen-based real-time PCR (Applied Biosystems®, Austin, USA) according to the manufacturer's instruction. Glyceraldehyde 3-phosphate dehydrogenase (GAPDH) gene was used as housekeeping gene. Relative gene expressions were normalized to GAPDH using the formula $2^{-\Delta\Delta CT}$ ($\Delta\Delta CT = \Delta CTsample - \Delta CTcontrol$). Template control and reverse transcriptase control were included in all RT-qPCR experiments. All qRT-PCR primers are listed in **Supplementary table 2**.

Quantification of rotavirus genome copy numbers

An amplicon of the SA11 (a fragment of VP6 gene from 564-718) was cloned into the pCR2.1-TOPO vector (Invitrogen, San Diego, CA) to generate a template for quantifying rotavirus genome copy number. The plasmid was extracted by Quick Plasmid Miniprep Kit (Invitrogen, Lohne, Germany) following manufacturer's instructions. A series of dilutions (from 10^{-2} to 10^{-}

[10]) were prepared and then were amplified and quantified by qRT-PCR to generate a standard curve. This standard curve was generated by plotting the log copy number versus the cycle threshold (CT) value (**Supplementary figure. S2)**. Copy numbers were calculated by using the following equation: Copy number (molecules/µl) = [concentration (ng/µl) × 6.022× 10^{23} (molecules/mol)]/[length of amplicon× 640 (g=/mol) × 10^9 (ng/g).

Determination of organoids cell death

The scoring process was performed as previously (Chen et al., 2019; Grabinger et al., 2014). In short, a minimum of 100 organoids were counted after 3 days of passaging. After 1.5 h incubation with SA11 rotavirus, HIOs were cultured in matrigel and treated with different agents for 48 h, then HIOs were stained by PI (red) which represented as dead cell, Hoechst(blue) which represented as nuclear, and Calcein (green) which represented as live cell. We define the HIOs with red signal more than green signal and also more than 50% of blue signal as positive, otherwise HIOs will be counted as negative. Detailed example is shown in **Supplementary figure. S4**. In optical microscopy imaging, positive HIOs were opaque and disorganized while negative HIOs were hyaline and in a spheroidal shape. The proportion of organoids apparently deteriorated was calculated as (viable/ total) %.

Western blot assay

Lysed cells were subjected to SDS-PAGE, and proteins were transferred to PVDF membrane (Immobilon-FL). DHODH (ab 54621, 1:1000, mouse monoclonal, Abcam), SA11 rotavirus VP4 (1:1000, HS-2, mouse monoclonal; provided by professor Harry Greenberg, Stanford University School of Medicine, USA) was detected by western blot analysis and β-actin protein was detected as loading control (sc-47778, 1:1000, mouse monoclonal; Santa Cruz). The intensity of the immunoreactive bands of blotted protein was quantified by the Odyssey V3.0 software.

Immunofluorescence analysis

After rotavirus infection, organoids were harvested and fixed in 4% paraformaldehyde in PBS at $4°C$ for 10 min. Fixed organoids were added into the CytoSpin II Cytocentrifuge (Shandon Scientifi Ltd, Runcorn, England), then spun down at 1000 rpm for 2 min. The slides containing

organoids were rinsed 3 times with PBS for 5 min each, followed by treatment with 0.1% (vol/vol) Tritonx100 for 4 min. Subsequently, the slides were twice rinsed with PBS for 5 min, followed by incubation with milk-tween-glycine medium (0.05% tween, 0.5% skim milk and 0.15% glycine) to block background staining for 30 min. Slides were incubated in a humidity chamber with anti-rotavirus antibody (1:250, mouse monoclonal; Abcam) and anti-EpCAM antibody (1:250, rabbit polyclonal; Abcam) diluted in milk-tween-glycine medium at 4 ºC overnight. Slides were washed 3 times for 5 min each in PBS prior to 1h incubation with 1:1000 dilutions of the anti-mouse IgG (H+L, Alexa Fluor® 594) and the anti-rabbit IgG (H+L, Alexa Fluor® 488) secondary antibodies. Nuclei were stained with DAPI (4, 6-diamidino-2-phenylindole; Invitrogen). Images were detected using Leica SP5 cell imaging system.

MTT assay

The CC_{50} values of GCT were determined by MTT assay (Fig. 1B, 1D) as previous study {Qu, 2018 #156}. Approximately 1×10^4 Caco2 cells were seeded per well in 96-well plate. After 48h, cells were incubated with 10 μL 5 mg/ml MTT for 3 h, then replaced with 100 ml dimethyl sulfoxide (DMSO) medium (Sigma). Absorbance (490 nm) was analyzed accordingly.

Statistics

All numerical results are reported as Mean ± SEM. The statistical significance of differences between means was assessed with the Mann-Whitney test (GraphPad Prism 5; GraphPad Software Inc., La Jolla, CA). The threshold for statistical significance was defined as $P \leq 0.05$.

**Supplementary table 3. List of broad-spectrum antiviral agents (BSAs) library.**

1	Abamectin	25	Cyclosporine	49	Hydroxychloroquine	73	Novobiocin
2	ABT-263	26	Dasatinib	50	Imatinib	74	Obatoclax
3	Acetylsalicylic acid	27	Dibucaine	51	Indomethacin	75	Omeprazole
4	Aciclovir	28	Diphyllin	52	Itraconazole	76	Pentosan polysulfate
5	Amiloride	29	Doxycycline	53	Ivermectin	77	Pirlindole
6	Amiodarone	30	DFMO	54	Kasugamycin	78	Quinine
7	Amodiaquine	31	Emetine	55	Lamivudine	79	Raloxifene
8	Apilimod	32	Emodine	56	Leflunomide	80	Rapamycin
9	Arbidol	33	Erlotinib	57	Lanatoside C (Isolanid)	81	Ribavirin
10	Artesunate	34	Esomeprazole	58	Lobucavir	82	Ritonavir
11	Azacitidine	35	Ezetimibe	59	Lopinavir	83	Regorafenib
12	Azithromycin	36	Famciclovir	60	Lovastatin	84	Simvastatin
13	BDA-366	37	Favipiravir	61	Luteolin	85	Sofosbuvir (PSI-7977)
14	Bepridil	38	Fenretinide (4-HPR)	62	Manidipine	86	Suramin
15	Berberine	39	Flavopiridol	63	Maribavir	87	Tamoxifen
16	Bortezomib	40	Fluoxetine	64	Memantine	88	Teicoplanin
17	Brequinar	41	Fluvastatin	65	Metformin	89	Tenofovir
18	Bromocriptine	42	Formoterol	66	Minocycline	90	Topotecan
19	Caffeine	43	Foscarnet	67	Mitoxantrone	91	Trifluridine
20	Camostat	44	Ganciclovir	68	Mycophenolic acid	92	Valacyclovir
21	Camptothecin	45	Gefitinib	69	Nafamostat	93	Verapamil
22	Chloroquine	46	Gemcitabine	70	Nelfinavir	94	Vidarabine
23	Cidofovir	47	Glycyrrhizin	71	Nitazoxanide		
24	Clofarabine	48	Homoharringtonine	72	Niclosamide		

Supplementary table 2. qRT-PCR primers (human gene) used in the study, from 5' to 3'.

Gene name	Sense primer	Antisense primer
SA11 Rotavirus	TGGTTAAACGCAGGATCGGA	AACCTTTCCGCGTCTGGTAG
RRV Rotavirus	GCTATTTGG AACGCAAGAG	TAGTGGTCACATTCGGAGTT
Human Patient Rotavirus	ACCATCTACACATGACCCTC	CACATAACGCCCCTATAGCC
Human GAPDH	GTCTCCTCTGACTTCAACAGCG	ACCACCCTGTTGCTGTAGTAGCCAA
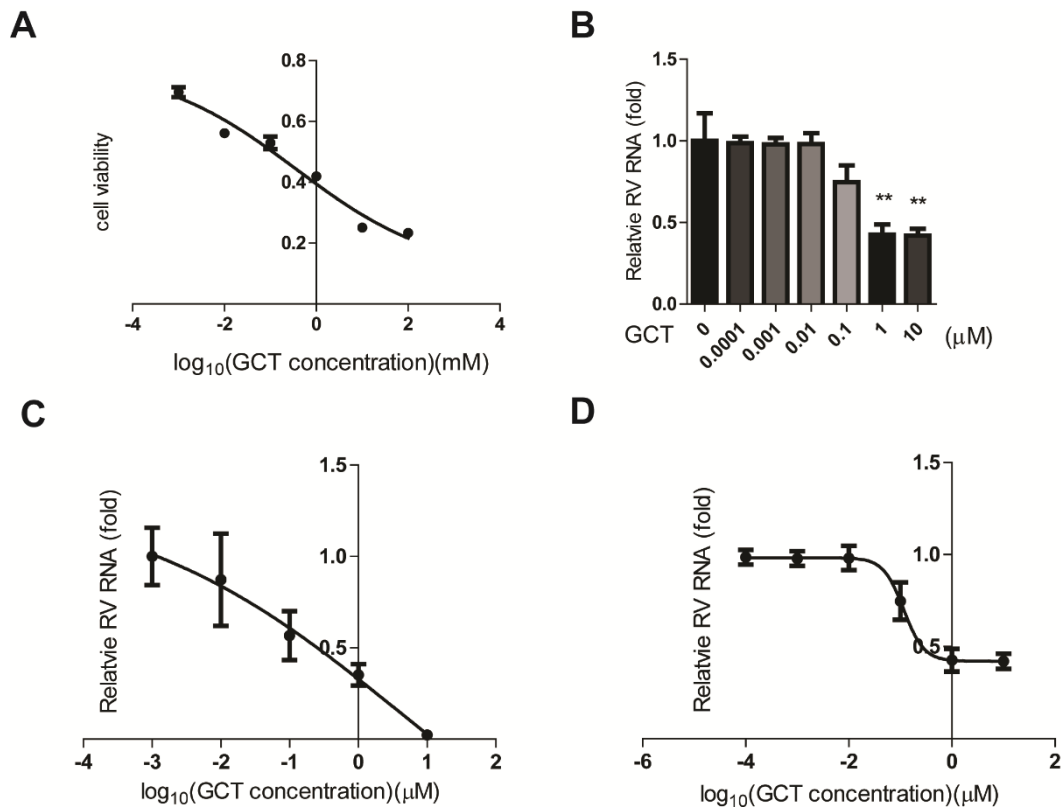
Supplementary Fig. S1. **Antiviral effect of gemcitabine (GCT) on MA104 cell line and its 50% inhibitory concentration (IC$_{50}$) curves**. (A) 50% cytotoxic concentration (CC$_{50}$) curves of GCT on MA104 cell line. (B) Dos-dependent inhibitory activity of GCT on MA104 cell line. (C) On Caco2 cell line, IC$_{50}$ is 3.977 μM. (D) On MA104 cell line, IC$_{50}$ is 0.1161 μM.
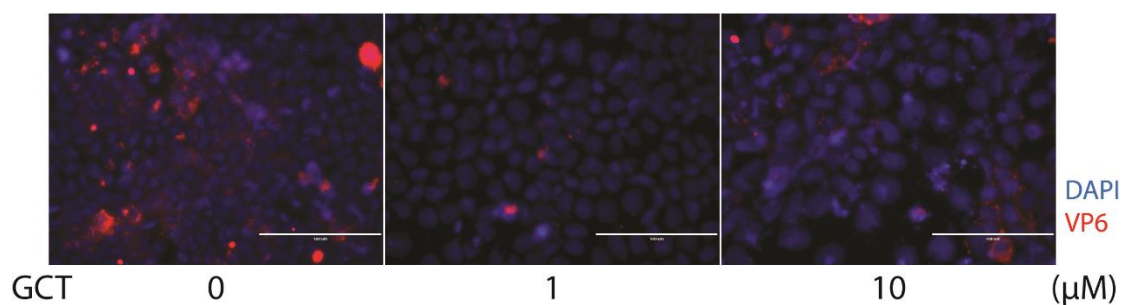
Supplementary Fig. S2. Indirect fluorescence microscopy for Caco2 cell line under 40* vision field.
The ratio of VP6 positive cells/ total cell number was quantified under these visions of field (n=6).
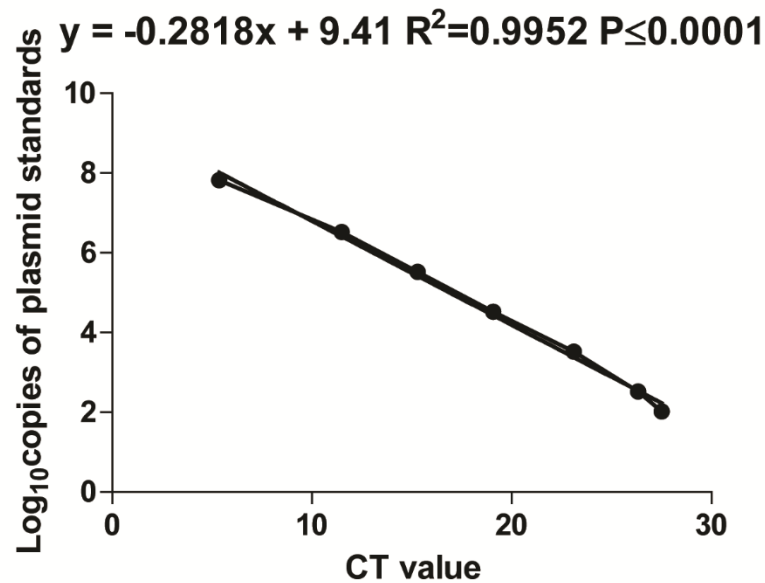
Supplementary Fig. S3. Standard curve for quantifying rotavirus genome copy numbers. An amplicon of the SA11 was cloned into the pCR2.1-TOPO vector. The plasmid was extracted, followed by a series of dilutions, from 10^{-2} to 10^{-10}, were prepared and then were amplified and quantified by qRT-PCR. Standard curve was generated by plotting the cycle threshold (CT) value regarding the log copy number.
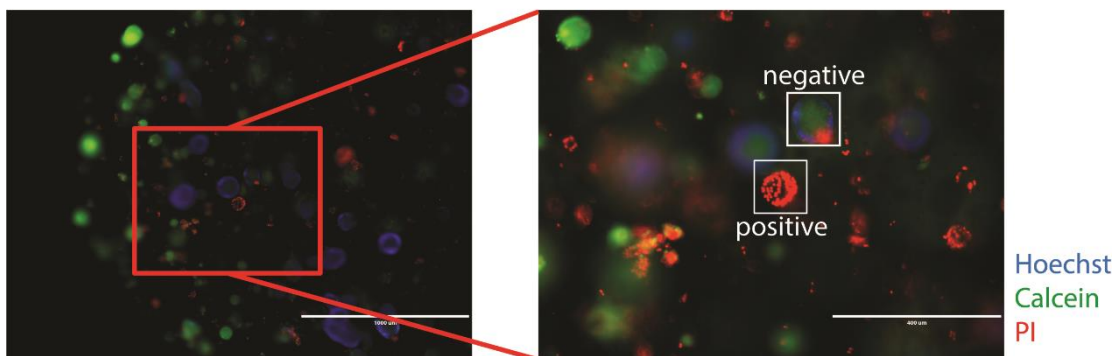
Supplementary Fig. S4. Determination of organoids cell death. Fluorescence microscopy images analysis of human intestinal organoids (HIOs) treated with gemcitabine (GCT) then stained by PI (red) which represented as dead cell, Hoechst (blue) which represented as nuclear, and Calcein (green) which represented as live cell. We define the lower left HIO (with red signal more than green signal and also more than 50% of blue signal) as positive HIO; on the contrary, HIOs like upper right one, will be counted as negative HIO. The proportion of deteriorated organoids was calculated as (viable/ total) %.

References

Chen, S., Ding, S., Yin, Y., Xu, L., Li, P., Peppelenbosch, M.P., Pan, Q., Wang, W., 2019. Suppression of pyrimidine biosynthesis by targeting DHODH enzyme robustly inhibits rotavirus replication. Antiviral Res 167, 35-44.

Grabinger, T., Luks, L., Kostadinova, F., Zimberlin, C., Medema, J.P., Leist, M., Brunner, T., 2014. Ex vivo culture of intestinal crypt organoids as a model system for assessing cell death induction in intestinal epithelial cells and enteropathy. Cell Death Dis 5, e1228.

Yin, Y., Bijvelds, M., Dang, W., Xu, L., van der Eijk, A.A., Knipping, K., Tuysuz, N., Dekkers, J.F., Wang, Y., de Jonge, J., Sprengers, D., van der Laan, L.J., Beekman, J.M., Ten Berge, D., Metselaar, H.J., de Jonge, H., Koopmans, M.P., Peppelenbosch, M.P., Pan, Q., 2015. Modeling rotavirus infection and antiviral therapy using primary intestinal organoids. Antiviral Res 123, 120-131.

Yin, Y., Chen, S., Hakim, M.S., Wang, W., Xu, L., Dang, W., Qu, C., Verhaar, A.P., Su, J., Fuhler, G.M., Peppelenbosch, M.P., Pan, Q., 2018a. 6-Thioguanine inhibits rotavirus replication through suppression of Rac1 GDP/GTP cycling. Antiviral Res 156, 92-101.

Yin, Y., Dang, W., Zhou, X., Xu, L., Wang, W., Cao, W., Chen, S., Su, J., Cai, X., Xiao, S., Peppelenbosch, M.P., Pan, Q., 2018b. PI3K-Akt-mTOR axis sustains rotavirus infection via the 4E-BP1 mediated autophagy pathway and represents an antiviral target. Virulence 9, 83-98.

Yin, Y., Wang, Y., Dang, W., Xu, L., Su, J., Zhou, X., Wang, W., Felczak, K., van der Laan, L.J., Pankiewicz, K.W., van der Eijk, A.A., Bijvelds, M., Sprengers, D., de Jonge, H., Koopmans, M.P., Metselaar, H.J., Peppelenbosch, M.P., Pan, Q., 2016. Mycophenolic acid potently inhibits rotavirus infection with a high barrier to resistance development. Antiviral Res 133, 41-49.

Chapter 8

Summary and Discussion

The development of rotavirus vaccines has made huge impact on global burden of rotavirus infection (1). This positive development has however diminished attention to quest for successful combat against rotavirus infection. However, the mortality of rotavirus disease remains considerably high in developing countries, especially in sub-Saharan Africa and south-east Asia (2). Additionally, some organ transplanted patients and IBD patients are still under the risk of contracting rotavirus infection (3). Moreover, recent research and case reports showed that rotavirus might be one of the viral causes of biliary atresia (4). So, investigation on rotavirus and focusing on antiviral treatment is still needed. This consideration led me to start research described this thesis, and here I want to summarize the result and outline my comprehension as what these results tell us.

Rotavirus infection and cytopathogenesis in development of biliary atresia

One important issue with respect to rotavirus is that the full extent of clinical complications provoked by the virus may have been underestimated. Biliary atresia (BA) is a neonatal liver disease characterized by progressive fibro-inflammatory obliteration of both intrahepatic and extrahepatic bile duct. The etiologies of BA remain largely unknown, and although some hypotheses as to how BA may come about, there is little actual data. Intriguingly, rotavirus infection might be a viral factor provoking this condition as a rotavirus-induced biliary atresia mouse model is a wildly established model for research on BA. In the present work I exploit liver organoids culture platforms to obtain more insight (5).

Results of my study indeed bolstered the case of a connection between rotavirus and BA. In total seven batches of biliary organoids from 3 different origins allowed productive infection with rotavirus, as evidenced by the generation of infectious viral particles, strongly suggesting that at least some type of cell in liver or bile duct is susceptible to rotavirus. Although I think this is an important step in making the case that rotavirus causes BA, I feel much more work is necessary and more research is now warranted: firstly, more rotavirus strains, and especially clinical isolated should be tested in more batches of organoids from different origins. Secondly, we should apply more differentiated organoids to test the infection, so that we can find out which type of cells are susceptible to rotavirus infection. Thirdly, mouse experimentation and infection of mouse biliary organoids may help us to get better understanding of the mechanism rotavirus-induced BA *in vivo*. Last but not the least, more

clinical evidence will help to reveal how rotavirus gets into neonatal bile duct. Does occur during gestation and can the virus overcome the placenta barrier or does infection occur in the birth canal?

Interferon mediated antiviral strategies

The Eukaryotic Translation Initiation Factor 4F (eIF4F) complex, containing a eukaryotic translation initiation factor 4A (eIF4A), a eukaryotic translation initiation factor 4E (eIF4E), and a eukaryotic translation initiation factor 4G (eIF4G), is a translation initiation factor that tightly regulates translation in response to a multitude of environmental conditions including viral infection (6). In our study, we found that blocking PDCD4 (a negative regulator of the eIF4F complex) elevates the activity of the three components of eIF4F complex and thereby inhibits rotavirus replication in host cells. Mounting evidence indicates that such inhibitory activity is the result of more efficient expression of antiviral proteins from the interferon signaling pathway. Thus, the eIF4F complex may become a promising target for development of new antiviral agents.

In line with this notion are especially the results of my studies in cell lines and intestinal organoids, which show that the interferon (IFNs) production, which follows rotavirus infection, can upregulate the expression of Interferon-stimulated genes (ISGs), but that cell autonomous endogenously produced IFNs are not able to limit rotavirus replication. This is mainly due to the ability of rotavirus to subvert the host innate immune response. However, exogenous treatment all three existing types of IFN treatment are effective in inhibiting rotavirus infection, and I also observed that combining IFNs with antiviral drugs also has a remarkable performance in limiting rotavirus infection, both in conventional cell lines and in the organoid model. Although further study should be done to identify which specific ISGs mediate the anti-rotavirus effect to complement the understanding of immunity against rotavirus, I feel my results indicate that IFN-mediated or IFN combined antiviral medication therapy should now be considered for managing problematic cases of rotavirus infection.

Nucleotides based anti-rotavirus strategies

Nucleotides play an important role in host cell metabolism but are obviously also essential for virus replication. Thus, targeting on purine or pyrimidine biosynthesis pathway might

effectively inhibit rotavirus replication and thus constitute a novel approach for potential novel anti-rotavirus therapy. Intriguingly, especially for organ transplanted patients, who are under the risk of rotavirus infection after surgery (3), a need for taking immunosuppressive drug exist and these drugs can be inhibitors of enzymes located in nucleotide producing pathways or be poorly metabolizible analogues of some intermediate products. Indeed such drugs have been described to exert potent antiviral activity against various types of virus (7-10). Therefore, taking this type of drugs would be a "kill two birds with one stone" solution, limiting rejection as well as virus infection at the same time. However, mechanisms of antiviral activity should be evaluated before clinical use, take 6-thioguanine (6-TG) and leflunomide (LFM) for instance, in my study, 6-TG exerts its antiviral activity through impairing Rac1 activation, and LFM can inhibit activity of the DHODH enzyme to limit rotavirus replication. However, in a previous HEV study, those two drugs have pro-viral effects on HEV infection in the Huh7 cell line (11). So, when considering using nucleotides based antiviral therapy, more comprehensive tests are required for specific drugs before clinical use is appropriate.

Broad-spectrum antiviral reagents screening strategy

Developing new drugs usually takes a long period of time require massive investments while risk of failure is high. Specifically, for rotavirus drug development, the potentially low return on investment ratio discourages widespread investment in the development of novel antiviral drugs. Faced with this problem, I proposed that repurposing existing drugs represents a cost-effective approach to identify antiviral treatment (12). In this line of thinking, screening of already clinically approved drugs screening should be a good way to reduce development costs. Among all kinds of drugs, broad-spectrum antiviral agents should be in the first round of the screening process. To be noticed in this respect, many antiviral drugs my host laboratory investigated are from the broad-spectrum antiviral agents (BSAAs) library. Setting drug libraries like BSAAs library is highly needed for humankind in order to have broader range of candidate drug options when viral pandemic (like the ongoing global COVID-19 pandemic) occurs.

Overall conclusions and future perspectives

In this thesis, I first established that rotavirus may be one of the causal factors with respect to biliary atresia, which also emphasized the importance of investigating rotavirus infection and

further illustrates the desperate need of novel antiviral treatment. Consequentially, we aimed at discovering anti-rotavirus strategies through targeting the interferon pathway, by inhibition of the nucleotide synthesis pathways and through broad-spectrum antiviral agents screening, respectively. These strategies provided insight to new antiviral drug development and provide a window to better treatment.

REFERENCES

1. Kirkwood CD, Ma L-F, Carey ME, Steele ADJV. 2019. The rotavirus vaccine development pipeline. 37:7328-7335.

2. Tate JE, Burton AH, Boschi-Pinto C, Parashar UD, Network WHOCGRS, Agocs M, Serhan F, de Oliveira L, Mwenda JM, Mihigo RJCID. 2016. Global, regional, and national estimates of rotavirus mortality in children< 5 years of age, 2000–2013. 62:S96-S105.

3. Yin Y, Metselaar HJ, Sprengers D, Peppelenbosch MP, Pan QJAJoT. 2015. Rotavirus in organ transplantation: drug-virus-host interactions. 15:585-593.

4. Hertel PM, Estes MKJCoig. 2012. Rotavirus and biliary atresia: can causation be proven? 28:10-17.

5. Broutier L, Andersson-Rolf A, Hindley CJ, Boj SF, Clevers H, Koo B-K, Huch MJNp. 2016. Culture and establishment of self-renewing human and mouse adult liver and pancreas 3D organoids and their genetic manipulation. 11:1724.

6. Montero H, García-Román R, Mora SIJV. 2015. eIF4E as a control target for viruses. 7:739-750.

7. Farasati NA, Shapiro R, Vats A, Randhawa PJT. 2005. Effect of leflunomide and cidofovir on replication of BK virus in an in vitro culture system. 79:116-118.

8. Takhampunya R, Ubol S, Houng H-S, Cameron CE, Padmanabhan RJJogv. 2006. Inhibition of dengue virus replication by mycophenolic acid and ribavirin. 87:1947-1952.

9. Wang Q-Y, Bushell S, Qing M, Xu HY, Bonavia A, Nunes S, Zhou J, Poh MK, de Sessions PF, Niyomrattanakit PJJov. 2011. Inhibition of dengue virus through suppression of host pyrimidine biosynthesis. 85:6548-6556.

10. Pan Q, de Ruiter PE, Metselaar HJ, Kwekkeboom J, de Jonge J, Tilanus HW, Janssen HL, van der Laan LJJH. 2012. Mycophenolic acid augments interferon-stimulated gene expression and inhibits hepatitis C Virus infection in vitro and in vivo. 55:1673-1683.

11. Wang Y, Wang W, Xu L, Zhou X, Shokrollahi E, Felczak K, Van Der Laan LJ, Pankiewicz KW, Sprengers D, Raat NJJAa, chemotherapy. 2016. Cross talk between nucleotide synthesis pathways with cellular immunity in constraining hepatitis E virus replication. 60:2834-2848.

12. Qu C, Li Y, Li Y, Yu P, Li P, Donkers JM, van de Graaf SF, Robert A, Peppelenbosch MP, Pan QJAr. 2019. FDA-drug screening identifies deptropine inhibiting hepatitis E virus involving the NF-κB-RIPK1-caspase axis. 170:104588.

Chapter 9

Nederlandse Samenvatting

Dutch Summary

Het rotavirus vormt een gesel die de mensheid hard treft. Deze ziekteverwekker infecteert onze darmen en veroorzaakt daar diarree, met als gevolg ziekte, uitdroging en kindersterfte. Ofschoon, eerst door verbeterde hygiëne en daarna door de introductie van vaccins de situatie sterk verbeterde, blijft rotavirusinfectie een groot probleem. In grote delen van de Derde Wereld is het nog steeds één van de belangrijkste oorzaken van kindersterfte. Daarnaast is het rotavirus ook gevaarlijk voor kwetsbare bevolkingsgroepen zoals transplantatiepatiënten en patiënten die immuunsysteemonderdrukkende medicijnen gebruiken. Tenslotte zou het zo kunnen zijn dat er klinische beelden bestaan die wel veroorzaakt worden door rotavirusinfectie, maar die niet als zodanig herkend worden. Zoals ik in **hoofdstuk 1** uitleg dreven deze overwegingen mij het onderzoek zoals beschreven in dit proefschrift uit te voeren, waarbij ik mij met name heb geconcentreerd op het geven van een aanzet met betrekking tot het ontwikkelen van nieuwe geneesmiddelen voor de behandeling van rotavirus infectie. Zulke geneesmiddelen bestaan namelijk momenteel niet en artsen zijn dus gedwongen om bij de behandeling van rotavirusinfectie zich grotendeels te beperken tot geven van vocht en zout, dit om uitdroging van de slachtoffer(tje)s tegen te gaan, terwijl er gehoopt wordt op spontaan herstel.

In **hoofdstuk 2** kijk naar afsluitingen van de galgang (zogenaamde biliaire atresie), een zeldzame ziekte bij pasgeborenen. Verlittekening van de galwegen veroorzaakt het ophopen van gal en indien er niet geopereerd wordt leidt dit tot steeds verder voortschrijdend leverfalen en uiteindelijk tot overlijden op jonge leeftijd. De oorzaak is onbekend, maar in dit hoofdstuk laat ik zien dat de cellen die galwegen bekleden geïnfecteerd kunnen worden met rotavirus (dit was nog niet bekend) en daar effecten veroorzaken die overeenstemming zijn met een rol voor het rotavirus bij het ontstaan van biliaire atresie. Ik kon deze resultaten publiceren in het vooraanstaande vaktijdschrift *mBio*. Ik laat dus zien dat problematiek geassocieerd met het rotavirusinfectie zelfs nog groter is dan gedacht.

In **Hoofdstuk 3** en **Hoofdstuk 4** kijk ik naar hoe ons aangeboren immuunsysteem rotavirusinfectie onder de duim kan houden. In hoofdstuk 3 doe ik daarbij een interessante observatie. Rotavirus heeft de eiwit-producerende machinerie van de cel nodig om zichzelf te kunnen vermenigvuldigen. Ik zie echter dat ons aangeboren immuunsysteem dezelfde eiwit-producerende machinerie nog harder nodig heeft om het virus effectief te kunnen bestrijden. Het remmen van de eiwit-producerende machinerie is dus een heilloze weg bij het ontwerpen van nieuwe therapie. Deze resultaten heb ik gepubliceerd in het vooraanstaande

wetenschappelijke tijdschrift *Nature Scientific Reports.* Vervolgens heb ik verder gekeken naar hoe het aangeboren immuunsysteem nog geholpen zou kunnen worden bij effectieve remming van virusvermenigvuldiging. Ik zie daarbij dat het geven van antivirale cytokinen (cytokinen zijn enigszins vergelijkbaar met hormonen) het aangeboren immuunsysteem zo sterk aanspoort dat het nu effectief het virus gaat bestrijden. Omdat dergelijke antivirale cytokinen ook echt aan mensen kunnen worden gegeven, geeft dit een duidelijk handvat bij het ontwerpen van nieuwe mogelijke therapie, gebaseerd op het aanjagen van de activiteit van ons eigen immuun systeem in haar gevecht met het rotavirus. Deze resultaten werden gepubliceerd in het vooraanstaande vaktijdschrift *Antiviral Research*.

Ofschoon dus bleek dat het remmen van de eiwitproductie niet de oplossing is bij het bestrijden van het rotavirus, bleef de mogelijkheid openliggen dat remming op RNA niveau wel effectief zou kunnen zijn. Rotavirussen bevatten hun genetische informatie in een dubbele RNA streng en als de aanmaak van de betrokken nucleotiden geremd wordt, zou dat heel wel een oplossing kunnen bieden bij indectie. Nucleotiden komen in twee smaken, pyrimidines en purines. Inderdaad zag ik dat remmers van pyrimidine biosynthese een sterk effect hadden tegen rotavirus (**Hoofdstuk 5**). Ook een remmer van purines (6-thioguanine) was effectief tegen rotavirus, maar dit effect bleek niet via purine biosynthese te lopen, maar via de immuunsysteemregulator p21Rac (**Hoofdstuk 6**). Onder voorwaarden kunnen zowel pyrimidine synthese inhibitoren alsook 6-thioguanine veilig aan patiënten worden gegeven en dus twee middelen zijn ook nieuwe mogelijkheden voor de behandeling van rotavirus infectie. Ik wist beide studies dan ook te publiceren als twee artikelen in het vooraanstaande vaktijdschrift *Antiviral Research*.

Belangrijke overwegingen bij de ontwikkeling van medicijnen zijn de kosten en moeite die men zich moet getroosten om vast te stellen dat de betreffende medicijnen veilig zijn. Bij bestaande medicatie, die reeds getest is, speelt dit uiteraard niet. Medicatie heeft vaak meerdere werkingen in het lichaam en het zou zo maar kunnen dat er bestaande medicatie is die toevallig ook effectief rotavirusinfectie kan bestrijden. Daarom besloot ik een grote bibliotheek van bestaande en reeds geteste medicijnen te onderzoeken op hun vermogen rotavirusinfectie te remmen. In **Hoofdstuk 7** beschrijf ik de resultaten en laat ik zien dat het antikanker medicijn gemcitabine heel krachtig is tegen rotavirus. Vooral voor kankerpatiënten die veel risico lopen op rotavirusinfectie zou dit wel eens een belangrijke overweging kunnen

vormen in de beslissing met welke medicatie zij behandeld moeten worden. Een publicatie is in voorbereiding.

Al met al heb ik het gevoel dat ik met dit proefschrift een aantal belangrijke nieuwe handvatten heb gevonden met over wanneer en hoe behandeling van het rotavirus uitgevoerd moet gaan worden. Ik hoop dan ook met dit proefschrift een bijdrage te hebben geleverd in het gevecht van de mensheid tegen dit virus.

Appendix

Acknowledgements

Publications

PhD Portfolio

Curriculum Vitae

Acknowledgements

After these four years of effort, I finally made it to summarize all achievements from my research and to compile them into this thesis. This work would never be possible without all your help from every aspect of my life. During these periods of time, after all the loss and gain, after all the pain and growth, I always had your support. Here, I would like to give all my best gratitude to all of you, my family, my promotor, co-promotor, colleagues, and friends in the Netherlands as well as in China.

To Dr. Qiuwei (Abdullah) Pan, you are a brilliant scientist with keen sense smell on research field, and you are so hard-working with humble attitude. I always admire your character toward to scientific research. During these four years of study, you have given me plenty of time and space to process my research, at the same time, you are always helpful for guiding me through all the difficulties. I have learned a lot from you, and it is an honor to be in our group under the supervision by you.

To Prof. Maikel P. Peppelenbosch, I treasure every group discussion with you, because it seems that you every time you can perfectly solve our problems, and come up with new inspiring ideas on our projects like a lighthouse leading the ship in a storm. Thanks for your support throughout all my PhD study.

To Prof. Luc van der Laan and Dr. Monique Verstegen, both of you are so kind to me, thanks for introducing project and sharing research resources to me even I am not a member of your group, I really enjoy attending the weekly organoids meeting you two held, and indeed I learned a lot from both of you.

To Prof. Hugo de Jonge and Dr. Marcel Bijvelds, thanks both of you for guiding me the technology of intestinal organoids culturing, you two are always very friendly and ready to help.

To Dr. Ron Smits, thanks for your tips while working in the lab, that helps me to form a good experimental habit.

To Dr. Gwenny Fuhler, you are a friendly and intelligent scientist, thanks for all the excellent questions you raised and all the good ideas you suggested, they helped me to enrich my project to a higher level, your optimistic attitude toward life always impressed me.

To Dr. Yuebang Yin, Dr. Lei Xu and Dr. Wenshi Wang, three of my respectful elder fellows, you taught me lot of skills on experiment and writing, moreover, you also helped me understanding the truth of life, I am so glad to be friend of you all, wish you all get big achievements in your present work.

To Dr. Wanlu Cao, Dr. Guoying Zhou, Dr. Wenhui Wang, Dr. Shan Li and, Dr. Pengyu Liu, thanks for guiding me with experimental skills as well as showing me the meaning of family, hope all of you and your family healthy and happy.

To Dr. Wen Dang and Dr. M. S. Hakim, I will never forget the moment when I was the paranimfen for both of your PhD defense in the same day! Thanks for your helping me with my experiment, I wish both of you have a bright future in your research field.

To Dr Meng Li, Dr. Changbo Qu and Dr. Buyun Ma, having discussion with all of you is extremely helpful for my project, it is so nice to have all of you as my colleagues as well as friends. Also, filming the defense of Changbo and Buyun was my honor to make the moment everlasting.

To Jiaye Liu and Zhouhong Ge, we came to Rotterdam in the same year with CSC scholarship, and we have been supported each other for four years, wish you both live a happy life as you expected. Special thanks to Jiaye for taking care of me when we were sharing the same apartment, I am so lucky to have you as my friend.

To Yang Li, Peifa Yu, Zhijiang Miao, Yunlong Li, Ruyi Zhang, Ling Wang, Shaojun Shi, Bingting Yu, Xiaopei Guo and Shanshan Li, all my younger fellows, you are all very helpful and friendly, hope all of you can get wonderful achievements in your research. Do not be shy, express yourself and enjoy the life in Netherland!

To Pengfei Li and Yining Wang, two paranimfen of my defense, both of you are hard-working and promising researchers, thanks for helping me with my experiment and my defense, wish both of you success!

To Suk yee Lam and Ketaryna Nesteruk, even we are not from the same group or working on the same project, we always can find some connection to make us friends. I will treasure all the moment we spend together.

To my former roommates: Rachid, Jorker, Ruby, Vincent, Thijmen, Yingying and Pauline, thanks for the help when we were sharing the office, all remember all the happiness we have experienced.

To my "trip" friends: Glüce, Anthonie, Lisanne, Floris, Michiel, Monique and Patrick, I am so happy to go for a short "trip" with all of you, you are so friendly and warm-hearted, we could be better friends if we had more time to spend. I wish you all the best.

To other MDL colleagues who helped me a lot: Petra, thanks for the experimental help, wish you can always enjoy your life. Jan, thanks for your management to the lab, you are so kind and warm-hearted. Leonie, thanks for your outstanding secretary work so that I can focus on my experimental work. Natasha and Kelly, you two just like tween sisters and always bring energy to our lab. Auke, also thank you for the management for our lab creating a perfect research environment for our study. And, many thanks to those colleagues not mentioned yet.

Then out of my department, there are also many friends in Rotterdam I should appreciated: Lico Lee, my performance partner, the Chinese singing star in Netherland, thanks for discovering my talent beyond doing research. Quan, Dan and Jialiang, thanks for offering me the part time job for performing and video shooting, I am incredibly happy to work with you. Mandy, you just like a big sister for me, and you always console me when I suffered. Then Yuke and Cong, you two are so lovely and always bring joy to me, thanks for staying with me.

To my master supervisor Prof. Meilin Jin, thanks for guiding me into this research field, and teaching me a lot of skills as well as the valuable quality for doing research, may all your wishes come true.

To my bachelor head teacher Prof. Xueying Hu, thank you for the help during my bachelor period, you found my potential. Wish you and your family well.

To my life-long friends in Wuhan, China: Yu Wang, Ge Liang, Pengcheng Liu Kailun Zhang, Xuan Chen and Xin Yin, thanks for keeping me company before I went to Netherland, and when I

went back China, you were the first group of friends I met, whatever I suffered, you always got my back, wish all of you have a better future and a happy family.

Finally, it is time to thanks my family: to my parents and grandparents, you are the greatest people in the world, you raised me up with all your love and unconditionally supporting me about every decision I made. To all my relatives in Wuhan and Liuzhou, thanks for your support helping me and my family for all time.

Publications list

1.   **<u>Chen, S.</u>**, Li, P.,Wang, Y., Yin, Y., de Ruiter, P., Verstegen, M. M., Peppelenbosch, M. P., Pan, Q. 2020. Rotavirus infection and cytopathogenesis in human biliary organoids potentially recapitulate biliary atresia development. ***mBio***.

2.   **<u>Chen, S.</u>**, Wang, Y., Li, P., Yin, Y., Bijvelds, M. J., de Jonge, H. R., Peppelenbosch, M. P., Kainov, D. E., Pan, Q. 2020. Drug screening identifies gemcitabine inhibiting rotavirus through alteration of pyrimidine nucleotide synthesis pathway. ***Antiviral Research***.

3.   Deuring, J. J., Li, M., Cao, W., **<u>Chen, S.</u>**, Wang, W., de Haar, C., van der Woude, C. J., Peppelenbosch, M. P. 2019. Pregnane X receptor activation constrains mucosal NF-κB activity in active inflammatory bowel disease. ***PloS one***.

4.   **<u>Chen, S.</u>**, Ding, S., Yin, Y., Xu, L., Li, P., Peppelenbosch, M. P., Pan, Q. , Wang, W. 2019. Suppression of pyrimidine biosynthesis by targeting DHODH enzyme robustly inhibits rotavirus replication. ***Antiviral research***.

5.   **<u>Chen, S.</u>**, Feng, C., Fang, Y., Zhou, X., Xu, L., Wang, W., Kong, X., Peppelenbosch, M. P., Pan, Q., Yin, Y. 2019. The eukaryotic translation initiation factor 4F complex restricts rotavirus infection via regulating the expression of IRF1 and IRF7. ***International journal of molecular sciences***.

6.   Dang, W., Xu, L., Ma, B., **<u>Chen, S.</u>**, Yin, Y., Chang, K. O., Peppelenbosch, M. P., Pan, Q. 2018. Nitazoxanide inhibits human norovirus replication and synergizes with ribavirin by activation of cellular antiviral response. ***Antimicrobial agents and chemotherapy***.

7.   Yin, Y., **<u>Chen, S.</u>**, Hakim, M. S., Wang, W., Xu, L., Dang, W., Qu, C., Verhaar, A. P., Su, J., Fuhler, G. M., Peppelenbosch, M. P., Pan, Q. 2018. 6-Thioguanine inhibits rotavirus replication through suppression of Rac1 GDP/GTP cycling. ***Antiviral research***.

8.   Hakim, M. S., Ding, S., **<u>Chen, S.</u>**, Yin, Y., Su, J., van der Woude, C. J., Fuhler, G. M., Peppelenbosch, M. P., Pan, Q., Wang, W. 2018. TNF-α exerts potent anti-rotavirus effects via the activation of classical NF-κB pathway. ***Virus research***.

9.   Hakim, M. S., **<u>Chen, S.</u>**, Ding, S., Yin, Y., Ikram, A., Ma, X., Wang, W., Peppelenbosch, M. P., Pan, Q. 2018. Basal interferon signaling and therapeutic use of interferons in controlling rotavirus infection in human intestinal cells and organoids. ***Scientific reports***.

10.   Dang, W., Xu, L., Yin, Y., **Chen, S.**, Wang, W., Hakim, M. S., Chang, K. O., Peppelenbosch, M. P., Pan, Q. 2018. IRF-1, RIG-I and MDA5 display potent antiviral activities against norovirus coordinately induced by different types of interferons. *Antiviral research*.

11.   Yin, Y., Dang, W., Zhou, X., Xu, L., Wang, W., Cao, W., **Chen, S.**, Su, J., Cai, X., Xiao, S., Peppelenbosch, M. P., Pan, Q. 2018. PI3K-Akt-mTOR axis sustains rotavirus infection via the 4E-BP1 mediated autophagy pathway and represents an antiviral target. *Virulence*.

12.   Cai, W., **Chen, S.**, Li, Y., Zhang, A., Zhou, H., Chen, H., Jin, M. 2016. 14-Deoxy-11, 12-didehydroandrographolide attenuates excessive inflammatory responses and protects mice lethally challenged with highly pathogenic A (H5N1) influenza viruses. *Antiviral Research*.

13.   Zou, Z., **Chen, S.**, Liu, Z., Jin, M. 2016. Identification and genetic analysis of H3N8 subtype influenza viruses isolated from domestic pigeons in Central China. *Virus genes*.

14.   Cai, W., Li, Y., **Chen, S.**, Wang, M., Zhang, A., Zhou, H., Chen, H., Jin, M. 2015. 14-Deoxy-11, 12-dehydroandrographolide exerts anti-influenza A virus activity and inhibits replication of H5N1 virus by restraining nuclear export of viral ribonucleoprotein complexes. *Antiviral Research*.

PhD Portfolio

Name of PhD student	Sunrui Chen
Department	Gastroenterology and Hepatology, Erasmus MC-University Medical Center, Rotterdam
PhD Period	October 2016 – October 2020
Promotor	Prof. dr. Maikel P. Peppelenbosch
Copromotor	Dr. Qiuwei Pan

PhD training

Seminars

• 2016-2020, Weekly MDL seminar program in experimental gastroenterology and hepatology (attending); (42 weeks/year; @1.5 h) (ECTS, 9.0).

• 2016-2020, Weekly MDL seminar program in experimental gastroenterology and hepatology (presenting); (preparation time 16 h; 2 times/year) (ECTS, 4.6).

• 2016-2020, Biweekly research group education (attending); (20 times/year; @1.5 h) (ECTS, 4.3).

• 2016-2020, Biweekly research group education (presenting); (preparation time 8 h; 4 times/year) (ECTS, 4.6).

General Courses and Workshops

• 2016, Basic and Translational Oncology 2016 (ECTS, 1.8).

• 2017, Course on Biomedical English Writing Course for MSc and PhD-students 2017 (ECTS, 2.0).

• 2018, Course in Virology 2018 (ECTS, 1.4).

• 2018, Course Scientific Integrity 2018 (ECTS, 0.3)

Academic Awards

• CSC Scholarship 2016, awarded by China Scholarship Council (CSC) (File No. 201606760056)

- Outstanding graduate 2014-2016, awarded by Huazhong Agricultural University

- DBN Encouragement Grant 2014-2015, awarded by Huazhong Agricultural University and DaBeiNong Sci-tech Group

- Student of Merit 2015-2016, awarded by Huazhong Agricultural University

- Student of Merit 2014-2015, awarded by Huazhong Agricultural University

- Student of Merit 2009-2012, awarded by Huazhong Agricultural University

- Grand Prize of The Second National Animal Medicine Skill Competition for College Students 2012, awarded by the China Veterinary Association

- Top ten singers in HZAU 2010 & 2015, awarded by Huazhong Agricultural University

Curriculum Vitae

Sunrui Chen was born on March 18th, 1991 in Wuhan, Hubei province, China. He was raised and finished his primary, secondary, and high school in his hometown.

In 2009, he started his bachelor study in veterinary medicine at the Huazhong Agricultural University, Wuhan, China (5 years). In 2014, he finished his study with a thesis entitled "The initial study of dehydroandrographolide anti-H5N1 influenza virus mechanism in vivo". And in the same year, he initiated his master research at the same university, in preventive veterinary medicine and under the supervision of Prof. Meilin Jin. He finished his master with a thesis book named "Detection of Tembusu virus antibody and the construction of Duck Enteritis Virus -Tembusu virus genetically engineered bivalent vaccine".

In 2016, with the support of China Scholarship Council (CSC) scholarship, he started his PhD research at the Department of Gastroenterology and Hepatology, Erasmus University Medical Center, Rotterdam, the Netherlands. Under the supervision of Prof. Maikel P. Peppelenbosch and Dr. Qiuwei Pan, he focuses on the development of novel antiviral strategies against rotavirus.